Lanthanide alkyl and silyl compounds: Synthesis, reactivity and catalysts for green chemistry

by

Aradhana Pindwal

A dissertation submitted to the graduate faculty

in partial fulfillment of the requirements for the degree of

DOCTOR OF PHILOSOPHY

Major: Inorganic Chemistry

Program of Study Committee:
Aaron D. Sadow, Major Professor
L. Keith Woo
Igor I. Slowing
Javier Vela
Jason Chen

Iowa State University

Ames, Iowa

2016

To my parents, sister Upasana and my husband Gaurav

TABLE OF CONTENTS

ACKNOWLEDGEMENTS

My graduate school journey began in August 2010 and I must confess that it has been a rollercoaster ride for me. From living away from my family and friends in India to learning to adjust to the new lifestyle and culture evolved me into a more responsible person. I came across a bunch of awesome people along this journey and here, I would like to sincerely thank them for guiding and helping me all throughout.

On the top of the list is my graduate school advisor, Dr. Aaron. D. Sadow who believed in me all throughout and moulded me into a real research scientist. I learnt a lot from him during this time and would treasure the knowledge gained all my life. I will never forget the early morning discussions I had with him in his office about research and paper writing skills I developed. I would also like to thank my committee members, Dr. L. Keith Woo, Dr. Javier Vela, Dr. Igor Slowing and Dr. Jason Chen for their support and guidance. In addition, I would like to thank my previous committee member Dr. Andreja Bakac. I would like to extend my thank you to CIF staff expecially Dr. Sarah Cady to accommodate my special requests to run overnight experiments and all the guidance about NMRs and other technical stuff. A special thanks to Dr. Arkady Ellern for running the X-ray crystallography and solving even the complicated structures in an efficient manner.

Next I would like to thank my awesome bunch of Sadow group members who kept me going even during the most difficult of times. I would like to thank Dr. James Dunne, Dr. KaKing Yan, Dr. Isaac Ho, Dr. Steven Neal, Dr. Kuntal Manna, Dr. Debabrata Mukherjee, Dr.

Songchen Xu, Dr. Nicole Lampland, Amy Zhu, Megan Hovey, Jake Fleckenstein, Naresh Eedugurala, Zak Weinstein, Brad Schmidt, Smita Patnaik, Kasuni Boteju, Abhranil Biswas, Yang Yun Chu. I would like to give a special mention to my fellow graduate student, Regina Reinig who has been my life support in the Sadow group. She has been with me through all thick and thin and I could not have survived without her support. Right from sharing food to serious discussions about our future and life to endless gossips and random shopping trip to the mall of America, we've done it all. I will miss you a lot but remember geographical distances will not distance our hearts.

Moreover, I would like to express my gratitude and thanks to my parents and sister, Upasana who have supported me and all my decisions all my life. You all have been an integral part of this journey and without your support and guidance it would be impossible to achieve this dream. I'm indebted to you all. Last but definitetly not the least, a big thank you to the love of my life, my husband Gaurav for always being there for me whenever I needed him. His constant support and love made this journey a really memorable one and I can't wait to start the next chapter of my life with him.

In the end, thank you all and I will cherish these moments all my life.

ABSTRACT

The last few decades have witnessed enormous research in the field of organometallic lanthanide chemistry. Our research group has developed a few rare earth alkyl compounds containing tris(dimethylsilyl)methyl ligand and explored their reactivity. This thesis focusses on extending the study of lanthanide alkyl and silyl compounds to develop strategies for their synthesis and explore their reactivity and role as catalysts in processes such as hydrosilylation and cross-dehydrocoupling.

Two novel ligands, alkyl, $–C(SiHMe_2)_3$ and silyl, $–Si(SiHMe_2)_3$ have been used to synthesize homoleptic organometallic lanthanide complexes. The silyl anion, $KSi(SiHMe_2)_3$, is prepared from the reaction of KO*t*Bu and $Si(SiHMe_2)_4$. A single crystal X-ray diffraction study shows that $KSi(SiHMe_2)_3$ crystallizes as a chain of alternating K cations and $Si(SiHMe_2)_3$ anions with K coordinated to the central Si atoms and the three Si-H moieties oriented toward the next K atom.

A series of lanthanum, cerium, praseodymium, neodymium, and samarium alkyl compounds and ytterbium and yttrium silyl compounds are synthesized and their characterization, reactivity and role as catalysts are described. These compounds are synthesized by salt metathesis reaction between the metal halide and an equiv. amount of $KC(SiHMe_2)_3$ and $KSi(SiHMe_2)_3$ ligands. The lanthanide tris(alkyl) compounds are solvent free compounds while lanthanide bis(silyl) compounds are THF coordinated and unstable at room temperature. All these compounds are highly air- and moisture-sensitive. Interestingly, spectroscopic characterization and X-ray analysis reveal that all the lanthanide alkyl compounds contain classical and non-classical β-SiH interactions with the metal center and undergo β-SiH

abstraction by Lewis acids, such as $B(C_6F_5)_3$ while the lanthanide silyl compounds lack such non-classical interactions with the metal center.

The reactions of $Ln\{C(SiHMe_2)_3\}_3$ (Ln = La, Ce, Pr, Nd) with one and two equiv. of $B(C_6F_5)_3$ gives $Ln\{C(SiHMe_2)_3\}_2HB(C_6F_5)_3$, and $LnC(SiHMe_2)_3\{HB(C_6F_5)_3\}_2$, respectively and an equiv. amount of 1,3-disilacyclobutane dimer, $\{Me_2Si\text{-}C(SiHMe_2)_2\}_2$ as the by-product. The monocations, $Ln\{C(SiHMe_2)_3\}_2HB(C_6F_5)_3$ are used as catalysts for hydrosilylation of α,β-unsaturated esters to selectively yield α-silyl esters. α-Silyl esters are isolated in high yields from a range of α,β-unsaturated esters and hydrosilanes.

The divalent bis(alkyl) lanthanide compounds, $Ln\{C(SiHMe_2)_3\}_2THF_2$ (Ln = Yb, Sm) are synthesized by salt metathesis of lanthanide halide and two equiv. of $KC(SiHMe_2)_3$ in THF. Reactions with one or two equiv. of $B(C_6F_5)_3$ generate $LnC(SiHMe_2)_3HB(C_6F_5)_3$ and an equiv. amount of 1,3-disilacyclobutane dimer, $\{Me_2Si\text{-}C(SiHMe_2)_2\}_2$. $Ln\{C(SiHMe_2)_3\}_2THF_2$ undergoes reaction with 1,3-di-tert-butylimidazol-2-ylidene (Im*t*Bu) to yield $Ln\{C(SiHMe_2)_3\}_2Im\textit{t}Bu$ in non-polar solvent. A single crystal X-ray diffraction and spectroscopic study of $Ln\{C(SiHMe_2)_3\}_2THF_2$ and $Ln\{C(SiHMe_2)_3\}_2Im\textit{t}Bu$ reveal the presence of classical and non-classical interactions with the metal center. $Ln\{C(SiHMe_2)_3\}_2Im\textit{t}Bu$ (Ln = Yb, Sm) is an efficient catalyst for cross-dehydrocoupling of organosilanes and amines to yield silazanes at room temperature in high yields. Kinetic studies of the catalytic system indicate a first-order dependence on silane and amine concentrations.

Lanthanide silyl compounds, $Yb\{Si(SiHMe_2)_3\}_2THF_3$ and $Cl_3Y\{Si(SiHMe_2)_3\}_2(Et_2O)].2K(Et_2O)_2$ are synthesized by salt metathesis of lanthanide halide and two or three equiv. of $KSi(SiHMe_2)_3$ ligand. $Yb\{Si(SiHMe_2)_3\}_2THF_3$ is the first example of homoleptic Ln(II) silyl compound characterized by X-ray diffraction having trigonal bipyramidal geometry around the ytterbium center. $Yb\{Si(SiHMe_2)_3\}_2THF_3$ reacts with ancillary ligand, $TlTo^M$ to yield $To^M{}_2Yb$ revealing lability of the silyl ligand.

CHAPTER 1: INTRODUCTION

General Introduction

Homoleptic lanthanide hydrocarbyl compounds[1]

The first homoleptic organometallic compound, $ZnEt_2$ was successfully synthesized and isolated in 1849 by Frankland which was highly reactive and pyrophoric.[2] A century later, significant progress was made in the synthesis of transition metal σ-hydrocarbyl compounds, however, homoleptic transition metal hydrocarbyl complexes such as $TiMe_4$, $ZrMe_4$ were highly unstable.[3] In the 1970s, Lappert and Wilkinson made break-through progress with the synthesis of new bulky hydrocarbyl ligands such as [CH_2SiMe_3], [$CH(SiMe_3)_2$], [CH_2CMe_3], or [CH_2Ph].[4] These new ligands paved way for synthesis and isolation of stable transition metal hydrocarbyl compounds.

In the area of rare earth organometallic chemistry, Wilkinson and Birmingham synthesized a series of $Ln(C_5H_5)_3$ compounds (Ln = Sc, Y, La, Ce, Pr, Nd, Sm, Gd, Dy, Er, Yb)[5] in 1954 but the first crystallographically characterized compound, $[Li(thf)_4][Lu(C_6H_3Me_2\text{-}2,6)_4]$ was synthesized by Hart containing the M–C σ bond.[6] In accordance to transition metal chemistry, [CH_2SiMe_3], [$CH(SiMe_3)_2$], [CH_2CMe_3], [$C(SiMe_3)_3$][7] ligands led to the development of organolanthanide chemistry. However, it was only in 1988 that the first crystallographically characterized neutral homoleptic lanthanide σ-hydrocarbyl compound, $Ln\{CH(SiMe_3)_2\}_3$ (Ln = La, Sm) was reported by Hitchcock.[8] These ligands and their variants are continued to be widely used to date in rare earth alkyl chemistry. Recently, ligands such as *t*-

butyl,[9] alkynyl,[10] and benzyl[11] have expanded the scope of ligands used in rare earth alkyl chemistry. Figure 1 shows some of the lanthanide alkyl complexes reported in literature.

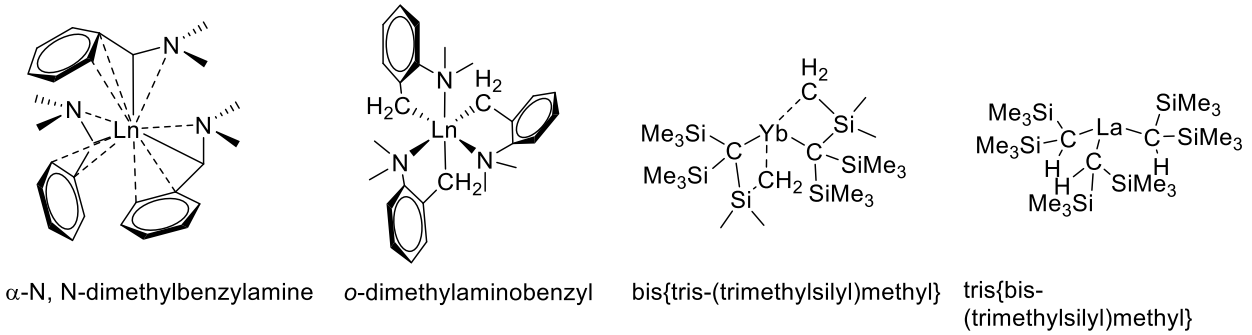

Figure 1. Examples of various hydrocarbyl compounds reported in literature

The ligands discussed thus far, do not contain any β-hydrogen such that the facile β-hydrogen elimination known in transition metal chemistry can be avoided. However, synthesis of ligands containing β-hydrogen provides us an opportunity to study the rare earth metal-ligand bonding and reactivity. The rare earth metal compounds containing β-hydrogen can exhibit interactions with the metal center. Such interactions are termed as 'agostic interactions', first coined by Malcolm Green to "discuss the various manifestations of covalent interactions between carbon-hydrogen groups and transition metal centers in organometallic compounds. The word agostic will be used to refer specifically to situations in which a hydrogen atom is covalently bonded simultaneously to both a carbon atom and a transition metal atom."[12] Although an agostic interaction refers to an M–H–C interaction, not all 3-center-2-electron bonds are agostic. For example, some of these interactions are better described as hydrogen-bonding.[13]

Rare earth alkyl compounds react via insertion, σ-bond metathesis, and protonolytic ligand substitution reactions which are important elementary steps in catalytic processes such as olefin polymerization,[14] hydrosilylation,[15] and dehydrocoupling.[16] Hydrosilylation presents a great opportunity for organic chemists to synthesize organosilanes which are useful in polymer

and medicinal chemistry. It is a well-known catalytic reaction for reduction of C=C, C=O and C=N bonds. A number of transition metal[17] and main group metal[18] catalysts are known to homogeneously hydrosilylate olefins, alkynes and carbonyl compounds. Catalytic hydrosilylation of aldehydes and ketones to give silyl ethers is a useful method for reversible protection of the C=O function or for its reduction to the corresponding alcohols. The reduction of the carbonyl group by hydrosilylation has been successfully used for the conversion of esters into primary alcohols.[19] Hydrosilylation of α,β-unsaturated carbonyl compounds followed by hydrolysis provides a novel and effective method of reduction to give the corresponding saturated carbonyl compounds or allylic alcohols. Hydrosilylation of linear and cyclic α,β-unsaturated ketones leads to 1,4-addition products.[20]

Despite a plethora of catalysts available for hydrosilylation of carbonyl compounds there are no organolanthanide catalysts reported to hydrosilylate α,β-unsaturated esters yet. Moreover, very few catalysts are known to hydrosilylate α,β-unsaturated esters to generate α-silyl esters.[21]

Another catalytic process of interest is the cross-dehydrocoupling of organosilanes and amines to yield silazanes. It presents an environment-friendly approach to synthesize silazanes because hydrogen gas is the only byproduct. Several catalysts have been developed for this process including rare earth metal complexes. Cui and group have demonstrated coordination of N-heterocyclic carbenes (NHCs) to rare earth amide compounds as efficient catalysts for cross-dehydrocoupling of silanes and amines over THF coordinated compounds.[22] Despite the synthesis of trivalent rare earth alkyl-NHC compounds reported in literature,[23] their catalytic chemistry is underdeveloped. In addition, divalent rare earth alkyl-NHC compounds are not known in literature yet.

Homoleptic lanthanide silyl compounds

The field of organosilicon chemistry has benefited extremely from contributions of Henry Gilman and co-workers. Gilman and group have synthesized first examples of polysilanes and tetrakis(trimethylsilyl)silane, the first tetrasilyl-substituted silane.[24] The first silyl anion, [tris-(trimethylsilyl)silyl]lithium was prepared by reacting methyllithium with tetrakis(trimethylsilyl)silane.[25] While metal silyl compounds exist for a range of metals in the periodic table but early transition metal silyl compounds[26] are limited and rare-earth silyl compounds are even more scarce with very few structurally characterized. A handful of the rare-earth silyl compounds reported in literature are shown in Figure 2.[27]

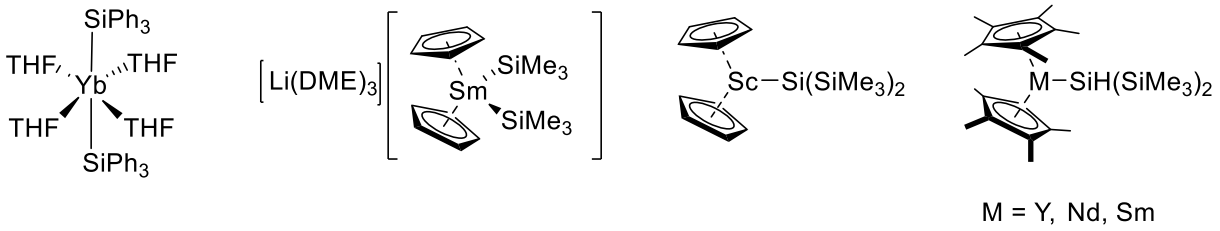

Figure 2: Examples of known rare-earth metal silyl complexes.

With the recent development of a polysilanylpotassium ligand by Marschner,[28] significant progress has been made in the field of silyl chemistry. However, similar to rare-earth hydrocarbyl compounds, rare-earth silyl compounds are also limited to ligands which do not contain β-hydrogen and thereby lack investigation of M-Si bond and reactivity.

This thesis contributes to the diversification and availability of potassium alkyl and silyl ligands through the development of the novel ligands, $KC(SiHMe_2)_3$ and $KSi(SiHMe_2)_3$ featuring β-SiH groups. The nucleophilicity of the SiH bond is investigated through abstraction reactions with Lewis acids. In addition, rare earth alkyl compounds are employed in catalytic transformations such as hydrosilylation and cross-dehydrocoupling of silanes and amines.

Thesis Organization

This thesis contains six chapters composed of manuscripts in preparation for journal submission. Chapter one gives a general introduction to the motivation behind the development of lanthanide alkyl and silyl compounds and catalysis. Chapter two through four are journal articles modified from manuscripts accepted in journal and in preparation for publication with in-depth discussion of the research conducted.

Chapter two describes the synthesis and characterization of homoleptic neutral, solvent-free lanthanide alkyl compounds with β-SiH containing $–C(SiHMe_2)_3$ ligand and their reactivity with other ligands such as $–N(SiHMe_2)_3$, BOx^{Me2} and $Ph(BOx^{Me2})$. The $La\{C(SiHMe_2)_3\}_3$ compound was synthesized by KaKing Yan and published in his thesis, however, I completed the series of lanthanide alkyl compounds and will be published in one paper.

Chapter three describes the reactivity of tris(dimethylsilyl)methyl lanthanide compounds with one and two equiv. of Lewis acid, $B(C_6F_5)_3$ resulting in the formation of monocation, $Ln\{C(SiHMe_2)_3\}_2HB(C_6F_5)_3$ and dication, $LnC(SiHMe_2)_3\{HB(C_6F_5)_3\}_2$ lanthanide alkyl hydridoborate compounds. Their characterization by NMR, IR spectroscopy and single crystal X-ray diffraction studies have been discussed in detail. $La\{C(SiHMe_2)_3\}_2HB(C_6F_5)_3$ and $LaC(SiHMe_2)_3\{HB(C_6F_5)_3\}_2$ were synthesized by KaKing Yan. The monocationic $Ln\{C(SiHMe_2)_3\}_2HB(C_6F_5)_3$ is described as an efficient catalyst for hydrosilylation of α,β-unsaturated esters to form α-silyl esters. The isolation of these α-silyl esters was carried out with the help of Smita Patnaik in our group. This presents the first example of rare-earth alkyl compound catalyzed hydrosilylation of α,β-unsaturated esters to yield α-silyl esters.

Chapter four discusses synthesis and characterization of lanthanide(II) alkyl complexes containing $–C(SiHMe_2)_3$ ligand with THF as the donor ligand and subsequent replacement of THF groups by N-heterocyclic carbenes. The NHC containing compounds are described as catalysts for cross-dehydrocoupling of silanes and amines and the kinetics of the catalytic reaction has been investigated. Chapter five describes the synthesis of bis(silyl) ytterbium and yttrium compounds with the new ligand $KSi(SiHMe_2)_3$ and that contains β-SiH functionality. The potassium silyl ligand was first synthesized and characterized by X-ray diffraction by Kaking Yan, and the optimized, scaled-up synthesis was developed by the combined efforts of Aradhana Pindwal and Nicole Lampland and is discussed in detail in Nicole Lampland's thesis. Iowa State University's crystallographer, Dr. Arkady Ellern, is credited with collecting data and solving all of the X-ray structures presented in this thesis.

References

[1] M. Zimmermann and R. Anwander, *Chemical Reviews* **2010**, *110*, 6194-6259.

[2] E. Frankland, *Quarterly Journal of the Chemical Society of London* **1850**, *2*, 263-296.

[3] a) K. Clauss and C. Beermann, *Angewandte Chemie-International Edition* **1959**, *71*, 627-627; b) N. J. Berthold and G. Groh, *Angewandte Chemie-International Edition* **1963**, *75*, 576-&; c) H. J. Berthold and G. Groh, *Angewandte Chemie-International Edition* **1966**, *5*, 516-&.

[4] a) M. R. Collier, M. F. Lappert and M. M. Truelock, *Journal of Organometallic Chemistry* **1970**, *25*, C036-&; b) G. Yagupsky, W. Mowat, Shortlan.A and Wilkinso.G, *Journal of the Chemical Society D-Chemical Communications* **1970**, 1369; c) W. Mowat, Shortlan.A, Wilkinso.G, G. Yagupsky, M. Yagupsky and N. J. Hill, *Journal of the Chemical Society-Dalton Transactions* **1972**, 533-&; d) M. R. Collier, M. F. Lappert and R. Pearce, *Journal of the Chemical Society-Dalton Transactions* **1973**, 445-451.

[5] G. Wilkinson and J. M. Birmingham, *Journal of the American Chemical Society* **1954**, *76*, 6210-6210.

[6] S. A. Cotton, A. J. Welch, Hursthou.Mb and F. A. Hart, *Journal of the Chemical Society-Chemical Communications* **1972**, 1225.

[7] C. Eaborn, P. B. Hitchcock, K. Izod and J. D. Smith, *Journal of the American Chemical Society* **1994**, *116*, 12071-12072.

[8] P. B. Hitchcock, M. F. Lappert, R. G. Smith, R. A. Bartlett and P. P. Power, *Journal of the Chemical Society-Chemical Communications* **1988**, 1007-1009.

[9] A. L. Wayda and W. J. Evans, *Journal of the American Chemical Society* **1978**, *100*, 7119-7121.

[10] a) G. B. Deacon and A. J. Koplick, *Journal of Organometallic Chemistry* **1978**, *146*, C43-C45; b) G. B. Deacon, A. J. Koplick, W. D. Raverty and D. G. Vince, *Journal of Organometallic Chemistry* **1979**, *182*, 121-141.

[11] a) L. E. Manzer, *Journal of Organometallic Chemistry* **1977**, *135*, C6-C9; b) L. E. Manzer, *Journal of the American Chemical Society* **1978**, *100*, 8068-8073; c) K. H. Thiele, K. Unverhau, M. Geitner and K. Jacob, *Zeitschrift Fur Anorganische Und Allgemeine Chemie* **1987**, *548*, 175-179.

[12] M. Brookhart and M. L. H. Green, *Journal of Organometallic Chemistry* **1983**, *250*, 395-408.

[13] a) L. Brammer, J. M. Charnock, P. L. Goggin, R. J. Goodfellow, T. F. Koetzle and A. G. Orpen, *Journal of the Chemical Society-Chemical Communications* **1987**, 443-445; b) L. Brammer, M. C. Mccann, R. M. Bullock, R. K. Mcmullan and P. Sherwood, *Organometallics* **1992**, *11*, 2339-2341.

[14] a) E. B. Coughlin and J. E. Bercaw, *Journal of the American Chemical Society* **1992**, *114*, 7606-7607; b) P. L. Watson, *Journal of the American Chemical Society* **1982**, *104*, 337-339; c) P. L. Watson and G. W. Parshall, *Accounts of Chemical Research* **1985**, *18*, 51-56.

[15] a) T. Sakakura, H. J. Lautenschlager and M. Tanaka, *Journal of the Chemical Society-Chemical Communications* **1991**, 40-41; b) P. F. Fu, L. Brard, Y. W. Li and T. J. Marks, *Journal of the American Chemical Society* **1995**, *117*, 7157-7168.

[16] a) C. M. Forsyth, S. P. Nolan and T. J. Marks, *Organometallics* **1991**, *10*, 2543-2545; b) E. Lu, Y. Yuan, Y. Chen and W. Xia, *ACS Catalysis* **2013**, *3*, 521-524.

[17] a) S. Chakraborty, J. A. Krause and H. Guan, *Organometallics* **2009**, *28*, 582-586; b) B. L. Tran, M. Pink and D. J. Mindiola, *Organometallics* **2009**, *28*, 2234-2243.

[18] a) F. Buch, H. Brettar and S. Harder, *Angewandte Chemie-International Edition* **2006**, *45*, 2741-2745; b) V. Leich, T. P. Spaniol, L. Maron and J. Okuda, *Chemical Communications* **2014**, *50*, 2311-2314.

[19] S. C. Berk, K. A. Kreutzer and S. L. Buchwald, *Journal of the American Chemical Society* **1991**, *113*, 5093-5095.

[20] T. Hagiwara, K. Taya, Y. Yamamoto and H. Yamazaki, *Journal of Molecular Catalysis* **1989**, *54*, 165-170.

[21] Y. Kim and S. Chang, *Angew Chem Int Ed Engl* **2015**.

[22] W. Xie, H. Hu and C. Cui, *Angew Chem Int Ed Engl* **2012**, *51*, 11141-11144.

[23] a) H. Schumann, D. M. M. Freckmann, S. Schutte, S. Dechert and M. Hummert, *Zeitschrift für anorganische und allgemeine Chemie* **2007**, *633*, 888-892; b) W. Fegler, T. P. Spaniol and J. Okuda, *Dalton Transactions* **2010**, *39*, 6774-6779.

[24] H. Gilman and C. L. Smith, *Journal of the American Chemical Society* **1964**, *86*, 1454-&.

[25] a) H. Gilman, J. M. Holmes and C. L. Smith, *Chemistry & Industry* **1965**, 848; b) H. Gilman and C. L. Smith, *Journal of Organometallic Chemistry* **1968**, *14*, 91-&.

[26] a) J. Arnold and T. D. Tilley, *Journal of the American Chemical Society* **1985**, *107*, 6409-6410; b) H. G. Woo and T. D. Tilley, *Journal of the American Chemical Society* **1989**, *111*, 3757-3758; c) N. S. Radu, T. D. Tilley and A. L. Rheingold, *Journal of Organometallic Chemistry* **1996**, *516*, 41-49.

[27] a) H. Schumann, J. A. Meesemarktscheffel and F. E. Hahn, *Journal of Organometallic Chemistry* **1990**, *390*, 301-308; b) B. K. Campion, R. H. Heyn and T. D. Tilley, *Organometallics* **1993**, *12*, 2584-2590; c) X. P. Cai, B. Gehrhus, P. B. Hitchcock and M. F. Lappert, *Canadian Journal of Chemistry-Revue Canadienne De Chimie* **2000**, *78*, 1484-1490.

[28] C. Marschner, *European Journal of Inorganic Chemistry* **1998**, 221-226.

CHAPTER 2: HOMOLEPTIC RARE EARTH ALKYL COMPOUNDS

Modified from a paper to be submitted to *J. Am. Chem. Soc.*

Aradhana Pindwal, KaKing Yan, Bradley M. Schmidt, Arkady Ellern, Steve Overbury, Igor S. Slowing, Aaron D. Sadow*

Abstract

The series of homoleptic rare earth tris(alkyl) complexes Ln{C(SiHMe$_2$)$_3$}$_3$ (Ln = La (**1a**), Ce (**1b**), Pr (**1c**), Nd (**1d**)) are synthesized through salt metathesis reactions of lanthanide triiodides and 3 equiv. of KC(SiHMe$_2$)$_3$. The isolated products **1a-d** do not contain THF or the KI byproduct in the final product, as determined by single crystal X-ray diffraction studies, NMR spectroscopy, and elemental analysis. Such studies of the series of complexes reveal isostructural pseudo-C_3-symmetric tris(alkyl) molecules containing two non-classical Ln←H-Si interactions per alkyl ligand, thereby generating six such interactions in one molecule. Infrared and ^{1}H NMR spectroscopic assignments, particularly of paramagnetic compounds, are further supported by preparation of deuterated analogues Ln{C(SiDMe$_2$)$_3$}$_3$ (Ln = La **1a-*d*$_9$**, Ce **1b-*d*$_9$**, Pr **1c-*d*$_9$**, Nd **1d-*d*$_9$**). These organometallic compounds persists in solution and the solid state up to 80 °C without formation of HC(SiHMe$_2$)$_3$ or the β-hydrogen elimination product {Me$_2$Si-C(SiHMe$_2$)$_2$}$_2$. Reactions of Ln{C(SiHMe$_2$)$_3$}$_3$ and ancillary proligands, such as bis-1,1-(4,4-dimethyl-2-oxazolinyl)ethane (**HBOx^{Me2}**) to give {BOx^{Me2}}Ln{C(SiHMe$_2$)$_3$}$_2$, demonstrates

these compounds as valuable synthetic organometallic starting materials in the chemistry of large lanthanide elements.

Introduction

Homoleptic organometallic compounds, which contain only one type of ligand bonded to a metal center,[1] have value in synthetic chemistry as homogeneous catalysts,[2] as well-defined starting materials for single-site grafting onto supports for catalysis,[3] as precursors for materials in chemical vapor deposition or other thermal decomposition processes,[4] and for combination with a range of ancillary ligands as an entry-point into reactive organometallic compounds.[5] New homoleptic organometallics, thus, can lead to new possibilities in synthesis and catalysis.

Studies of homoleptic rare earth tris(alkyl) starting materials have typically focused on β-hydrogen-free alkyl ligands, namely CH_2SiMe_3,[6] $CH(SiMe_3)_2$,[7] and $CH_2C_6R_5$.[8] Applications of homoleptic trivalent compounds containing these ligands, particularly those of the abundant light lanthanides (La, Ce, Pr, Nd), are limited by their short lifetimes at room temperature, challenging multistep syntheses (in the case of $CH(SiMe_3)_2$), or the difficulty to exclude THF or salt byproducts from the metal center's coordination sphere. For example, $La(CH_2Ph)_3THF_3$, $Ce(CH_2Ph)_3THF_3$, and their derivatives readily extrude toluene at room temperature. Ligand design strategies have sought to overcome these difficulties.

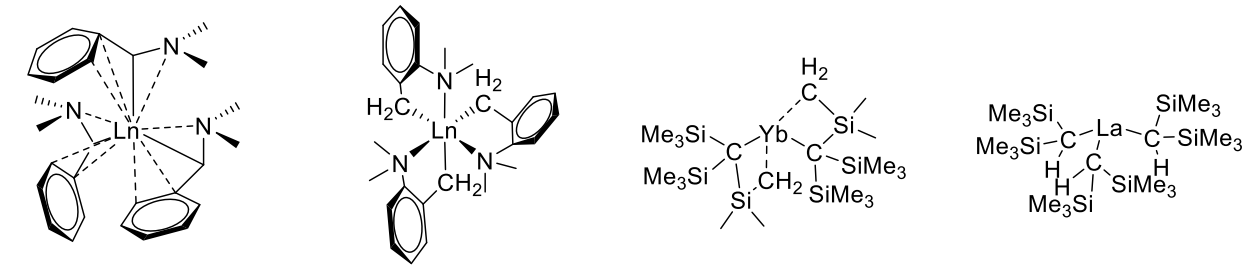

Figure 1. Examples of various hydrocarbyl compounds reported in literature

For example, α-metalated *N*,*N*-dimethylbenzylamine lanthanide complexes are persistent at room temperature,[9] and chelating *ortho*-dimethylaminobenzyl ligands stabilize the organolanthanide complexes presumably due to intramolecular coordination.[10] The bulky alkyl ligand -$C(SiMe_3)_3$, provides homoleptic isolable, donor-solvent free compounds but is restricted to divalent Ln(II) compounds.[11] Interestingly, non-classical Ln←Me-Si interactions were observed in $Yb\{C(SiMe_3)_3\}_2$[11] and $La\{CH(SiMe_3)_2\}_3$.[7] In addition, both of these donor-free homoleptic rare earth alkyls adopt solid-state structures that are distorted with respect to VSEPR predictions. $Yb\{C(SiMe_3)_3\}_2$ is bent (C-Yb-C 137°), and $La\{CH(SiMe_3)_2\}_3$ is pyramidal ($\sum_{CLaC}$ = 330°), rather than trigonal planar. The significant steric profile is the key to the persistence of these compounds.

The choice of alkyl ligand, however, may not need to be limited to the β-hydrogen-free hydrocarbyl groups. For example, $[Ln\textit{t}Bu_4]^-$[12] and $Cp_2Lu\textit{t}Bu(THF)$[13] are isolable and eliminate isobutylene under only relatively forcing conditions. In catalysis, particularly ethylene polymerization, ultra-high molecular weight products are obtained from rare earth catalysts, and presumably the long polymer chains are accessible partly because β-hydrogen elimination is slow.[14] In such a scenario, the presence of β-hydrogen may stabilize reactive alkyl groups, as in

Cp^*_2ScEt[15] and other agostic compounds.[16] Moreover, valuable aspects of metal-ligand bonding and reactivity is ignored in the absence of studies of β-hydrogen containing complexes.

An alternative means for stabilizing metal centers in homoleptic compounds, utilized mainly for amides, involves the β-silicon and β-hydrogen containing ligands such as tetramethyldisilazide $–N(SiHMe_2)_2$ and tert-butyl dimethylsilazide $–N(tBu(SiHMe_2))$ ligands.[17] Tetramethyldisilazide has been widely studied in d^0 and f-element chemistry.[18] Early metal and rare earth silazides containing β-SiH often form agostic-type structures evident from low energy Si-H vibrations and deviation from Ln-N-Si angles within a given silylamide ligand.[18b, c] A few examples of tetramethyldisilazido *ansa*-lanthanidocene compounds containing $–N(SiHMe_2)_2$ ligand exhibit an unusual β-Si-H diagostic interactions.[19] (Note that the polarization of Si-H bonds are inverted in comparison to C-H bonds, thus we refer to three-center-two electron Ln←H-Si as non-classical or agostic-like.)[20] A limitation of amide ligands, however, is the potential for eliminated amine to participate as a base, or in the case of silazanes as a silylating agent. In addition, conversions of tetramethyldisilazido rare earth compounds are hindered by the relatively low pKa of tetramethyldisilazane,[18c] and for these reasons dimethylsilyl substituted alkyl ligands combine the desirable stabilization of β-agostic-like silazido ligands with the reactivity of Ln-C bonds.

Previously, our group has reported the β-SiH-containing tris(alkyl)yttrium complex $Y\{C(SiHMe_2)_3\}_3$[21] and bis(alkyl) $M\{C(SiHMe_2)_3\}_2THF_2$ (M = Ca, Yb).[22] These complexes contain non-classical M←H-Si interactions, and the divalent compounds $M\{C(SiHMe_2)_3\}_2THF_2$ (M = Ca, Yb) react with Lewis acids such as $B(C_6F_5)_3$ through an intramolecular β-hydrogen abstraction pathway. In this work, we report the synthesis of trivalent homoleptic tris(alkyl)

complexes of lanthanum, cerium, praseodymium, and neodymium, i.e., the lightest and largest of the rare earth centers. The large ionic radii (6-coordinate La^{+3} (1.03 Å), 6-coordinate Ce^{+3} (1.01 Å), 6-coordinate Pr^{+3} (0.99 Å), 6-coordinate Nd^{+3} (0.98 Å)[23] make the synthesis of homoleptic, donor-free alkyls of these metal particularly challenging. The unusual structures, compared to $Ln\{CH(SiMe_3)_2\}_3$,[7] and diagnostic spectroscopic properties allow detailed characterization of both diamagnetic and paramagnetic members of the series. In addition, initial applications as organometallic synthetic precursors have been demonstrated.

Results and Discussion.

Synthesis and characterization of $Ln\{C(SiHMe_2)_3\}_3$ (Ln = La (1a), Ce (1b), Pr (1c), Nd (1d)). The homoleptic rare earth tris(alkyl) complexes are synthesized by reaction of $LnI_3(THF)_n$ (n = 4 for La, Ce; n = 3 for Pr, Nd) and 3 equiv. of $KC(SiHMe_2)_3$ in benzene for 12 h at room temperature. Crude $La\{C(SiHMe_2)_3\}_3$ and $Ce\{C(SiHMe_2)_3\}_3$ are obtained as pale yellow solids and form hexagon-shaped colorless crystals upon recrystallization from pentane. $Pr\{C(SiHMe_2)_3\}_3$ crystallizes as green plate-like crystals from toluene, while $Nd\{C(SiHMe_2)_3\}_3$ forms blue block-like crystals from pentane. In contrast to lanthanide iodide precursors, the combination of anhydrous rare earth halides $LaBr_3$, $LaCl_3$, $CeCl_3$, or $NdCl_3$ and $KC(SiHMe_2)_3$ in benzene or THF at room temperature does not provide the corresponding organometallic compounds. The identity of **1a** as $La\{C(SiHMe_2)_3\}_3$ is firmly established by a single crystal X-ray diffraction study (see below) and elemental analysis.

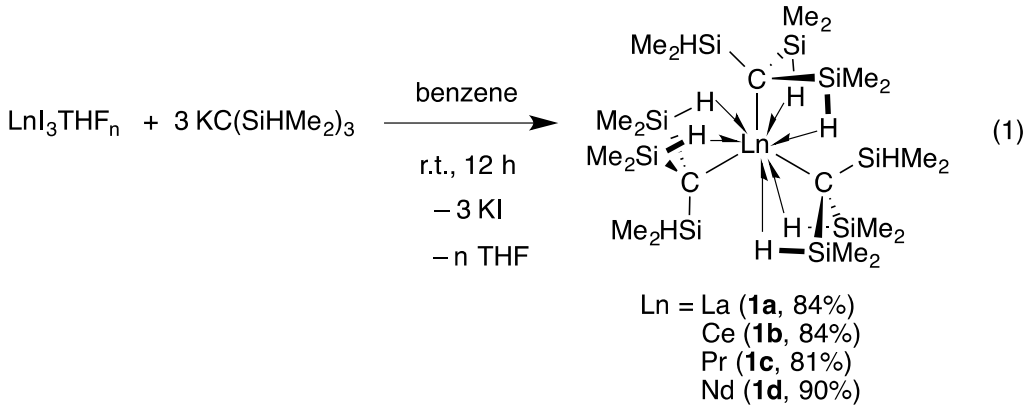

(1)

The selectively isotopically labeled Ln{C(SiDMe$_2$)$_3$}$_3$ (**1**-d_9, eq. 2) are also synthesized from KC(SiDMe$_2$)$_3$[22] to facilitate characterization of **1a-d** and study their fluxional processes.

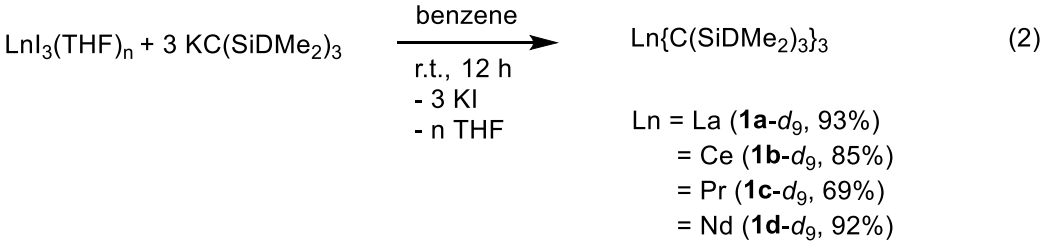

(2)

Similar infrared spectra (Figure 2) were measured for all four non-labeled compounds, and the ν_{SiH} region from 1800-2200 cm^{-1} was particularly informative. All four spectra contained a band at ca. 2107 cm^{-1} assigned to the stretching mode of a 2-center-2-electron SiH group. The spectra also contained a lower energy band at ~1830 cm^{-1} assigned to the SiH mode in a three-center-two-electron Ln←H-Si moiety. The assignment of both of these bands is supported by isotopically labeled samples Ln{C(SiDMe$_2$)$_3$}$_3$, which contained two bands at ~1529-30 and 1324-29 cm^{-1}, while the ν_{SiH} bands noted above are not observed. Thus, the infrared spectra indicate the series of tris(alkyl) lanthanide are isostructural.

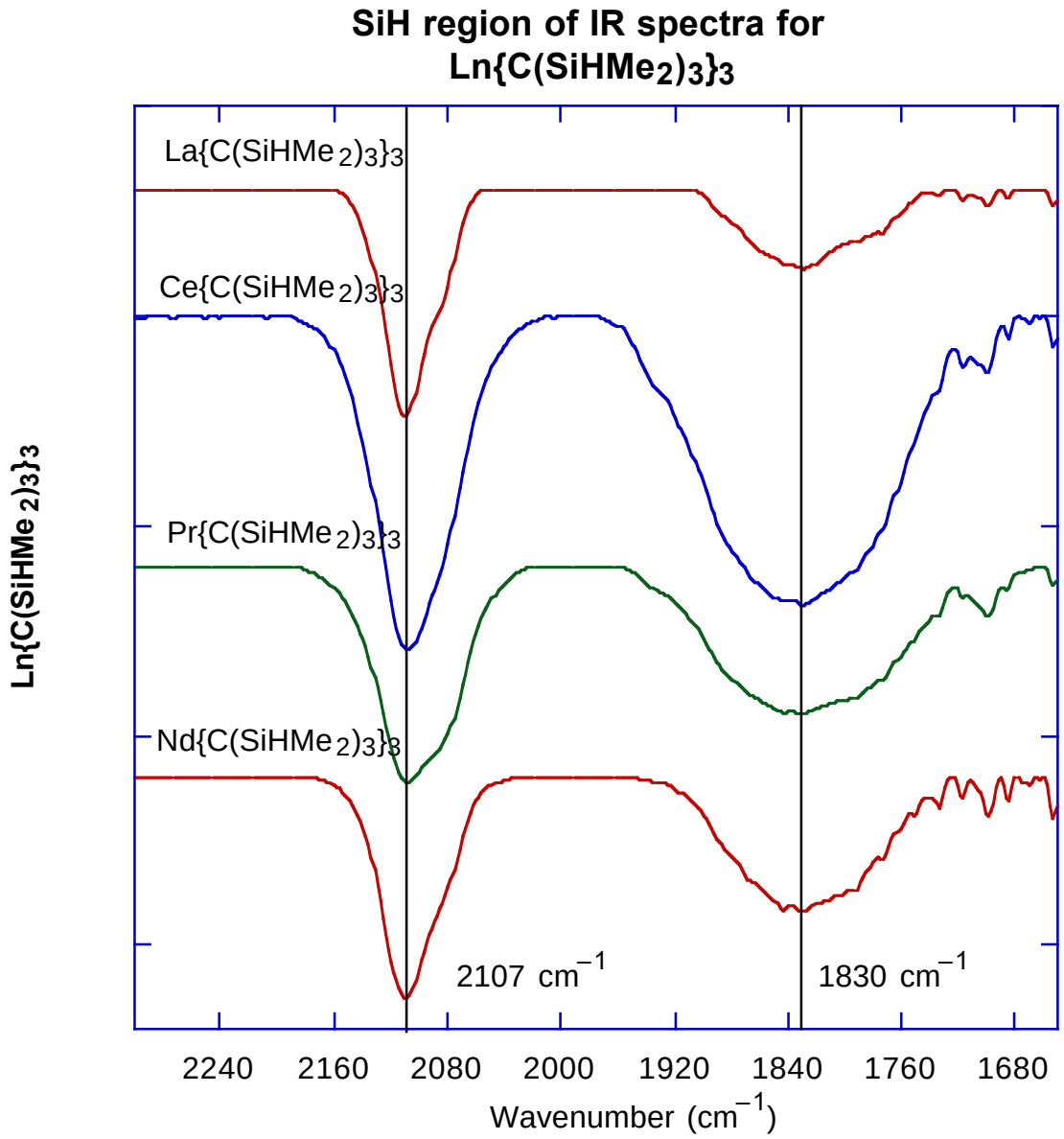

Figure 2. Infrared spectra of SiH region for $Ln\{C(SiHMe_2)_3\}_3$ (La: **1a**; Ce: **1b**; Pr: **1c**; Nd: **1d**)

The ^{1}H NMR spectrum of diamagnetic **1a**, acquired at room temperature in benzene-d_6, contained barely resolved doublet and multiplet resonances at 0.41 ppm ($^3J_{HH}$ = 3.3 Hz) at 4.26 ppm ($^1J_{SiH}$ = 137 Hz). The 6:1 integrated ratio of these signals indicated that the product contained only $SiHMe_2$ organic groups, which appeared equivalent at room temperature. The ^{1}H

NMR spectrum of **1a**-d_9 contained only a singlet at 0.41 ppm, while the ^{2}H NMR spectrum contained a resonance at 4.26 ppm.

The low $^1J_{SiH}$ value of **1a** is similar to the averaged value in fluxional Y{C(SiHMe$_2$)$_3$}$_3$,[20] so low temperature NMR experiments were performed on **1a**. As the temperature of a sample in toluene-d_8 was lowered, the SiH ^{1}H NMR resonance broadened to the coalescence point at 210 K. At 190 K, two SiH resonances at 4.78 ppm (3 H, $^1J_{SiH}$ = 186 Hz) and 4.04 ppm (6 H, $^1J_{SiH}$ = 114 Hz) and three methyl resonances at 0.55, 0.49, and 0.42 ppm (18 H each) were resolved in the ^{1}H NMR spectrum. The downfield signal and its $^1J_{SiH}$ value are similar to those in HC(SiHMe$_2$)$_3$ (4.33 ppm, 180 Hz). The upfield-shifted 4.04 ppm signal and its lower silicon-hydrogen coupling constant are similar to those of signals observed in low temperature NMR spectra of Y{C(SiHMe$_2$)$_3$}$_3$ (108 Hz). Although the yttrium compound shows the same temperature-dependent pattern of ^{1}H NMR signals as **1a**, the chemical shift range is larger in the lighter congener. In that compound and in **1a**, the fluxional behavior and the NMR parameters are assigned to six non-classical (agostic-type) interactions between the β-SiH and the rare earth center. A COSY experiment performed on **1a** at 190 K contained correlations between two SiMe$_2$ resonances at 0.49 and 0.55 ppm and the upfield SiH at 4.04 ppm, thus assigning these signals to the SiHMe$_2$ groups involved in agostic-like interactions with the La center, while the upfield signal at 0.42 ppm was assigned to a normal SiHMe$_2$ group. Thus, compound **1a** contains two types of SiHMe$_2$, one of which contains diastereotopic methyls, rather than three inequivalent SiHMe$_2$ groups.

Likewise, the room temperature ^{13}C{^{1}H} NMR spectrum of **1a** in toluene-d_8 contained only two resonances, at 31.8 (assigned to *C*(SiHMe$_2$)$_3$) and 3.6 ppm, whereas three upfield resonances at 4.42, 3.40, and 2.25 ppm and one downfield resonance at 30.15 ppm were

observed in the spectrum acquired at 190 K. The observation of only one downfield $^{13}C\{^{1}H\}$ NMR signal indicates that there is only one type of $C(SiHMe_2)_3$ group in the complex. This signal is more shielded than $La\{CH(SiMe_3)_2\}_3$ (75.2 ppm),[7] but downfield of $Y\{C(SiHMe_2)_3\}_3$ (r.t., 17.3 ppm). The two most upfield ^{13}C NMR signals are assigned to non-classical $SiH\mathit{Me}_2$ groups on the basis of ^{1}H-^{13}C HMQC experiments.

The temperature-dependent fluxionality is also observed in the ^{29}Si INEPT NMR spectra, which contained one resonance at –13.1 ppm at room temperature and two signals at –9.3 and –18.5 ppm at 190 K. Although the two types of SiH's give very different one-bond coupling constants, the ^{29}Si NMR chemical shifts are surprisingly similar. Note that downfield ^{29}Si NMR signals would be expected from structures in which the Si-H bond is partly broken from an arrested β-H elimination, either in the form of a partially-formed silene or a partly-formed silylium site.[23]

Despite the paramagnetic Ce, Pr, and Nd centers in complexes **1b**, **1c**, and **1d**, NMR and IR spectroscopic data suggest similar structures as the lanthanum compound described above. For example, the room temperature ^{1}H NMR spectrum of $Ce\{C(SiHMe_2)_3\}_3$ contained two broad peaks at 1.0 (54 H, 89 Hz at half-height) and 4.9 ppm (9 H, 169 Hz at half-height) which were assigned to $SiMe_2$ and SiH, respectively. The ^{1}H NMR spectrum of the deuterated analogue $Ce\{C(SiDMe_2)_3\}_3$ (**1b-*d*$_9$**) supported these assignments on the basis of a single resonance detected at 0.66 ppm, while the ^{2}H NMR spectrum contained a signal at 3.98 ppm assigned to the SiD moiety. Although these chemical shifts are similar to those of the diamagnetic lanthanum analogue obtained at room temperature, they in fact represent signals averaged by a fast exchange process as in **1a**. The ^{1}H NMR spectrum acquired at 200 K contained sharp, paramagnetically shifted signals at 10.6, 9.3 and –11.6 ppm (18 H each) and broad resonances at

24.5 and –19.7 ppm assigned to classical and non-classical SiH, respectively, assigned on the basis of their 1:2 integrated ratio and their absence in ^{1}H NMR spectra of **1b-*d*$_9$**. The ^{13}C{^{1}H} NMR spectrum of Ce{C(SiHMe$_2$)$_3$}$_3$ acquired at room temperature revealed only a single resonance at 11.5 ppm that splits into three resonances at 36.1, 33.2 and –4.2 ppm at low temperature. Unfortunately, ^{29}Si NMR signals were not detected at room temperature or at low temperature in ^{1}H-^{29}Si HMBC or ^{29}Si INEPT experiments.

The room temperature ^{1}H NMR spectra of Pr{C(SiHMe$_2$)$_3$}$_3$ and Nd{C(SiHMe$_2$)$_3$}$_3$ each contained two ^{1}H NMR resonances, but we were unable to detect signals in ^{13}C or ^{29}Si NMR spectra using direct or indirect detection methods. For both compounds, broad ^{1}H NMR signals with similar chemical shifts of 2.18 (540 Hz at half-height) and 1.78 ppm (775 Hz at half-height) for praseodymium and neodymium, respectively, were measured and assigned to silylmethyl groups on the basis of their integration of 6 H with respect to the second peak. The second peak, which was attributed to the SiH group, exhibited a greater averaged paramagnetic chemical shift for Nd (27.8 ppm) than Pr (12.03 ppm), giving the trend Ce (f^1) < Pr (f^2) < Nd (f^3). However, an opposite trend is observed for chiral lanthanide complexes, Ln(*i*Pr-BOPA){N(SiMe$_3$)$_2$}$_2$ (Ln = Pr, Nd) where the SiMe$_3$ signal is observed at –8.59 and –5.96 ppm for Pr and Nd, respectively.[24] The assignments were supported by the deuterium-labeled compounds' ^{1}H NMR spectrum, which showed a SiMe$_2$ peak at 1.7 ppm for **1d**-d_9. Only four resonances were resolved in the low temperature ^{1}H NMR spectra of Pr{C(SiHMe$_2$)$_3$}$_3$ and Nd{C(SiHMe$_2$)$_3$}$_3$ rather than the five signals in **1a** and **1b**.

The variable temperature NMR experiments indicate that bridging Ln←H–Si and terminal Si–H exchange occurs at rates on the NMR timescale. The rate of exchange between the three inequivalent methyl groups is the same as SiH exchange and can be used to study the exchange

process. The linewidths of the methyl signals in the $^{13}C\{^{1}H\}$ NMR spectra for **1a** were acquired from 153 K to 297 K in pentane-d_{12}, which was used to extend the temperature range of the study, were simulated using iNMR to obtain rate constant for the exchange process.[25] The temperature dependent rate constants over this range, fit to the Eyring equation, provided $\Delta H^{\ddagger}$ of 8.2(3) kcal·mol^{-1} and $\Delta S^{\ddagger}$ of –1(2) cal·mol^{-1}K^{-1}. These activation parameters are different from the corresponding values for the exchange process in Y{C(SiHMe$_2$)$_3$}$_3$ which were previously measured in toluene-d_8 as 13.4(3) kcal·mol^{-1} and 11(1) cal·mol^{-1}K^{-1}.[20] Given the similar structures and spectroscopic properties of Y{C(SiHMe$_2$)$_3$}$_3$ and La{C(SiHMe$_2$)$_3$}$_3$, the exchange process distinct kinetic parameters were unexpected. We re-measured these values for Y{C(SiHMe$_2$)$_3$}$_3$ in pentane-d_{12} from 180 K to 260 K to obtain $\Delta H^{\ddagger}$ = 11.2(2) kcal·mol^{-1} and $\Delta S^{\ddagger}$ = 3(1) cal·mol^{-1}K^{-1}, and these values likely reflect a more reasonable comparison of rate between the smaller and larger lanthanide tris(alkyls). Qualitatively, the exchange rate between SiH groups in the La compound is much faster (coalescence at ~180 K) in comparison to Y{C(SiHMe$_2$)$_3$}$_3$ (coalescence at 230 K).

The temperature dependent fluxional processes were measured for the related labeled compounds La{C(SiDMe$_2$)$_3$}$_3$ and Y{C(SiDMe$_2$)$_3$}$_3$, giving activation parameters listed in Table **1**. Although the $\Delta H^{\ddagger}$ and $\Delta S^{\ddagger}$ values are the same within 3σ error, the isotope effect k_H/k_D for both lanthanum and yttrium are *inverse* at low temperature.

Table 1. Activation parameters for Ln⇠H–Si/Si–H exchange in $Ln\{C(SiHMe_2)_3\}_3$ (Ln = La, Y)

Compound	**$\Delta H^{\ddagger}$ (kcal·mol^{-1})**	**$\Delta S^{\ddagger}$ (cal·mol^{-1}·K^{-1})**
$La\{C(SiHMe_2)_3\}_3$ (**1a**)	8.2(4)	–1(2)
$La\{C(SiDMe_2)_3\}_3$ (**1a**-d_9)	7.7(3)	–4(2)
$Y\{C(SiHMe_2)_3\}_3$	11.2(3)	3(1)
$Y\{C(SiDMe_2)_3\}_3$	10.5(3)	0(1)

Since compounds **1b-d** are colored the absorption properties were studied using UV-Vis spectroscopy. A broad absorption feature in the visible or near UV region was observed around 409 nm (ε = 294 $M^{-1}cm^{-1}$) for $Ce\{C(SiHMe_2)_3\}_3$ assigned to 5d → 4f intershell transitions. However, for $Pr\{C(SiHMe_2)_3\}_3$ and $Nd\{C(SiHMe_2)_3\}_3$ more than one absorption peak is observed at 458 nm (ε = 19.4 $M^{-1}cm^{-1}$) and 468 nm (ε = 16.5 $M^{-1}cm^{-1}$) for $Pr\{C(SiHMe_2)_3\}_3$ and 538 nm (ε = 28.5 $M^{-1}cm^{-1}$), 593 (ε = 37.4 $M^{-1}cm^{-1}$), 604 nm (ε = 70 $M^{-1}cm^{-1}$) and 611 nm (ε = 39.5 $M^{-1}cm^{-1}$) for $Nd\{C(SiHMe_2)_3\}_3$ suggesting multiple transitions in the visible region.

The $Ln\{C(SiHMe_2)_3\}_3$ (Ln = La, Ce, Pr, Nd) compounds are highly crystalline, and single crystal X-ray diffraction experiments provide the molecular structures (see Figures 3-6 (**1a-1d**) for significant bond distances and angles). In some examples, average values of crystallographically distinct distances and angles are given, and in these cases the standard deviation reflects statistical deviation of the data set rather than the crystallographically determined estimated standard deviation (E.S.D.) for a single value. All four compounds crystallize in the P-1 space group (Z = 2). The lanthanum, cerium, and praseodymium derivatives are isostructural, with similar unit cell parameters and only the $Ln\{C(SiHMe_2)_3\}_3$ molecule in the asymmetric unit. The smallest metal of the series, neodymium, co-crystallizes with a benzene

molecule, but the molecular geometry of all four compounds are essentially identical. The structures of **1a-d** have been examined in depth. The discussion will primarily focus on the lanthanum compound **1a**, with comparisons to **1b-d** provided as appropriate. Interestingly, the previously reported yttrium derivative $Y\{C(SiHMe_2)_3\}_3$ form high-quality crystals that diffract well,[20] but a convergent solution is not available partly as a result of three-fold twinned habit.

Several structural features of the $Ln\{C(SiHMe_2)_3\}_3$ are important, including the geometry and symmetry of the molecules, the geometry of the $C(SiHMe_2)_3$ ligands, and the six nonclassical Ln←H-Si bonding interactions featured in the $Ln–C(SiHMe_2)_3$ structures. The molecular structures contain three $C(SiHMe_2)_3$ ligands coordinated to the lanthanide center. The central carbons of the ligands (e.g. C1, C2, and C3) and La1 in $La\{C(SiHMe_2)_3\}_3$ are located in a plane, which is demonstrated by the sum of the C-La-C angles of 359.9°, and each of the C-La-C angles is 120.0 ± 0.7°. The compounds **1b-d** are also characterized by C-Ln-C angles of 120 ± 0.8°. The three ligands are related by pseduo-C_3 operations, and the two $SiHMe_2$ groups containing bridging La←H-Si interactions within each $C(SiHMe_2)_3$ ligand are related by a reflection. That mirror plane is located in the plane that contains La1, C1-3, Si3, Si5, and Si9, giving the overall $Ln\{C(SiHMe_2)_3\}_3$ molecules approximate C_{3h} symmetry. For La (**1a**), Ce (**1b**), and Pr (**1c**), the $SiHMe_2$ groups of Si3, Si5, and Si9 are also related by the C_3 operations, but these are oriented with all classical SiH's pointing to one face of the plane (rather than remaining in the plane as required for true C_{3h} symmetry) to give pseudo-C_3 symmetry. A C_3-symmetric structure was predicted in the gas-phase by DFT calculations $Y\{C(SiHMe_2)_3\}_3$ by Lein and Harrison. However, perfect C_3 symmetry is not observed for the crystallographically determined structures in the La-Nd series of compounds. There is no crystallographically imposed symmetry, and slight variations in interatomic distances and angles are observed between the

three $C(SiHMe_2)_3$ ligands in the compounds. In addition to the co-crystallized benzene molecule, the Nd compound **1d** is distinct from **1a-c** in its conformation of the $C(SiHMe_2)_3$ ligands. While Si3, Si5, and Si9 atoms of the $SiHMe_2$ groups are contained in the Nd1, C1, C2, and C3 plane, only two SiH groups are pointed to one side of the plane, while the third points to the other face.

Moreover, the planar structures of **1a-d** contrast the geometry of $La\{CH(SiMe_3)_2\}_3$, which is pyramidal at the La center, with C-La-C angles ca. 110° ($\sum$= 330°).[7] That compound contains three equivalent and short La-C_α distances (2.515(9) Å) as well as three short La-Me close contacts (~3.12 Å) described as β-agostic La⋯C-Si interactions. To our knowledge, $La\{CH(SiMe_3)_2\}_3$ is the only previously reported donor-free lanthanum compound containing only hydrocarbyl ligands. Other donor-free homoleptic lanthanum compound reported include $La\{N(SiMe_3)_3)_2\}_3$ having P31c space group, however, no X-ray data is reported.[27]

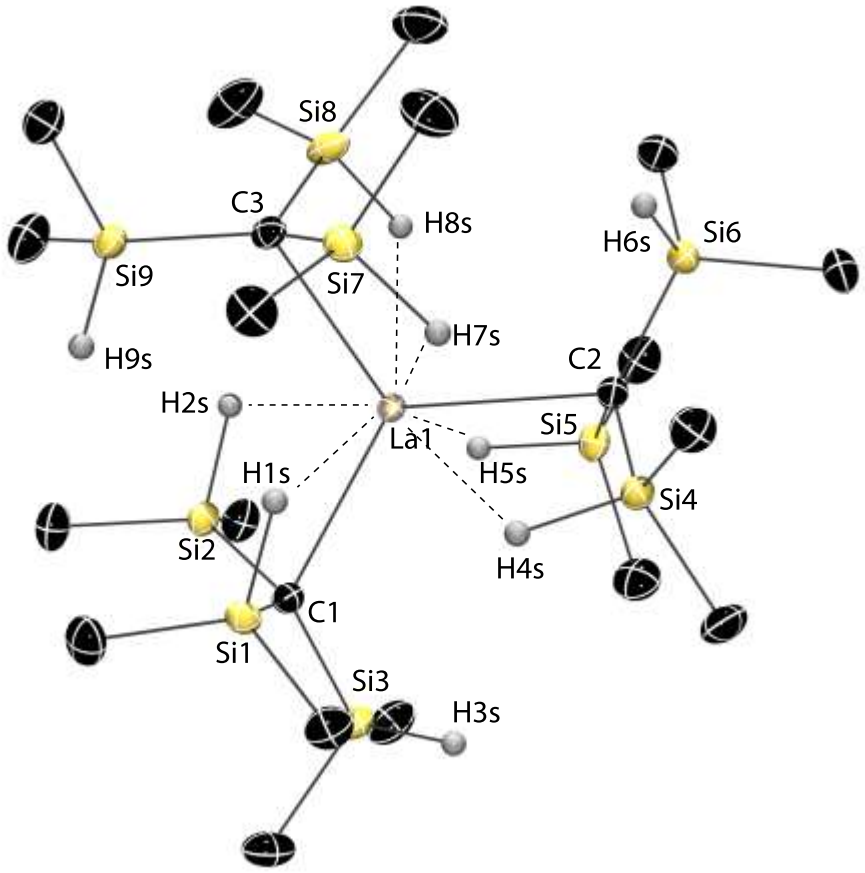

Figure 3. Rendered thermal ellipsoid plot of La{C(SiHMe$_2$)$_3$}$_3$ (**1a**) looking down the C_3 axis. Ellipsoids are plotted at 35% probability. Hydrogen atoms bonded to silicon were located objectively in the Fourier difference map and are included in the representation. All other H atoms are not plotted for clarity. Dashed curves between La1 and H1s, H2s, H4s, H6s, H7s, and H8s highlight short La-H distances. Significant interatomic distances (Å): La1-C1, 2.695(2); La1-C2, 2.679(2); La1-C3, 2.685(2); La1-Si1, 3.227(9); La1-Si2, 3.218(9); La1-Si4, 3.230(9); La1-Si5, 3.250(9); La1-Si7, 3.248(7); La1-Si8, 3.212(9); La1-H1s, 2.41(2); La1-H2s, 2.49(2); La1-H4s, 2.45(2); La1-H6s, 2.51(2); La1-H7s, 2.48(2); La1-H8s, 2.45(2); Si1-H1s, 1.51(2); Si2-H2s, 1.48(2); Si3-H3s, 1.40(2); Si4-H4s, 1.50(2); Si5-H5s, 1.45(2); Si6-H6s, 1.46(3); Si7-H7s, 1.47(3); Si8-H8s, 1.50(3); Si9-H9s, 1.36(2); C1-Si1, 1.839(2); C1-Si2, 1.828(2); C1-Si3,

1.848(2); C2-Si4, 1.833(1); C2-Si5, 1.850(2); C2-Si6, 1.819(2); C3-Si7, 1.820(1); C3-Si8, 1.832(2); C3-Si9, 1.854(2). Significant interatomic angles (°): C1-La1-C2, 119.70(5); C1-La1-C3,119.23(5); C2-La1-C3, 120.99(5); La1-C1-Si1, 88.30(7); La1-C1-Si2, 88.54(7); La1-C1-Si3, 126.16(9); La1-C2-Si4, 89.38(7);. La1-C2-Si5, 118.72(9); La1-C2-Si6, 90.44(7); La1-C3-Si7, 90.18(7); La1-C3-Si8, 88.56(7); La1-C3-Si9, 121.41(9).

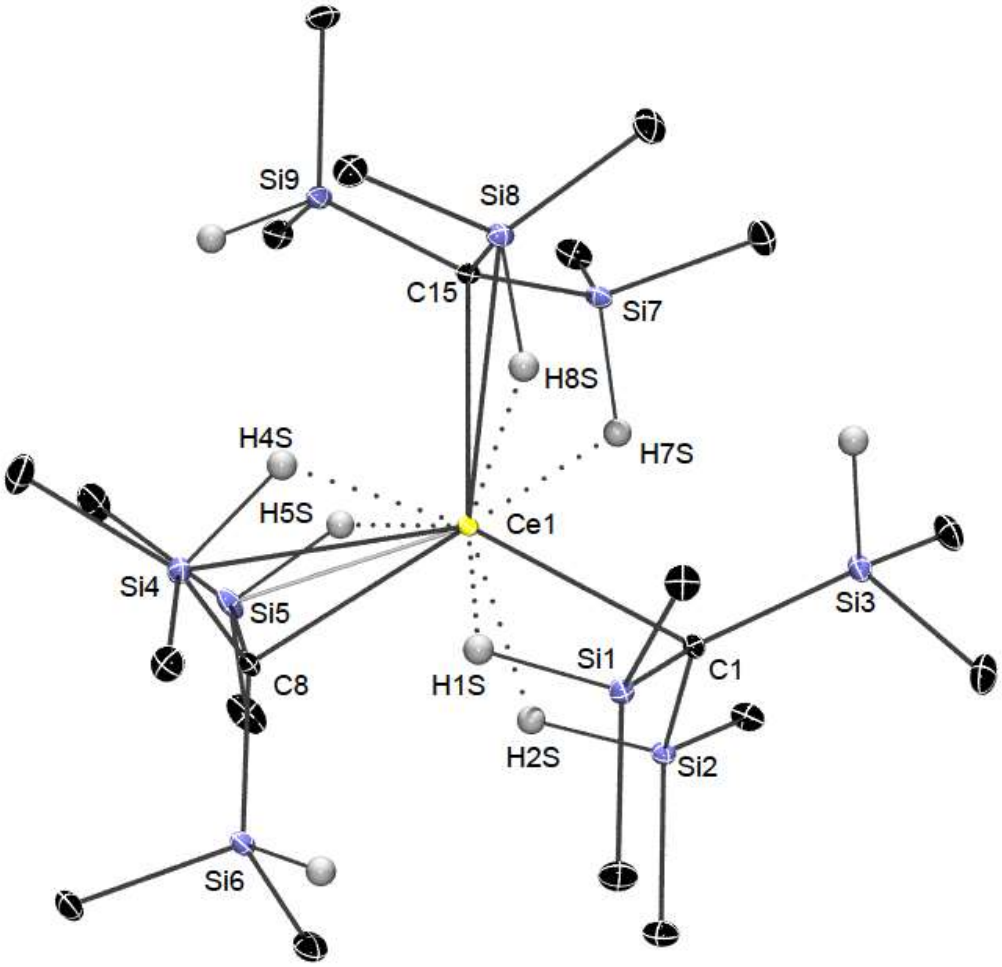

Figure 4. Rendered thermal ellipsoid plot of Ce{C(SiHMe$_2$)$_3$}$_3$ (**1b**) looking down the C_3 axis. Ellipsoids are plotted at 35% probability. Hydrogen atoms bonded to silicon were located

objectively in the Fourier difference map and are included in the representation. All other H atoms are not plotted for clarity. Dashed curves between Ce1 and H1s, H2s, H4s, H5s, H7s, and H8s highlight short Ce-H distances. Significant interatomic distances (Å): Ce1-C1, 2.659(2); Ce1-C8, 2.672(2); Ce1-C15, 2.651(2); Ce1-Si1, 3.221(9); Ce1-Si2, 3.185(1); Ce1-Si4, 3.192(1); Ce1-Si5, 3.191(7); Ce1-Si7, 3.204(1); Ce1-Si8, 3.224(1); Ce1-H1s, 2.48(3); Ce1-H2s, 2.43(3); Ce1-H4s, 2.44(3); Ce1-H5s, 2.44(3); Ce1-H7s, 2.44(3); Ce1-H8s, 2.53(3); Si1-H1s, 1.46(3); Si2-H2s, 1.47(3); Si3-H3s, 1.39(3); Si4-H4s, 1.48(3); Si5-H5s, 1.46(3); Si6-H6s, 1.42(3); Si7-H7s, 1.42(3); Si8-H8s, 1.46(3); Si9-H9s, 1.43(3); C1-Si1, 1.820(2); C1-Si2, 1.837(3); C1-Si3, 1.852(3); C8-Si4, 1.832(3); C8-Si5, 1.838(3); C8-Si6, 1.844(2); C15-Si7, 1.830(3); C15-Si8, 1.820(3); C15-Si9, 1.852(2). Significant interatomic angles (°): C1-Ce1-C8, 119.28(8); C1-Ce1-C15, 121.16(8); C8-Ce1-C15, 119.49(7); Ce1-C1-Si1, 89.94(9); Ce1-C1-Si2, 88.24(9); Ce1-C1-Si3, 122.37(1); Ce1-C8-Si4, 88.19(9);. Ce1-C8-Si5, 88.08(9); Ce1-C8-Si6, 127.08(1); Ce1-C15-Si7, 89.32(9); Ce1-C15-Si8, 90.32(1); Ce1-C15-Si9, 119.46(1).

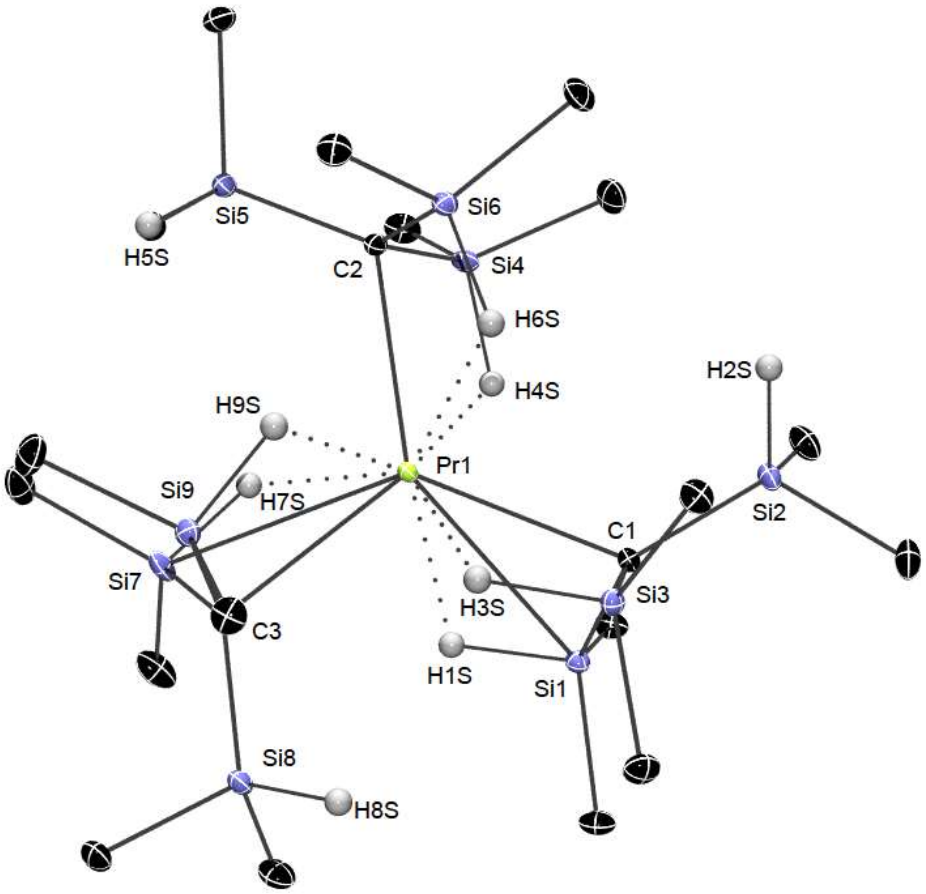

Figure 5. Rendered thermal ellipsoid plot of Pr{C(SiHMe$_2$)$_3$}$_3$ (**1c**) looking down the C_3 axis. Ellipsoids are plotted at 35% probability. Hydrogen atoms bonded to silicon were located objectively in the Fourier difference map and are included in the representation. All other H atoms are not plotted for clarity. Dashed curves between Pr1 and H1s, H3s, H4s, H6s, H7s, and H9s highlight short Pr-H distances. Significant interatomic distances (Å): Pr1-C1, 2.638(2); Pr1-C2, 2.632(2); Pr1-C3, 2.652(2); Pr1-Si1, 3.162(8); Pr1-Si3, 3.199(7); Pr1-Si4, 3.180(8); Pr1-Si6, 3.201(8); Pr1-Si7, 3.171(6); Pr1-Si9, 3.167(8); Pr1-H1s, 2.40(2); Pr1-H3s, 2.47(2); Pr1-H4s, 2.41(2); Pr1-H6s, 2.54(2); Pr1-H7s, 2.39(2); Pr1-H9s, 2.44(2); Si1-H1s, 1.47(2); Si2-H2s, 1.38(2); Si3-H3s, 1.45(2); Si4-H4s, 1.46(2); Si5-H5s, 1.40(2); Si6-H6s, 1.47(2); Si7-H7s,

1.47(2); Si8-H8s, 1.35(2); Si9-H9s, 1.46(2); C1-Si1, 1.834(2); C1-Si2, 1.849(2); C1-Si3, 1.819(2); C2-Si4, 1.830(2); C2-Si5, 1.847(2); C2-Si6, 1.823(2); C3-Si7, 1.837(1); C3-Si8, 1.846(2); C3-Si9, 1.828(2). Significant interatomic angles (°): C1-Pr1-C2, 121.04(6); C1-Pr1-C3,119.32(6); C2-Pr1-C3, 119.57(6); Pr1-C1-Si1, 88.07(8); Pr1-C1-Si2, 122.72(1); Pr1-C1-Si3, 89.79(8); Pr1-C2-Si4, 89.04(8);. Pr1-C2-Si5, 119.90(9); Pr1-C2-Si6, 89.98(8); Pr1-C3-Si7, 87.93(7); Pr1-C3-Si8, 127.51(1); Pr1-C3-Si9, 87.97(1).

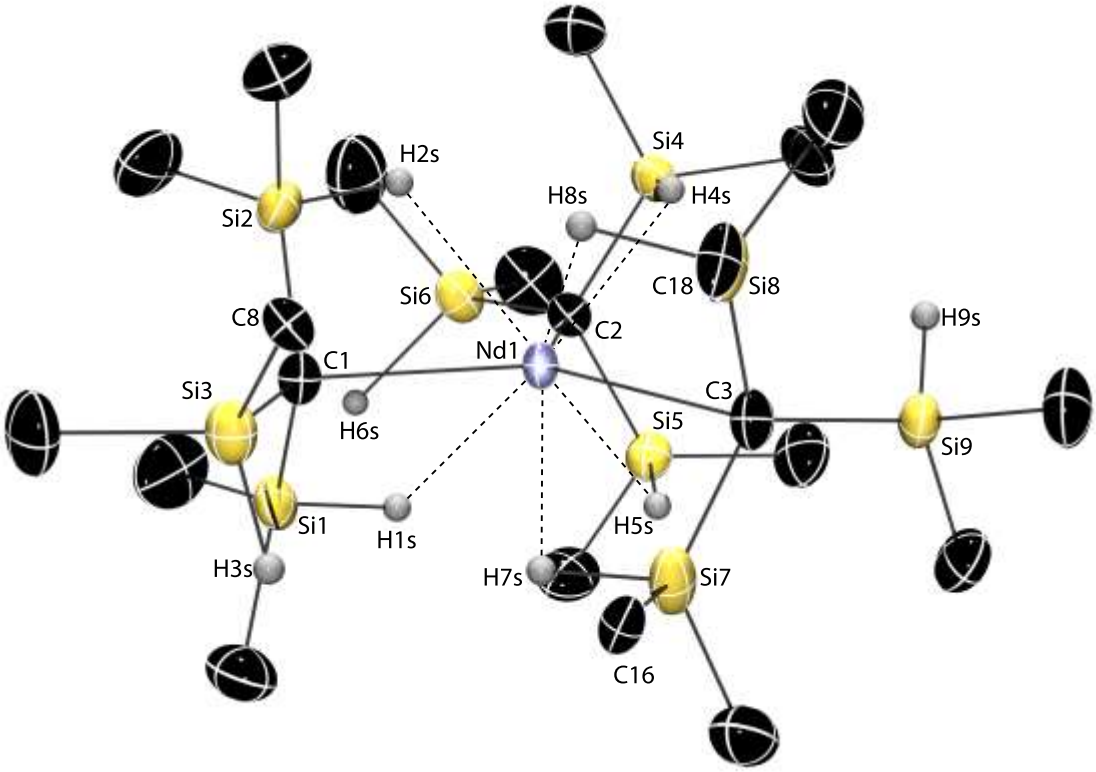

Figure 6. Rendered thermal ellipsoid plot showing a side-view of Nd{C(SiHMe$_2$)$_3$}$_3$ (**1d**). Ellipsoids are plotted at 50% probability, with the exception of C8, C16, and C18 which are plotted at 25% probability for clarity. Hydrogen atoms bonded to silicon were located objectively in the Fourier difference map, and these are included in the figure. All other H atoms and a co-crystallized benzene molecule are not included for clarity. Significant interatomic distances (Å): Nd1-C1, 2.623(2); Nd1-C8, 2.623(2); Nd1-C15, 2.632(3); Nd1-Si1, 3.1349(9); Nd1-Si2,

3.1727(8); Nd1-Si4, 3.152(1); Nd1-Si5, 3.1435(8); Nd1-Si7, 3.1456(9); Nd1-Si8, 3.1672(7); C1-Si1, 1.830(3); C1-Si3, 1.848(3). Significant interatomic angles (°): C1-Nd1-C2, 119.04(8); C1-Nd1-C3, 121.01(8); C2-Nd1-C3, 119.88(8); Nd1-C1-Si1, 87.6(1); Nd1-C1-Si2, 89.1(1); Nd1-C1-Si3, 128.5(1); Nd1-C2-Si4, 88.2(1); Nd1-C2-Si5, 87.9(1); Nd1-C2-Si6, 129.9(1); Nd1-C3-Si7, 87.9(1); Nd1-C3-Si8, 88.6(1); Nd1-C3-Si9, 123.5(1).

The La–C distances (La1-C1, 2.697(2), La1-C2, 2.679(2), La1-C3, 2.684(2) Å) in $La\{C(SiHMe_2)_3\}_3$ are long, ca. 0.16 Å longer than the distances in $La\{CH(SiMe_3)_2\}_3$. Other tris(alkyl)lanthanum compounds structurally characterized by single-crystal X-ray diffraction include six-coordinate $La(CH_2Ph)_3THF_3$ and $La(CH_2C_6H_4\text{-}4\text{-}Me)_3THF_3$, and these also contain shorter La-CH_2 interatomic distances of 2.648 ± 2 and 2.627 ± 2 Å,[8a] respectively. The La-C distances in the chelating benzyl compounds $La\{CH(NMe_2)Ph\}_3$ (2.65 ± 1 Å)[9] and $La\{CH_2C_6H_4NMe_2)_3$ (2.64 ± 1 Å)[10] are also shorter than the La-C distances in **1a**.

Each $C(SiHMe_2)_3$ ligand in **1a** contains two short La-H and two short La-Si distances. The La-H distances range from 2.41 to 2.51 Å, and although the limitations of X-ray diffraction and the large La ion require care in discussing H atom positions (see Si-H distance discussion below), these distances are shorter than the La-H distances of 2.70(3) and 2.66(4) Å in diagostic tetramethyldisilazido lanthanum compound $Me_2Si(C_5Me_4)_2LaN(SiHMe_2)_2$[19] and the corresponding solvent-free silyamide $La\{N(SiHMe_2)_2\}_3$[26] having La-H distance of 2.56(6) Å. The La-Si distances in $La\{C(SiHMe_2)_3\}_3$ range from 3.21–3.25 Å and are similar to the sum of La and Si covalent radii (3.18 Å)[27] and the distances in $Me_2Si(C_5Me_4)_2LaN(SiHMe_2)_2$[19] (3.244(1) and 3.246(1) Å). The La-Si distances in the β-SiC agostic $Cp^*La\{CH(SiMe_3)_2\}_2$ of 3.35(1) and 3.42(1) Å are significantly longer than in **1a**.[28] Additional structural evidence for a

multicenter interaction between La and the $C(SiHMe_2)_3$ ligands comes from La-C-Si angles, which are ≤90° for the $SiHMe_2$ groups with close La-H and La-Si contacts. These groups also have small La-C-Si-H torsion angles, which vary from 0.36–10.68°.

Distortions of the $–C(SiHMe_2)_3$ group accompany the multicenter La-$C(SiHMe_2)_3$ interaction. For example, the Si-H distances of groups involved in non-classical interactions with the La center are longer than those involved in 2-center-2-electron interactions. This analysis is subject to the limitation of X-ray crystallography mentioned above, which can be illustrated by comparison of Si-H distances across compounds **1a-d**, where the identity of the Ln center might be expected to have only a minor effect on the distances across the series. The average Si-H distance in those groups that point toward the Ln center is 1.47 ± 0.02 Å, whereas the classical Si-H distances show considerable variation 1.4 ± 0.1 Å (an order of magnitude larger than crystallographic E.S.D.s). For compound **1a** in particular, the two of the $C(SiHMe_2)_3$ groups show large differences between two center and multicenter SiH moieties. In the most extreme example, non-classical Si7-H7s and Si8-H8s distances 1.47(3) and 1.50(3) Å are notably longer than the classical Si9-H9s of 1.36(2) Å. However, it should be noted that Si4-H4s, Si5-H5s, and Si6-H6s are the same within error. Interestingly, the Si-C distances associated with non-classical La-H-Si structures are also generally shorter than those of classical $SiHMe_2$ groups. Across the **1a-d** series, the average Si-C distance of non-classical moieties is 1.828 ± 0.006 Å, whereas the average Si-C distance for non-bridging SiH groups is 1.849 ± 0.003 Å. In a selected $C(SiHMe_2)_3$ ligand in **1a** as a particular example, the C3-Si7 and C3-Si8 distances in bridging La-H-Si structures of 1.820(1) and 1.832(2) Å are shorter than the C3-Si9 distance in the non-bridged Si of 1.854(2) Å. Previously, structures of ytterbium(II) and calcium(II) neutral and cationic compounds containing the $C(SiHMe_2)_3$ ligand were characterized by single crystal X-ray

diffraction. In contrast to La{C(SiHMe$_2$)$_3$}$_3$, those compounds, such as Yb{C(SiHMe$_2$)$_3$}$_2$THF$_2$ and YbC(SiHMe$_2$)$_3$HB(C$_6$F$_5$)$_3$THF$_2$ do not give evidence for lengthened SiH bonds or shortened SiC bonds in non-classical moieties.[21] The neutron structure of β-CSi agostic Cp*La{CH(SiMe$_3$)$_2$}$_2$ shows statistically longer Si-C bonds involved in non-classical bonding,[28] and **1a-d** show different behavior as might be expected given the different role the Si-C group plays in the multicenter interaction.

The angles associated with the central carbon in the C(SiHMe$_2$)$_3$ ligands also highlight its distorted geometry. In general, acute or nearly acute ∠Ln-C-Si angles (average over **1a-d**: 88.8 ± 0.9°) are associated with the bridging Ln←H-Si structures, while angles associated with non-bridging Si are obtuse (average over **1a-d**: 124 ± 4°) and show greater variation. The average sum of the Si-C-Si angles around the central carbon in **1a-d** is 350 ± 2°. In most C(SiHMe$_2$)$_3$ ligands, there are two Si-C-Si angles that are ~120°, with the third angle ~110°. For example, the Si1-C1-Si2, Si1-C1-Si3, and Si2-C1-Si3 angles in **1a** are 110.0(1), 119.3(1), and 120.1(1)°, and in this example the smallest angle is associated with the Si involved in multicenter interactions with the La center. However, the pairing of the small angle with the two non-classical Si centers is not systematic across the **1a-d** series. Even in **1a**, the other two C(SiHMe$_2$)$_3$ ligands have wider angles associated (e.g. Si4-C2-Si5, 120.5(1)° where Si4 and Si5 are involved in La←H-Si bridging structure).

The Ln-C distances follow the trends expected on the basis of the ionic radii of the metal center (La > Ce > Pr > Nd), although comparison of adjacent Ln{C(SiHMe$_2$)$_3$}$_3$ shows that the shortest distance of the larger Ln is within 3σ of longest distance of the smaller Ln compound. For example, comparison of the shortest La–C and longest Ce–C distances (La1–C2, 2.679(2) vs Ce1–C2, 2.672(3) Å) or the statistical distribution of Ln-C distances (La–C, 2.687 ± 0.008; Ce–

C, 2.661 ± 0.009; Pr–C, 2.641 ± 0.008; Nd–C, 2.627 ± 0.004 Å) highlight the similarities and differences across series. Aside from the series $Ln(CH_2Ph)_3THF_3$ which has been crystallographically characterized for lanthanum - neodymium,[8c] generally few series of homoleptic monometallic lanthanide alkyls have been crystallographically characterized for comparison. The Ln–C bonds in the six-coordinate benzyl compounds are shorter than in $Ln\{C(SiHMe_2)_3\}_3$.[8a] $Ce\{CH(SiMe_3)_2\}_3$ is pyramidal and isomorphous with $La\{CH(SiMe_3)_2\}_3$,[29] and the Ce–C distance of 2.475(7) Å is much shorter than the distances in $Ce\{C(SiHMe_2)_3\}_3$ of 2.651(2), 2.659(2), 2.672(2) Å.

Interestingly, **1a-d** are all thermally robust, with $t_{1/2}$ approximately 80 h at 80 °C for decomposition to the alkane, $HC(SiHMe_2)_3$. The β-elimination product $Me_2Si{=}C(SiHMe_2)_2$ or its disilacyclobutane [2+2] dimer are not observed in ^{1}H NMR spectra of thermalized solutions of **1a-d**.

Reactions of $La\{C(SiHMe_2)_3\}_3$ and ancillary proligands, such as bis-1,1-(4,4-dimethyl-2-oxazolinyl)ethane (**$MeHC(Ox^{Me2})_2$**) and bis-1,1-(4,4-dimethyl-2-oxazolinyl)methylphenyl (**$PhHC(Ox^{Me2})_2$**) to give $\{MeC(Ox^{Me2})_2\}La\{C(SiHMe_2)_3\}_2$ (**2a**) and $\{Ph(Ox^{Me2})_2\}La\{C(SiHMe_2)_3\}_2$ (**3a**), respectively (eq. 3).

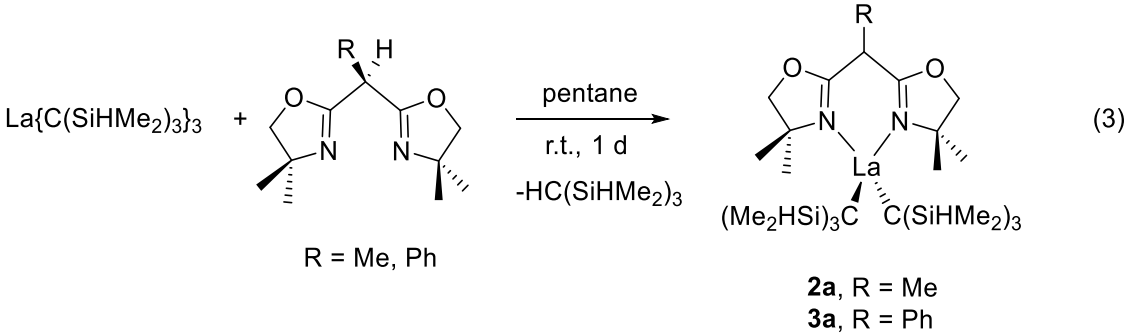

(3)

^{1}H NMR spectra of compounds **2a** and **3a** contained barely resolved multiplets at 4.60 ppm ($^1J_{SiH}$ = 163 Hz) and 4.65 ppm ($^1J_{SiH}$ = 143 Hz), respectively, assigned to the SiH groups.

The oxazolinyl methylene peaks were observed as singlets at 3.52 ppm (4 H) for **2a** and at 3.37 ppm (4 H) for **3a** while the oxazolinyl methyls were also observed as singlets at 1.30 ppm (12 H) and 1.35 ppm (12 H) for compounds **2a** and **3a**, respectively suggesting there is a mirror plane of symmetry. The IR spectrum of **2a** shows two stretching bands, one at 2113 cm^{-1} for classical SiH interaction and another broad band at 1872 cm^{-1} is poorly resolved from band at 1906 cm^{-1} for non-classical SiH interaction. The ν_{CN} stretching bands are observed as sharp peaks at 1588 and 1572 cm^{-1}. For **3a** these bands are observed at 2107, 1914 and 1876 cm^{-1} (ν_{SiH}) and a single broad band at 1564 cm^{-1} (ν_{CN}).

In addition, these homoleptic tris(alkyl) lanthanides may be starting materials for other rare earth compounds through protonolytic alkane elimination. For example compounds **1a-d** and 3 equiv. of tetramethyldisilazide react at room temperature to yield $Ln\{N(SiHMe_2)_2\}_3$ quantitatively in micromole-scale reactions. The tris(disilazido)lanthanoid compounds are readily isolated from the $HC(SiHMe_2)_3$ byproduct by extraction with hexamethyldisiloxane.

$$Ln\{C(SiHMe_2)_3\}_3 + HN(SiHMe_2)_2 \xrightarrow[\text{r.t., 1 h}]{\text{pentane}} Ln\{N(SiHMe_2)_2\}_3 + 3\ HC(SiHMe_2)_3 \qquad (4)$$

Ln = Ce (**4b**, 75%)
Nd (**4d**, 76%)

$$Pr\{C(SiHMe_2)_3\}_3 + HN(SiHMe_2)_2 \xrightarrow[60^oC,\ 4\ h]{\text{benzene}} Pr\{N(SiHMe_2)_2\}_3 + 3\ HC(SiHMe_2)_3 \qquad (5)$$

(**4c**, 71%)

$La\{N(SiHMe_2)_2\}_3$[28] and $Ce\{N(SiHMe_2)_2\}_3$[18b] have been previously prepared by reaction of $Ln\{N(SiMe_3)_2\}_3\}$ and $HN(SiHMe_2)_2$. $[La\{N(SiHMe_2)_2\}_3]_2$ (**4a**) crystallizes as a C_1-symmetric dimer, while the cerium analogue is not crystallographically characterized. The IR spectrum of $[Ce\{N(SiHMe_2)_2\}_3]_2$ (**4b**) contained bands at 2079 and 1915 cm^{-1} assigned to two-center-two-electron Si–H groups and three-center-two-electron bridging Ln←H-Si structures

which is similar to that reported for La analogue (2092, 1920 cm^{-1}) suggesting similar dimeric structures. $[Nd\{N(SiHMe_2)_2\}_3]_2$ (**4d**) was also synthesized in similar fashion and the IR stretching bands were observed at 2091 and 1922 cm^{-1}. However, the previously unknown $[Pr\{N(SiHMe_2)_2\}_3]_2$ (**4c**) was synthesized under more forcing conditions of 60 °C for 4 h in benzene. The infrared spectrum of compound **4c** contained absorption bands at 2121 and 1929 cm^{-1} similar to La analogue.

Conclusion

We have shown synthesis and characterization of new solvent-free, homoleptic rare earth alkyl compounds containing nine β-hydrogens which are nucleophilic in nature. These compounds do not undergo β-H elimination at elevated temperatures and rather decompose to the corresponding alkane. NMR and IR spectroscopy along with X-ray data gives us a good understanding of the molecular structure and bonding in these molecules. The variable temperature NMR studies have been performed on $La\{C(SiHMe_2)_3\}_3$ and $Y\{C(SiHMe_2)_3\}_3$ and their deuterated analogues which indicates exchange between Ln⇽H-Si and terminal Si-H on NMR timescale. The rate of exchange between three inequivalent methyls in the ligand was used to study the exchange rate. An inverse isotope effect k_H/k_D was found for both lanthanum and yttrium at low temperature. In addition, utility of $La\{C(SiHMe_2)_3\}_3$ is demonstrated by reactions with $HN(SiHMe_2)_2$ and $HBOx^{Me2}$ ligands, which are of value for synthesis of larger organometallic compounds.

Experimental Section

All manipulations were performed under a dry argon atmosphere using standard Schlenk techniques or under a nitrogen atmosphere in a glovebox unless otherwise indicated. Water and oxygen were removed from benzene and pentane solvents using an IT PureSolv system. Benzene-d_6 was heated to reflux over Na/K alloy and vacuum-transferred. The compounds $LaI_3(THF)_4$, $CeI_3(THF)_4$, $PrI_3(THF)_3$ and $NdI_3(THF)_3$ were modified from literature procedures,[30] $KC(SiHMe_2)_3$,[20] were prepared following literature procedures.

^1H, ^{11}B, $^{13}C\{^1H\}$, and $^{29}Si\{^1H\}$ NMR spectra were collected on a Bruker DRX-400 spectrometer, a Bruker Avance III-600 spectrometer, or an Agilent MR 400 spectrometer. ^{11}B NMR spectra were referenced to an external sample of $BF_3{\cdot}Et_2O$. Infrared spectra were measured on a Bruker Vertex 80. Elemental analyses were performed using a Perkin-Elmer 2400 Series II CHN/S. X-ray diffraction data was collected on a Bruker APEX II diffractometer.

$La\{C(SiHMe_2)_3\}_3$ (1a). $LaI_3(THF)_4$ (0.365 g, 0.452 mmol) and $KC(SiHMe_2)_3$ (0.310 g, 1.36 mmol) were stirred in 10 mL of benzene at room temperature for 1.5 h. Evaporation of the volatile materials, pentane extraction (3 × 5 mL), and evaporation of the pentane afforded a spectroscopically pure sticky yellow solid (0.269 g, 0.380 mmol, 84.0%). This solid was recrystallized at –30 °C from a minimal amount of pentane to obtain **1a** as colorless crystals. ^1H NMR (benzene-d_6, 600 MHz, 25 °C): δ 4.26 (m, $^1J_{SiH}$ = 138.7 Hz, 9 H, SiH), 0.41 (d, $^3J_{HH}$ = 3.2 Hz, 54 H, $SiMe_2$). ^1H NMR (toluene-d_8, 600 MHz, –94 °C): δ 4.78 (m, 3 H, SiH), 4.04 (6 H, La←*H*$SiMe_2$), 0.55 (br, 18 H, La←HSi*Me*$_2$), 0.49 (br, 18 H, La←HSi*Me*$_2$), 0.42 (br, 18 H, $SiMe_2$). $^{13}C\{^1H\}$ NMR (benzene-d_6, 150 MHz, 25 °C): δ 31.8 (LaC), 3.64 ($SiMe_2$). $^{13}C\{^1H\}$

NMR (toluene-d_8, 150 MHz, –94 °C): δ 30.00 (LaC), 4.31 ($SiHMe_2$), 3.29 (La←$HSiMe_2$), 2.14 (La←$HSiMe_2$). $^{29}Si\{^1H\}$ NMR (benzene-d_6, 119 MHz, 25 °C): δ –13.1. $^{29}Si\{^1H\}$ NMR (toluene-d_8, 119 MHz, –94 °C): δ –9.3 ($^1J_{SiH}$ = 110 Hz, La←$HSiMe_2$), –18.5 ($^1J_{SiH}$ = 185 Hz, $SiHMe_2$). IR (KBr, cm^{-1}): 2953 s, 2900 m, 2108 s (ν_{SiH}), 1829 s br (ν_{SiH}), 1590 w, 1415 w, 1254 s, 1025 s br, 889 s br, 835 s, 777 s, 689 s. Anal. Calcd for $C_{21}H_{63}Si_9La$: C, 35.66; H, 8.98. Found: C, 36.56; H, 9.24. Mp, 114-117 °C.

$La\{C(SiDMe_2)_3\}_3$ (1a-d_9). $LaI_3(THF)_4$ (0.209 g, 0.259 mmol) and $KC(SiDMe_2)_3$ (0.180 g, 0.777 mmol) were stirred in 10 mL of benzene room temperature for 1.5 h. The product was isolated as a pale yellow solid following the procedure for **1a** described above (0.171 g, 0.238 mmol, 92.8%). ^1H NMR (benzene, 600 MHz, 25 °C): δ 0.41 (s, $SiMe_2$). ^2H NMR (benzene, 600 MHz, 25 °C): δ 3.4 (s, Si*D*Me_2). $^{13}C\{^1H\}$ NMR (benzene, 150 MHz, 25 °C): δ 2.98 ($SiMe_2$). $^{13}C\{^1H\}$ NMR (toluene-d_8, 150 MHz, –94 °C): δ 4.31, 3.31, 2.12 ($SiMe_2$). ^{29}Si NMR (benzene, 119.3 MHz, 25 °C): δ –13.7. IR (KBr, cm^{-1}): 2981 m, 2954 s, 2899 s, 1515 s br, (ν_{SiD}), 1414 w, 1327 s (ν_{SiD}), 1252 s, 1014 w, s, 938 s, 894 s, 855 m, 834 s br, 812 s, 778 s, 756 br, 704 s, 648 w, 583 s.

$Ce\{C(SiHMe_2)_3\}_3$ (1b). $CeI_3(THF)_4$ (0.362 g, 0.449 mmol) and $KC(SiHMe_2)_3$ (0.307 g, 1.34 mmol) were stirred in benzene (10 mL) at room temperature for 12 h. The $Ce\{C(SiHMe_2)_3\}_3$ product was isolated following the procedure for **1a** described above as spectroscopically pure material (0.251 g, 0.354 mmol, 79.2%). This solid was recrystallized at –30 °C from a minimal amount of pentane to obtain colorless crystals of **1b**. ^1H NMR (benzene-d_6, 600 MHz, 25 °C): δ 5.0 (br, 9 H, SiH), 1.0 (br, 54 H, $SiMe_2$). ^1H NMR (toluene-d_8, 600 MHz, –76 °C): δ 24.5 (3 H,

br, SiH), 10.6 (s, 18 H, $SiMe_2$), 9.3 (s, 18 H, $SiMe_2$), –11.6 (s, 18 H, $SiMe_2$), –19.7 (6 H, br, Ce←*H*$SiMe_2$). $^{13}C\{^1H\}$ NMR (benzene-d_6, 150 MHz, 25 °C): δ 11.85 ($SiMe_2$). $^{13}C\{^1H\}$ NMR (toluene-d_8, 150 MHz, –73 °C): δ 36, 33, –4 ($SiMe_2$). IR (KBr, cm^{-1}): 2952 s, 2899 s, 2107 s (ν_{SiH}), 1829 s br (ν_{SiH}), 1590 w, 1493 s, 1417 w, 1253 s, 1026 s br, 951 s br, 885 s, 834 w, 777 s, 679 s. Anal. Calcd. for $C_{21}H_{63}Si_9Ce$: C, 35.59; H, 8.96. Found: C, 35.44; H, 9.26. Mp, 117-121 °C.

Ce{C(SiDMe$_2$)$_3$}$_3$ (1b-*d*$_9$). $CeI_3(THF)_4$ (0.183 g, 0.226 mmol) and $KC(SiDMe_2)_3$ (0.157 g, 0.678 mmol) were stirred in benzene (10 mL) at room temperature for 12 h. The product was isolated following the procedure for **1a** described above (0.143 g, 0.199 mmol, 88.2%). ^1H NMR (benzene, 600 MHz, 25 °C): δ 0.66 (br, $SiMe_2$). ^2H NMR (benzene, 600 MHz, 25 °C): δ 3.98 (s, Si*D*Me_2). $^{13}C\{^1H\}$ NMR (benzene-d_6, 150 MHz, 25 °C): δ 11.29 ($SiMe_2$). $^{13}C\{^1H\}$ NMR (toluene-d_8, 150 MHz, –73 °C): δ 36, 33, –4 ($SiMe_2$). IR (KBr, cm^{-1}): 2953 s, 2897 s, 2798 s, 1530 s (ν_{SiD}), 1406 s, 1326 s (ν_{SiD}), 1250 s, 1191 s, 1021 s, 936 br, 897 br, 779 s.

Pr{C(SiHMe$_2$)$_3$}$_3$ (1c). $PrI_3(THF)_3$ (0.162 g, 0.220 mmol) and $KC(SiHMe_2)_3$ (0.173 g, 0.760 mmol) were stirred in benzene (10 mL) at room temperature for 12 h. The product was isolated as spectroscopically pure material (0.146 g, 0.206 mmol, 93.7%) following the procedure for **1a** described above. This material was recrystallized at –30 °C from a minimal amount of toluene to obtain **1c** as yellow-green X-ray quality crystals. ^1H NMR (benzene-d_6, 600 MHz, 25 °C): δ 12 (br, 9 H, SiH), 2.2 (br, 54 H, $SiMe_2$). ^1H NMR (toluene-d_8, 600 MHz, –74 °C): δ –47 (br, SiH), 20.7 (s, $SiMe_2$), 19.9 (s, $SiMe_2$), –24.9 (s, $SiMe_2$). IR (KBr, cm^{-1}): 2954 s, 2899 s, 2108 s (ν_{SiH}),

1830 s br (ν_{SiH}), 1509 w, 1464 s, 1253 s, 1029 s br, 953 s br, 911 s, 887 w, 835 s, 679 s. Anal. Calcd. for $C_{21}H_{63}Si_9Pr$: C, 35.55; H, 8.95. Found: C, 35.43; H, 8.83. Mp, 115-118 °C.

Pr{C(SiDMe$_2$)$_3$}$_3$ (1c-*d*$_9$). $PrI_3(THF)_3$ (0.116 g , 0.157 mmol) and $KC(SiDMe_2)_3$ (0.126 g, 0.544 mmol) were stirred in benzene (10 mL) at room temperature for 12 h. The yellow product (0.091 g, 0.127 mmol, 68.8%) was isolated following the procedure describe above for **1a**. ^{1}H NMR (benzene, 600 MHz, 25 °C): δ 2.1 (br, $SiMe_2$). ^{1}H NMR (benzene-d_6, 600 MHz, 25 °C): δ 2.0 (br, $SiMe_2$). ^{1}H NMR (toluene-d_8, 600 MHz, –74 °C): δ 20.5 (s, $SiMe_2$), 19.8 (s, $SiMe_2$), –25.1 (s, $SiMe_2$). IR (KBr, cm^{-1}): 2953 s, 2898 s, 1529 s (ν_{SiD}), 1409 s, 1329 s (ν_{SiD}), 1251 s, 937 br, 897 br, 832 s, 779 s, 707 s.

Nd{C(SiHMe$_2$)$_3$}$_3$ (1d). $NdI_3(THF)_3$ (0.204 g, 0.275 mmol) and $KC(SiHMe_2)_3$ (0.189 g, 0.827 mmol) were stirred in benzene (10 mL) at room temperature for 12 h. The spectroscopically pure product (0.176 g, 0.247 mmol, 89.7%) was isolated following the procedure for **1a** described above. This solid was recrystallized at –30 °C from a minimal amount of pentane to obtain **1d** as blue-green crystals. ^{1}H NMR (benzene-d_6, 600 MHz, 25 °C): δ 27.8 (br, SiH), 1.78 (br, $SiMe_2$). IR (KBr, cm^{-1}): 2954 s, 2900 s, 2108 s (ν_{SiH}), 1829 s br (ν_{SiH}), 1418 w, 1253 s, 1192 s br, 1058 br, 952 s br, 886 s, 835 w, 778 s, 689 s. Anal. Calcd. for $C_{21}H_{63}Si_9Nd$: C, 35.39; H, 8.91. Found: C, 35.48; H, 9.11. Mp, 119-122 °C.

Nd{C(SiDMe$_2$)$_3$}$_3$ (1d-*d*$_9$). $NdI_3(THF)_3$ (0.183 g, 0.248 mmol) and $KC(SiDMe_2)_3$ (0.172 g, 0.743 mmol) were stirred in benzene (10 mL) at room temperature for 12 h. The yellow solid product (0.165 g, 0.229 mmol, 92.2%) was isolated following the prodedure for **1a**. ^{1}H NMR (benzene,

600 MHz, 25 °C): δ 1.7 (br, $SiMe_2$). ^{1}H NMR (toluene-d_8, 600 MHz, –79 °C): δ 15.4 (s, $SiMe_2$), 14.6 (s, $SiMe_2$), –17.5 (s, $SiMe_2$). IR (KBr, cm^{-1}): 2953 s, 2898 s, 2798 s, 1528 s (ν_{SiD}), 1467 s, 1408 s, 1328 s (ν_{SiD}), 1251 s, 1155 s, 939 br, 898 br, 833 s, 812 s, 779 s.

{MeC(Ox^{Me2})$_2$}La{C(SiHMe$_2$)$_3$}$_2$ (2a). La{C($SiHMe_2$)$_3$}$_3$ (0.609 g, 0.861 mmol) and MeHC(Ox^{Me2})$_2$ (0.193 g, 0.861 mmol) were stirred in pentane (5 mL) at 25 °C for 12 h. The volatile materials were evaporated, and the residue was extracted with hexamethyldisiloxane (3 × 5 mL). Evaporation of the hexamethyldisiloxane afforded {Box^{Me2}}La{C($SiHMe_2$)$_3$}$_2$ (0.462 g, 0.622 mmol, 72.3 %) in good yield as a sticky solid. ^{1}H NMR (benzene-d_6, 600 MHz, 25 °C): δ 4.60 (m, 6 H, SiH), 3.51 (s, 4 H, CNCMe$_2$C*H*$_2$O), 2.40 (s, 3 H, *Me*C), 1.30 (s, 12 H, CNC*Me*$_2$CH$_2$O), 0.42 (d, 36 H, $SiMe_2$). ^{13}C{^{1}H} NMR (benzene-d_6, 150 MHz, 25 °C): δ 171.3 (*C*NCMe$_2$CH$_2$O), 78.2 (CNC*Me*$_2$CH$_2$O), 66.3 (CNCMe$_2$*C*H$_2$O), 28.0 (CN*C*Me$_2$CH$_2$O), 13.6 (*Me*C), 3.2 ($SiMe_2$). ^{1}H–^{29}Si HMBC NMR (benzene-d_6, 119.3 MHz, 25 °C): δ –17.7 ($SiHMe_2$). ^{15}N{^{1}H} NMR (benzene-d_6, 61 MHz, 25 °C): δ –165.9 (CNCMe$_2$*C*H$_2$O). IR (KBr, cm^{-1}): 2960 s, 2895 s, 2112 s (ν_{SiH}), 1872 s br (ν_{SiH}), 1588 s (ν_{CN}), 1572 s (ν_{CN}), 1498 s, 1446 w, 1365 s, 1293 s, 1250 s, 1189 s, 1150 s, 1073 s br, 1024 s br, 943 s br, 895 br, 834 w, 768 s, 741 s, 700 s, 678 s, 635 s, 568 s. Anal. Calcd for $C_{26}H_{62}LaN_2O_2Si_6$: C, 42.08; H, 8.42; N, 3.77. Found: C, 41.98; H, 8.38; N, 3.65. Mp, 110-112 °C.

{PhC(Ox^{Me2})$_2$}La{C(SiHMe$_2$)$_3$}$_2$ (3a). La{C($SiHMe_2$)$_3$}$_3$ (0.124 g, 0.176 mmol) and PhHC(Ox^{Me2})$_2$ (0.050 g, 0.176 mmol) were stirred in pentane (2 mL) at 25 °C for 12 h. The product {PhBox^{Me2}}La{C($SiHMe_2$)$_3$}$_2$ (0.105 g, 0.131 mmol, 74.2 %) was isolated following the

procedure for **2a** as a sticky yellow solid. ^{1}H NMR (benzene-d_6, 600 MHz, 25 °C): δ 7.76 (d, 2 H, *ortho*-C_6H_5), 7.36 (m, 3 H, *para*- and *meta*-C_6H_5), 4.65 (m, 6 H, SiH), 3.37 (s, 4 H, $CNCMe_2CH_2O$), 1.35 (s, 12 H, $CNCMe_2CH_2O$), 0.44 (d, 36 H, $SiMe_2$). $^{13}C\{^{1}H\}$ NMR (benzene-d_6, 150 MHz, 25 °C): δ 171.4 ($CNCMe_2CH_2O$), 139.0 (C_6H_5), 133.7 (C_6H_5), 126.2 (C_6H_5), 78.1 ($CNCMe_2CH_2O$), 66.1 ($CNCMe_2CH_2O$), 27.9 ($CNCMe_2CH_2O$), 3.3 ($SiMe_2$). ^{1}H-^{29}Si HMBC NMR (benzene-d_6, 119.3 MHz, 25 °C): δ –17.2 ($SiHMe_2$). $^{15}N\{^{1}H\}$ NMR (benzene-d_6, 61 MHz, 25 °C): δ –168.1 ($CNCMe_2CH_2O$). IR (KBr, cm^{-1}): 2964 s, 2896 s, 2107 s (ν_{SiH}), 1914 (ν_{SiH}), 1876 s br (ν_{SiH}), 1564 s (ν_{CN}), 1478 s, 1436 w, 1376 s, 1299 s, 1251 s, 1187 s, 1165 s, 1044 s br, 943 s br, 919 s br, 897 br, 836 w, 809 s, 775 s, 757 s, 700 s, 679 s, 657 s. Anal. Calcd for $C_{26}H_{62}LaN_2O_2Si_6$: C, 46.29; H, 8.02; N, 3.48. Found: C, 42.20; H, 8.08; N, 3.35. Mp, 109-111 °C.

$Ce\{N(SiHMe_2)_2\}_3$ (4b). $Ce\{C(SiHMe_2)_3\}_3$ (0.094 g, 0.132 mmol) and $HN(SiHMe_2)_2$ (0.053 g, 0.397 mmol) were stirred in pentane (3 mL) at room temperature for 1 h. The volatile materials were evaporated, the residue was extracted with hexamethyldisiloxane (2 × 3 mL). Evaporation of the hexamethyldisiloxane afforded analytically pure $Ce\{N(SiHMe_2)_2\}_3$ as a sticky yellow solid (0.053 g, 0.099 mmol, 75.3%). ^{1}H NMR (toluene-d_8, 600 MHz, 25 °C): δ 2.78 (br, $SiMe_2$). IR (KBr, cm^{-1}): 2955 s, 2898 m, 2854 w, 2079 s br (ν_{SiH}), 1915 s br (ν_{SiH}), 1514 w, 1416 w, 1250 s, 1041 s br, 974 s br, 893 s, 837 s, 788 s, 764 s, 686 s, 626 m, 593 m. Anal. Calcd. for $C_{12}H_{42}Si_6N_3Ce$: C, 26.83; H, 7.88; N, 7.82. Found: C, 26.76; H, 7.56; N, 7.42. Mp, 125-128 °C.

$Pr\{N(SiHMe_2)_2\}_3$ (4c). $Pr\{C(SiHMe_2)_3\}_3$ (0.042 g, 0.058 mmol) and $HN(SiHMe_2)_2$ (0.023 g, 0.173 mmol) were heated in benzene (2 mL) at 60 °C for 4 h. The volatile materials were

evaporated, the residue was extracted with hexamethyldisiloxane (2 × 2 mL), and evaporation of the hexamethyldisiloxane afforded analytically pure $Pr\{N(SiHMe_2)_2\}_3$ as a sticky yellow-green solid (0.022 g, 0.041 mmol, 70.7%). ^{1}H NMR (benzene-d_6, 600 MHz, 25 °C): δ 2.81 (br, $SiMe_2$), 2.57 (br, $SiMe_2$). IR (KBr, cm^{-1}): 2957 s, 2900 m, 2121 s br (ν_{SiH}), 1929 s br (ν_{SiH}), 1456 w, 1417 w, 1377 w, 1251 s, 1177 m br, 1045 s br, 894 s, 837 s, 788 s, 763 s, 689 s, 627 m, 593 m. Anal. Calcd. for $C_{12}H_{42}Si_6N_3Pr$: C, 26.79; H, 7.87; N, 7.81. Found: C, 26.61; H, 7.82; N, 7.75.

$Nd\{N(SiHMe_2)_2\}_3$ (4d). $Nd\{C(SiHMe_2)_3\}_3$ (0.121 g, 0.168 mmol) and $HN(SiHMe_2)_2$ (0.067 g, 0.504 mmol) were stirred in pentane (3 mL) at room temperature for 1 h. Workup following the procedure for **2a** afforded analytically pure $Nd\{N(SiHMe_2)_2\}_3$ as a sticky blue solid (0.069 g, 0.127 mmol, 75.6 %). ^{1}H NMR (toluene-d_8, 600 MHz, 25 °C): δ 5.86 (br, $SiMe_2$), 5.10 (br, SiH), 1.00 (br, SiH). IR (KBr, cm^{-1}): 2954 s, 2899 m, 2855 w, 2091 s br (ν_{SiH}), 1922 s br (ν_{SiH}), 1416 w, 1250 s, 1177 m, 1046 s br, 895 s, 837 s, 798 s, 764 s, 688 s, 628 m, 596 m. Anal. Calcd. for $C_{12}H_{42}Si_6N_3Nd$: C, 26.63; H, 7.82; N, 7.76. Found: C, 26.71; H, 7.57; N, 7.67. Mp, 123-125 °C.

References

[1] a) U. Zucchini, Albizzat.E and U. Giannini, *Journal of Organometallic Chemistry* **1971**, *26*, 357-&; b) W. Kruse, *Journal of Organometallic Chemistry* **1972**, *42*, C39; c) A. J. Shortland and G. Wilkinson, *Journal of the Chemical Society, Dalton Transactions* **1973**, 872-876; d) K. Mertis and G. Wilkinson, *Journal of the Chemical Society, Dalton Transactions* **1976**, 1488-1492; e) A. L. Wayda and W. J. Evans, *Journal of the American Chemical Society* **1978**, *100*, 7119-7121; f) W. G. Van der Sluys, C. J. Burns and A. P. Sattelberger, *Organometallics* **1989**, *8*, 855-857; g)

P. M. Morse and G. S. Girolami, *Journal of the American Chemical Society* **1989**, *111*, 4114-4116; h) S. Kleinhenz, V. Pfennig and K. Seppelt, *Chemistry-a European Journal* **1998**, *4*, 1687-1691; i) F. T. Edelmann, D. M. M. Freckmann and H. Schumann, *Chemical Reviews* **2002**, *102*, 1851-1896; j) A. Tsuboyama, H. Iwawaki, M. Furugori, T. Mukaide, J. Kamatani, S. Igawa, T. Moriyama, S. Miura, T. Takiguchi, S. Okada, M. Hoshino and K. Ueno, *Journal of the American Chemical Society* **2003**, *125*, 12971-12979; k) S. Fortier, B. C. Melot, G. Wu and T. W. Hayton, *Journal of the American Chemical Society* **2009**, *131*, 15512-15521; l) M. Zimmermann and R. Anwander, *Chemical Reviews* **2010**, *110*, 6194-6259.

[2] a) A. M. Kawaoka, M. R. Douglass and T. J. Marks, *Organometallics* **2003**, *22*, 4630-4632; b) T. J. Woodman, Y. Sarazin, S. Garratt, G. Fink and M. Bochmann, *Journal of Molecular Catalysis A: Chemical* **2005**, *235*, 88-97.

[3] a) F. Quignard, A. Choplin and J. M. Basset, *Journal of the Chemical Society-Chemical Communications* **1991**, 1589-1590; b) F. Quignard, C. Lecuyer, C. Bougault, F. Lefebvre, A. Choplin, D. Olivier and J. M. Basset, *Inorganic Chemistry* **1992**, *31*, 928-930; c) J. A. N. Ajjou and S. L. Scott, *Organometallics* **1997**, *16*, 86-92; d) C. Coperet, M. Chabanas, R. P. Saint-Arroman and J. M. Basset, *Angewandte Chemie-International Edition* **2003**, *42*, 156-181.

[4] a) A. H. Cowley, B. L. Benac, J. G. Ekerdt, R. A. Jones, K. B. Kidd, J. Y. Lee and J. E. Miller, *Journal of the American Chemical Society* **1988**, *110*, 6248-6249; b) G. S. Sandhu and P. Fazan in *Chemical vapor deposition using organometallic precursors*, *Vol.* Google Patents, **2001**; c) M. Putkonen and L. Niinistö in *Organometallic Precursors for Atomic Layer Deposition*, (Ed. R. A. Fischer), Springer Berlin Heidelberg, Berlin, Heidelberg, **2005**, pp. 125-145.

[5] a) K. C. Hultzsch, T. P. Spaniol and J. Okuda, *Angewandte Chemie International Edition* **1999**, *38*, 227-230; b) L. Zhang, T. Suzuki, Y. Luo, M. Nishiura and Z. Hou, *Angewandte Chemie International Edition* **2007**, *46*, 1909-1913; c) B. Wang, D. Cui and K. Lv, *Macromolecules* **2008**, *41*, 1983-1988; d) S. Li, D. Cui, D. Li and Z. Hou, *Organometallics* **2009**, *28*, 4814-4822; e) B. Wang, T. Tang, Y. Li and D. Cui, *Dalton Transactions* **2009**, 8963-8969; f) M. Nishiura and Z. Hou, *Nat Chem* **2010**, *2*, 257-268; g) X. Xu, Y. Chen, J. Feng, G. Zou and J. Sun, *Organometallics* **2010**, *29*, 549-553; h) I. Aillaud, C. Olier, Y. Chapurina, J. Collin, E. Schulz, R. Guillot, J. Hannedouche and A. Trifonov, *Organometallics* **2011**, *30*, 3378-3385; i) Y. Pan, T. Xu, Y.-S. Ge and X.-B. Lu, *Organometallics* **2011**, *30*, 5687-5694; j) S. Long, B. Wang, H. Xie, C. Yao, C. Wu and D. Cui, *New Journal of Chemistry* **2015**, *39*, 7682-7687.

[6] a) M. F. Lappert and R. Pearce, *Journal of the Chemical Society-Chemical Communications* **1973**, 126-126; b) J. L. Atwood, W. E. Hunter, R. D. Rogers, J. Holton, J. Mcmeeking, R. Pearce and M. F. Lappert, *Journal of the Chemical Society-Chemical Communications* **1978**, 140-142; c) H. Schumann, D. M. M. Freckmann and S. Dechert, *Zeitschrift Fur Anorganische Und Allgemeine Chemie* **2002**, *628*, 2422-2426.

[7] P. B. Hitchcock, M. F. Lappert, R. G. Smith, R. A. Bartlett and P. P. Power, *Journal of the Chemical Society-Chemical Communications* **1988**, 1007-1009.

[8] a) S. Bambirra, A. Meetsma and B. Hessen, *Organometallics* **2006**, *25*, 3454-3462; b) S. Bambirra, D. van Leusen, C. G. J. Tazelaar, A. Meetsma and B. Hessen, *Organometallics* **2007**, *26*, 1014-1023; c) A. J. Wooles, D. P. Mills, W. Lewis, A. J. Blake and S. T. Liddle, *Dalton Transactions* **2010**, *39*, 500-510; d) W. Huang, B. M. Upton, S. I. Khan and P. L. Diaconescu, *Organometallics* **2013**, *32*, 1379-1386.

[9] A. C. Behrle and J. A. R. Schmidt, *Organometallics* **2011**, *30*, 3915-3918.

[10] S. Harder, *Organometallics* **2005**, *24*, 373-379.

[11] C. Eaborn, P. B. Hitchcock, K. Izod and J. D. Smith, *Journal of the American Chemical Society* **1994**, *116*, 12071-12072.

[12] a) H. Schumann, J. Muller, N. Bruncks, H. Lauke, J. Pickardt, H. Schwarz and K. Eckart, *Organometallics* **1984**, *3*, 69-74; b) H. Schumann, W. Genthe, E. Hahn, J. Pickardt, H. Schwarz and K. Eckart, *Journal of Organometallic Chemistry* **1986**, *306*, 215-225; c) W. Noh and G. S. Girolami, *Polyhedron* **2007**, *26*, 3865-3870.

[13] W. J. Evans, J. H. Meadows, A. L. Wayda, W. E. Hunter and J. L. Atwood, *Journal of the American Chemical Society* **1982**, *104*, 2015-2017.

[14] R. Kempe, *Chemistry – A European Journal* **2007**, *13*, 2764-2773.

[15] B. J. Burger, M. E. Thompson, W. D. Cotter and J. E. Bercaw, *Journal of the American Chemical Society* **1990**, *112*, 1566-1577.

[16] W. Scherer and G. S. McGrady, *Angewandte Chemie International Edition* **2004**, *43*, 1782-1806.

[17] W. S. Rees, O. Just, H. Schumann and R. Weimann, *Angewandte Chemie-International Edition in English* **1996**, *35*, 419-422.

[18] a) R. Anwander, O. Runte, J. Eppinger, G. Gerstberger, E. Herdtweck and M. Spiegler, *Journal of the Chemical Society-Dalton Transactions* **1998**, 847-858; b) A. R. Crozier, A. M. Bienfait, C. Maichle-Mossmer, K. W. Tornroos and R. Anwander, *Chem Commun (Camb)* **2013**, *49*, 87-89; c) A. M. Bienfait, C. Schadle, C. Maichle-Mossmer, K. W. Tornroos and R. Anwander, *Dalton Trans* **2014**, *43*, 17324-17332.

[19] J. Eppinger, M. Spiegler, W. Hieringer, W. A. Herrmann and R. Anwander, *Journal of the American Chemical Society* **2000**, *122*, 3080-3096.

[20] M. Brookhart and M. L. H. Green, *Journal of Organometallic Chemistry* **1983**, *250*, 395-408.

[21] K. Yan, A. V. Pawlikowski, C. Ebert and A. D. Sadow, *Chem Commun (Camb)* **2009**, 656-658.

[22] K. Yan, B. M. Upton, A. Ellern and A. D. Sadow, *Journal of the American Chemical Society* **2009**, *131*, 15110-15111.

[23] R. D. Shannon, *Acta Crystallographica* **1976**, *A32*, 751-767.

[24] K. Yan, G. Schoendorff, B. M. Upton, A. Ellern, T. L. Windus and A. D. Sadow, *Organometallics* **2013**, *32*, 1300-1316.

[25] a) D. Bravo-Zhivotovskii, G. Korogodsky and Y. Apeloig, *Journal of Organometallic Chemistry* **2003**, *686*, 58-65; b) D. Bravo-Zhivotovskii, R. Dobrovetsky, D. Nemirovsky, V. Molev, M. Bendikov, G. Molev, M. Botoshansky and Y. Apeloig, *Angewandte Chemie* **2008**, *120*, 4415-4417.

[26] *iNMR (http://www.inmr.net)*

[27] D. C. Bradley, J. S. Ghotra and F. A. Hart, *Journal of the Chemical Society, Dalton Transactions* **1973**, 1021-1023.

[28] H. F. Yuen and T. J. Marks, *Organometallics* **2008**, *27*, 155-158.

[29] W. T. Klooster, L. Brammer, C. J. Schaverien and P. H. M. Budzelaar, *Journal of the American Chemical Society* **1999**, *121*, 1381-1382.

[30] A. G. Avent, C. F. Caro, P. B. Hitchcock, M. F. Lappert, Z. N. Li and X. H. Wei, *Dalton Transactions* **2004**, 1567-1577.

[31] a) P. N. Hazin, J. C. Huffman and J. W. Bruno, *Organometallics* **1987**, *6*, 23-27; b) G. B. Deacon, T. C. Feng, P. C. Junk, G. Meyer, N. M. Scott, B. W. Skelton and A. H. White, *Australian Journal of Chemistry* **2000**, *53*, 853-865.

CHAPTER 3: HYDROSILYLATION OF α,β-UNSATURATED ESTERS TO α-SILYL ESTERS BY LANTHANIDE ALKYL HYDRIDOBORATES

Modified from a paper to be submitted to *ACS Catalysis*

Aradhana Pindwal, Smita Patnaik, KaKing Yan, Arkady Ellern, Aaron D. Sadow*

Abstract

Reactions of $Ln\{C(SiHMe_2)_3\}_3$ with one or two equiv. of $B(C_6F_5)_3$ afford zwitterionic bis(alkyl)lanthanide compounds $Ln\{C(SiHMe_2)_3\}_2HB(C_6F_5)_3$ (Ln = La (**1a**), Ce (**1b**), Pr (**1c**), Nd (**1d**)) or $LnC(SiHMe_2)_3\{HB(C_6F_5)_3\}_2$ (Ln = La (**2a**), Ce (**2b**), Pr (**2c**), Nd (**2d**)), respectively, via β-hydrogen abstraction. The isolated products **1a-d** have been spectroscopically studied exhibiting the presence of two non-classical Ln⇽H-Si interactions per alkyl ligand. Single crystal X-ray diffraction studies of **1b** and **2d** are presented which reveal the non-classical, 3-center-2-electron bonding with the two non-classical SiH's of one $C(SiHMe_2)_3$ ligand facing the classical SiH of the next ligand. Surprisingly, IR bands assigned to non-classical interactions from 1700-2000 cm^{-1} were not observed in **2a-d**, suggesting lack of 3-center-2-electron bonding, but it also does not rule out the multi-center bonding. Compounds **1a-d** have been employed in the catalytic hydrosilylation of α,β-unsaturated esters at room temperature to give, almost instantaneously synthetically valuable α-silyl esters as the sole product in high yields with a turnover number of 2200. These catalytic transformations are selective for secondary silanes

while primary silanes do not react and tertiary silanes yields silyl ketene acetals as the catalytic product. The route to synthesis of α-silyl esters does not involve a retro-Brook rearrangement.

Introduction

Catalytic hydrosilylation is an important method for reducing unsaturated C=C, C=O and C=N functional groups and for generating silicon-containing compounds which are useful in medicinal, polymer and materials chemistry.[1] For example, the sequence of hydrosilylation, followed by oxidation is a valuable route to alcohols, and cross-coupling of silanes is a useful method for C-C bond formation,[2] and the silyl group can also be retained as a protecting group, which is important in organic synthesis. Tamao-Fleming oxidation utilizes silanes bearing a phenyl group to provide a hydroxyl group with retention in configuration while Hiyama-Denmark coupling requires silanols and siloxanes for Pd-catalyzed C-C bond formation. Transition-metal,[3] main group metal,[4] organolanthanides,[5] and Lewis acids[6] have been employed in the reduction of olefins, alkynes, and many carbonyl compounds via hydrosilylation process. However, the literature and commercial processes for hydrosilylation of carbonyl compounds have traditionally been dominated by late transition metal-based catalysts, while the oxophilicity of early transition metals, group 1 and 2 main group metals, and f-elements have excluded these elements from application in such catalysis. Metal-oxygen containing species are intermediates in many proposed metal-mediated mechanisms, and this strong polar bond is typically unreactive toward silanes. In a rare example, group 2 metal complex, [{Me-Nacnac^{Dipp}}CaH.THF]$_2$ (Me-Nacnac^{Dipp} = (2,6-*i*(C_3H_7)$_2$$C_6H_3$)NCMe)$_2$CH) catalyzed 1,2-hydrosilylation of ketones via- a hypervalent six-coordinate silicon atom.[7]

Late-transition-metal catalyzed hydrosilylation of α,β-unsaturated esters by tertiary silanes could generate four possible products, namely, α- and β-adducts resulting from 1,2-addition to the C=C bond or adducts from 1,2- and 1,4-addition across the C=O bond (Scheme 1).

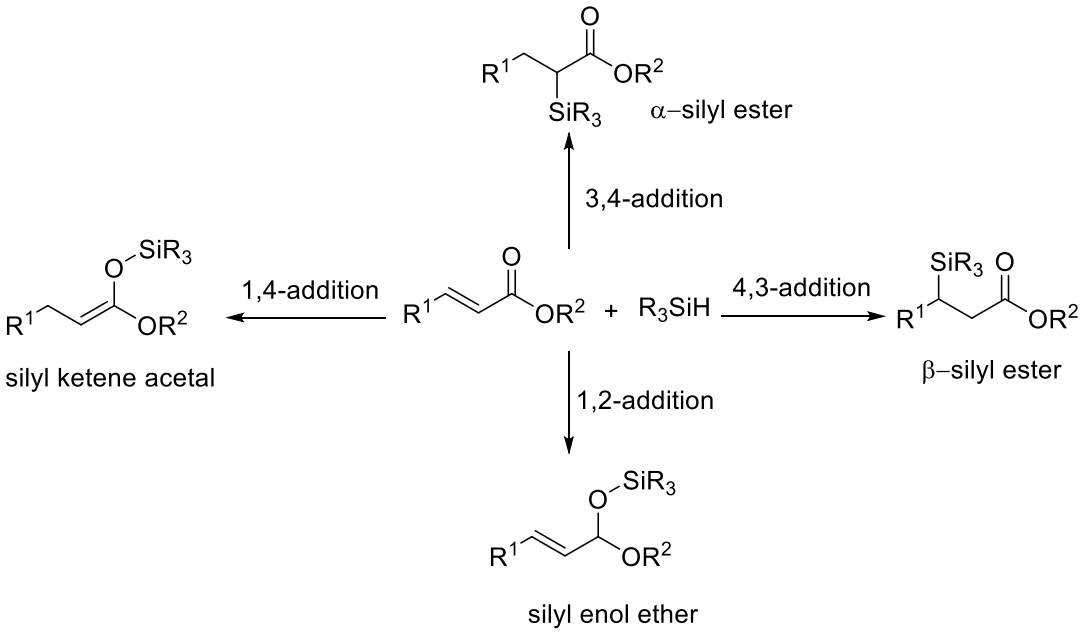

Scheme 1. Possible products for hydrosilylation of α,β-unsaturated esters with tertiary silanes.

Controlling the products in these types of catalytic reactions is challenging, with most examples giving mixtures, and α-silyl esters are difficult to access selectively. For example, the $Co_2(CO)_8$-catalyzed hydrosilylation of acrylates by tertiary silanes forms a mixture of silane products that include α- and β-adducts and silyl ketene acetals resulting from the 1,4-addition pathway.[8] On the other hand, H_2PtCl_6 catalyzes hydrosilylation of methacrylates with tertiary hydrosilanes to yield β-adducts.[9] Hydrosilylation of methyl methacrylate by Et_3SiH catalyzed by rhodium complexes yields product of the 1,4-O-silylation, which is accompanied by the β-adduct.[10]

These selectivity challenges may be addressed by new reaction pathways. Recently, $B(C_6F_5)_3$ was discovered to catalyze the addition of α,β-unsaturated esters and tertiary silanes,

giving silyl ketene acetals that isomerize to α-silyl esters through a $B(C_6F_5)_3$-catalyzed retro-Brook rearrangement.[11] This system is, however, best with substituted esters, and acrylates and methacrylates conversions are not reported. Alternatively, we observed that a zwitterionic magnesium hydridoborate complex affords silyl ketene acetals, without subsequent rearrangement.[12] The key to this transformation is hypothesized to be the zwitterionic structure of the $To^MMg[HB(C_6F_5)_3]$ (To^M = tris(4,4-dimethyl-2-oxazolinyl)phenylborate), and this motivated consideration of other $[M]HB(C_6F_5)_3$ complexes in catalytic hydrosilylations. In fact, zwitterionic early metal compounds such as $(C_5R_5)_2ZrH\{HB(C_6F_5)_3\}$ are catalysts for olefin polymerization[13] and silane polymerization,[14] and a magnesium hydridoborate catalyzes the hydroboration of carbon dioxide,[15] further suggesting the potential for this zwitterionic moiety in catalysis.

Organometallic hydridoborate compounds may be formed by abstraction of a metal hydride by $B(C_6F_5)_3$,[16] by H_2 or silane treatment of $[M](\mu\text{-Me})B(C_6F_5)_3$,[17] or from mixtures of metal alkyls, silanes, and $B(C_6F_5)_3$.[18] Recently, we have studied a convenient alternative route, in which β-SiH-containing early main-group metal or divalent rare earth alkyl compounds and $B(C_6F_5)_3$ react by β-hydride abstraction.[19] In the present work, we have investigated this abstraction chemistry with light trivalent lanthanide compounds $Ln\{C(SiHMe_2)_3\}_3$ (Ln = La, Ce, Pr, Nd). We describe the synthesis, characterization, and highly active catalytic hydrosilylation chemistry by organo-rare earth hydridoborate complexes, focused upon the first examples of rare earth catalyzed hydrosilylations of α,β-unsaturated esters. The apparent pathway for hydrosilylation is distinguished from transition-metal and $B(C_6F_5)_3$-catalyzed reactions to give the first catalytic synthesis of SiH-substituted α-silyl esters.

Results and Discussion

Reaction with one equiv. of $B(C_6F_5)_3$. The reactions of $Ln\{C(SiHMe_2)_3\}_3$ (Ln = La, Ce, Pr, Nd) and one equiv. of $B(C_6F_5)_3$ in benzene at room temperature for 30 min. yield zwitterionic $Ln\{C(SiHMe_2)_3\}_2HB(C_6F_5)_3$ (**1a-d**) and 0.5 equiv. of the disilacyclobutane $[(Me_2HSi)_2C–SiMe_2]_2$. The borane-derived moiety in the products is $[HB(C_6F_5)_3]$ rather than $(Me_2HSi)_3C$-$B(C_6F_5)_3$, and these products suggest that the reaction proceeds by an intermolecular β-hydrogen abstraction. Previously, reactions of $B(C_6F_5)_3$ and divalent organometallics $M\{C(SiHMe_2)_3\}_2L_2$ (M = Ca, Yb; L_2 = THF, TMEDA) were shown to provide related metal hydridoborates and disilacyclobutane products.[19b] $Ce\{C(SiHMe_2)_3\}_2HB(C_6F_5)_3$ is isolated by crystallization from toluene at –40 °C as colorless crystals.

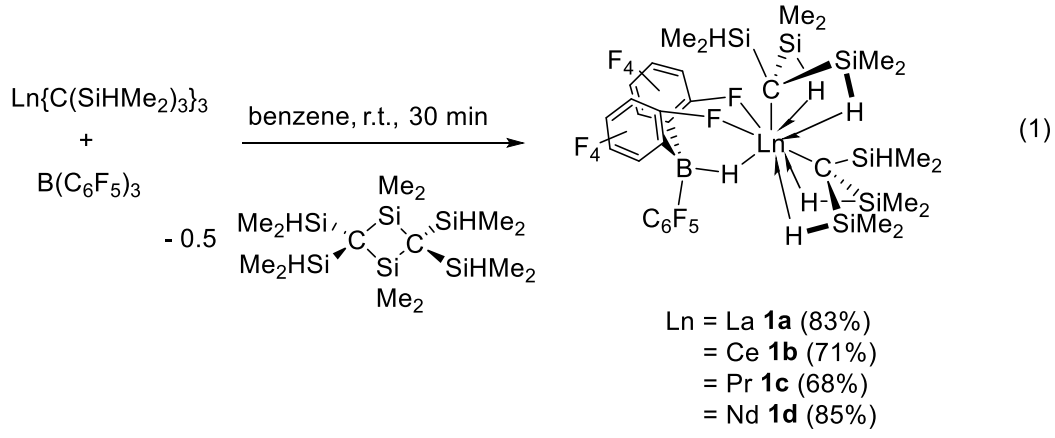

(1)

Ln = La **1a** (83%)
= Ce **1b** (71%)
= Pr **1c** (68%)
= Nd **1d** (85%)

The ^{11}B NMR spectrum of compound **1a** contained a broad doublet at –18 ppm ($^1J_{BH}$ = 68 Hz) and provided good evidence for hydrogen abstraction. Its ^1H NMR spectrum contained singlet resonances at 0.21 ppm (6 H, $SiMe_2$) and 4.45 ppm (1 H, $^1J_{SiH}$ = 135.2 Hz, SiH) assigned to the remaining $C(SiHMe_2)_3$ ligands. In comparison to the $La\{C(SiHMe_2)_3\}_3$ starting material, the $SiMe_2$ peak is shifted slightly upfield by 0.2 ppm and the SiH signal shifted downfield by 0.2

ppm, although the $^{1}J_{SiH}$ constants for La{C(SiHMe$_2$)$_3$}$_3$ and **1a** are similar. The $^{1}J_{SiH}$ values are averaged over three-center-two-electron and two-center-two-electron SiH moieties through a fast exchange process in neutral divalent dialkyls, neutral trivalent trialkys, and zwitterionic trivalent dialkyls. The one-bond coupling constants are smaller in the zwitterionic **1a** compared to Ln{C(SiHMe$_2$)$_3$}$_2$L$_2$ (Ln = Ca, Yb; L$_2$ = THF, TMEDA) and ~2 Hz smaller than in La{C(SiHMe$_2$)$_3$}$_3$. This difference between neutral and zwitterionic compounds may be related to the presence of two donor groups (THF or TMEDA) in the neutral divalent compounds, weaker SiH bonds in 3-c-2-e interactions resulting from the increased charge in the zwitterionic compounds. Interestingly, the rate of exchange in **1a** is faster than in La{C(SiHMe$_2$)$_3$}$_3$. Kinetic data for exchange between agostic-like and classical SiH in La{C(SiHMe$_2$)$_3$}$_3$ suggests a dissociative process with no entropic contribution to the barrier, but this process is fast on the NMR timescale even at 190 K for **1a**. Thus, the faster rate of exchange in **1a** may be interpreted as evidence for weaker La←H-Si interactions in the zwitterionic compound.

The room temperature ^{13}C{^{1}H} NMR spectrum acquired in toluene-d_8 contained two resonances at 47.4 (LaC) and 1.46 ppm (SiMe$_2$) assigned to the C(SiHMe$_2$)$_3$ group. The former signal is ca. 16 ppm downfield compared to the neutral starting materials. The ^{19}F NMR spectrum contained three resonances at –133.6, –156.3 and –161.0 ppm assigned to *ortho*, *meta*, and *para*-fluorines, respectively on equivalent C$_6$F$_5$ rings. One of the methods to identify between zwitterionic species and solvent separated ion pair is to measure the chemical shifts for *para*- and *meta*- fluorines in ^{19}F NMR. Previously, Horton suggested a difference in the chemical shifts of the *meta*- and *para*-fluorine resonances [Δδ (*m*,*p*-F)] greater than 3.5 ppm is associated with coordination, whereas a value less than 3.0 ppm indicates non-coordination.[20] Thus, our observation of Δδ (*m*,*p*-F) = 4.7 ppm indicates zwitterionic species.The ^{11}B NMR spectra of

compounds **1b**, **1c**, and **1d** contained paramagnetically shifted broad signals at –45, –68, and –4 ppm, respectively, indicating that the $\{(Me_2HSi)_3C\}_2Ln^+$ and $HB(C_6F_5)_3$ groups interact in solution, as was suggested by the ^{19}F NMR spectrum of **1a**. In addition, ^1H NMR spectra of **1b-d** each contained only one signal at 3.99 (Ce), 10.1 (Pr) and 5.6 ppm (Nd) corresponding to the $SiMe_2$ group. The ^1H NMR spectra of the corresponding **1b-d-*d*$_7$** compounds showed the $SiMe_2$ peak at 4.22 (Ce), 10.1 (Pr) 5.6 ppm (Nd) further supporting the assignment. In ^{19}F NMR spectra of **1b**, **1c**, and **1d**, only two signals were detected (e.g., for **1b**: –157.1 and –162.4 ppm) in a 1:2 ratio assigned to *para*- and *meta*- fluorine on the C_6F_5. These chemical shifts were similar for **1a-d**, with the signals assigned to *ortho*- F in **1a** not detected in **1b-d**.

Through IR spectroscopy, the SiH group in the alkyl ligand is a powerful handle to compare the paramagnetic and diamagnetic compounds, which suggests that **1a-d** are isostructural. Two ν_{SiH} bands were observed at 2110 and 1787 cm^{-1} for **1a**, 2117 and 1795 cm^{-1} for **1b**, 2113 and 1796 cm^{-1} for **1c** and 2113 and 1792 cm^{-1} for **1d**. The latter signal is red-shifted by 40 cm^{-1} in comparison to $Ln\{C(SiHMe_2)_3\}_3$, and this change and the lower average $^1J_{SiH}$ in cationic vs. neutral compounds suggest weaker Si-H bonds in the zwitterionic species. In addition, bands at 2262 (**1a**), 2268 (**1b**), 2258 (**1c**), and 2255 cm^{-1} (**1d**) were assigned to the ν_{BH}. These signals were not observed in $Ln\{C(SiDMe_2)_3\}_2DB(C_6F_5)_3$ (**1b-d-*d*$_7$**), however corresponding ν_{BD} and ν_{SiD} overlapped with signals from the $B(C_6F_5)_3$ group and were not assigned.

A single crystal X-ray diffraction study of **1b** reveals that two $C(SiHMe_2)_3$ ligands coordinate to the Ce center through similar structures as in $Ce\{C(SiHMe_2)_3\}_3$, in which each $C(SiHMe_2)_3$ ligand contains two bridging Ce←H-Si interactions. The third $C(SiHMe_2)_3$ ligand was substituted for a tridentate $HB(C_6F_5)_3$ group. As shown in Figure 1, these ligands are

oriented in a head-to-tail fashion, with the two non-classical SiH's of one $C(SiHMe_2)_3$ facing the classical SiH of the next ligand. Interestingly, the $HB(C_6F_5)_3$ is oriented similarly, with the two F atoms coordinated to Ce facing the classical $SiHMe_2$ group of the neighboring $C(SiHMe_2)_3$ and the B-H facing the non-classical SiHs of the other neighboring ligand.

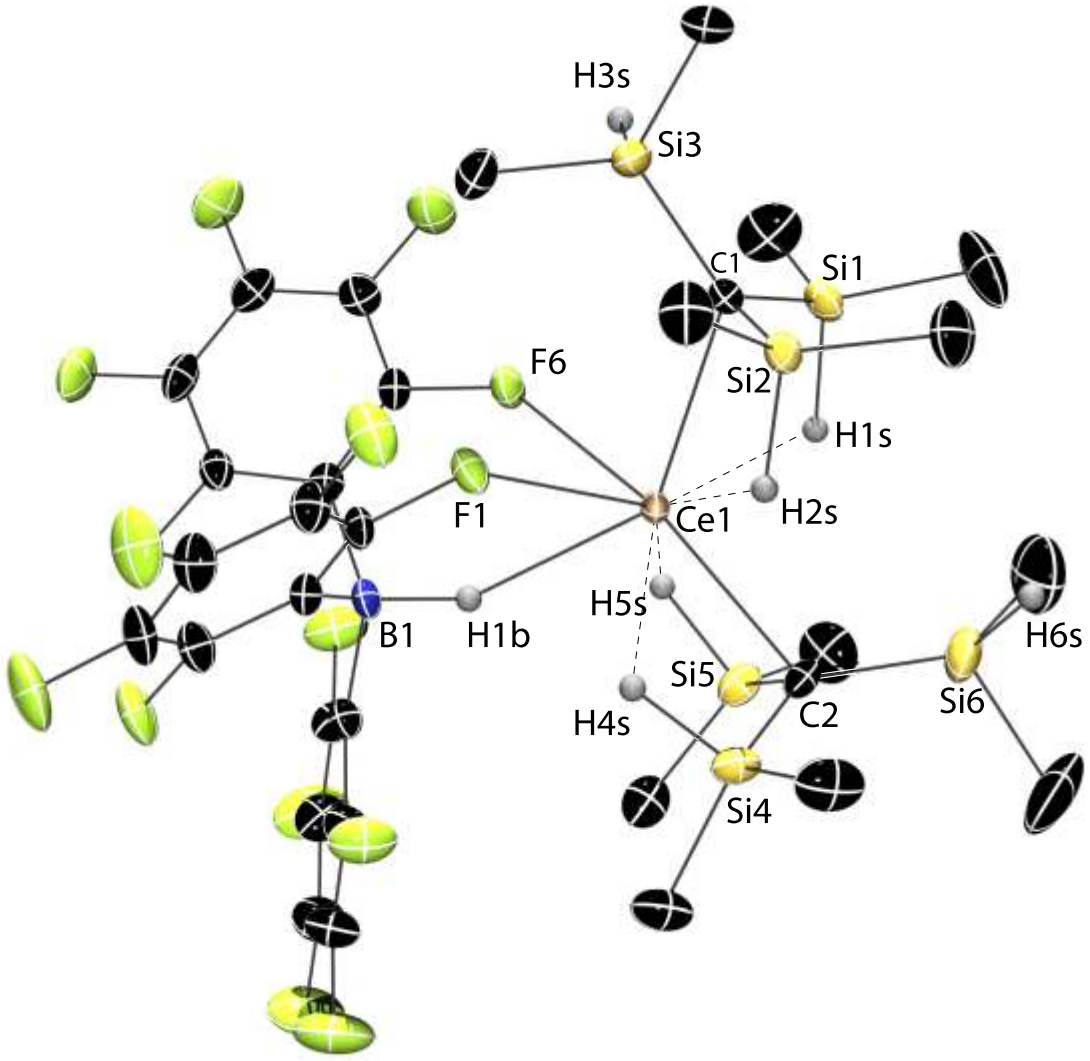

Figure 1. ORTEP diagram of $Ce\{C(SiHMe_2)_3\}_2HB(C_6F_5)_3$ (**1b**). Ellipsoids are plotted at 50% probability. Hydrogen atoms bonded to silicon were located objectively in the Fourier difference map. Significant interatomic distances (Å): Ce1-C1, 2.580(2); Ce1-C2, 2.615(2); Ce1-F1, 2.610(1); Ce1-F6, 2.584(1); Ce1-H1s, 2.39(3); Ce1-H2s, 2.42(3); Ce1-H4s, 2.42(4); Ce1-H5s,

2.44(3); Ce1-Si1, 3.132(1); Ce1-Si2, 3.1664(9); Ce1-Si4, 3.153(1); Ce1-Si5, 3.1542(9); C1-Si1, 1.840(2); C1-Si2, 1.834(2); C1-Si3, 1.854(3); C2-Si4, 1.832(3); C2-Si5, 1.835(2); C2-Si6, 1.856(3); Si1-H1s, 1.54(4); Si2-H2s, 1.49(3); Si3-H3s, 1.47(3); Si4-H4s, 1.49(3); Si5-H5s, 1.48(3); Si6-H6s, 1.61(3). Significant interatomic angles (°): Ce1-C1-Si1, 88.5(1); Ce1-C1-Si2, 90.0(1); Ce1-C1-Si3, 126.4(1); C1-Ce1-C2, 122.26(9); Ce1-C2-Si4, 88.5(1); Ce1-C2-Si5, 88.4(1); C1-C2-Si6, 119.1(1); Si1-C1-Si2, 118.8(1); Si1-C1-Si3, 113.2(1); Si2-C1-Si3, 116.2(1); Si4-C2-Si5, 120.5(1); Si4-C2-Si6, 113.6(1); Si5-C2-Si6, 119.4(1).

The Ce-C and Ce-Si distances in **1b** are shorter than in $Ce\{C(SiHMe_2)_3\}_3$. The Ce1-C1 and Ce1-C2 distances are 2.582(3) and 2.615(2) Å. The average of these (2.60 ± 0.02 Å) is 0.06 Å shorter than in the neutral species (2.661 ± 0.008 Å). The Yb-C distance in $YbC(SiHMe_2)_3HB(C_6F_5)_3THF_2$[19b] is 2.59(2) Å which is comparable to **1b** given their similar ionic radii (6-coordinate Yb^{2+} (1.02 Å); 6-coordinate Ce^{3+} (1.01 Å)).[21] The Ce-Si distances (for the Si1, Si2, Si4 and Si5 participating in the Ce←H-Si structure) in **1b** are 3.15 ± 0.01 Å, which is 0.05 Å shorter than the average in $Ce\{C(SiHMe_2)_3\}_3$ (3.20 ± 0.01 Å). The C-Si distances in $C(SiHMe_2)_3$ ligand in both $Ce\{C(SiHMe_2)_3\}_3$ and **1b** are similar and show a related trend, that is, the average C-Si distances (1.835 ± 0.003 Å) associated with the non-classical Ce←H-Si interactions are shorter than those associated with classical SiH's (1.855 ± 0.001 Å). Furthermore, the Ce center in **1b** may be considered to be planar, based on the sum of C-Ce-C and C-Ce-centroid angles of 360° (with the centroid defined as the average position of the H1B, F1, and F6 atoms). The only other structurally characterized cerium hydridoborate compound reported in literature is $[1,2,4\text{-}(Me_3C)_3C_5H_2]_2Ce(H)BPh_3$).[22]

Reaction with two equiv. of $B(C_6F_5)_3$. Reactions of two equiv. of $B(C_6F_5)_3$ and $Ln\{C(SiHMe_2)_3\}_3$ (Ln = La, Ce, Pr, Nd) in benzene at room temperature for 30 minutes afford bis(hydridoborate) $LnC(SiHMe_2)_3\{HB(C_6F_5)_3\}_2$ (**2a-d**) and 1 equiv. of disilacyclobutane $[(Me_2SiH)_2C\text{-}SiMe_2]_2$ via β-hydrogen abstraction. Interestingly, the last alkyl group in **2a-d** is not affected by treatment with $B(C_6F_5)_3$. In comparison, all of the alkyl groups in divalent $Yb\{C(SiHMe_2)_3\}_2THF_2$ are removed by excess $B(C_6F_5)_3$, resulting in an alkyl group-free dicationic product.[19b]

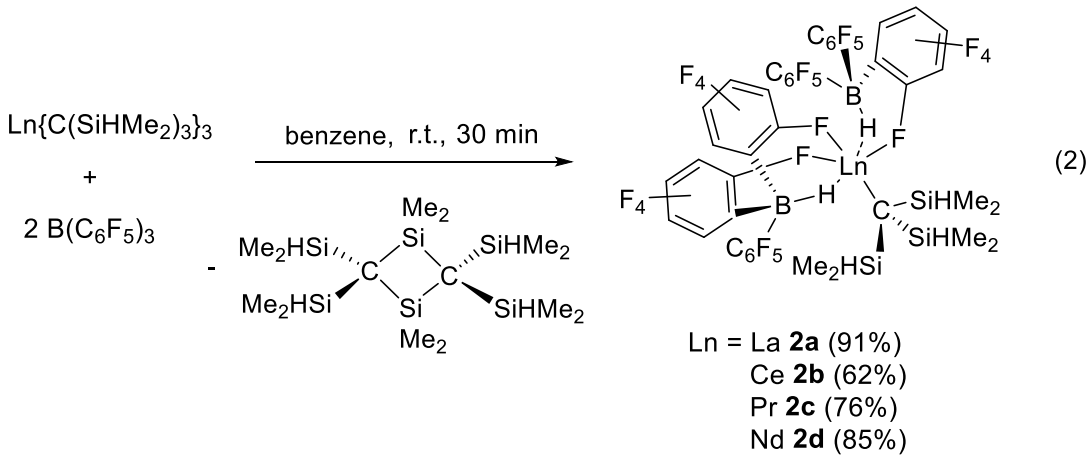

(2)

Ln = La **2a** (91%)
Ce **2b** (62%)
Pr **2c** (76%)
Nd **2d** (85%)

The ^1H NMR spectrum of **2a** contained one doublet resonance at 0.00 ppm ($SiMe_2$) and a multiplet at 4.38 ppm ($^1J_{SiH}$ = 135 Hz, SiH) in the expected 6:1 ratio of integrals. The dimethylsilyl signal moved 0.2 ppm systematically upfield from neutral $La\{C(SiHMe_2)_3\}_3$ to zwitterionic **1a** to bis(hydridoborate) **2a**, whereas the SiH signal in the **1a** and **2a** were downfield of the neutral species. The $SiMe_2$ signals for paramagnetic **2b-d** were broad at 4.55 (Ce), 14.12 (Pr), and 8.29 ppm (Nd) and assignments were confirmed by deuterium-labeled derivatives while no SiH peak was observed. The ^{13}C NMR signal for the $C(SiHMe_2)_3$ ligand at 56.9 ppm was also further downfield, following the trend **2a** > **1a** > $La\{C(SiHMe_2)_3\}_3$. Although ^{13}C NMR spectra of the paramagnetic derivatives were featureless, the ^{11}B NMR spectra of **2a-d** contained signals

at -17.4 ppm –7.47 ppm, –23.4, and 25.1 ppm that revealed persistent Ln-HB(C_6F_5)$_3$ interaction. As in zwitterionic **1b-d**, only *meta*- and *para*-F signals were detected in the ^{19}F NMR spectra of **2b-d**, suggesting that the *ortho*-F directly interact with the paramagnetic centers. Interestingly, the only band in the SiH region of IR spectra for **2a-d** appeared at 2110 cm^{-1}. The surprising lack of signals from 1700 – 2000 cm^{-1} for **2a-d**, does not provide evidence for 3-center-2-electron bonding, but as a negative result, it also does not unambiguously rule out multi-center bonding.

A single crystal X-ray diffraction study of **2d** reveals that one C($SiHMe_2$)$_3$ ligand is coordinated to the Nd center while the other two coordination sites are taken up by tridentate HB(C_6F_5)$_3$ groups. The C($SiHMe_2$)$_3$ ligand is oriented such that two non-classical SiH's face the Nd center. There are a total of three Nd-F interactions in the molecule including two bridging *ortho*-F atoms from one B(C_6F_5)$_3$ group and the third bridging *ortho*-F atom from the other B(C_6F_5)$_3$ group. The Nd-F distances are 2.616(6) Å, 2.857(6) Å from one B(C_6F_5)$_3$ group and 2.600(7) Å from other B(C_6F_5)$_3$ group. These distances are similar to the one observed in the crystal structure of **1b**. In addition to one C($SiHMe_2$)$_3$ group and two B(C_6F_5)$_3$ groups, a toluene molecule also coordinates to the Nd center. The coordination of crystallization solvent molecule in the crystal structure of Nd compounds is not unusual as we observe coordinated toluene in (η-C_6H_5Me)Nd[N(C_6F_5)$_2$]$_3$.[23] Also, compound Nd{C($SiHMe_2$)$_3$}$_3$, co-crystallizes with benzene molecule. The distances between Nd1 and carbons of the toluene molecule (e.g.C71, C72, C73, C74, C75) range between 2.954(1) to 3.026(1) Å which is shorter than the distance between Nd and carbons of the toluene molecule in (η-C_6H_5Me)Nd[N(C_6F_5)$_2$]$_3$[23] (2.98(2) to 3.324(1) Å) suggesting a stronger coordination of toluene molecule. The Nd1-C1 distance is ca. 0.11 Å shorter than that observed in Nd{C($SiHMe_2$)$_3$}$_3$ suggesting that the positive charge generated on the Nd center due to Lewis acid mediated H abstraction from two alkyl groups causes the

molecule to shrink. Similarly, Nd-Si distances also shorten to 3.135(3) (Nd1-Si1) and 3.101(4) Å (Nd1-Si2) from av. 3.152 Å in $Nd\{C(SiHMe_2)_3\}_3$. This presents the first example of crystallographically characterized Nd alkyl bis(hydridoborate).

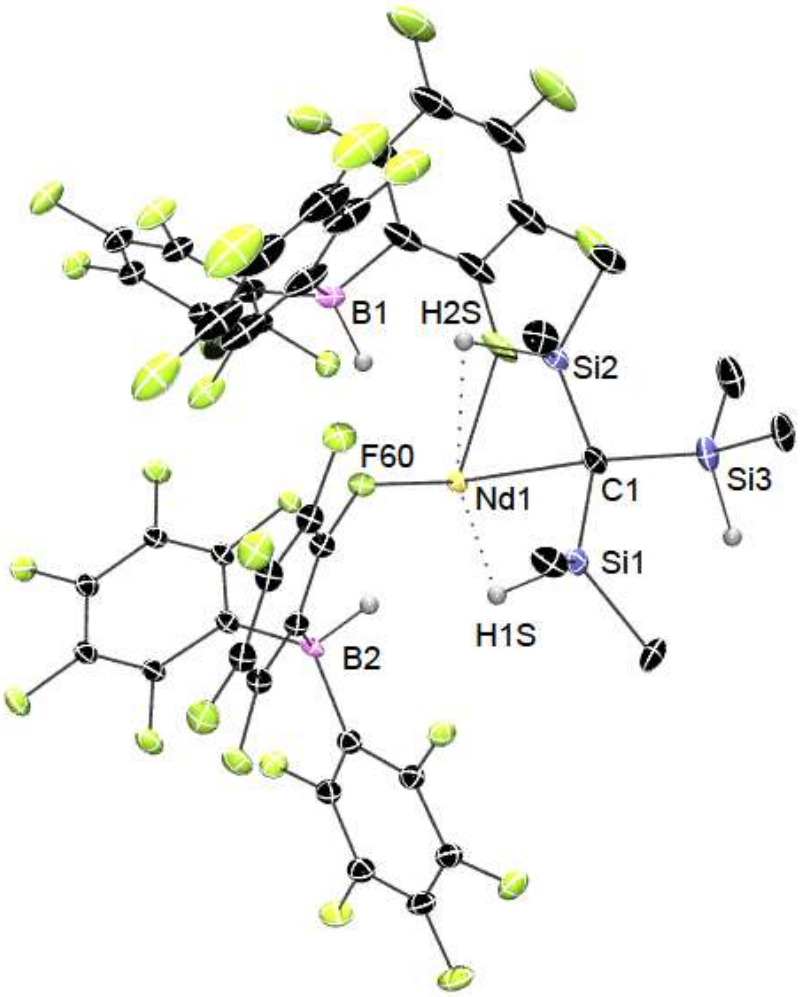

Figure 2. ORTEP diagram of $NdC(SiHMe_2)_3\{HB(C_6F_5)_3\}_2$ (**2d**). Ellipsoids are plotted at 50% probability. Hydrogen atoms bonded to silicon were located objectively in the Fourier difference map. Significant interatomic distances (Å): Nd1-C1, 2.512(2); Nd1-F24, 2.857(6); Nd1-F30, 2.614(6); Nd1-F60, 2.600(7); Nd1-Si1, 3.135(3); Nd1-Si2, 3.101(4); C1-Si1, 1.844(1); C1-Si2, 1.839(1); C1-Si3, 1.870(1). Significant interatomic angles (°): Nd1-C1-Si1, 90.7(5); Nd1-C1-

Si2, 89.6(5); Nd1-C1-Si3, 132.8(6); Si1-C1-Si2, 119.4(7); Si1-C1-Si3, 112.9(6); Si2-C1-Si3, 110.3(7).

Hydrosilylation of α,β-unsaturated acrylates. The trivalent $Ln\{C(SiHMe_2)_3\}_3$, **1a-d**, **2a-d**, as well as divalent $LnC(SiHMe_2)_3HB(C_6F_5)_3$ (Ln = Yb, Sm) were investigated as catalysts for hydrosilylation of α,β-unsaturated esters in comparison to $B(C_6F_5)_3$ and $To^MMgHB(C_6F_5)_3$. Remarkably, the addition of secondary silanes and acrylates to give α-silyl esters is catalyzed effectively by compounds **1a-d**, which provide the products in high yield (Table 1). In contrast, **1a-d** catalyze hydrosilylation of acrylates with tertiary silanes to give silyl ketene acetals while primary silanes do not react with acrylates at room temperature or at 60 °C for one day.

These results also contrast the catalytic action of $To^MMgHB(C_6F_5)_3$, which provides silyl ketene acetals for additions of secondary and tertiary silanes to methacrylates, but polymerizes acrylates rather than catalyzing their hydrosilylation.[12] Neither divalent $LnC(SiHMe_2)_3HB(C_6F_5)_3THF_2$, trivalent $Ln\{C(SiHMe_2)_3\}_3$, nor di-zwitterionic **2a-d** provide either hydrosilylation product. Because compounds **1a-d** appeared to have equivalent reactivity in the catalyst screening and the cerium complex **1b** is purified by crystallization, all further conversions employed **1b**. The α-silyl ester products are obtained in benzene, toluene, methylene chloride and chloroform, and chloroform was used for subsequent reactions for convenience. Remarkably, catalyst loadings of 0.05 mol% give full conversion within 5 mins. Lower catalyst loadings do not give full conversion, and under those conditions a turnover number of 2200 is measured. In fact, the reaction between the silanes and acrylates is catalyzed within a minute of adding catalyst **1b** as the catalyst changes color from pale yellow to colorless providing a TOF of 37 s^{-1}.

Table 1. Comparison of compounds **1a-d** as catalysts, solvents for hydrosilylation of methyl acrylate and $PhMeSiH_2$.

Entry	**Reaction**	**Variable**	**NMR Yield (%)**
1.	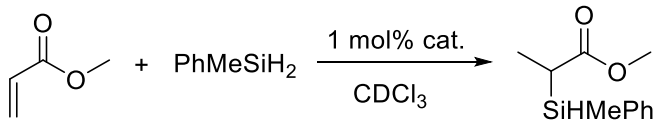	Catalyst **1a** **1b** **1c** **1d**	 81 84 81 82
2.	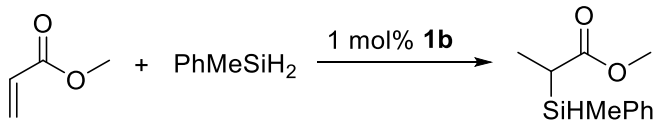	Solvent C_6D_6 CD_2Cl_2 $CDCl_3$	 72 75 81
3.	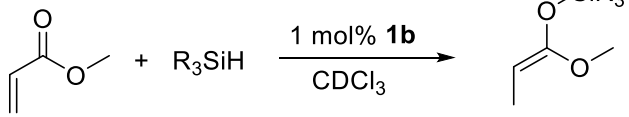	Silane $BnMe_2SiH$ Et_3SiH $(CH_2=CH)$ Me_2SiH	 71 74 68
4.	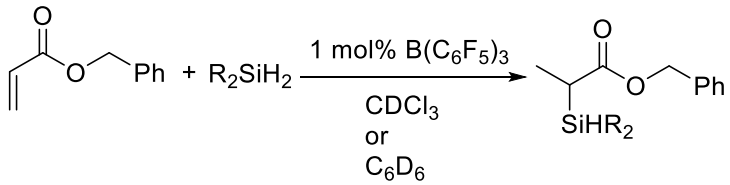	Silane Ph_2SiH_2 $PhMeSiH_2$ Et_2SiH_2	 64 60 62

The α-silyl ester products were unambiguously identified by NMR and infrared spectroscopies. For example, the ^{1}H NMR spectrum of the isolated methyl α-diphenylsilylpropionate contained a doublet resonance at 4.94 ppm (chloroform-d, $^{3}J_{HH}$ = 3.0 Hz, $^{1}J_{SiH}$ = 205 Hz) with silicon satellites, and thus assigned to SiH that was coupled to the α-methine resonance at 2.73 ppm. The resonance assigned to the α-methine appeared as a quartet of doublets ($^{3}J_{HH}$ = 7.2 Hz) resulting from SiH and CH_3 (1.35 ppm) coupling. These signals, as well as the phenyl signals, correlated with the ^{29}Si NMR signal at –9.33 ppm observed in a ^{1}H-^{29}Si HMBC experiment. Moreover, the ^{13}C{^{1}H} spectrum contained a resonance at 175.93 ppm assigned to carbonyl carbon. In a ^{1}H-^{13}C HMBC experiment, a crosspeak between this signal and the ^{1}H NMR signal assigned to the α-methyl was observed. Finally, a band in the infrared spectrum at 1725 cm^{-1} is was consistent with the ν_{CO} of an ester.

A range of silyl esters have been prepared using catalyst **1b** (Table 2). The products have been isolated in chloroform as the solvent however, we report the isolation of $Ph_2HSiCHCO_2Me$ in chloroform and toluene.

Table 2: **1b** catalyzed hydrosilylation of acrylates and secondary silanes

Entry	**Silane**	**Acrylate**	**Product**	**Yield (isolated)[a]**
1.	$PhMeSiH_2$	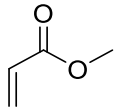	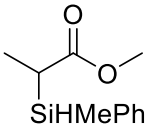	84 (82)
2.	Ph_2SiH_2	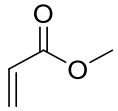	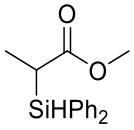	81 (80) 72[b] (72)[c]
3.	Et_2SiH_2	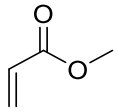	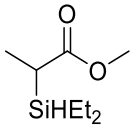	82 (81)
4.	$PhMeSiH_2$	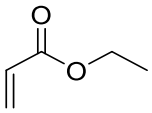	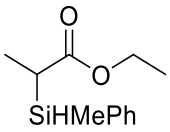	88 (85)
5.	Ph_2SiH_2	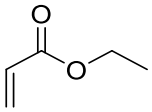	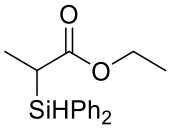	77 (74)
6.	Et_2SiH_2	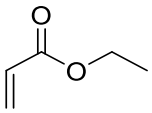	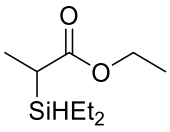	82 (79)
7.	$PhMeSiH_2$	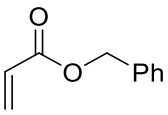	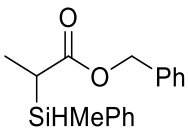	83 (81)
8.	Et_2SiH_2	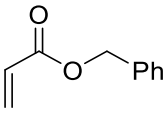	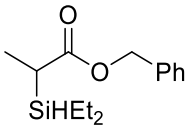	78 (77)

Table 2 continued

9.	$PhMeSiH_2$	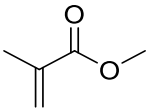	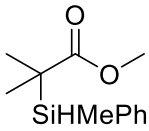	89[d] (88)
10.	$PhMeSiH_2$	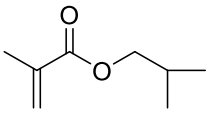	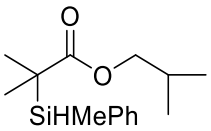	82 (81)
11.	Ph_2SiH_2	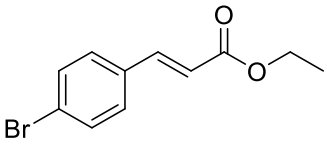	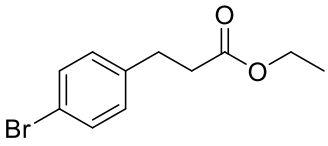	85 (82)
12.	Et_2SiH_2	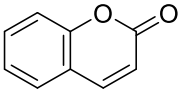	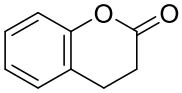	84 (81)

Conditions: 1 mol% $Ce\{C(SiHMe_2)_3\}_2HB(C_6F_5)_3$, silane : acrylate = 1:1, solvent = chloroform, [a]room temperature, [b]NMR yield in benzene-d_6, [c]isolated yield from toluene, [d]0 °C, 1 h.

Alternatively, $B(C_6F_5)_3$ is known to catalyze 1,2-hydrosilylation of tertiary silanes and esters.[6a] Free $B(C_6F_5)_3$ could be present in the reaction via dissociation of **1b** therefore, its catalytic reactivity was studied. 1 mol% of $B(C_6F_5)_3$ as catalyst in benzene-d_6 or chloroform-*d* for reaction between $PhMeSiH_2$ and methyl acrylate did not result in 3,4-addition hydrosilylated ester but instead gave a number of unidentified species in ^{1}H NMR.

Recently, Chang *et al*.[11] have reported that $B(C_6F_5)_3$ catalyzes hydrosilylation of α,β-unsaturated esters and amides to afford α-silyl carbonyl compounds. The mechanistic studies revealed two step procedure: fast 1,4-hydrosilylation of the carbonyl group followed by slow silyl group migration of the silyl ether intermediate. To investigate this pathway in our system, hydrosilylation of ethyl trans-4-bromocinnamate with Ph_2SiH_2 and $PhMe_2SiH$ catalyzed by **1b** was carried out in chloroform-*d*. However, no α-silyl ester was observed after one day at room

temperature while $B(C_6F_5)_3$ catalyzed reaction of ethyl trans-4-bromocinnamate with Ph_2SiH_2 was very messy in ^1H NMR with several unidentified species. When the reaction between Ph_2SiH_2 and methyl methacrylate was catalyzed by 1 mol% **1b** followed by 5 mol% $B(C_6F_5)_3$, methane and a new unidentified silyl containing product was obtained suggesting cleavage of the methacrylate. Similar cleavage of methacrylate was observed when the reaction was catalyzed by $B(C_6F_5)_3$. Thus, formation of α-silyl esters is not catalyzed by $B(C_6F_5)_3$ and that catalyzed by **1b** does not follow similar pathway as reported in literature.

We also independently synthesized $PhMeHSiO(MeO)C=CMe_2$ from $To^MMgHB(C_6F_5)_3$ catalyzed reaction of benzyl methacrylate and $PhMeSiH_2$[12] and then added catalytic amounts of catalyst **1b** and no silicon migration product, $PhMeHSiCMe_2CO_2CH_2Ph$ was not detected in ^1H NMR after one day.

Conclusion

In conclusion, we have successfully demonstrated the synthesis and characterization of trivalent rare earth alkyl hydridoborate compounds featuring non-classical interactions. Their role as hydrosilylation catalysts has been probed for α,β-unsaturated esters and secondary silanes. Moreover, tertiary silanes with α,β-unsaturated esters generate silyl ketene acetals while primary silanes do not react. The catalytic results presented here reveal the first example of rare-earth metal alkyl borate catalyzed hydrosilylation of α,β-unsaturated esters to generate α-silyl esters in quantitative yields. The reactions are instantaneous with low catalyst loading and quantitative yields under mild conditions. The pathway for the synthesis of α-silyl esters is not

via retro-Brook rearrangement as isolated silyl ketene acetals are not converted to α-silyl esters catalytically.

Experimental Section

All manipulations were performed under a dry argon atmosphere using standard Schlenk techniques or under a nitrogen atmosphere in a glovebox unless otherwise indicated. Water and oxygen were removed from benzene and pentane solvents using an IT PureSolv system. Benzene-d_6, chloroform-*d* were heated to reflux over Na/K alloy and CaH_2, respectively, and vacuum-transferred. $B(C_6F_5)_3$[19] and $To^MMgHB(C_6F_5)_3$[7] were prepared following literature procedures. $PhMeSiH_2$ was prepared by reaction of chlorosilane with $LiAlH_4$. Ph_2SiH_2, Et_2SiH_2 were purchased from Sigma Aldrich and degassed by three freeze-pump-thaw cycles prior to use. Methyl acrylate, ethyl acrylate, benzyl acrylate, methyl methacrylate and isobutyl methacrylate were purchased from TCI America and degassed by three freeze-pump-thaw cycles prior to use.

La{C(SiHMe$_2$)$_3$}$_2$HB(C$_6$F$_5$)$_3$ (1a). $B(C_6F_5)_3$ (0.068 g, 0.134 mmol) was added to a benzene (4 mL) solution of $La\{C(SiHMe_2)_3\}_3$ (0.095 g, 0.134 mmol) in small portions. The resulting yellow mixture was stirred at room temperature for 30 min. The solvent was evaporated under reduced pressure to give a yellow paste. The residue was washed with pentane (3 × 5 mL) and the volatiles were evaporated to dryness in vacuo to give $La\{C(SiHMe_2)_3\}_2HB(C_6F_5)_3$ as a pale orange solid (0.115 g, 0.112 mmol, 83.3%). ^{1}H NMR (benzene-d_6, 600 MHz, 25 °C): δ 4.45 (m, $^1J_{SiH}$ = 135.2 Hz, 6 H, SiH), 0.21 (d, $^3J_{HH}$ = 3.4 Hz, 36 H, $SiMe_2$). ^{11}B NMR (benzene-d_6, 192 MHz, 25 °C): δ -17.5 (d, $^1J_{BH}$ = 68.0 Hz). $^{13}C\{^1H\}$ NMR (benzene-d_6, 150 MHz, 25 °C): δ 150.2

(br, C_6F_5), 148.7 (br, C_6F_5), 141.0 (br, C_6F_5), 139.0 (br, C_6F_5), 137.3 (br, C_6F_5), 48.1 (LaC), 2.2 ($SiMe_2$). ^{19}F NMR (benzene-d_6, 564 MHz, 25 °C): δ –133.6 (6 F, *ortho*- C_6F_5), –156.3 (3 F, *para*- C_6F_5), –161.0 (6 F, *meta*- C_6F_5). $^{29}Si\{^1H\}$ NMR (benzene-d_6, 119 MHz, 25 °C): δ –11.2 ($SiHMe_2$). IR (KBr, cm^{-1}): 2958 m, 2904 w, 2263 m br (ν_{BH}), 2109 m br (ν_{SiH}), 1787 m br (ν_{SiH}), 1646 m, 1603 w, 1516 s, 1467 s br, 1372 m, 1283 s, 1258 s, 1110 s br, 1079 s br, 959 s br, 896 s br, 837 s br, 786 s, 673 m. Anal. Calcd for $BC_{32}F_{15}H_{43}Si_6La$: C, 37.28; H, 4.20. Found: C, 37.81; H, 4.00. mp = 171 °C dec.

La{C(SiDMe$_2$)$_3$}$_2$DB(C$_6$F$_5$)$_3$ (1a-*d*$_7$). $B(C_6F_5)_3$ (0.058 g, 0.011 mmol) was added to a benzene (4 mL) solution of $La\{C(SiDMe_2)_3\}_3$ (0.081 g, 0.011 mmol) in small portions. The resulting yellow mixture was stirred at room temperature for 30 min. The solvent was evaporated under reduced pressure to give a yellow paste. The residue was washed with pentane (3 × 5 mL) and the volatiles were evaporated to dryness in vacuo to give $La\{C(SiDMe_2)_3\}_2DB(C_6F_5)_3$ as a pale orange solid (0.101 g, 0.010 mmol, 85.5%). ^1H NMR (benzene, 600 MHz, 25 °C): δ 0.22 (s, 36 H, $SiMe_2$). ^2H NMR (benzene, 600 MHz, 25 °C): δ 4.44 (s, 6 D, Si*D*Me$_2$). ^{11}B NMR (benzene, 192 MHz, 25 °C): δ –18.3 (s). $^{13}C\{^1H\}$ NMR (benzene, 150 MHz, 25 °C): δ 150.1 (br, C_6F_5), 148.6 (br, C_6F_5), 140.9 (br, C_6F_5), 138.9 (br, C_6F_5), 137.2 (br, C_6F_5), 47.6 (LaC), 2.1 ($SiMe_2$). ^{19}F NMR (benzene, 564 MHz, 25 °C): δ –137.4 (d, 6 F, *ortho*- C_6F_5), –152.1 (t, 3 F, *para*- C_6F_5), –160.4 (t, 6 F, *meta*- C_6F_5). $^{29}Si\{^1H\}$ NMR (benzene, 119 MHz, 25 °C): δ –12.4 ($SiHMe_2$). IR (KBr, cm^{-1}): 2959 m, 2903 w, 1646, 1607 w br, 1516 s br, 1466 s br, 1413 w br, 1370 m, 1257 s br, 1099 s br, 1081 s br, 976 s, 933 w br, 891 s br, 841 s, 814 w br, 790 m, br.

$LaC(SiHMe_2)_3\{HB(C_6F_5)_3\}_2$ (2a). $B(C_6F_5)_3$ (0.130 g, 0.184 mmol) was added to a benzene (4 mL) solution of $La\{C(SiHMe_2)_3\}_3$ (0.193 g, 0.377 mmol) in small portions. The resulting yellow mixture was stirred at room temperature for 30 min. The solvent was evaporated under reduced pressure to give a yellow paste. The residue was washed with pentane (3 × 5 mL) and the volatiles were evaporated to dryness in vacuo to give $LaC(SiHMe_2)_3\{HB(C_6F_5)_3\}_2$ as an off-white solid (0.226 g, 0.167 mmol, 90.6%). ^{1}H NMR (benzene-d_6, 600 MHz, 25 °C): δ 4.38 (m, $^1J_{SiH}$ = 134.7 Hz, 3 H, SiH), 2.27-2.96 (br q, 1 H, HB), 0.00 (d, $^3J_{HH}$ = 3.6 Hz, 18 H, $SiMe_2$). ^{11}B NMR (benzene-d_6, 192 MHz, 25 °C): δ –17.7 (d, $^1J_{BH}$ = 58.4 Hz). $^{13}C\{^1H\}$ NMR (benzene-d_6, 150 MHz, 25 °C): δ 149.9 (br, C_6F_5), 148.4 (br, C_6F_5), 141.2 (br, C_6F_5), 139.5 (br, C_6F_5), 138.9 (br, C_6F_5), 137.2 (br, C_6F_5), 56.9 (LaC), 1.4 ($SiMe_2$). ^{19}F NMR (benzene-d_6, 564 MHz, 25 °C): δ –137.0 (br, 6 F, *ortho*-C_6F_5), –158.7 (br, 3 F, *para*- C_6F_5), –163.3 (6 F, *meta*- C_6F_5). $^{29}Si\{^1H\}$ NMR (benzene-d_6, 119 MHz, 25 °C): δ –10.3 ($SiHMe_2$). IR (KBr, cm^{-1}): 2963 m, 2252 m br (ν_{BH}), 2106 m br (ν_{SiH}), 1649 m, 1606 w, 1518 s, 1468 s br, 1375 m, 1283 s, 1267 s, 1117 s br, 1081 s br, 974 s, 953 s, 896 s br, 842 s br, 790 m, 672 m. Anal. Calcd for $B_2C_{48}F_{30}H_{35}Si_3La$: C, 40.41; H, 2.47. Found: C, 40.84; H, 2.59. mp = 170 -173 °C.

$LaC(SiDMe_2)_3\{DB(C_6F_5)_3\}_2$ (2a-d_5). $B(C_6F_5)_3$ (0.132 g, 0.026 mmol) was added to a benzene (4 mL) solution of $La\{C(SiDMe_2)_3\}_3$ (0.092 g, 0.013 mmol) in small portions. The resulting yellow mixture was stirred at room temperature for 30 min. The solvent was evaporated under reduced pressure to give a yellow paste. The residue was washed with pentane (3 × 5 mL) and the volatiles were evaporated to dryness in vacuo to give $La\{C(SiDMe_2)_3\}\{DB(C_6F_5)_3\}_2$ as an off-white solid (0.151 g, 0.011 mmol, 86.3%). ^{1}H NMR (benzene, 600 MHz, 25 °C): δ 0.00 (s, 18 H,

$SiMe_2$). ^2H NMR (benzene, 600 MHz, 25 °C): δ 4.40 (s, 6 D, Si*D*Me_2). ^{11}B NMR (benzene, 192 MHz, 25 °C): δ –18.0 (s). $^{13}C\{^1H\}$ NMR (benzene, 150 MHz, 25 °C): δ 149.4 (br, C_6F_5), 147.9 (br, C_6F_5), 138.1 (br, C_6F_5), 136.6 (br, C_6F_5), 134.3 (br, C_6F_5), 133.2 (br, C_6F_5), 0.73 ($SiMe_2$). ^{19}F NMR (benzene, 564 MHz, 25 °C): δ –130.6 (6 F, *ortho*-C_6F_5), –154.8 (3 F, *para*-C_6F_5), –160.2 (6 F, *meta*-C_6F_5). $^{29}Si\{^1H\}$ NMR (benzene, 119 MHz, 25 °C): δ –10.9 ($SiHMe_2$). IR (KBr, cm^{-1}): 2961 m, 2906 w, 1648, 1607 w br, 1518 s, 1467 s br, 1370 s, 1265 s br, 1101 s br, 1082 s br, 979 s, 947 s br, 877 s br, 843 s, 791 s, br, 706 s.

$Ce\{C(SiHMe_2)_3\}_2HB(C_6F_5)_3$ (1b). $B(C_6F_5)_3$ (0.045 g, 0.088 mmol) was added to a benzene (4 mL) solution of $Ce\{C(SiHMe_2)_3\}_3$ (0.062 g, 0.088 mmol) in small portions. The resulting yellow mixture was stirred at room temperature for 1 h. The solvent was evaporated under reduced pressure to give a yellow paste. The residue was washed with pentane (2 × 5 mL) and the volatiles were evaporated to dryness in vacuo to give $Ce\{C(SiHMe_2)_3\}_2HB(C_6F_5)_3$ as a pale yellow solid (0.065 g, 0.063 mmol, 71.4%). This solid was recrystallized at –30 °C from a minimal amount of toluene to obtain as **2b** colorless crystals. ^1H NMR (benzene-d_6, 600 MHz, 25 °C): δ 3.99 ($SiMe_2$). ^{11}B NMR (benzene-d_6, 192 MHz, 25 °C): δ –44.8 (s). $^{13}C\{^1H\}$ NMR (benzene-d_6, 150 MHz, 25 °C): δ 30.60, 15.81, 4.53, 2.14, -1.16 (unidentified). ^{19}F NMR (benzene-d_6, 564 MHz, 25 °C): δ –157.1 (3 F, *para*-C_6F_5), –162.4 (6 F, *meta*-C_6F_5). IR (KBr, cm^{-1}): 2957 m, 2903 w, 2268 m br (ν_{BH}), 2117 s (ν_{SiH}), 1795 m br (ν_{SiH}), 1646 m, 1605 w, 1516 s, 1466 s br, 1372 m, 1256 s, 1113 s br, 1087 s br, 1026 br, 986 s br, 908 s br, 878 s br, 790 s, 683 m. Anal. Calcd. for $BC_{32}F_{15}H_{43}Si_6Ce$: C, 37.24; H, 4.20. Found: C, 36.83; H, 4.40. mp = 175 °C dec.

Ce{C(SiDMe$_2$)$_3$}$_2$DB(C$_6$F$_5$)$_3$ (1b-*d*$_7$). B(C$_6$F$_5$)$_3$ (0.039 g, 0.055 mmol) was added to a benzene (4 mL) solution of Ce{C(SiDMe$_2$)$_3$}$_3$ (0.028 g, 0.055 mmol) in small portions. The resulting yellow mixture was stirred at room temperature for 1 h. The solvent was evaporated under reduced pressure to give a yellow paste. The residue was washed with pentane (2 × 5 mL) and the volatiles were evaporated to dryness in vacuo to give Ce{C(SiDMe$_2$)$_3$}$_2$DB(C$_6$F$_5$)$_3$ as a pale yellow solid (0.027 g, 0.027 mmol, 48.9%). ^{1}H NMR (benzene, 600 MHz, 25 °C): δ 4.22 (SiMe$_2$). ^{11}B NMR (benzene, 192 MHz, 25 °C): δ –46.0 (br). ^{19}F NMR (benzene, 564 MHz, 25 °C): δ –156.0 (3 F, *para*-C$_6$F$_5$), –161.7 (6 F, *meta*- C$_6$F$_5$). IR (KBr, cm^{-1}): 2959 m, 2904 w, 1647, 1516 s br, 1467 s br, 1371 br, 1258 br, 1102 s br, 1080 s br, 977 s br, 889 s br, 842 s.

CeC(SiHMe$_2$)$_3${HB(C$_6$F$_5$)$_3$}$_2$ (2b). B(C$_6$F$_5$)$_3$ (0.199 g, 0.389 mmol) was added to a benzene (4 mL) solution of Ce{C(SiHMe$_2$)$_3$}$_3$ (0.138 g, 0.195 mmol) in small portions. The resulting yellow mixture was stirred at room temperature for 1 h. The solvent was evaporated under reduced pressure to give a yellow paste. The residue was washed with pentane (2 × 5 mL) and the volatiles were evaporated to dryness in vacuo to give CeC(SiHMe$_2$)$_3${HB(C$_6$F$_5$)$_3$}$_2$ as a pale yellow solid (0.164 g, 0.121 mmol, 62.1%). ^{1}H NMR (benzene-*d*$_6$, 600 MHz, 25 °C): δ 4.55 (SiMe$_2$). ^{11}B NMR (benzene-*d*$_6$, 192 MHz, 25 °C): δ –7.47 (s). ^{13}C{^{1}H} NMR (benzene-*d*$_6$, 150 MHz, 25 °C): δ 149.41 (C$_6$F$_5$), 147.77 (C$_6$F$_5$), 138.99 (C$_6$F$_5$), 137.25 (C$_6$F$_5$), -1.15 (SiMe$_2$). ^{19}F NMR (benzene-*d*$_6$, 564 MHz, 25 °C): δ –154.74 (3 F, *para*-C$_6$F$_5$) , –161.5 (6 F, *meta*-C$_6$F$_5$). IR (KBr, cm^{-1}): 2964 m, 2263 (ν_{BH}), 2117 s (ν_{SiH}), 1648 m, 1605 w, 1518 s, 1467 s br, 1375 m,

1268 s, 1115 s br, 1085 s br, 972 s br, 957 s br, 895 s br, 841 s. Anal. Calcd. for $B_2C_{43}F_{30}H_{23}Si_3Ce$: C, 38.10; H, 1.71. Found: C, 37.89; H, 1.92. mp = 174-178 °C.

$CeC(SiDMe_2)_3\{DB(C_6F_5)_3\}_2$ (2b-d_5). $B(C_6F_5)_3$ (0.096 g, 0.187 mmol) was added to a benzene (4 mL) solution of $Ce\{C(SiDMe_2)_3\}_3$ (0.067 g, 0.094 mmol) in small portions. The resulting yellow mixture was stirred at room temperature for 1 h. The solvent was evaporated under reduced pressure to give a yellow paste. The residue was washed with pentane (2 × 5 mL) and the volatiles were evaporated to dryness in vacuo to give $CeC(SiDMe_2)_3\{DB(C_6F_5)_3\}_2$ as a pale yellow solid (0.106 g, 0.078 mmol, 83.5%). ^{1}H NMR (benzene, 600 MHz, 25 °C): δ 4.61 ($SiMe_2$). ^{11}B NMR (benzene, 192 MHz, 25 °C): δ –7.68 (s). ^{19}F NMR (benzene, 564 MHz, 25 °C): δ –154.9 (3 F, *para*-C_6F_5), –162.0 (6 F, *meta*-C_6F_5). IR (KBr, cm^{-1}): 2962 m, 2904 w, 1648 s, 1608 w, 1517 s br, 1467 s br, 1370 m, 1263 s br, 1100 s br, 1084 s br, 973 s br, 945 s br, 844 s br, 798 s br, 706 m br.

$Pr\{C(SiHMe_2)_3\}_2HB(C_6F_5)_3$ (1c). $B(C_6F_5)_3$ (0.041 g, 0.081 mmol) was added to a benzene (4 mL) solution of $Pr\{C(SiHMe_2)_3\}_3$ (0.057 g, 0.081 mmol) in small portions. The resulting yellow mixture was stirred at room temperature for 1 h. The solvent was evaporated under reduced pressure to give a yellow paste. The residue was washed with pentane (2 × 5 mL) and the volatiles were evaporated to dryness in vacuo to give $Pr\{C(SiHMe_2)_3\}_2HB(C_6F_5)_3$ as a pale yellow solid (0.057 g, 0.055 mmol, 67.8%). ^{1}H NMR (benzene-d_6, 600 MHz, 25 °C): δ 10.11 ($SiMe_2$). ^{11}B NMR (benzene-d_6, 192 MHz, 25 °C): δ –68.1 (br). ^{19}F NMR (benzene-d_6, 564 MHz, 25 °C): δ –157.7 (3 F, *para*-C_6F_5) , –164.5 (6 F, *meta*-C_6F_5). IR (KBr, cm^{-1}): 2957 m, 2904

w, 2258 br (ν_{BH}), 2113 s (ν_{SiH}), 1795 m br (ν_{SiH}), 1646 m, 1516 s, 1467 s br, 1372 m, 1258 s, 1109 s br, 1079 s br, 973 s br, 960 s br, 894 s br, 836 s br, 786 s, 675 m. Anal. Calcd. for $BC_{32}F_{15}H_{43}Si_6Pr$: C, 37.20; H, 4.19. Found: C, 37.45; H, 4.07. mp = 181 °C dec.

Pr{C(SiDMe$_2$)$_3$}$_2$DB(C$_6$F$_5$)$_3$ (1c-*d*$_7$). $B(C_6F_5)_3$ (0.059 g, 0.15 mmol) was added to a benzene (4 mL) solution of $Pr\{C(SiDMe_2)_3\}_3$ (0.082 g, 0.15 mmol) in small portions. The resulting yellow mixture was stirred at room temperature for 1 h. The solvent was evaporated under reduced pressure to give a yellow paste. The residue was washed with pentane (2 × 5 mL) and the volatiles were evaporated to dryness in vacuo to give $Pr\{C(SiDMe_2)_3\}_2DB(C_6F_5)_3$ as a pale yellow solid (0.092 g, 0.089 mmol, 78.6%). ^{1}H NMR (benzene, 600 MHz, 25 °C): δ 10.07 ($SiMe_2$). ^{11}B NMR (benzene, 192 MHz, 25 °C): δ –68.2 (br). ^{19}F NMR (benzene, 564 MHz, 25 °C): δ –157.4 (3 F, *para*-C_6F_5), –164.3 (6 F, *meta*-C_6F_5. IR (KBr, cm^{-1}): 2960 m, 2904 w, 1646 s, 1516 s br, 1467 s br, 1370 br, 1314 br, 1258 br, 1099 s br, 1081 s br, 977 s br, 890 s br, 842 s.

PrC(SiHMe$_2$)$_3${HB(C$_6$F$_5$)$_3$}$_2$ (2c). $B(C_6F_5)_3$ (0.098 g, 0.192 mmol) was added to a benzene (4 mL) solution of $Pr\{C(SiHMe_2)_3\}_3$ (0.068 g, 0.096 mmol) in small portions. The resulting yellow mixture was stirred at room temperature for 1 h. The solvent was evaporated under reduced pressure to give a yellow paste. The residue was washed with pentane (2 × 5 mL) and the volatiles were evaporated to dryness in vacuo to give $PrC(SiHMe_2)_3\{HB(C_6F_5)_3\}_2$ as a pale yellow solid (0.099 g, 0.073 mmol, 76.3%). ^{1}H NMR (benzene-*d*$_6$, 600 MHz, 25 °C): δ 14.12 ($SiMe_2$). ^{11}B NMR (benzene-*d*$_6$, 192 MHz, 25 °C): δ –23.4 (br). ^{19}F NMR (benzene-*d*$_6$, 564 MHz, 25 °C): δ –154.8 (3 F, *para*-C_6F_5), –163.9 (6 F, *meta*-C_6F_5). IR (KBr, cm^{-1}): 2963 m, 2914

w, , 2257 w br (ν_{BH}), 2113 s (ν_{SiH}), 1648 m, 1605 w, 1518 s, 1467 s br, 1372 m, 1266 s, 1114 s br, 1085 s br, 971 s br, 953 s br, 895 s br, 840 s br, 791 s, 769 m. Anal. Calcd. for $B_2C_{43}F_{30}H_{23}Si_3Pr$: C, 38.07; H, 1.71. Found: C, 37.45; H, 4.07. mp = 170-173 °C.

$PrC(SiDMe_2)_3\{DB(C_6F_5)_3\}_2$ (2c-d_5). $B(C_6F_5)_3$ (0.151 g, 0.294 mmol) was added to a benzene (4 mL) solution of $Pr\{C(SiDMe_2)_3\}_3$ (0.106 g, 0.147 mmol) in small portions. The resulting yellow mixture was stirred at room temperature for 1 h. The solvent was evaporated under reduced pressure to give a yellow paste. The residue was washed with pentane (2 × 5 mL) and the volatiles were evaporated to dryness in vacuo to give $PrC(SiDMe_2)_3\{DB(C_6F_5)_3\}_2$ as a pale yellow solid (0.156 g, 0.115 mmol, 76.1%). ^{1}H NMR (benzene, 600 MHz, 25 °C): δ 14.14 ($SiMe_2$). ^{19}F NMR (benzene, 564 MHz, 25 °C): δ –153.9 (3 F, *para*-C_6F_5), –163.7 (6 F, *meta*-C_6F_5) . IR (KBr, cm^{-1}): 2964 m, 2907 w, 1648 s, 1607 w, 1517 s br, 1467 s br, 1370 m, 1267 s br, 1101 s br, 1083 s br, 974 s br, 944 s br, 877 s br, 845 s br, 796 s br, 706 m br.

$Nd\{C(SiHMe_2)_3\}_2HB(C_6F_5)_3$ (1d). The compound was prepared following the procedure for **2a**, with $B(C_6F_5)_3$ (0.033 g, 0.065 mmol) and $Nd\{C(SiHMe_2)_3\}_3$ (0.046 g, 0.065 mmol) giving $Nd\{C(SiHMe_2)_3\}_2HB(C_6F_5)_3$ as a green solid (0.057 g, 0.055 mmol, 84.7%). ^{1}H NMR (benzene-d_6, 600 MHz, 25 °C): δ 5.63 ($SiMe_2$). ^{11}B NMR (benzene-d_6, 192 MHz, 25 °C): δ –4.2 (s). ^{19}F NMR (benzene-d_6, 564 MHz, 25 °C): δ –156.6 (3 F, *para*-C_6F_5), –162.9 (6 F, *meta*-C_6F_5) . IR (KBr, cm^{-1}): 2959 m, 2904 w, 2255 m br (ν_{BH}), 2114 s (ν_{SiH}), 1792 m br (ν_{SiH}), 1646 m, 1605 w, 1516 s, 1467 s br, 1372 m, 1258 s, 1110 s br, 1080 s br, 972 s br, 960 s br, 894 s br, 835 br, 786

s, 681 m. Anal. Calcd. for $BC_{32}F_{15}H_{43}Si_6Nd$: C, 37.24; H, 4.20. Found: C, 37.51; H, 4.56. mp = 178 °C dec.

$Nd\{C(SiDMe_2)_3\}_2DB(C_6F_5)_3$ (1d-d_7). The compound was prepared following the procedure for **2a**, with $B(C_6F_5)_3$ (0.102 g, 0.200 mmol) and $Nd\{C(SiDMe_2)_3\}_3$ (0.144 g, 0.200 mmol) affording $Nd\{C(SiDMe_2)_3\}_2DB(C_6F_5)_3$ as a green solid (0.152 g, 0.146 mmol, 48.9%). ^{1}H NMR (benzene, 600 MHz, 25 °C): δ 5.59 (br, $SiMe_2$). ^{11}B NMR (benzene, 192 MHz, 25 °C): δ –4.0 (br). ^{19}F NMR (benzene, 564 MHz, 25 °C): δ –156.6 (3 F, *para*-C_6F_5), –162.9 (6 F, *meta*-C_6F_5). IR (KBr, cm^{-1}): 2959 m, 2903 w, 1646, 1607 br, 1516 s br, 1467 s br, 1370 br, 1312 br, 1258 br, 1101 s br, 1080 s br, 977 s br, 892 s br, 841 s.

$NdC(SiHMe_2)_3\{HB(C_6F_5)_3\}_2$ (2d). The compound was prepared following the procedure for **3a**, with $B(C_6F_5)_3$ (0.067 g, 0.132 mmol) and $Nd\{C(SiHMe_2)_3\}_3$ (0.047 g, 0.066 mmol) providing $NdC(SiHMe_2)_3\{HB(C_6F_5)_3\}_2$ as a green solid (0.076 g, 0.056 mmol, 84.8%). ^{1}H NMR (benzene-d_6, 600 MHz, 25 °C): δ 10.69 (C_7H_8), 8.29 ($SiMe_2$), 5.43 (C_7H_8), 2.92 (C_7H_8), –3.63 (C_7H_8). ^{11}B NMR (benzene-d_6, 192 MHz, 25 °C): δ 25.1 (s). $^{13}C\{^1H\}$ NMR (benzene-d_6, 150 MHz, 25 °C): δ 132.03 (C_6F_5), –1.12 ($SiMe_2$). ^{19}F NMR (benzene-d_6, 564 MHz, 25 °C): δ –154.24 (3 F, *para*-C_6F_5), –161.76 (6 F, *meta*-C_6F_5). IR (KBr, cm^{-1}): 2963 m,, 2257 m br (ν_{BH}), 2111 s (ν_{SiH}),, 1648 m, 1606 w, 1518 s, 1467 s br, 1372 m, 1282 s, 1266 s br, 1116 s br, 1081 s br, 973 s br, 954 s br, 895 s br, 842 br, 790 s. Anal. Calcd. for $B_2C_{43}F_{30}H_{23}Si_3Nd$: C, 37.98; H, 1.71. Found: C, 38.09; H, 1.92. mp = 181-184 °C.

$NdC(SiDMe_2)_3\{DB(C_6F_5)_3\}_2$ (2d-d_5). The compound was prepared following the procedure for **3a**, with $B(C_6F_5)_3$ (0.087 g, 0.170 mmol) and $Nd\{C(SiDMe_2)_3\}_3$ (0.061 g, 0.085 mmol) $NdC(SiDMe_2)_3\{DB(C_6F_5)_3\}_2$ (**3d**-d_3) was obtained as a green solid (0.098 g, 0.072 mmol, 85.0%). ^{1}H NMR (benzene-d_6, 600 MHz, 25 °C): δ 8.29 (br, $SiMe_2$). ^{11}B NMR (benzene, 192 MHz, 25 °C): δ 37.8 (s). ^{19}F NMR (benzene, 564 MHz, 25 °C): δ –153.4 (3 F, *para*-C_6F_5), –162.3 (6 F, *meta*-C_6F_5) . IR (KBr, cm^{-1}): 2962 m, 2907 w, 1648 s, 1607 w, 1517 s br, 1465 s br, 1371 m, 1282 s br, 1261 s br, 1124 s br, 1102 s br, 1082 s br, 975 s br, 943 s br, 880 s br, 845 s br, 799 s br, 704 m.

Catalytic hydrosilylation of acrylates using 1b as catalyst

Reaction of $PhMeSiH_2$ and methyl acrylate. $Ce\{C(SiHMe_2)_3\}_2HB(C_6F_5)_3$ (0.015 g, 0.014 mmol), methyl acrylate (0.122 g, 1.41 mmol), and $PhMeSiH_2$ (0.175 g, 1.41 mmol) were stirred in benzene for 30 min at room temperature. The solution was passed through celite and benzene was removed under reduced pressure, leaving behind a colorless gel. The remaining residue was purified by silica gel column chromatography (hexane:ethyl acetate = 9.8:0.2) to afford diastereomers of, $PhMe(H)Si(H)MeCCO_2Me$ (0.242 g, 1.16 mmol, 82.4%). ^{1}H NMR (chloroform-*d*, 600 MHz): δ 0.44 (d, $^3J_{HH}$ = 3.6 Hz, 3 H, SiMe), 0.47 (d, $^3J_{HH}$ = 3.6 Hz, 3 H, SiMe), 1.23 (d, $^3J_{HH}$ = 7.2 Hz, 3 H, CH*Me*), 1.25 (d, $^3J_{HH}$ = 7.2 Hz, 3 H, CH*Me*), 2.85 (qd, $^3J_{HH}$ = 5.4 Hz, $^3J_{HH}$ = 1.8 Hz, 1 H, C*H*Me), 3.59 (s, 1 H, CO_2*Me*), 3.61 (s, 1 H, CO_2*Me*), 4.42 (m, $^1J_{SiH}$ = 200 Hz, 1 H, SiH), 4.46 (m, $^1J_{SiH}$ = 200 Hz, 1 H, SiH), 7.37-7.44 (m, 3 H, C_6H_5), 7.54 (m, 2 H, C_6H_5). ^{13}C{^{1}H} NMR (chloroform-*d*, 150 MHz,): δ –7.04 (SiMe), –6.71 (SiMe), 11.63 (CH*Me*), 12.05 (CH*Me*), 28.38 (*C*HMe), 51.48 (CO_2*Me*), 51.49 (CO_2*Me*), 128.17 (C_6H_5), 128.18 (C_6H_5), 130.15 (C_6H_5), 130.16 (C_6H_5), 133.43 (*ipso*-C_6H_5), 133.78 (*ipso*-C_6H_5), 134.76 (C_6H_5), 134.80

(C_6H_5), 176.17 (*C*=O), 176.23 (*C*=O). $^{29}Si\{^1H\}$ (chloroform-*d*, 119 MHz): δ –7.2 (SiH). IR (KBr, cm^{-1}): 3071 (w), 3050 (w), 2961 (m), 2917 (s), 2849 (s), 2131 (s, ν_{SiH}), 1724 (s, ν_{CO}), 1578 (br s), 1540 (m), 1462 (m), 1430 (s), 1376 (br m), 1358 (br m), 1319 (s), 1256 (br s), 1194 (s), 1181 (s), 1143 (m), 1116 (s), 1085 (m), 1046 (m), 1020 (m), 988 (m), 960 (m), 877 (s), 860 (s), 835 (s), 789 (m), 729 (s). MS (EI): *m/z* = 207.1 [M-1]

$Ph_2HSi(H)MeCCO_2Me$. $Ce\{C(SiHMe_2)_3\}_2HB(C_6F_5)_3$ (0.019 g, 0.018 mmol), dissolved in chloroform (2 mL), was added to a mixture of methyl acrylate (0.155 g, 1.80 mmol) and Ph_2SiH_2 (0.332 g, 1.80 mmol), and the resulting homogeneous solution was allowed to stir for 30 min at room temperature. The solution was passed through celite, and the volatile materials were evaporated under reduced pressure leaving behind a colorless gel. This residue was purified by silica gel column chromatography (hexane:ethyl acetate = 9:1) to afford $Ph_2HSi(H)MeCCO_2Me$ (0.388 g, 1.43 mmol, 79.7%) as a colorless liquid. ^1H NMR (chloroform-*d*, 600 MHz): δ 1.35 (d, $^3J_{HH}$ = 7.3 Hz, 3 H, CH*Me*), 2.73 (qd, $^3J_{HH}$ = 7.2 Hz, $^3J_{HH}$ = 2.8 Hz, 1 H, C*H*Me), 3.49 (s, 1 H, CO_2Me), 4.94 (d, $^3J_{HH}$ = 2.7 Hz, $^1J_{SiH}$ = 205 Hz, 1 H, SiH), 7.38-7.43 (m, 6 H, C_6H_5), 7.60 (m, 2 H, C_6H_5), 7.65 (m, 2 H, C_6H_5). $^{13}C\{^1H\}$ NMR (chloroform-*d*, 150 MHz): δ 12.52 (CH*Me*), 27.88 (*C*HMe), 51.51 (CO_2*Me*), 128.22 (C_6H_5), 128.32 (C_6H_5), 130.32 (C_6H_5), 130.36 (C_6H_5), 131.86 (C_6H_5), 131.94 (C_6H_5), 134.53 (*ipso*-C_6H_5), 135.60 (C_6H_5), 135.65 (C_6H_5), 175.98 (*C*=O). $^{29}Si\{^1H\}$ (chloroform-*d*, 119 MHz): δ –9.9 (SiH). IR (KBr, cm^{-1}): 3070 (m), 3050 (m), 3002 (w), 2949 (w), 2918 (w), 2874 (w), 2850 (w), 2136 (s ν_{SiH}), 1725 (s ν_{CO}), 1590 (m), 1487 (w), 1459 (w), 1429 (s), 1379 (w), 1320 (br s), 1245 (br m), 1196 (br s), 1118 (s), 1066 (br m), 1024 (s), 997 (m), 817 (s), 734 (s), 698 (s). MS (EI): *m/z* = 269.1 [M–1].

$Et_2HSi(H)MeCCO_2Me$. $Ce\{C(SiHMe_2)_3\}_2HB(C_6F_5)_3$ (0.024 g, 0.023 mmol) dissolved in chloroform (2 mL) was added to a mixture of methyl acrylate (0.201 g, 2.34 mmol) and Et_2SiH_2 (0.207 g, 2.34 mmol). The resulting homogeneous solution was allowed to stir for 30 min at room temperature. The solution was passed through celite, and the volatile species were removed under reduced pressure leaving behind a colorless gel. This residue was purified by silica gel column chromatography (hexane:diethyl ether = 9:1) to afford $Et_2HSi(H)MeCCO_2Me$ (0.331 g, 1.90 mmol, 81.1%) as a colorless liquid. ^{1}H NMR (chloroform-*d*, 600 MHz): δ 0.69 (m, 4 H, $SiCH_2CH_3$), 0.997 (t, $^3J_{HH}$ = 7.9 Hz, 3 H, $SiCH_2CH_3$) 1.012 (t, $^3J_{HH}$ = 7.9 Hz, 3 H, $SiCH_2CH_3$), 1.24 (d, $^3J_{HH}$ = 7.2 Hz, 3 H, $CHMeSiHEt_2$), 2.23 (qd, $^3J_{HH}$ = 7.2 Hz, $^3J_{HH}$ = 2.2 Hz, 1 H, $CHMeSiHEt_2$), 3.65 (s, 3 H, OMe), 3.71 (m, $^1J_{SiH}$ = 190 Hz, 1 H, SiH). $^{13}C\{^1H\}$ NMR (chloroform-*d*, 150 MHz): δ 1.96 ($SiCH_2CH_3$), 2.23 ($SiCH_2CH_3$), 8.10 ($SiCH_2CH_3$), 12.00 ($CHMeSiHEt_2$), 26.23 ($CHMeSiHEt_2$), 51.46 (O*Me*), 176.85 (CO_2Me). $^{29}Si\{^1H\}$ (chloroform-*d*, 119 MHz): δ 4.4. IR (KBr, cm^{-1}): 2961 (s), 2915 (m), 2877 (m), 2849 (w), 2118 (s ν_{SiH}), 1729 (s ν_{CO}), 1463 (m), 1434 (w), 1414 (w), 1380 (w), 1319 (br s), 1260 (br s), 1193 (br s), 1181 (br s), 1144 (m), 1088 (br s), 1016 (s), 972 (w), 860 (m), 805 (br s), 717 (w). MS (EI): *m/z* = 173.1 [M – 1].

$PhMeHSi(H)MeCCO_2Et$. $Ce\{C(SiHMe_2)_3\}_2HB(C_6F_5)_3$ (0.018 g, 0.017 mmol) dissolved in chloroform (2 mL) was added to a mixture of ethyl acrylate (0.171 g, 1.71 mmol) and $PhMeSiH_2$ (0.213 g, 1.71 mmol), and the resulting homogeneous solution was allowed to stir for 30 min at room temperature. The solution was passed through celite, and chloroform was removed under reduced pressure leaving behind a colorless gel. This residue was purified by silica gel column

chromatography (hexane:ethyl acetate = 9.7:0.3) to afford diastereomers of PhMeHSi(H)MeCCO$_2$Et (0.322 g, 1.45 mmol, 84.7%) as a colorless liquid. ^{1}H NMR (chloroform-*d*, 600 MHz): δ 0.45 (d, $^3J_{HH}$ = 3.7 Hz, 3 H, Si*Me*), 0.47 (d, $^3J_{HH}$ = 3.7 Hz, 3 H, Si*Me*), 1.148 (t, $^3J_{HH}$ = 7.2 Hz, 3 H, CO$_2$CH$_2$C*H*$_3$), 1.164 (t, $^3J_{HH}$ = 7.2 Hz, 3 H, CO$_2$CH$_2$C*H*$_3$), 1.22 (d, $^3J_{HH}$ = 7.3 Hz, 3 H, CH*Me*SiHMePh), 1.24 (d, $^3J_{HH}$ = 7.3 Hz, 3 H, CH*Me*SiHMePh), 2.36 (m, 2 H, C*H*MeSiHMePh), 4.06 (m, 4 H, CO$_2$C*H*$_2$CH$_3$), 4.12 (qd, $^3J_{HH}$ = 3.6 Hz, $^3J_{HH}$ = 0.6 Hz, $^1J_{SiH}$ = 200 Hz, 1 H, SiH), 4.45 (qd, $^3J_{HH}$ = 2.4 Hz, $^3J_{HH}$ = 1.2 Hz, $^1J_{SiH}$ = 200 Hz, 1 H, SiH), 7.37-7.43 (m, 6 H, C$_6$H$_5$), 7.55 (m, 4 H, C$_6$H$_5$). ^{13}C{^{1}H} NMR (chloroform-*d*, 150 MHz): δ –6.92 (SiMe), –6.73 (SiMe), 11.64 (COC*Me*), 12.05 (COC*Me*), 14.47 (CO$_2$CH$_2$*C*H$_3$), 14.50 (CO$_2$CH$_2$*C*H$_3$), 28.40 (CO*C*Me), 60.24 (CO$_2$*C*H$_2$CH$_3$), 128.15 (C$_6$H$_5$), 130.12 (C$_6$H$_5$), 133.58 (*ipso*-C$_6$H$_5$), 133.92 *(ipso*-C$_6$H$_5$), 134.82 (C$_6$H$_5$), 134.86 (C$_6$H$_5$), 175.75 (*C*OCMe), 175.80 (*C*OCMe). ^{29}Si{^{1}H} (chloroform-*d*, 119 MHz): δ –7.3 (SiH). IR (KBr, cm^{-1}): 3071 (w), 3052 (w), 2977 (m), 2963 (m), 2930 (m), 2873 (w), 2851 (w), 2132 (s ν_{SiH}), 1719 (s ν_{CO}), 1463 (m), 1423 (m), 1389 (w), 1378 (m), 1366 (w), 1314 (br s), 1254 (br m), 1240 (m), 1184 (br s), 1143 (s), 1117 (br m), 1059 (s), 1016 (m), 978 (w), 876 (s), 835 (s), 792 (m), 730 (s), 699 (s). MS (EI): *m/z* = 221.0 [M–1].

Ph$_2$HSi(H)MeCCO$_2$Et. Ce{C(SiHMe$_2$)$_3$}$_2$HB(C$_6$F$_5$)$_3$ (0.018 g, 0.017 mmol) dissolved in chloroform (2 mL) was added to a mixture of ethyl acrylate (0.171 g, 1.71 mmol) and Ph$_2$SiH$_2$ (0.315 g, 1.71 mmol), and the resulting homogeneous solution was allowed to stir for 30 min at room temperature. The solution was passed through celite, and chloroform was removed under reduced pressure leaving behind a colorless gel. This residue was purified by silica gel column chromatography (hexane:ethyl acetate = 9.5:0.5) to afford Ph$_2$HSi(H)MeCCO$_2$Et (0.361 g, 1.27

mmol, 74.3%) as a colorless liquid. ^{1}H NMR (chloroform-*d*, 600 MHz): δ 1.02 (t, $^{3}J_{HH}$ = 7.2 Hz, 3 H, $CO_2CH_2CH_3$), 1.37 (d, $^{3}J_{HH}$ = 7.3 Hz, 3 H, CH*Me*), 2.73 (qd, $^{3}J_{HH}$ = 7.2 Hz, $^{3}J_{HH}$ = 2.7 Hz, 1 H, C*H*Me), 3.96 (m, 2 H, $CO_2CH_2CH_3$), 4.97 (d, $^{3}J_{HH}$ = 2.7 Hz, $^{1}J_{SiH}$ = 205 Hz, 1 H, SiH), 7.39-7.48 (m, 6 H, C_6H_5), 7.63 (m, 2 H, C_6H_5), 7.67 (m, 2 H, C_6H_5). ^{13}C{^{1}H} NMR (chloroform-*d*, 150 MHz): δ 12.46 (COC*Me*), 14.16 ($CO_2CH_2CH_3$), 27.82 (CO*C*Me), 60.31 ($CO_2CH_2CH_3$), 128.16 (C_6H_5), 128.25 (C_6H_5), 130.25 (C_6H_5), 130.28 (C_6H_5), 131.98 (C_6H_5), 132.00 (C_6H_5), 134.49 (*ipso*-C_6H_5), 135.64 (C_6H_5), 135.65 (C_6H_5), 135.85 (C_6H_5), 175.49 (*C*OCMe). ^{29}Si{^{1}H} (chloroform-*d*, 119 MHz): δ –9.8 (SiH). IR (KBr, cm^{-1}): 3071 (w), 3050 (w), 2964 (s), 2905 (m), 2875 (w), 2135 (s ν_{SiH}), 1717 (s ν_{CO}), 1429 (s), 1313 (m), 1261 (s), 1185 (br s), 1143 (w), 1109 (br m), 1016 (br s), 863 (m), 804 (s), 734 (s), 698 (s). MS (EI): *m/z* = 283.1 [M–1].

$Et_2HSi(H)MeCCO_2Et$. $Ce\{C(SiHMe_2)_3\}_2HB(C_6F_5)_3$ (0.016 g, 0.015 mmol) dissolved in chloroform (2 mL) was added to a mixture of ethyl acrylate (0.151 g, 1.51 mmol) and Et_2SiH_2 (0.133 g, 1.51 mmol) and the resulting homogeneous solution was allowed to stir for 30 min at room temperature. The solution was passed through celite, and chloroform was removed under reduced pressure leaving behind a colorless gel. The residue was purified by silica gel column chromatography (hexane:diethyl ether = 9.5:0.5) to afford $Et_2HSi(H)MeCCO_2Et$ (0.225 g, 1.19 mmol, 79.2%) as a colorless liquid. ^{1}H NMR (chloroform-*d*, 600 MHz): δ 0.70 (m, 4 H, $SiCH_2CH_3$), 1.011 (t, $^{3}J_{HH}$ = 7.9 Hz, 3 H, $SiCH_2CH_3$) 1.028 (t, $^{3}J_{HH}$ = 8.0 Hz, 3 H, $SiCH_2CH_3$), 1.242 (d, $^{3}J_{HH}$ = 7.3 Hz, 3 H, CH*Me*$SiHEt_2$), 1.250 (t, $^{3}J_{HH}$ = 7.2 Hz, 3 H, $CO_2CH_2CH_3$), 2.22 (qd, $^{3}J_{HH}$ = 7.2 Hz, $^{3}J_{HH}$ = 2.1 Hz, 1 H, C*H*$MeSiHEt_2$), 3.72 (m, $^{1}J_{SiH}$ = 189 Hz, 1 H, SiH), 4.12 (m, 2 H, $CO_2CH_2CH_3$). ^{13}C{^{1}H} NMR (chloroform-*d*, 150 MHz): δ 2.00 ($SiCH_2CH_3$), 2.31

($SiCH_2CH_3$), 8.18 ($SiCH_2CH_3$), 12.00 ($CHMeSiHEt_2$), 14.61 ($CO_2CH_2CH_3$), 26.32 ($CHMeSiHEt_2$), 60.15 ($CO_2CH_2CH_3$), 176.41 (CO_2Me). $^{29}Si\{^1H\}$ (chloroform-*d*, 119 MHz): δ 4.2. IR (KBr, cm^{-1}): 2938 (br s), 2913 (br s), 2877 (s), 2115 (s ν_{SiH}), 1723 (s ν_{CO}), 1463 (m), 1414 (w), 1379 (w), 1366 (m), 1315 (s), 1237 (br s), 1182 (br s), 1143 (s), 1083 (m), 1050 (m), 1015 (s), 978 (s), 900 (m), 859 (w), 819 (s), 770 (m), 715 (m). MS (EI): *m/z* = 187.1 [M – 1].

PhMeHSi(H)MeCCO$_2$CH$_2$Ph. $Ce\{C(SiHMe_2)_3\}_2HB(C_6F_5)_3$ (0.008 g, 0.007 mmol), dissolved in chloroform (2 mL), was added to a mixture of benzyl acrylate (0.118 g, 0.727 mmol) and $PhMeSiH_2$ (0.090 g, 0.727 mmol) and the resulting homogeneous solution was allowed to stir for 30 min at room temperature. The solution was passed through celite, and the volatile materials were removed under reduced pressure, leaving behind a colorless gel. The residue was purified by silica gel column chromatography (hexane:ethyl acetate = 9:1) to afford PhMeHSi(H)MeCCO$_2$CH$_2$Ph (0.167 g, 0.587 mmol, 80.6%) as a colorless liquid. ^1H NMR (chloroform-*d*, 600 MHz): δ 0.43 (d, $^3J_{HH}$ = 3.8 Hz, 3 H, SiMe), 0.45 (d, $^3J_{HH}$ = 3.7 Hz, 3 H, SiMe), 1.28 (d, $^3J_{HH}$ = 7.1 Hz, 3 H, CH*Me*), 1.30 (d, $^3J_{HH}$ = 7.1 Hz, 3 H, CH*Me*), 2.46 (m, 2 H, C*H*Me), 4.45 (vq, $^3J_{HH}$ = 3.0 Hz, $^1J_{SiH}$ = 200 Hz, 1 H, SiH), 4.49 (vq, $^3J_{HH}$ = 2.4 Hz, $^1J_{SiH}$ = 200 Hz, 1 H, SiH), 5.04 (d, 1 H, $^2J_{HH}$ = 12.3 Hz, CH_2Ph), 5.07 (d, 1 H, $^2J_{HH}$ = 12.3 Hz, CH_2Ph), 5.08 (s, 2 H, CO_2CH_2Ph), 7.28 (m, 4 H, C_6H_5), 7.29-7.36 (m, 10 H, C_6H_5), 7.36-7.37 (m, 2 H, C_6H_5), 7.38-7.40 (m, 4 H, C_6H_5). $^{13}C\{^1H\}$ NMR (chloroform-*d*, 150 MHz): δ –6.93 (SiMe), –6.85 (SiMe), 11.70 (CH*Me*), 12.08 (CH*Me*), 28.46 (*C*HMe), 28.49 (*C*HMe), 66.29 (CO_2CH_2Ph), 128.19 (C_6H_5), 128.26 (C_6H_5), 128.39 (C_6H_5), 128.54 (C_6H_5), 128.57 (C_6H_5), 128.65 (C_6H_5), 130.13 (C_6H_5), 130.16 (C_6H_5), 133.37 (*ipso*-C_6H_5), 133.67 (*ipso*-C_6H_5), 134.83 (C_6H_5), 134.87 (C_6H_5), 136.40 (C_6H_5), 136.45 (C_6H_5), 175.60 (*C*=O), 175.65 (*C*=O). $^{29}Si\{^1H\}$ (chloroform-*d*,

119 MHz): δ –7.4 (SiH). IR (KBr, cm^{-1}): 3070 (m), 3051 (m), 3032 (w), 2963 (m), 2935 (w), 2917 (w), 2875 (w), 2849 (w), 2134 (s ν_{SiH}), 1720 (s ν_{CO}), 1578 (w), 1541 (w), 1497 (w), 1457 (s), 1429 (s), 1376 (s), 1313 (br s), 1258 (s), 1176 (br s), 1140 (m), 1117 (m), 1084 (br m), 1027 (m), 952 (br w), 911 (s), 877 (s), 836 (s), 732 (s), 698 (s). MS (EI): *m/z* = 283.0 [M–1].

$Et_2HSi(H)MeCCO_2CH_2Ph$. $Ce\{C(SiHMe_2)_3\}_2HB(C_6F_5)_3$ (0.013 g, 0.013 mmol) dissolved in chloroform (2 mL) was added to a mixture of benzyl acrylate (0.204 g, 1.26 mmol) and Et_2SiH_2 (0.111 g, 1.26 mmol) and the resulting homogeneous solution was allowed to stir for 30 min at room temperature. The solution was passed through celite, and chloroform was removed under reduced pressure, leaving behind a colorless gel. The residue was purified by silica gel column chromatography (hexane:ethyl acetate = 9.5:0.5) to afford $Et_2HSi(H)MeCCO_2CH_2Ph$ (0.243 g, 0.97 mmol, 77.1%) as a colorless liquid. ^{1}H NMR (chloroform-*d*, 600 MHz): δ 0.66 (m, 4 H, $SiCH_2CH_3$), 0.976 (t, $^3J_{HH}$ = 8.0 Hz, 3 H, $SiCH_2CH_3$) 0.991 (t, $^3J_{HH}$ = 8.0 Hz, 3 H, $SiCH_2CH_3$), 1.27 (d, $^3J_{HH}$ = 7.2 Hz, 3 H, $CHMeSiHEt_2$), 2.29 (qd, $^3J_{HH}$ = 7.2 Hz, $^3J_{HH}$ = 2.2 Hz, 1 H, $CHMeSiHEt_2$), 3.74 (m, $^1J_{SiH}$ = 190 Hz, 1 H, SiH), 5.111 (s, 2 H, CH_2Ph), 5.114 (s, 2 H, CH_2Ph), 7.31–7.35 (m, 2 H, C_6F_5), 7.36 (m, 3 H, C_6F_5). $^{13}C\{^1H\}$ NMR (chloroform-*d*, 150 MHz): δ 1.98 ($SiCH_2CH_3$), 2.23 ($SiCH_2CH_3$), 8.14 ($SiCH_2CH_3$), 8.15 ($SiCH_2CH_3$), 12.02 ($CHMeSiHEt_2$), 26.39 ($CHMeSiHEt_2$), 66.19 (OCH_2Ph), 128.26 (C_6F_5), 128.52 (C_6F_5), 128.67 (C_6F_5), 136.59 (C_6F_5), 176.24 (*C*=O). $^{29}Si\{^1H\}$ (chloroform-*d*, 119 MHz): δ 4.4 (SiH). IR (KBr, cm^{-1}): 3067 (m), 3034 (m), 2958 (s), 2935 (w), 2914 (s), 2875 (w), 2113 (s ν_{SiH}), 1722 (s ν_{CO}), 1498 (m), 1456 (s), 1413 (m), 1378 (m), 1314 (br s), 1232 (m), 1174 (br s), 1138 (s), 1085 (m), 1011 (m), 974 (br m), 817 (s), 697 (s). MS (EI): *m/z* = 249.1 [M-1].

PhMeHSiCMe$_2$CO$_2$Me. Ce{C(SiHMe$_2$)$_3$}$_2$HB(C$_6$F$_5$)$_3$ (0.014 g, 0.013 mmol) dissolved in chloroform (2 mL) was added to a mixture of methyl methacrylate (0.132 g, 1.32 mmol), and PhMeSiH$_2$ (0.164 g, 1.32 mmol) at 0 °C and the solution was allowed to react for 1 h at the same temperature. The solution was allowed to come to room temperature and passed through celite, and chloroform was removed under reduced pressure, leaving behind a colorless gel. The residue was purified by silica gel column chromatography (hexane:ethyl acetate = 9.5:0.5) to afford PhMeHSiCMe$_2$CO$_2$Me (0.258 g, 1.16 mmol, 87.8%) as a colorless liquid. ^{1}H NMR (chloroform-*d*, 600 MHz): δ 0.43 (d, $^3J_{HH}$ = 3.6 Hz, 3 H, SiMe), 1.25 (s, 3 H, CMe$_2$), 1.29 (s, 3 H, CMe$_2$), 3.59 (s, CO$_2$Me), 4.30 (q, $^3J_{HH}$ = 3.6 Hz, $^1J_{SiH}$ = 199 Hz, 1 H, SiH), 7.36-7.38 (m, 2 H, *m*-C$_6$H$_5$), 7.41 (m, 1 H, *p*-C$_6$H$_5$), 7.51 (m, 2 H, *o*-C$_6$H$_5$). ^{13}C{^{1}H} NMR (chloroform-*d*, 150 MHz): δ –7.7 (SiMe), 21.52 (C*Me*$_2$), 21.78 (C*Me*$_2$), 32.15 (*C*Me$_2$), 51.68 (CO$_2$*Me*), 128.03 (C$_6$H$_5$), 130.15 (C$_6$H$_5$), 133.47 (*ipso*-C$_6$H$_5$), 135.26 (C$_6$H$_5$), 178.26 (*C*=O). ^{29}Si{^{1}H} (chloroform-*d*, 119 MHz): δ –1.2 (SiH). IR (KBr, cm^{-1}): 3091 (m), 3070 (m), 3034 (m), 2977 (m), 2961 (m), 2923 (s), 2867 (m), 2852 (m), 2131 (s ν_{SiH}), 1739 (s ν_{CO}), 1716 (s ν_{CO}), 1588 (m), 1467 (s), 1423 (w), 1367 (w), 1343 (m), 1258 (br m), 1190 (br s), 1154 (s), 1117 (s), 1029 (w), 1015 (s), 906 (s), 875 (s), 830 (s), 733 (s), 697 (s). MS (EI): *m/z* = 222.1 [M].

PhMeHSiCMe$_2$CO$_2$CH$_2$CHMe$_2$. Ce{C(SiHMe$_2$)$_3$}$_2$HB(C$_6$F$_5$)$_3$ (0.017 g, 0.016 mmol) dissolved in chloroform (2 mL) was added to a mixture of isobutyl methacrylate (0.231 g, 1.63 mmol), and PhMeSiH$_2$ (0.203 g, 1.63 mmol) and the resulting homogeneous solution was allowed to stir for 30 min at room temperature. The solution was passed through celite, and chloroform was removed under reduced pressure, leaving behind a colorless gel. The residue was purified by

silica gel column chromatography (hexane:ethyl acetate = 9.7:0.2) to afford $PhMeHSiCMe_2CO_2CH_2CHMe_2$ (0.351 g, 1.33 mmol, 81.4%) as a colorless liquid. ^{1}H NMR (chloroform-*d*, 600 MHz): δ 0.45 (d, $^3J_{HH}$ = 3.7 Hz, 3 H, SiMe), 0.88 (d, $^3J_{HH}$ = 1.9 Hz, 3 H, CH*Me*$_2$), 0.89 (d, $^3J_{HH}$ = 1.9 Hz, 3 H, CH*Me*$_2$), 1.27 (s, 3 H, C*Me*$_2$), 1.31 (s, 3 H, C*Me*$_2$), 1.84 (sept, $^3J_{HH}$ = 6.7 Hz, 1 H, C*H*Me$_2$), 3.77 (m, 2 H, C*H*$_2$CHMe$_2$), 4.34 (q, $^3J_{HH}$ = 3.7 Hz, $^1J_{SiH}$ = 199 Hz, 1 H, SiH), 7.35-7.38 (m, 2 H, *m*-C_6H_5), 7.41 (m, 1 H, *p*-C_6H_5), 7.53 (m, 2 H, *o*-C_6H_5). ^{13}C{^{1}H} NMR (chloroform-*d*, 150 MHz): δ –7.59 (SiMe), 19.35 (CO_2CH_2CH*Me*$_2$), 21.49 (C*Me*$_2$), 21.88 (C*Me*$_2$), 27.95 (CO_2CH_2*C*HMe$_2$), 32.19 (*C*Me$_2$), 70.71 (CO_2*C*H$_2$CHMe$_2$), 128.02 (C_6H_5), 130.10 (C_6H_5), 133.53 (C_6H_5), 133.93 (*ipso*-C_6H_5), 135.30 (C_6H_5), 177.86 (*C*=O). ^{29}Si{^{1}H} (chloroform-*d*, 119 MHz): δ –1.3 (SiH). IR (KBr, cm^{-1}): 3071 (m), 3052 (m), 2960 (br s), 2931 (br m), 2872 (s), 2132 (s ν_{SiH}), 1712 (br ν_{CO}), 1468 (s), 1429 (m), 1386 (w), 1368 (m), 1243 (br s), 1156 (br s), 1125 (s), 1033 (s), 875 (s), 831 (s), 791 (s), 732 (s), 699 (s). MS (EI): *m/z* = 264.1 [M].

References

[1] a) B. Marciniec and J. Guliński, *Journal of organometallic chemistry* **1993**, *446*, 15-23; b) B. Marciniec, *Hydrosilylation : a comprehensive review on recent advances*, Springer, [New York], **2009**, p.

[2] a) S. E. Denmark and R. F. Sweis, *Accounts of Chemical Research* **2002**, *35*, 835-846; b) S. E. Denmark and R. F. Sweis, *Chemical and Pharmaceutical Bulletin* **2002**, *50*, 1531-1541.

[3] a) A. J. Chalk and J. F. Harrod, *Journal of the American Chemical Society* **1965**, *87*, 16-21; b) I. Ojima, M. Nihonyanagi and Y. Nagai, *Journal of the Chemical Society, Chemical*

Communications **1972**, 938a-938a; c) K. B in *Platinum complexes of unsaturated siloxanes and platinum containing organopolysiloxanes, Vol.* Google Patents, **1973**; d) I. Ojima and T. Kogure, *Organometallics* **1982**, *1*, 1390-1399; e) I. E. Markó, S. Stérin, O. Buisine, G. Mignani, P. Branlard, B. Tinant and J.-P. Declercq, *Science* **2002**, *298*, 204-206; f) I. Ojima, Z. Li and J. Zhu in *Recent Advances in the Hydrosilylation and Related Reactions*, John Wiley & Sons, Ltd, **2003**, pp. 1687-1792; g) S. Díez-González and S. P. Nolan, *Organic Preparations and Procedures International* **2007**, *39*, 523-559; h) S. Park and M. Brookhart, *Organometallics* **2010**, *29*, 6057-6064.

[4] a) F. Buch, H. Brettar and S. Harder, *Angewandte Chemie-International Edition* **2006**, *45*, 2741-2745; b) V. Leich, T. P. Spaniol, L. Maron and J. Okuda, *Chemical Communications* **2014**, *50*, 2311-2314.

[5] P. F. Fu, L. Brard, Y. W. Li and T. J. Marks, *Journal of the American Chemical Society* **1995**, *117*, 7157-7168.

[6] a) D. J. Parks and W. E. Piers, *Journal of the American Chemical Society* **1996**, *118*, 9440-9441; b) D. J. Parks, J. M. Blackwell and W. E. Piers, *Journal of Organic Chemistry* **2000**, *65*, 3090-3098.

[7] J. Spielmann and S. Harder, *European journal of inorganic chemistry* **2008**, *2008*, 1480-1486.

[8] K. Takeshita, Y. Seki, K. Kawamoto, S. Murai and N. Sonoda, *Journal of Organic Chemistry* **1987**, *52*, 4864-4868.

[9] E. Yoshii, Kobayash.Y, T. Koizumi and T. Oribe, *Chemical & Pharmaceutical Bulletin* **1974**, *22*, 2767-2769.

[10] S. A. Bruno in *1,4-O-metallation process and composition, Vol.* Google Patents, **1988**.

[11] Y. Kim and S. Chang, *Angew Chem Int Ed Engl* **2015**.

[12] N. L. Lampland, A. Pindwal, S. R. Neal, S. Schlauderaff, A. Ellern and A. D. Sadow, *Chem. Sci.* **2015**, *6*, 6901-6907.

[13] X. Yang, C. L. Stern and T. J. Marks, *Angewandte Chemie International Edition in English* **1992**, *31*, 1375-1377.

[14] A. D. Sadow and T. D. Tilley, *Organometallics* **2001**, *20*, 4457-4459.

[15] M. D. Anker, M. Arrowsmith, P. Bellham, M. S. Hill, G. Kociok-Kohn, D. J. Liptrot, M. F. Mahon and C. Weetman, *Chemical Science* **2014**, *5*, 2826-2830.

[16] a) D. A. Walker, T. J. Woodman, D. L. Hughes and M. Bochmann, *Organometallics* **2001**, *20*, 3772-3776; b) S. Dagorne, S. Bellemin-Laponnaz and R. Welter, *Organometallics* **2004**, *23*, 3053-3061; c) S. Milione, F. Grisi, R. Centore and A. Tuzi, *Organometallics* **2006**, *25*, 266-274.

[17] a) L. Jia, X. Yang, C. L. Stern and T. J. Marks, *Organometallics* **1997**, *16*, 842-857; b) I. A. Guzei, R. A. Stockland, Jr and R. F. Jordan, *Acta Crystallographica Section C* **2000**, *56*, 635-636; c) A. D. Sadow and T. D. Tilley, *Journal of the American Chemical Society* **2003**, *125*, 9462-9475.

[18] a) P. B. Glaser and T. D. Tilley, *Journal of the American Chemical Society* **2003**, *125*, 13640-13641; b) S. Dagorne, I. Janowska, R. Welter, J. Zakrzewski and G. Jaouen, *Organometallics* **2004**, *23*, 4706-4710.

[19] a) K. Yan, J. J. Duchimaza Heredia, A. Ellern, M. S. Gordon and A. D. Sadow, *Journal of the American Chemical Society* **2013**, *135*, 15225-15237; b) K. Yan, B. M. Upton, A. Ellern and A. D. Sadow, *Journal of the American Chemical Society* **2009**, *131*, 15110-15111.

[20] a) A. D. Horton and J. de With, *Organometallics* **1997**, *16*, 5424-5436; b) A. D. Horton, J. de With, A. J. van der Linden and H. van de Weg, *Organometallics* **1996**, *15*, 2672-2674.

[21] R. D. Shannon, *Acta Crystallographica* **1976**, *A32*, 751-767.

[22] E. L. Werkema, R. A. Andersen, A. Yahia, L. Maron and O. Eisenstein, *Organometallics* **2009**, *28*, 3173-3185.

[23] D. R. Click, B. L. Scott and J. G. Watkin, *Chemical Communications* **1999**, 633-634.

[24] A. G. Massey and A. J. Park, *Journal of Organometallic Chemistry* **1964**, *2*, 245-250.

Supporting Information.

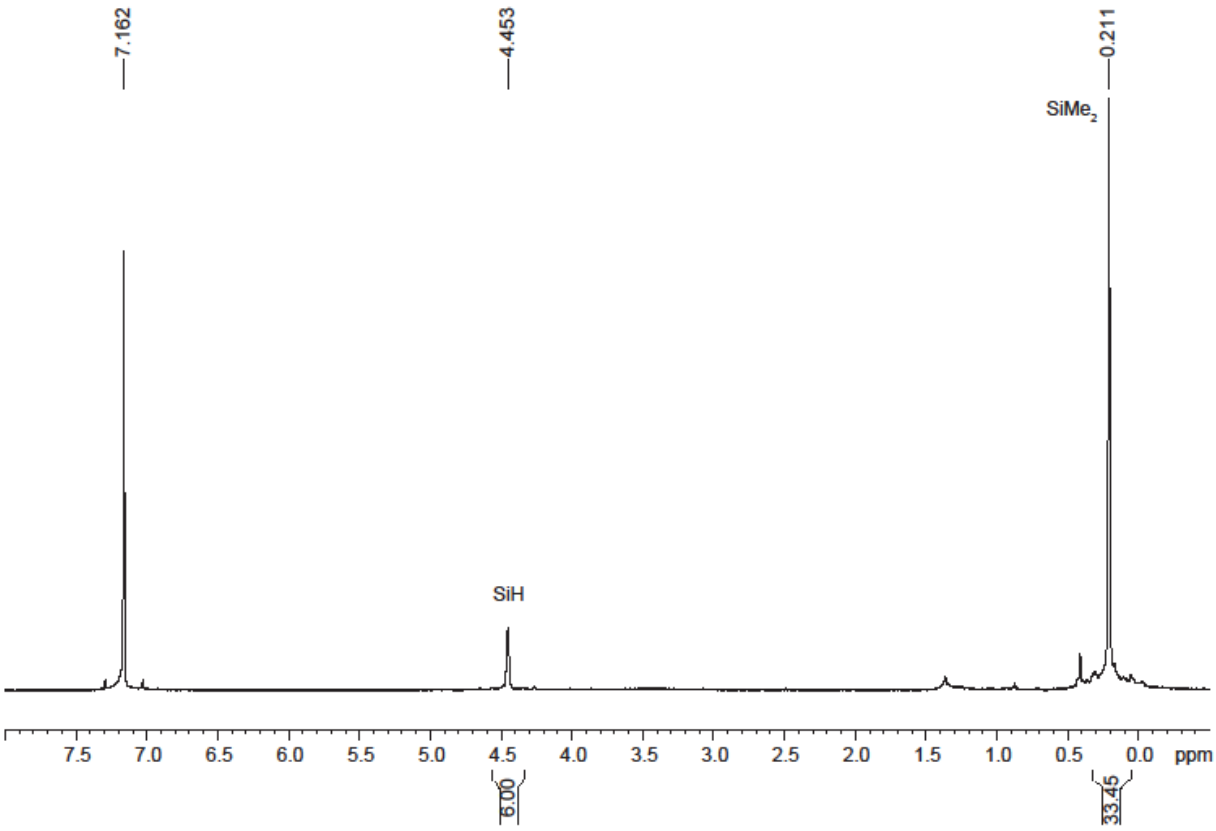

Figure S1. ^{1}H NMR (600 MHz, benzene-d_6) of La{C(SiHMe$_2$)$_3$}$_2$HB(C$_6$F$_5$)$_3$ (**1a)**.

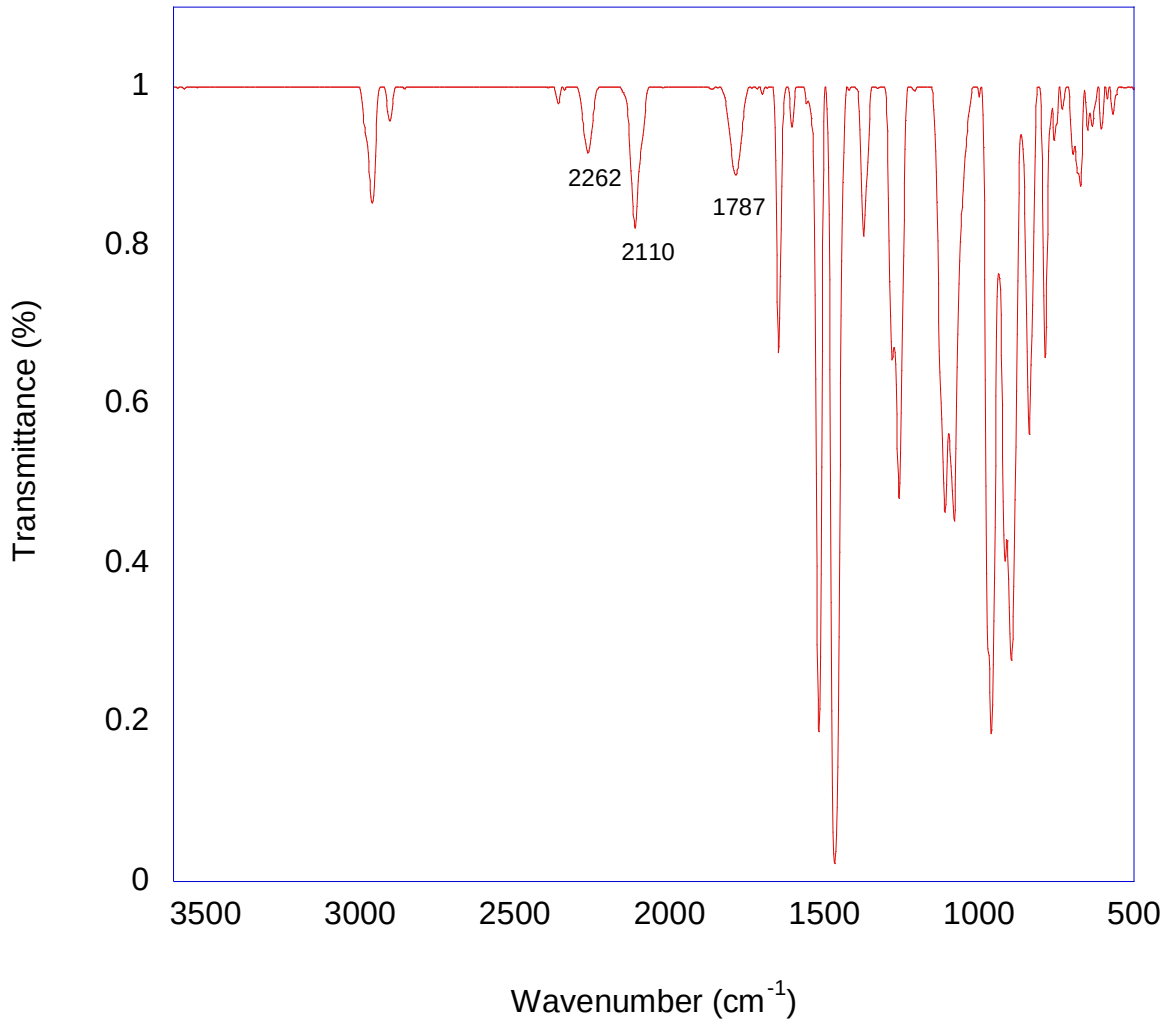

Figure S2. IR (KBr) spectrum of La{C(SiHMe$_2$)$_3$}$_2$HB(C$_6$F$_5$)$_3$ (**1a)**.

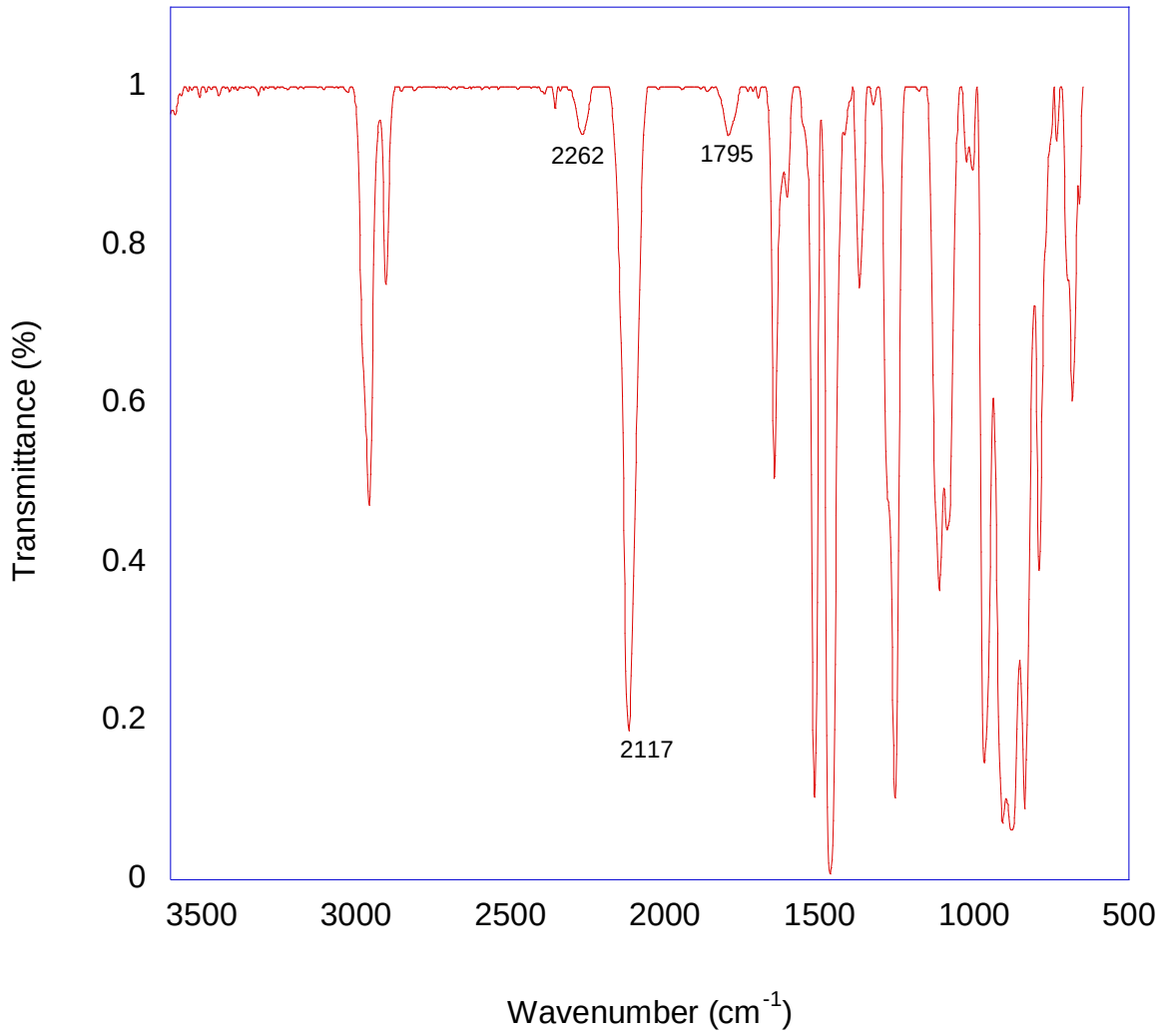

Figure S3. IR (KBr) spectrum of $Ce\{C(SiHMe_2)_3\}_2HB(C_6F_5)_3$ (**1b)**.

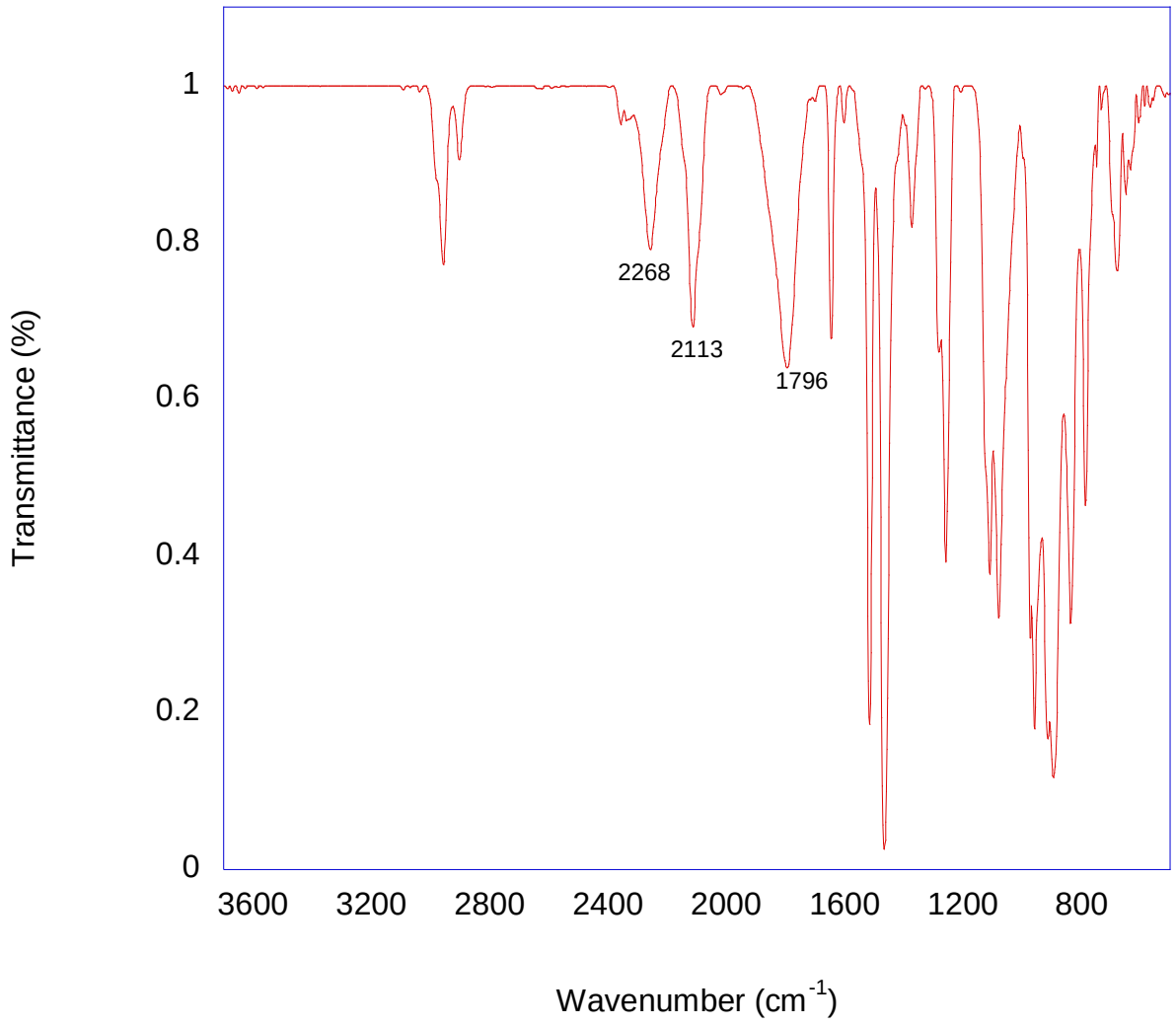

Figure S4. IR (KBr) spectrum of $Pr\{C(SiHMe_2)_3\}_2HB(C_6F_5)_3$ (**1c)**.

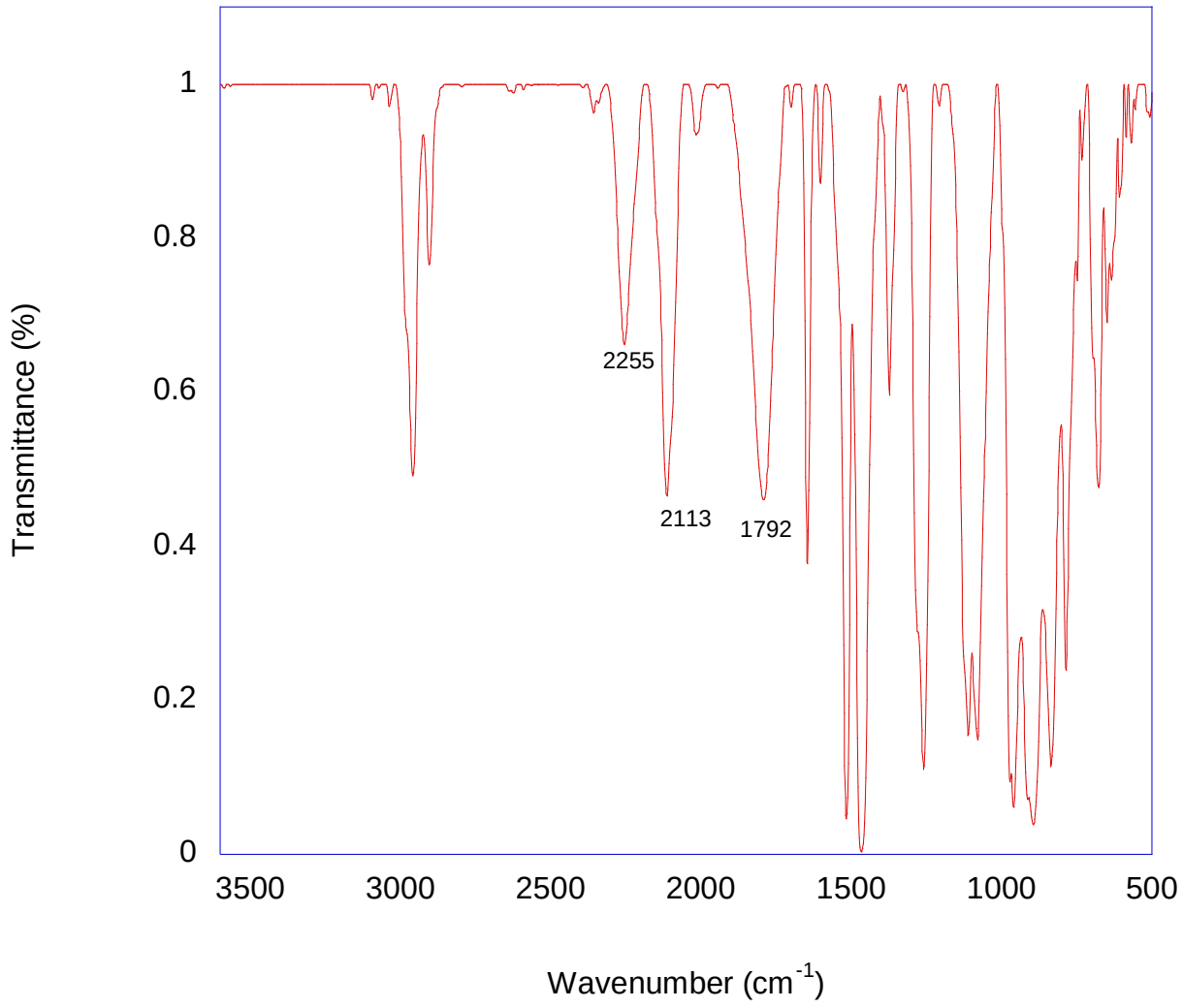

Figure S5. IR (KBr) spectrum of $Nd\{C(SiHMe_2)_3\}_2HB(C_6F_5)_3$ (**1d)**.

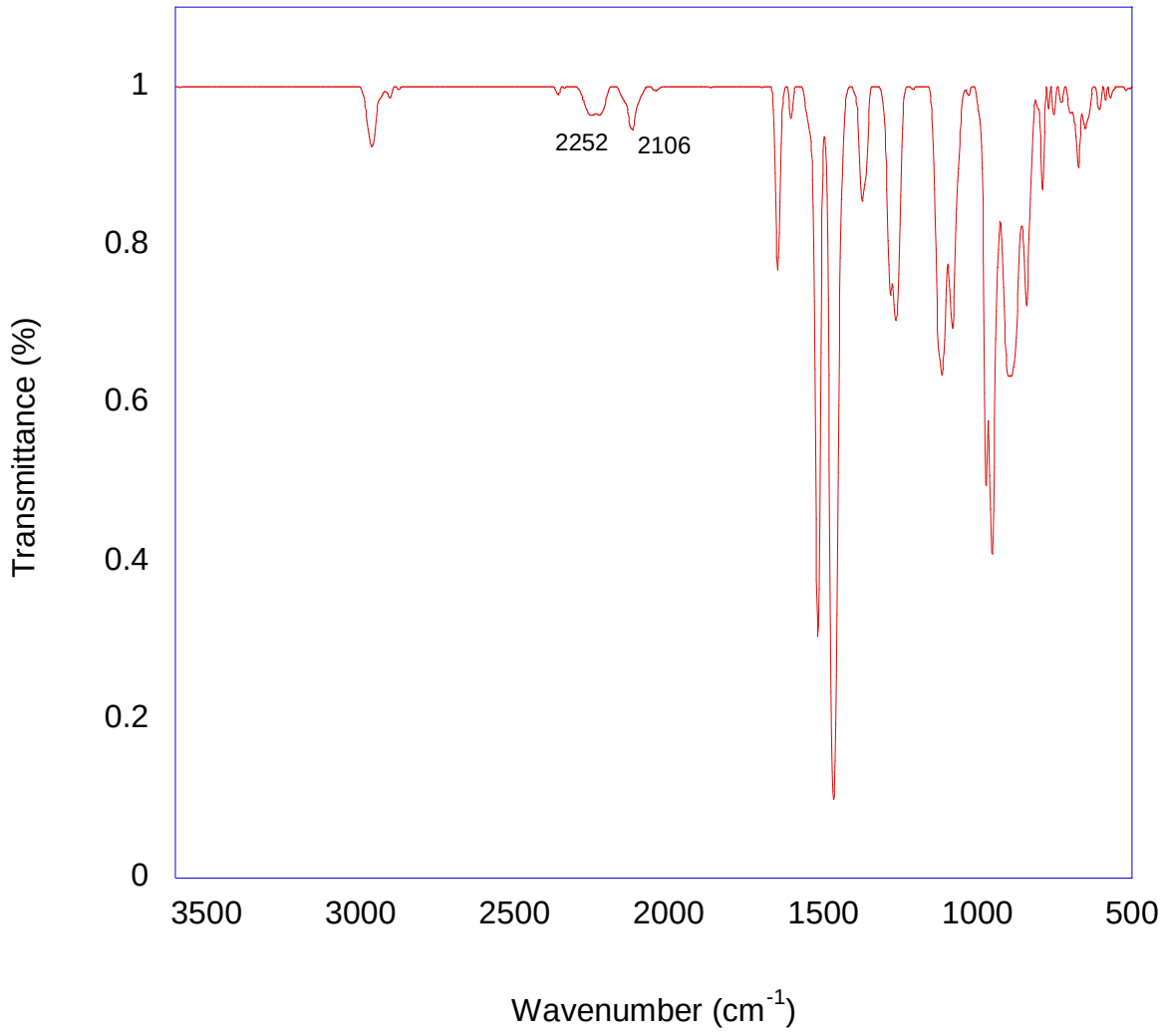

Figure S6. IR (KBr) spectrum of $LaC(SiHMe_2)_3\{HB(C_6F_5)_3\}_2$ **(2a)**.

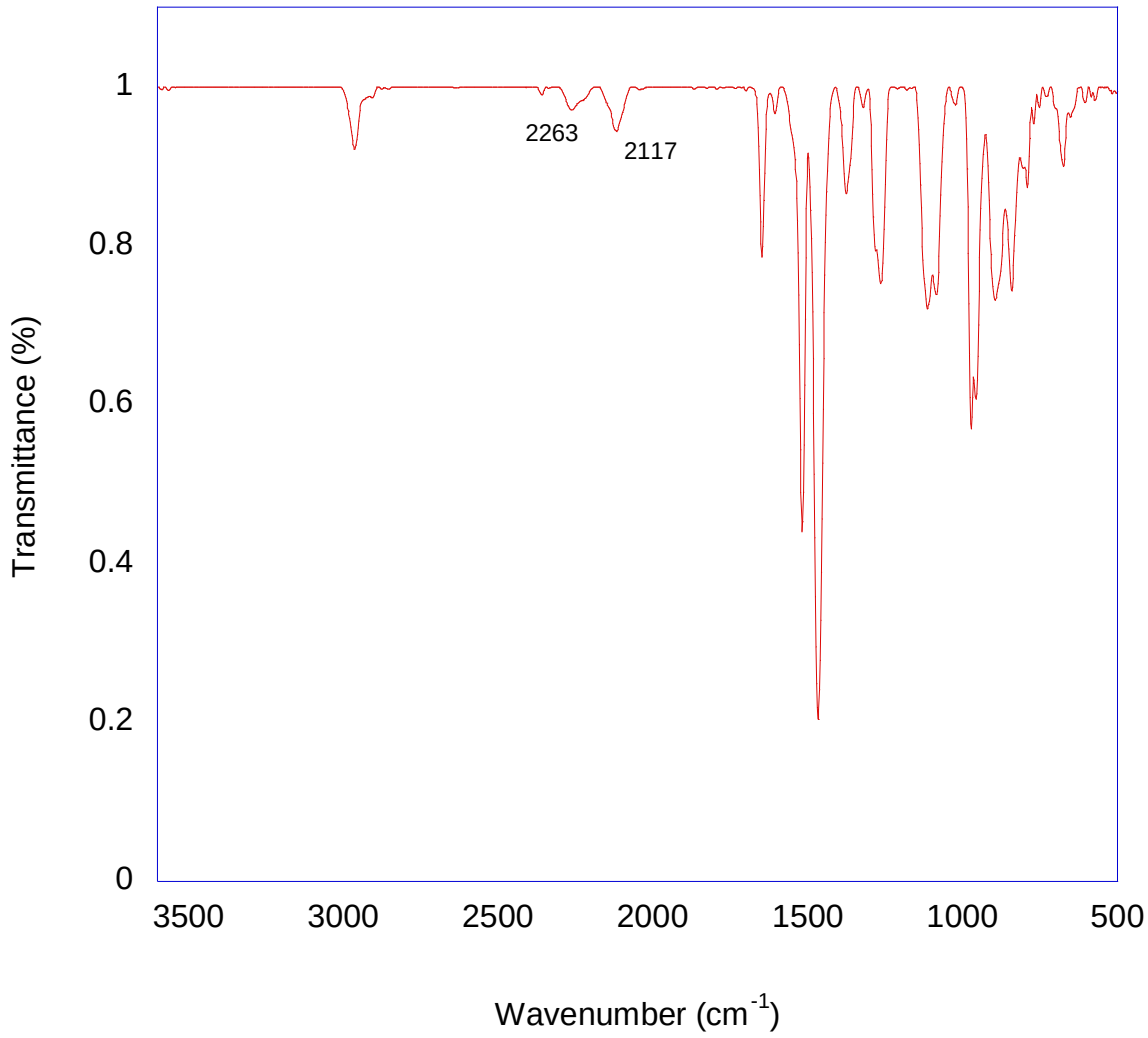

Figure S7. IR (KBr) spectrum of $CeC(SiHMe_2)_3\{HB(C_6F_5)_3\}_2$ (**2b)**.

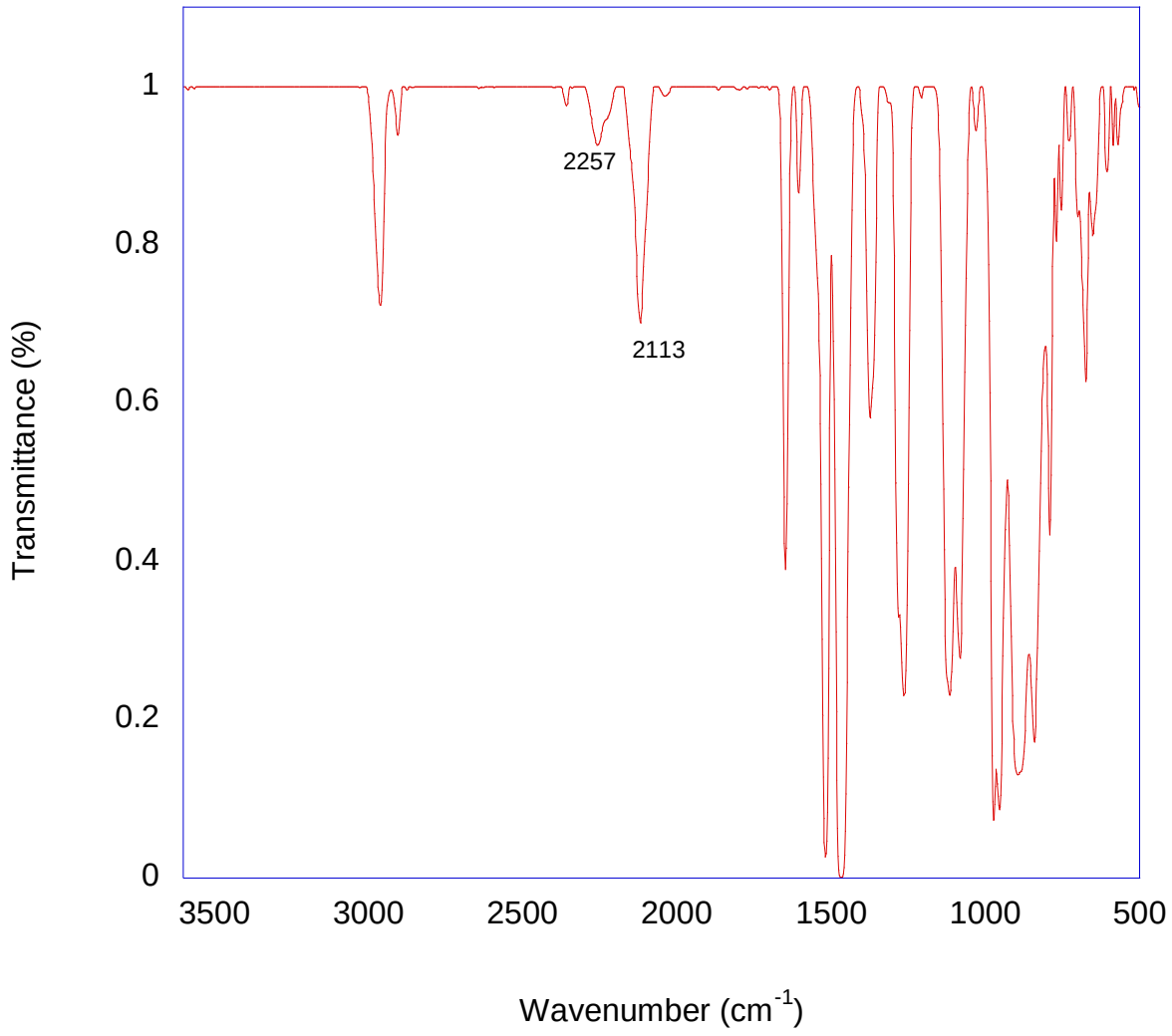

Figure S8. IR (KBr) spectrum of $PrC(SiHMe_2)_3\{HB(C_6F_5)_3\}_2$ (**2c)**.

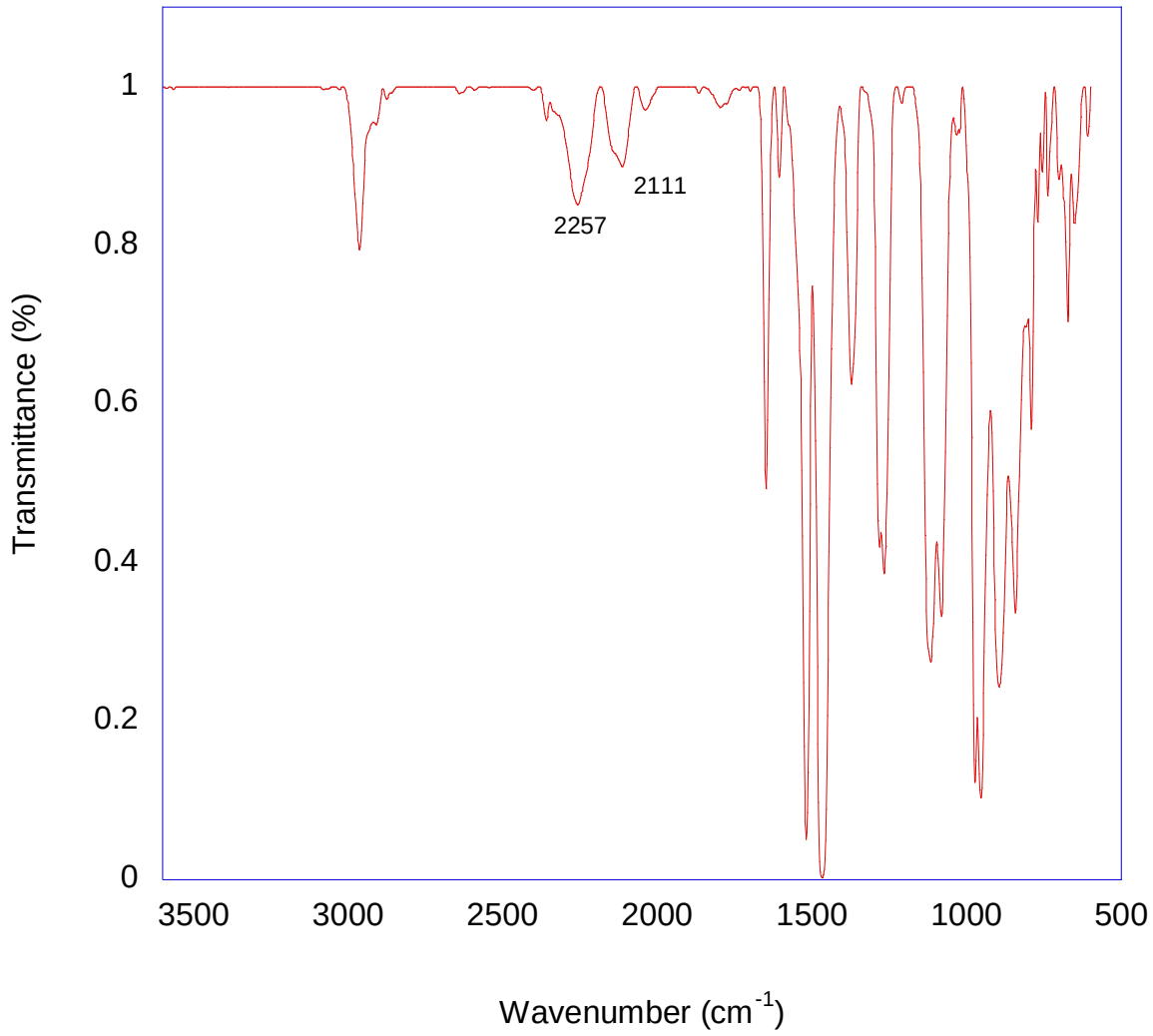

Figure S9. IR (KBr) spectrum of $NdC(SiHMe_2)_3\{HB(C_6F_5)_3\}_2$ (**2d)**.

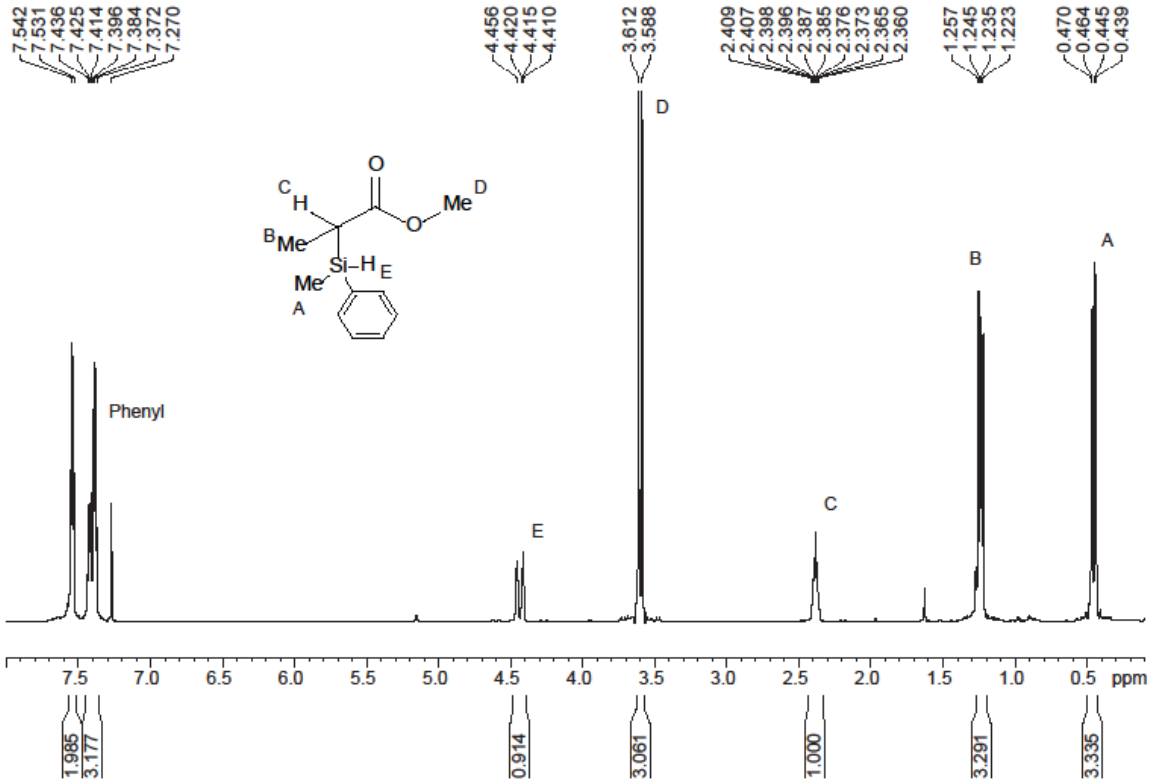

Figure S10. ^{1}H NMR spectrum (600 MHz, chloroform-*d*) for catalytic reaction of methyl acrylate and $PhMeSiH_2$ to yield diastereomers of $PhMeHSi(H)MeCCO_2Me$.

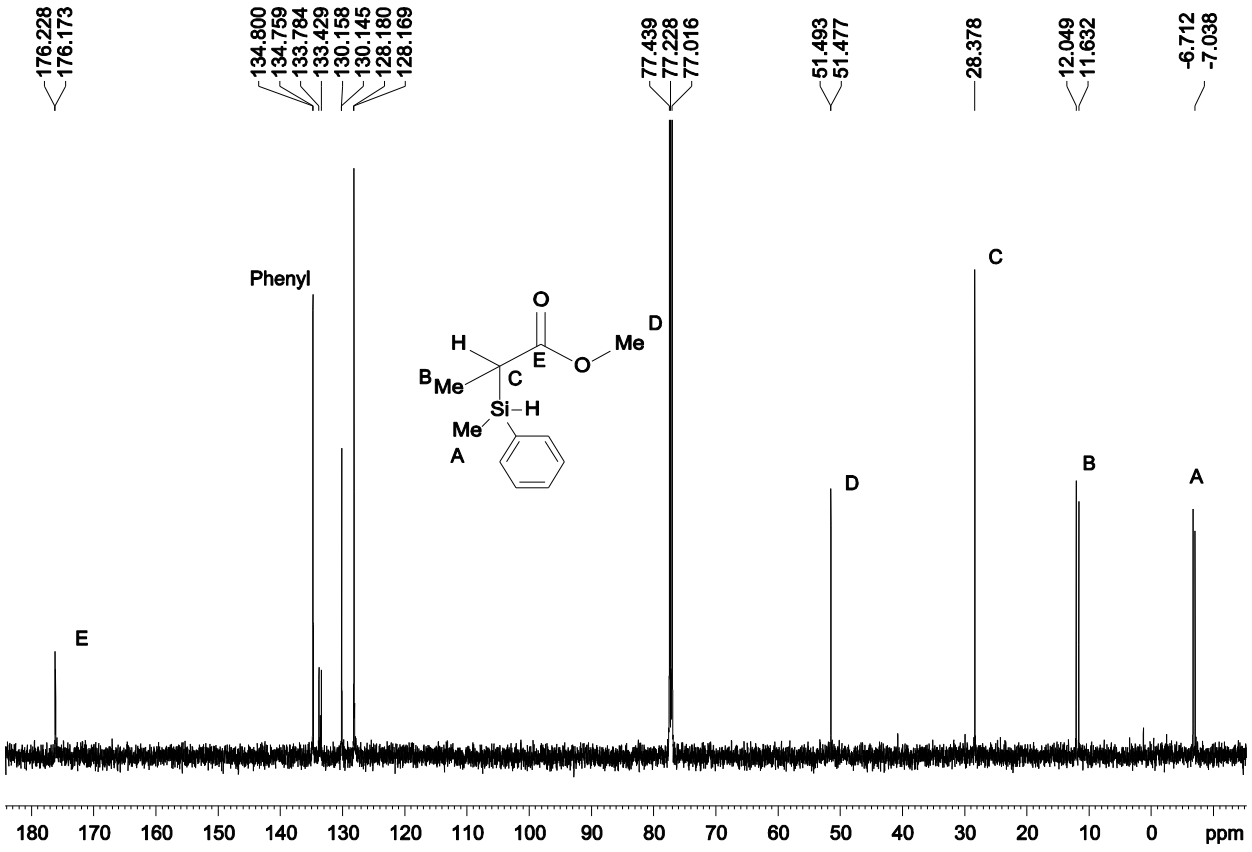

Figure S11. $^{13}C\{^{1}H\}$ NMR spectrum (150 MHz, chloroform-*d*) for catalytic reaction of methyl acrylate and $PhMeSiH_2$ to yield diastereomers of $PhMeHSi(H)MeCCO_2Me$.

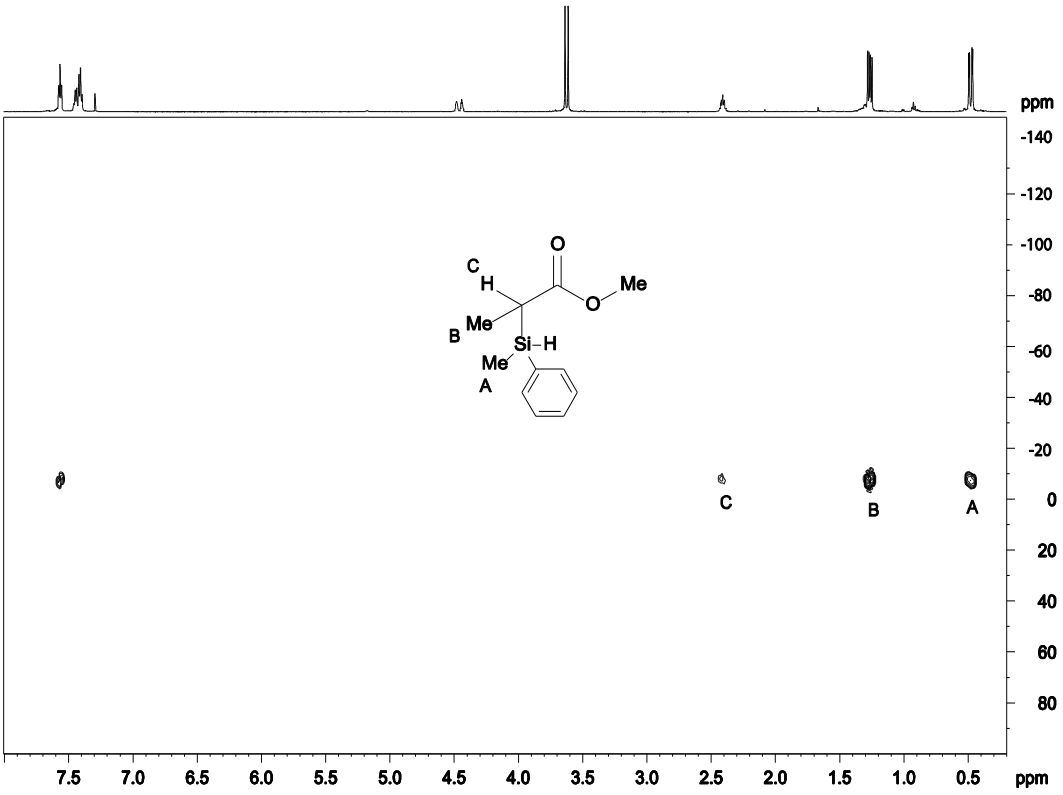

Figure S12. ^{1}H-^{29}Si NMR HMBC experiment (119 MHz, chloroform-*d*) for catalytic reaction of methyl acrylate and $PhMeSiH_2$ to yield diastereomers of $PhMeHSi(H)MeCCO_2Me$.

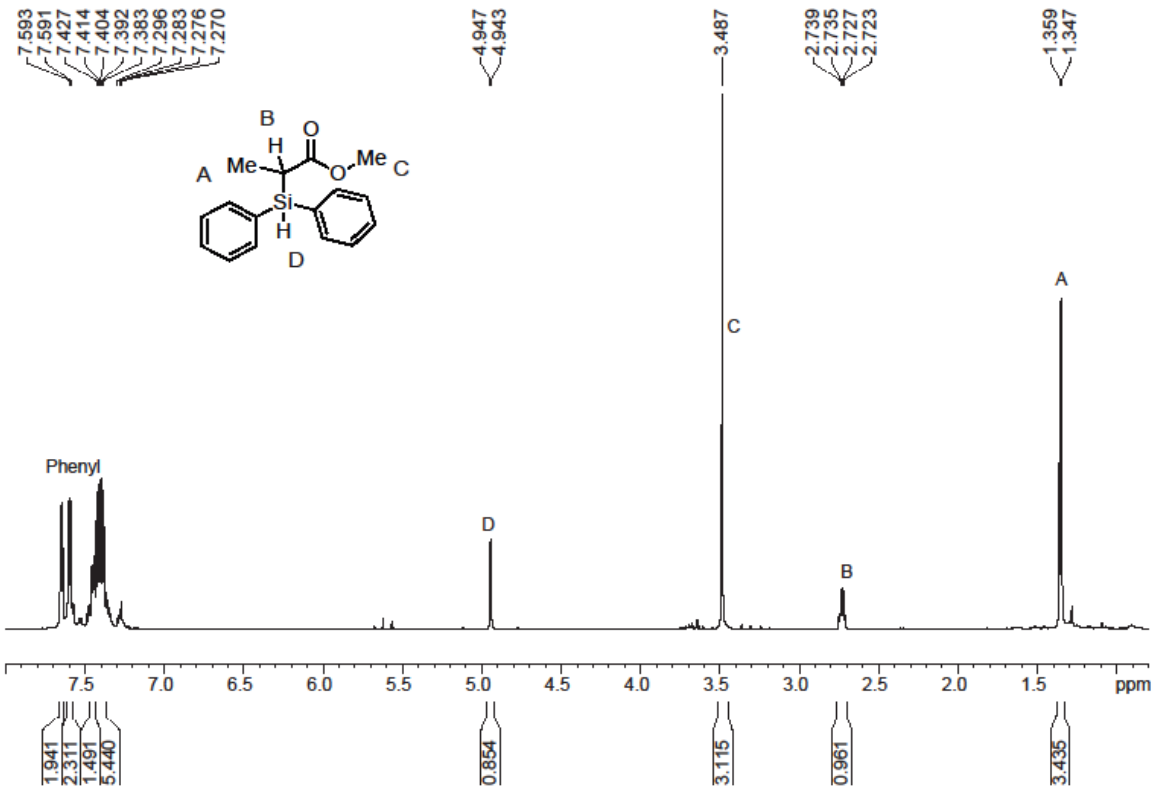

Figure S13. ^{1}H NMR spectrum (600 MHz, chloroform-*d*) for catalytic reaction of methyl acrylate and Ph_2SiH_2 to yield $Ph_2HSi(H)MeCCO_2Me$.

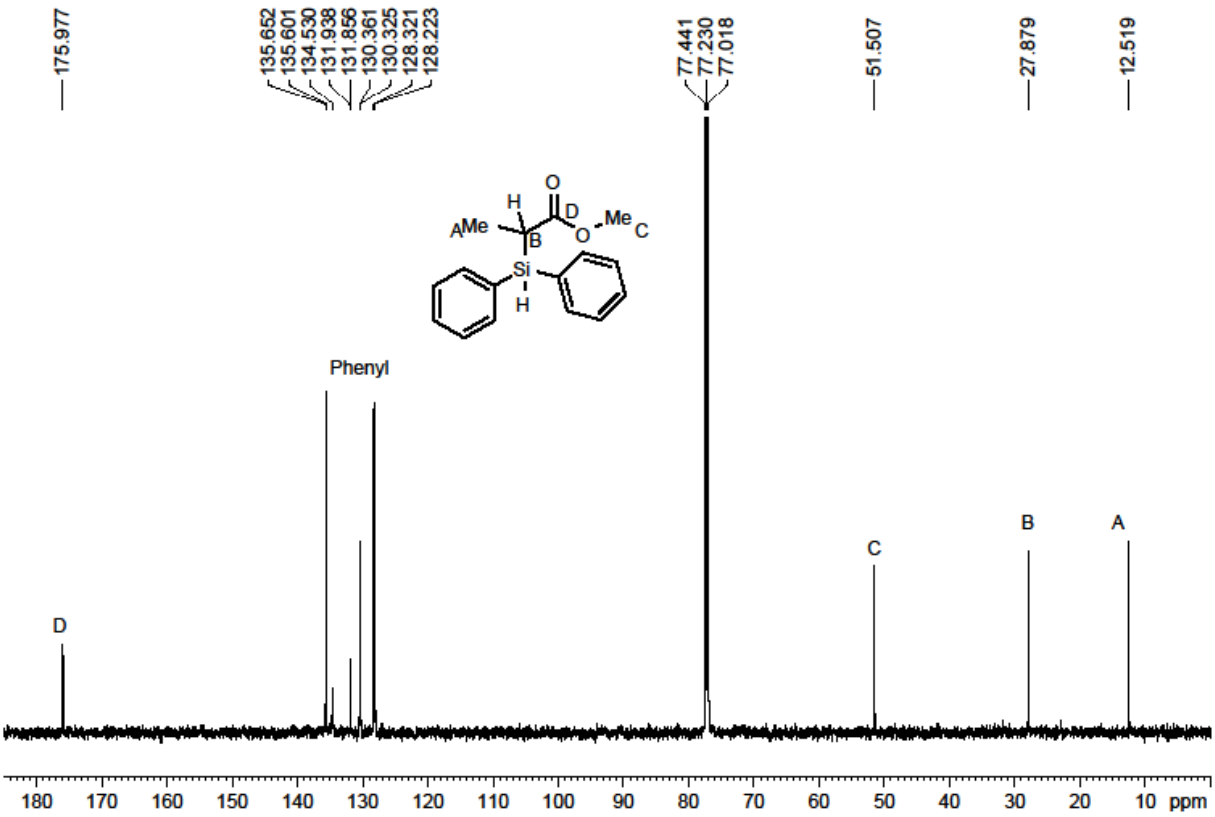

Figure S14. $^{13}C\{^{1}H\}$ NMR spectrum (150 MHz, chloroform-*d*) for catalytic reaction of methyl acrylate and Ph_2SiH_2 to yield $Ph_2HSi(H)MeCCO_2Me$.

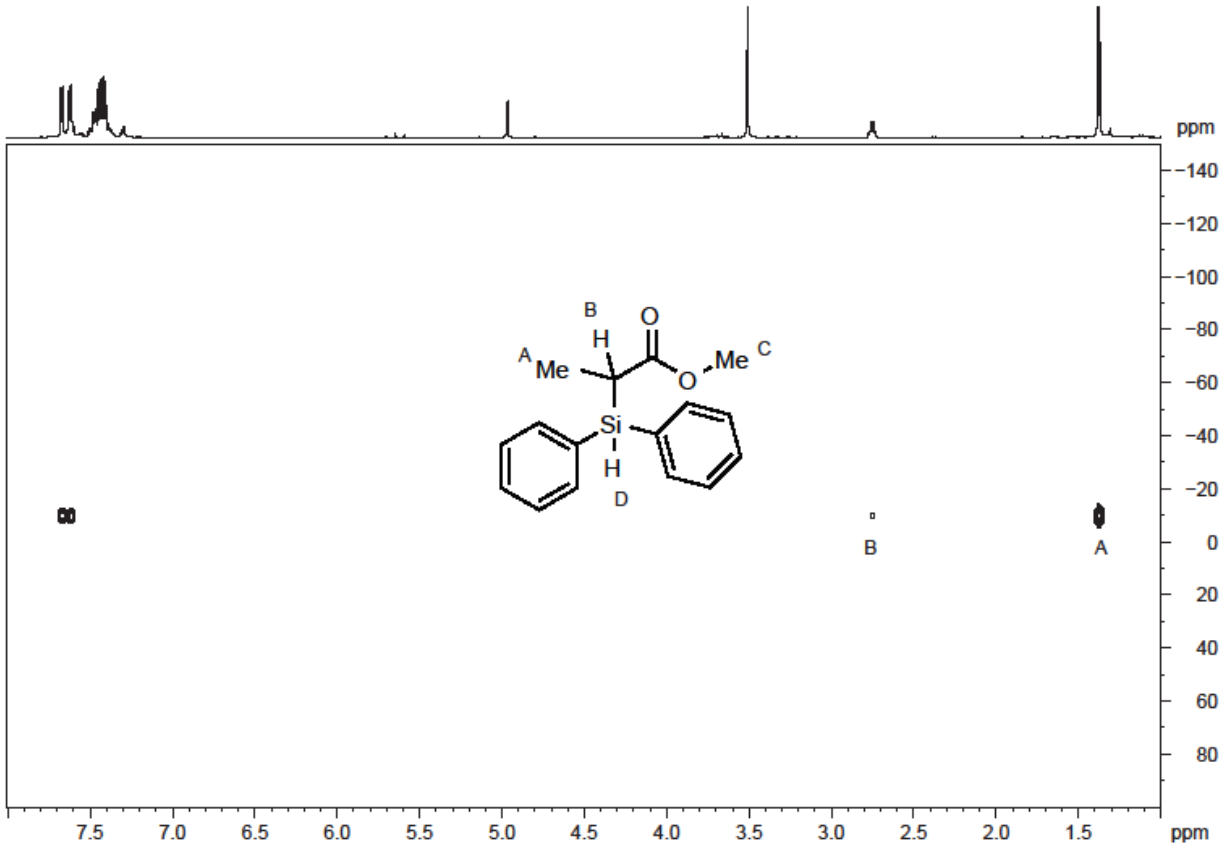

Figure S15. ^{1}H-^{29}Si NMR HMBC experiment (119 MHz, chloroform-*d*) for catalytic reaction of methyl acrylate and Ph_2SiH_2 to yield $Ph_2HSi(H)MeCCO_2Me$.

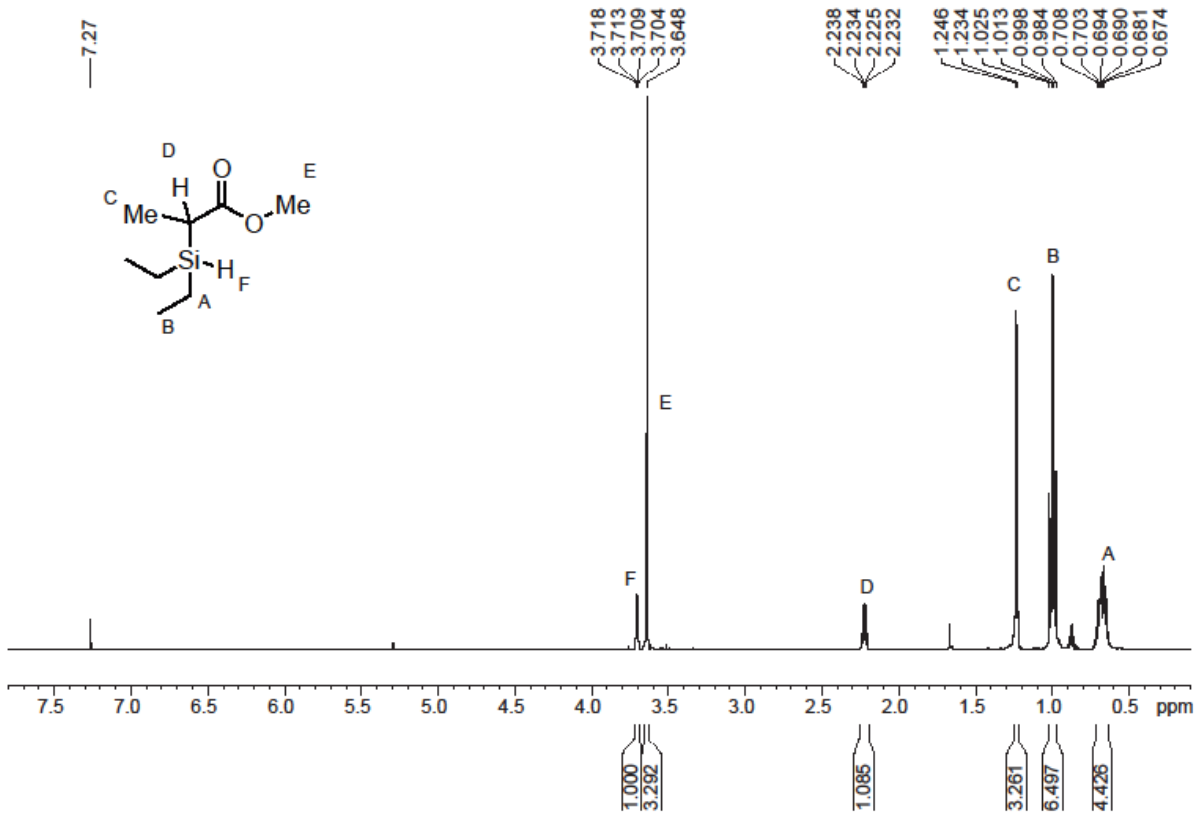

Figure S16. ^{1}H NMR spectrum (600 MHz, chloroform-*d*) for catalytic reaction of methyl acrylate and Et_2SiH_2 to yield $Et_2HSi(H)MeCCO_2Me$.

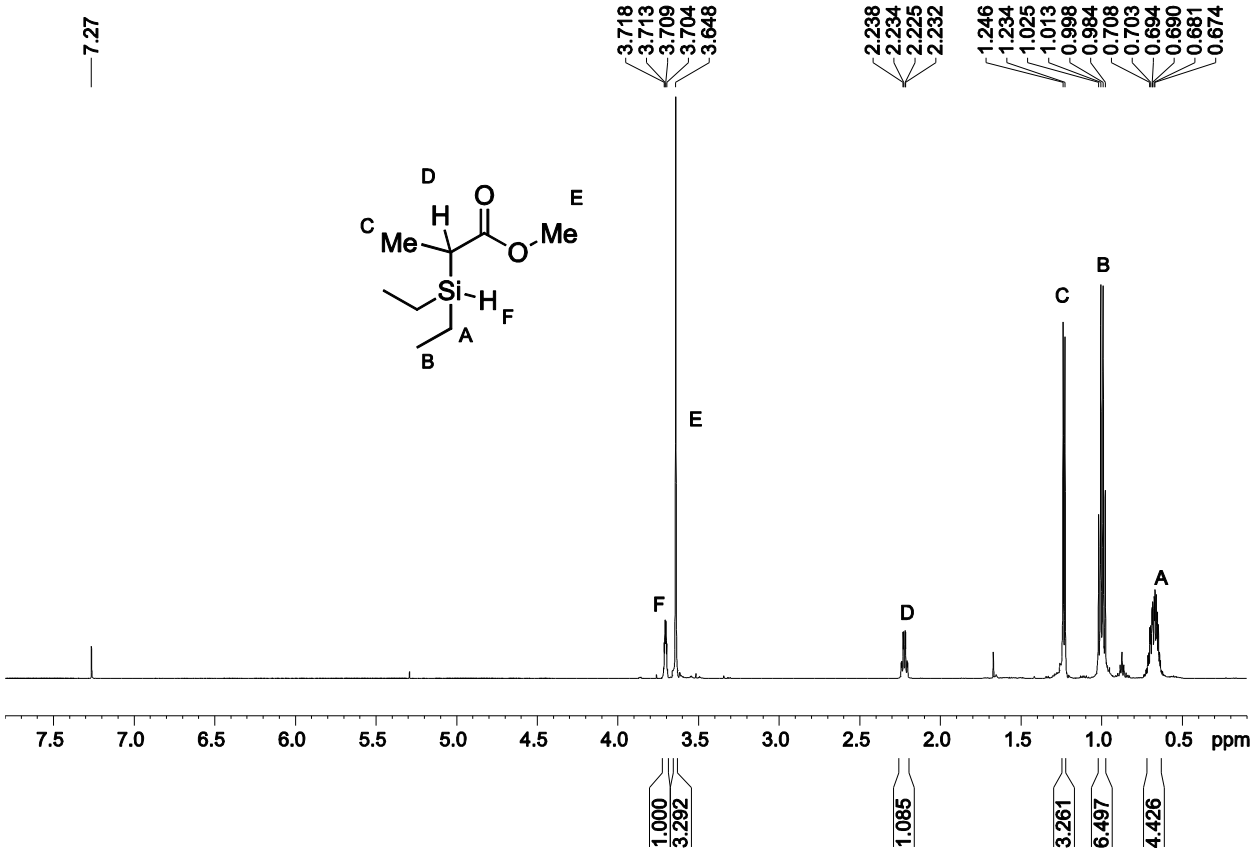

Figure S17. $^{13}C\{^{1}H\}$ NMR spectrum (150 MHz, chloroform-*d*) for catalytic reaction of methyl acrylate and Et_2SiH_2 to yield $Et_2HSi(H)MeCCO_2Me$.

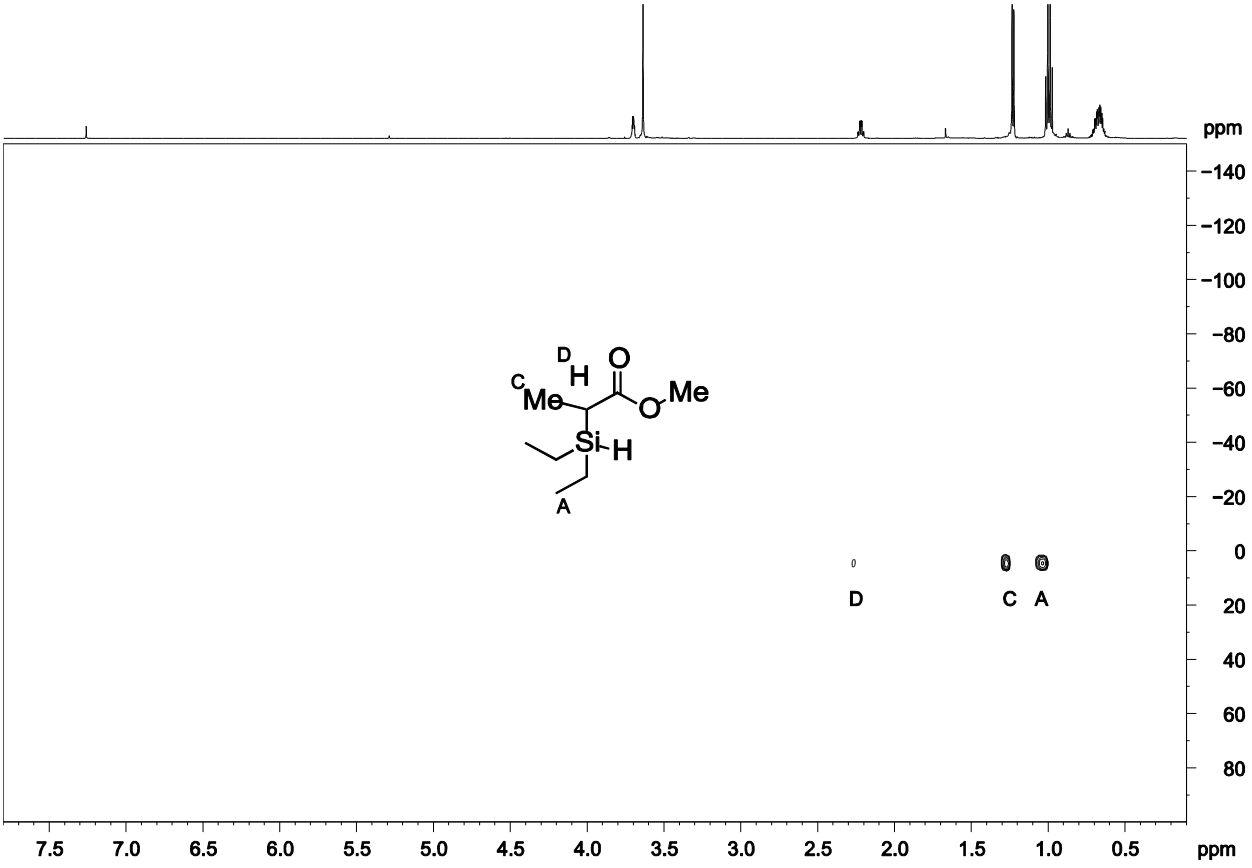

Figure S18. ^{1}H-^{29}Si NMR HMBC experiment (119 MHz, chloroform-*d*) for catalytic reaction of methyl acrylate and Et_2SiH_2 to yield $Et_2HSi(H)MeCCO_2Me$.

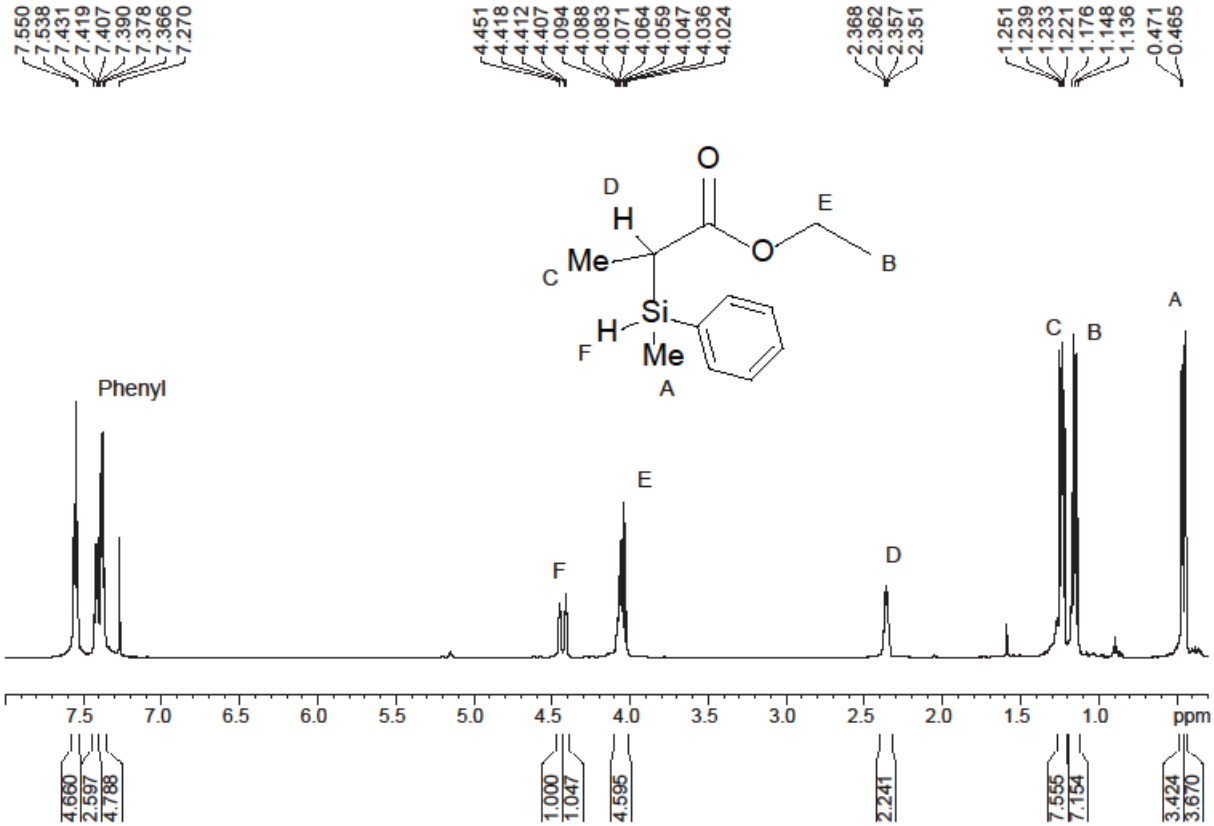

Figure S19. ^{1}H NMR spectrum (600 MHz, chloroform-*d*) for catalytic reaction of ethyl acrylate and $PhMeSiH_2$ to yield diastereomers of $PhMeHSi(H)MeCCO_2Et$.

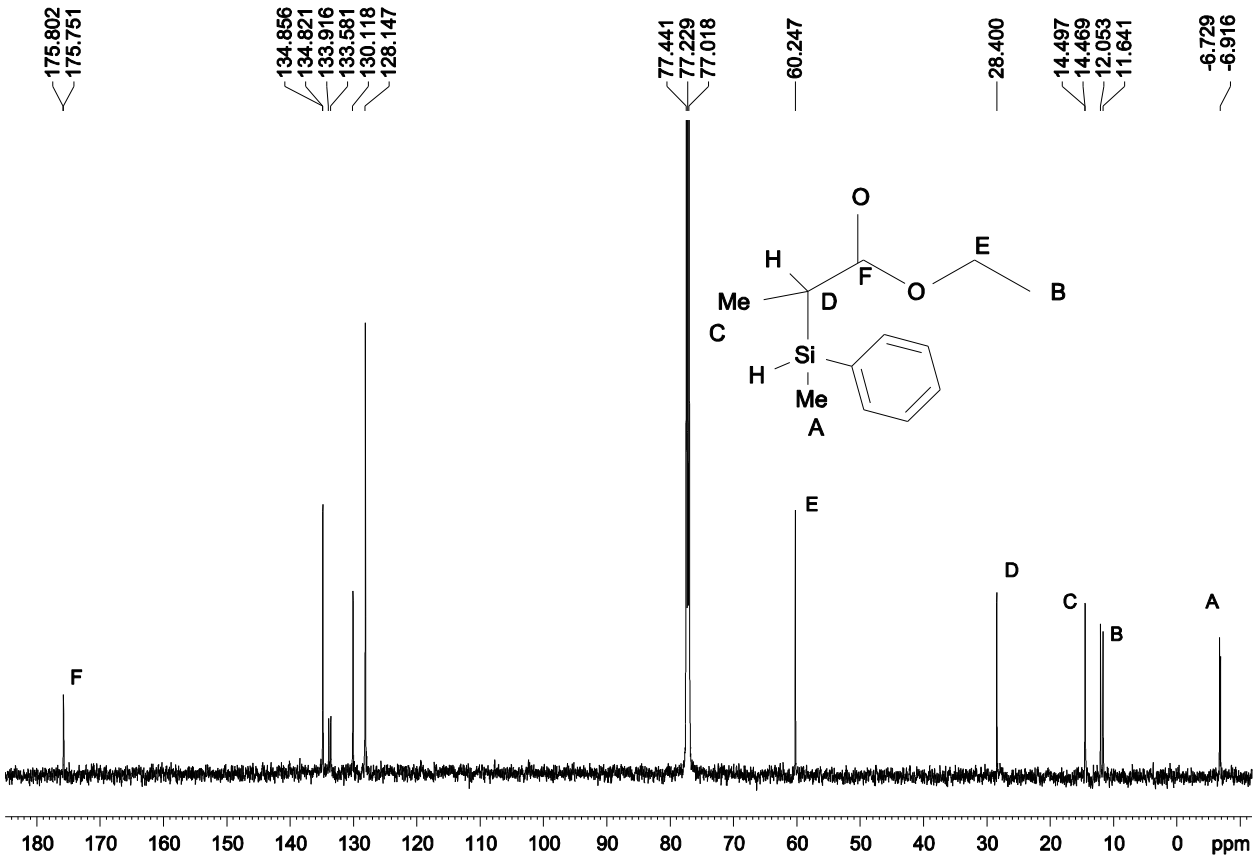

Figure S20. $^{13}C\{^{1}H\}$ NMR spectrum (150 MHz, chloroform-*d*) for catalytic reaction of ethyl acrylate and $PhMeSiH_2$ to yield diastereomers of $PhMeHSi(H)MeCCO_2Et$.

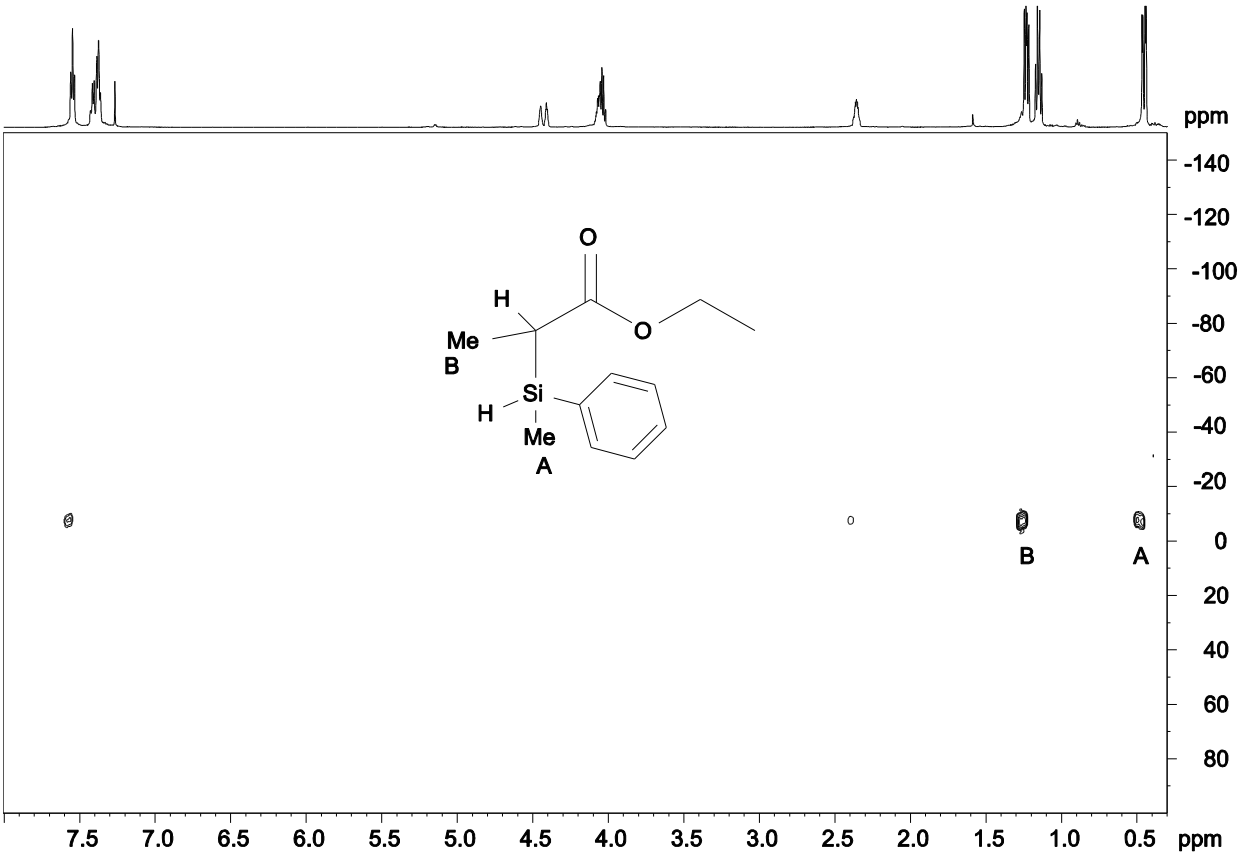

Figure S21. ^{1}H-^{29}Si NMR HMBC experiment (119 MHz, chloroform-*d*) for catalytic reaction of ethyl acrylate and $PhMeSiH_2$ to yield diastereomers of $PhMeHSi(H)MeCCO_2Et$.

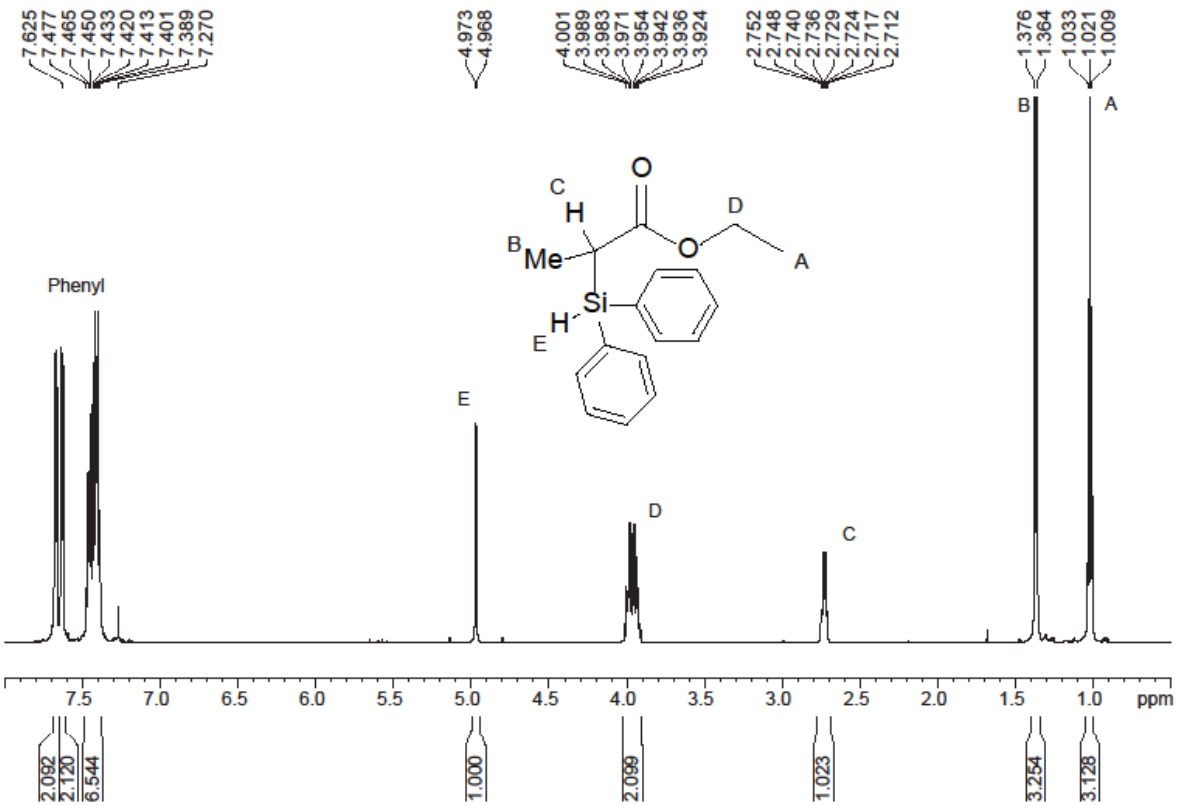

Figure S22. ^{1}H NMR spectrum (600 MHz, chloroform-*d*) for catalytic reaction of ethyl acrylate and Ph_2SiH_2 to yield $Ph_2HSi(H)MeCCO_2Et$.

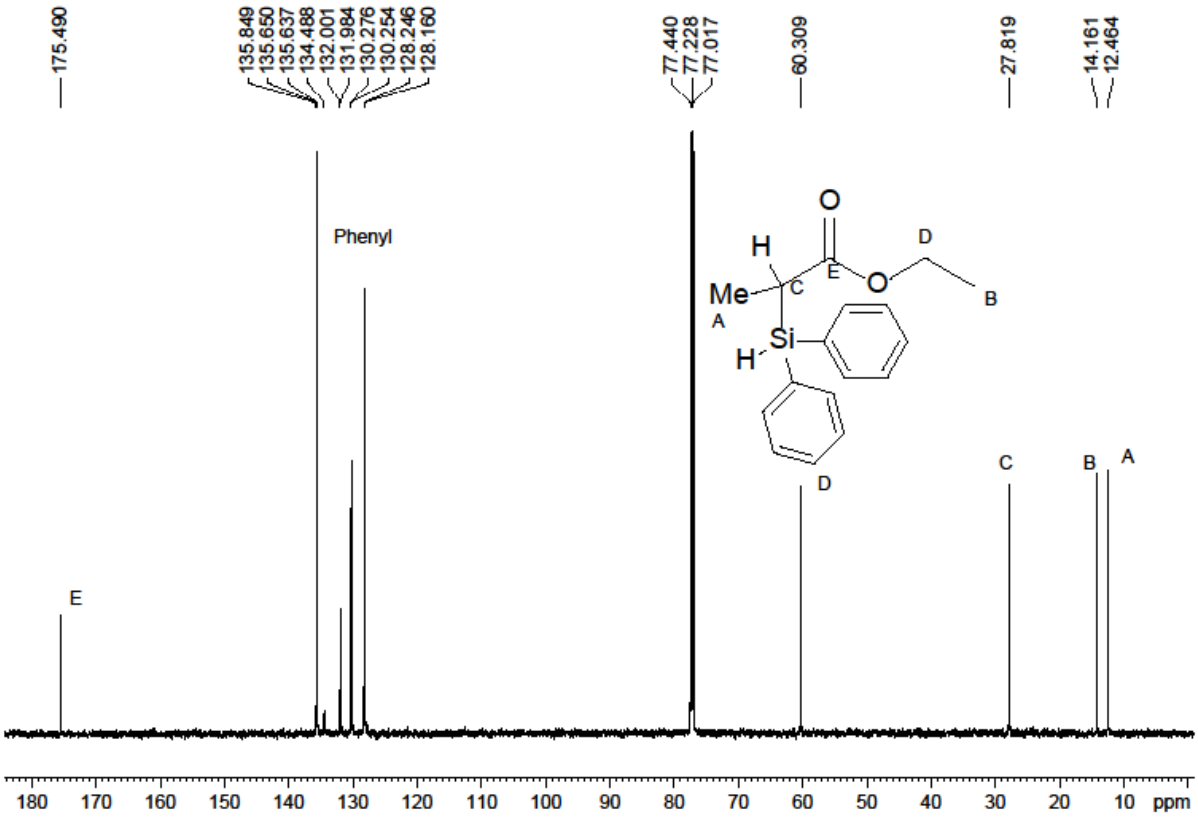

Figure S23. $^{13}C\{^{1}H\}$ NMR spectrum (150 MHz, chloroform-*d*) for catalytic reaction of ethyl acrylate and Ph_2SiH_2 to yield $Ph_2HSi(H)MeCCO_2Et$.

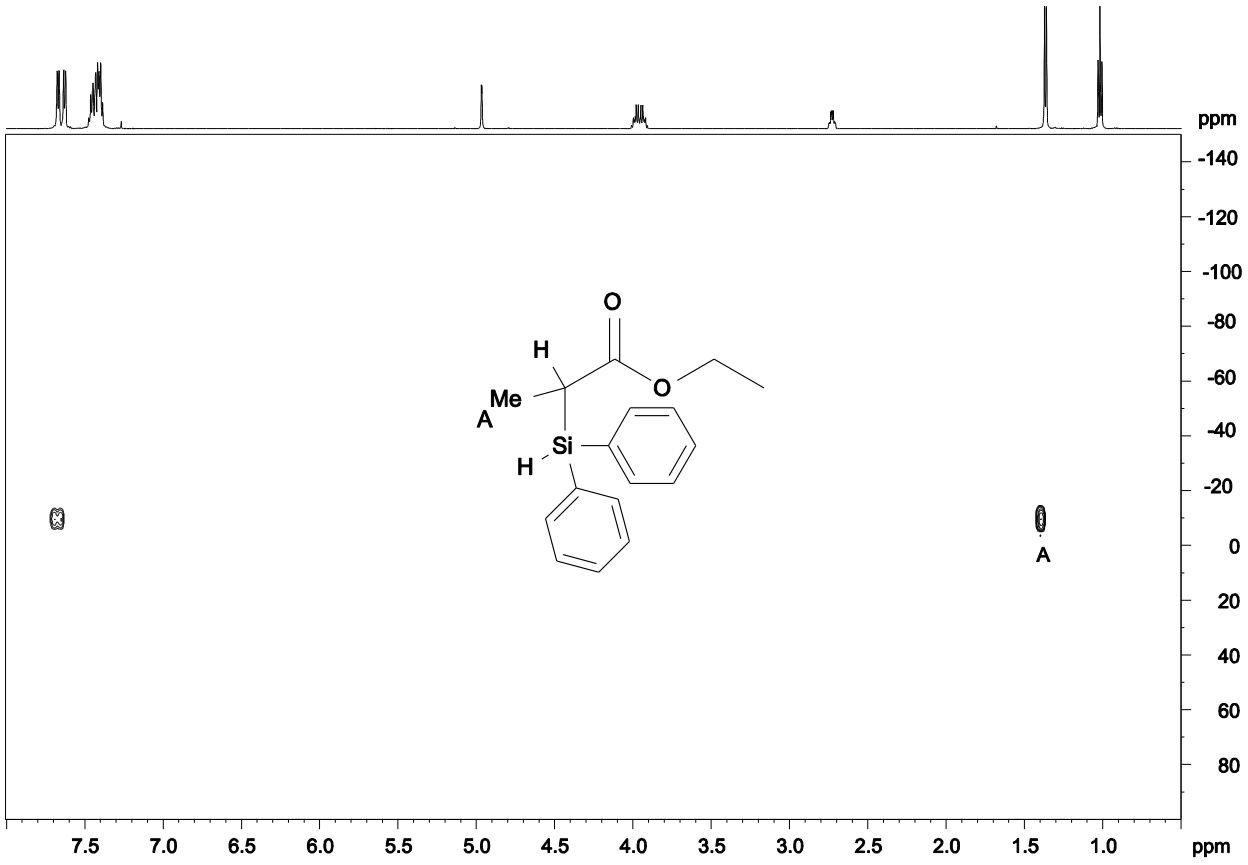

Figure S24. ^{1}H-^{29}Si NMR HMBC experiment (119 MHz, chloroform-*d*) for catalytic reaction of ethyl acrylate and Ph_2SiH_2 to yield $Ph_2HSi(H)MeCCO_2Et$.

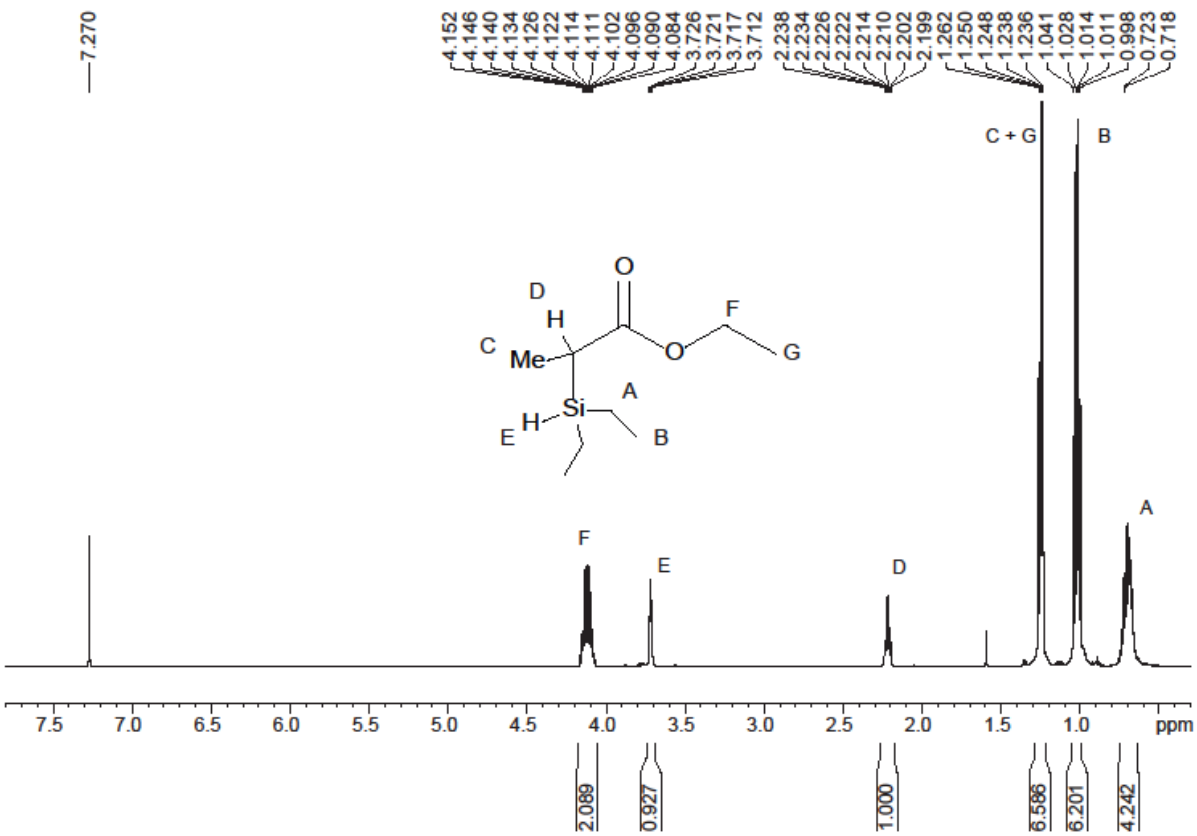

Figure S25. ^{1}H NMR spectrum (600 MHz, chloroform-*d*) for catalytic reaction of ethyl acrylate and Et_2SiH_2 to yield $Et_2HSi(H)MeCCO_2Et$.

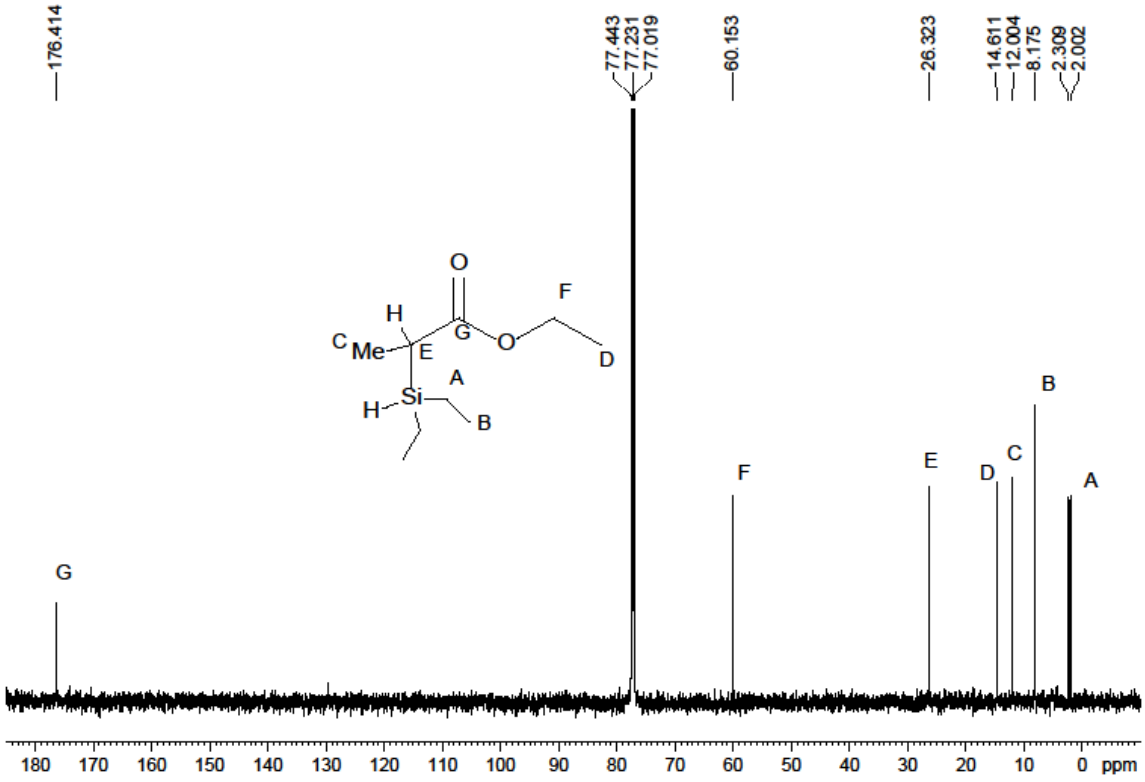

Figure S26. $^{13}C\{^{1}H\}$ NMR spectrum (150 MHz, chloroform-*d*) for catalytic reaction of ethyl acrylate and Et_2SiH_2 to yield $Et_2HSi(H)MeCCO_2Et$.

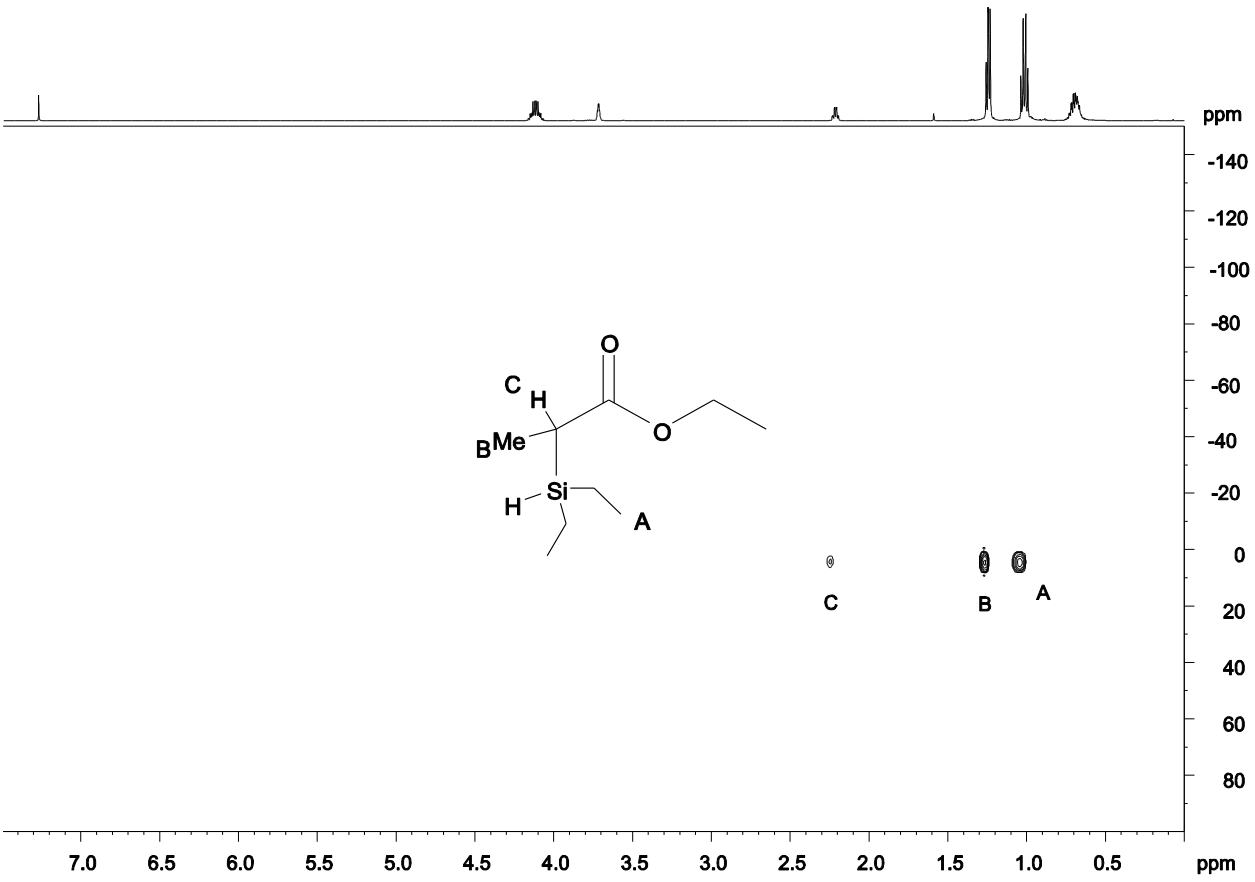

Figure S27. ^{1}H-^{29}Si NMR HMBC experiment (119 MHz, chloroform-*d*) for catalytic reaction of ethyl acrylate and Et_2SiH_2 to yield $Et_2HSi(H)MeCCO_2Et$.

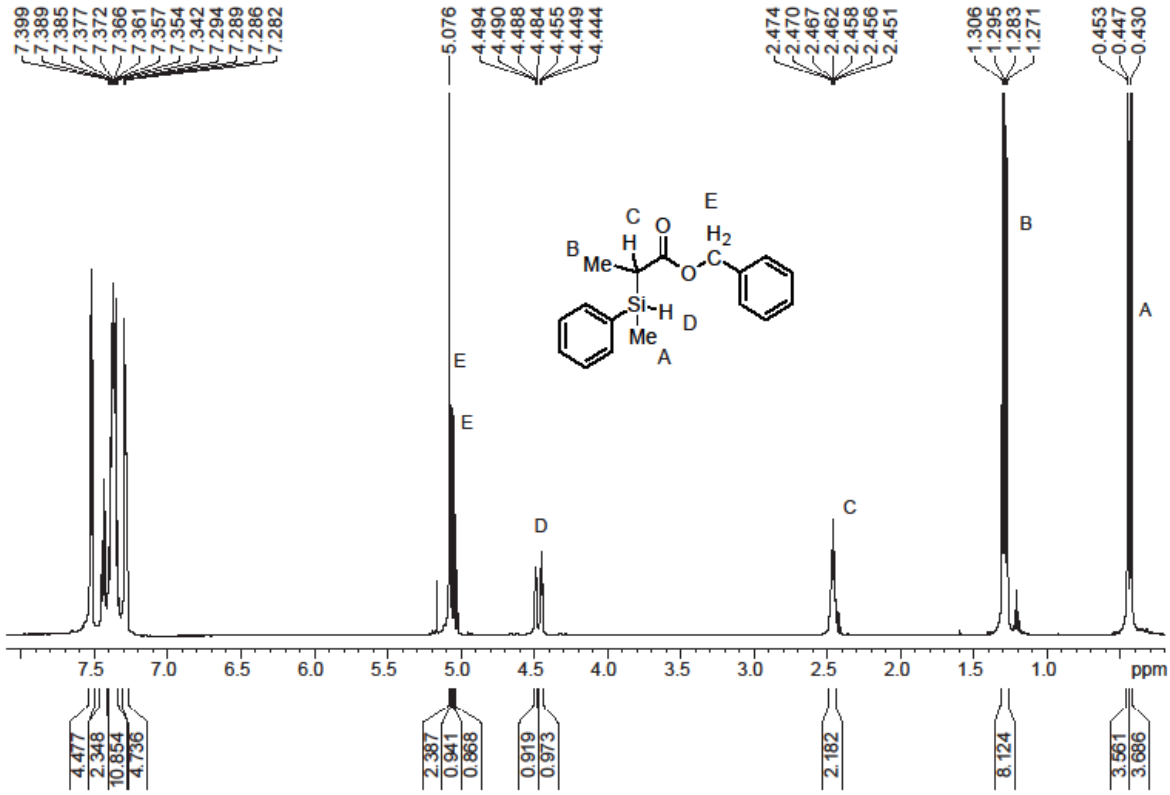

Figure S28. ^{1}H NMR spectrum (600 MHz, chloroform-*d*) for catalytic reaction of benzyl acrylate and $PhMeSiH_2$ to yield diastereomers of $PhMeHSi(H)MeCCO_2CH_2Ph$.

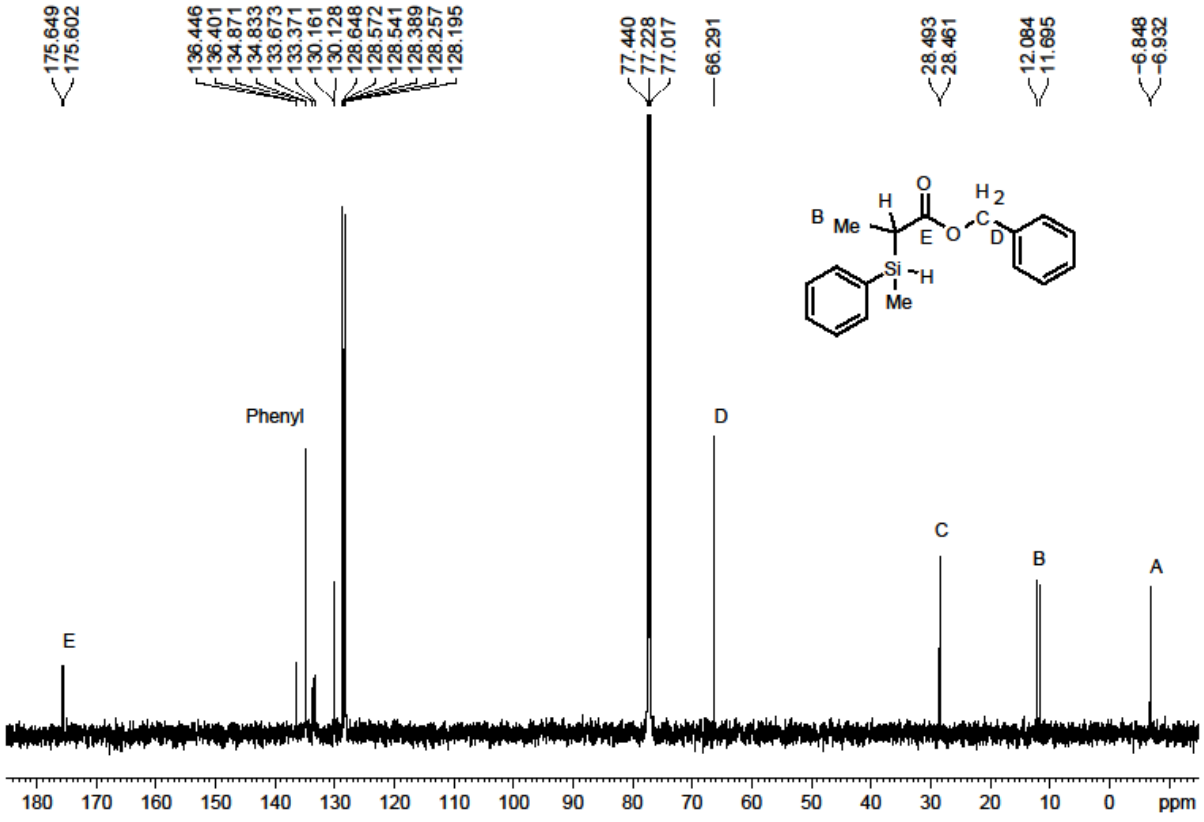

Figure S29. $^{13}C\{^{1}H\}$ NMR spectrum (150 MHz, chloroform-*d*) for catalytic reaction of benzyl acrylate and $PhMeSiH_2$ to yield diastereomers of $PhMeHSi(H)MeCCO_2CH_2Ph$.

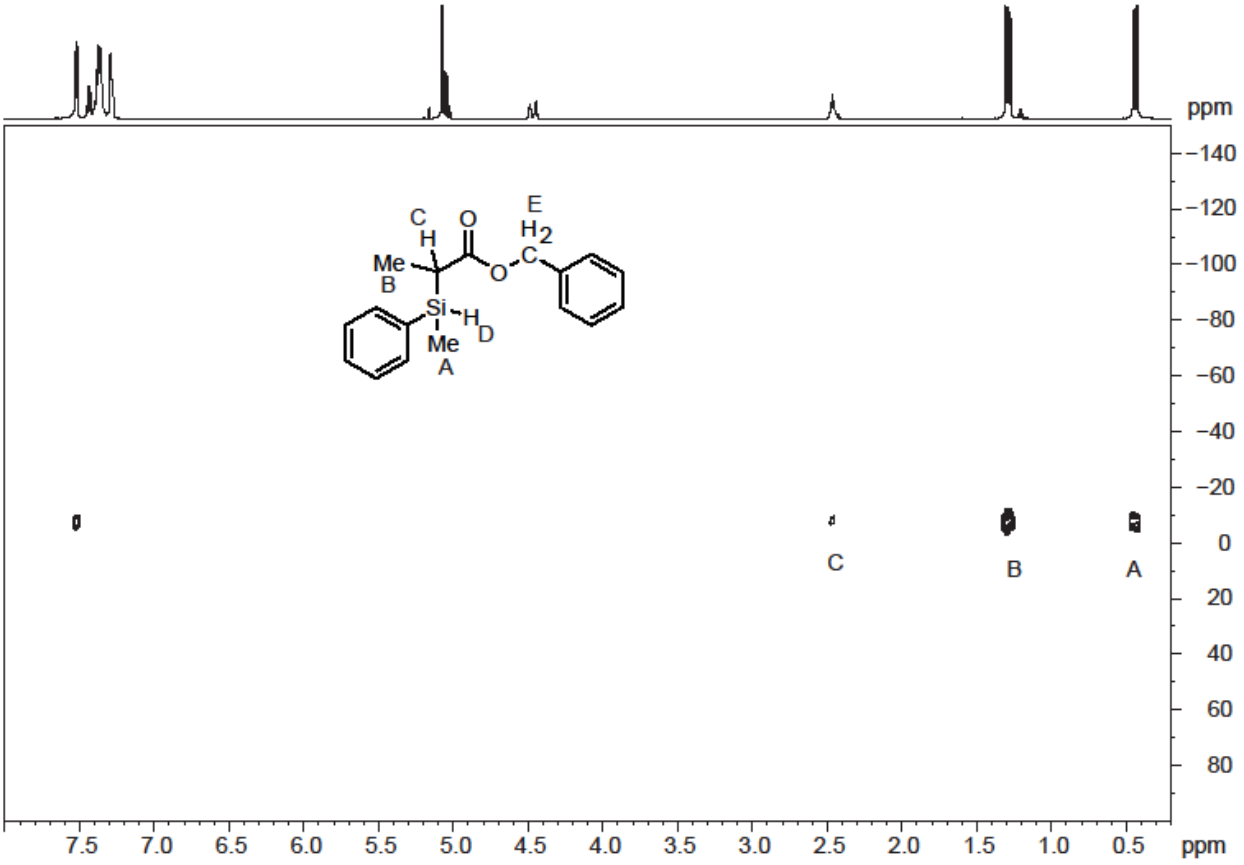

Figure S30. ^{1}H-^{29}Si NMR HMBC experiment (119 MHz, chloroform-*d*) for catalytic reaction of benzyl acrylate and $PhMeSiH_2$ to yield diastereomers of $PhMeHSi(H)MeCCO_2CH_2Ph$.

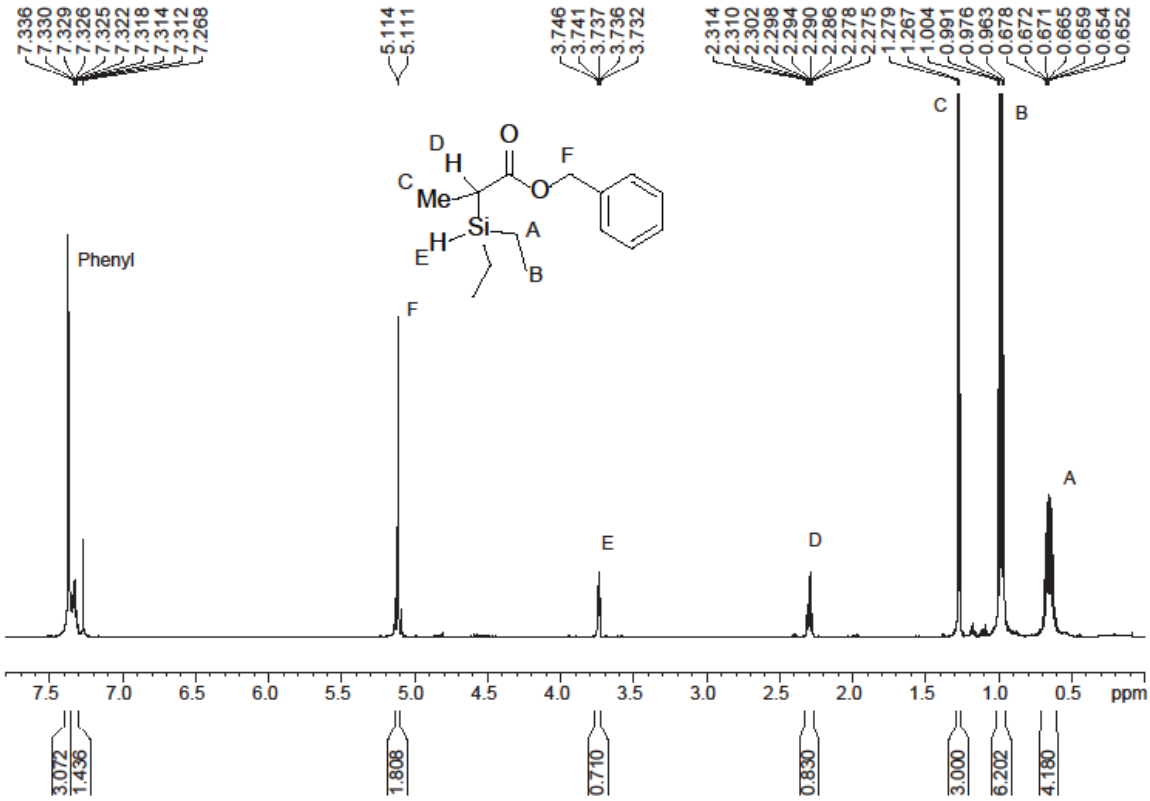

Figure S31. ^{1}H NMR spectrum (600 MHz, chloroform-*d*) for catalytic reaction of benzyl acrylate and Et_2SiH_2 to yield $Et_2HSi(H)MeCCO_2CH_2Ph$.

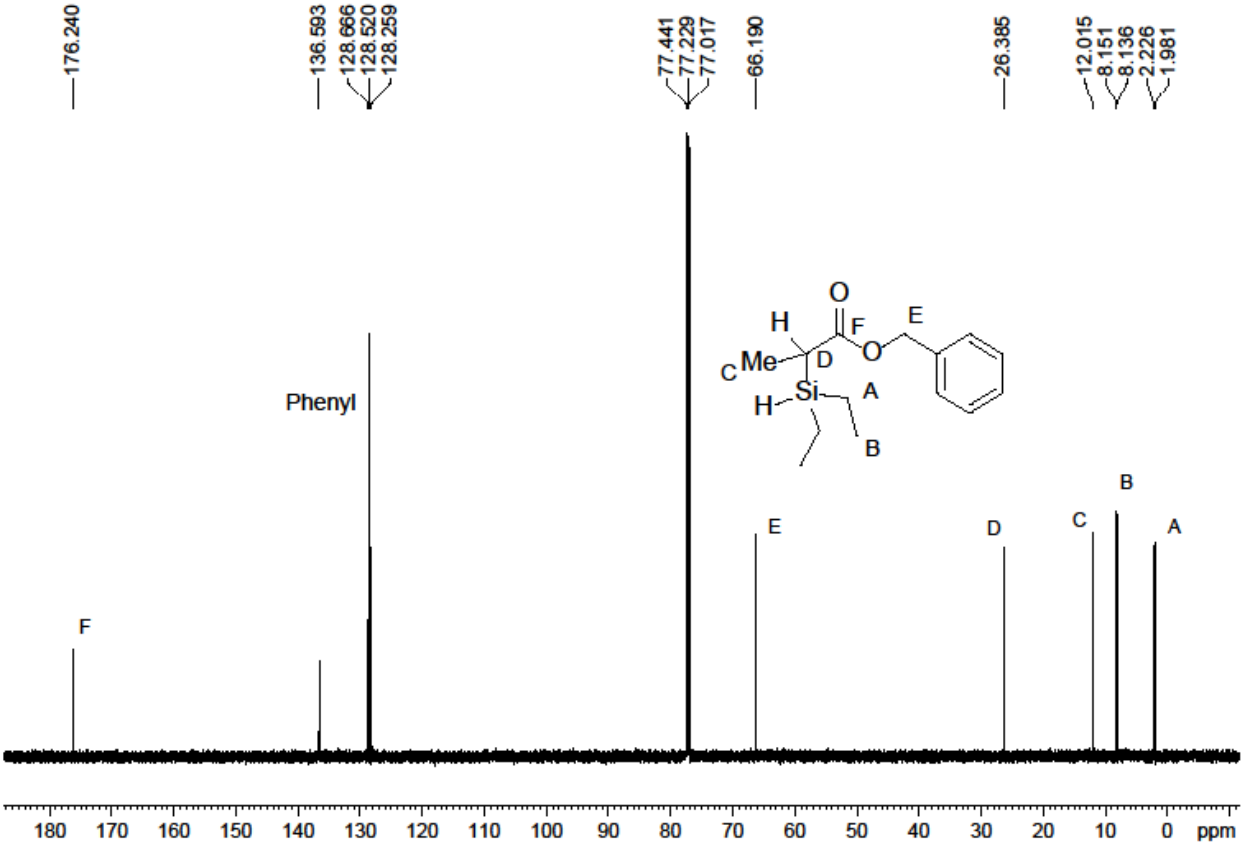

Figure S32. $^{13}C\{^{1}H\}$ NMR spectrum (150 MHz, chloroform-*d*) for catalytic reaction of benzyl acrylate and Et_2SiH_2 to yield $Et_2HSi(H)MeCCO_2CH_2Ph$.

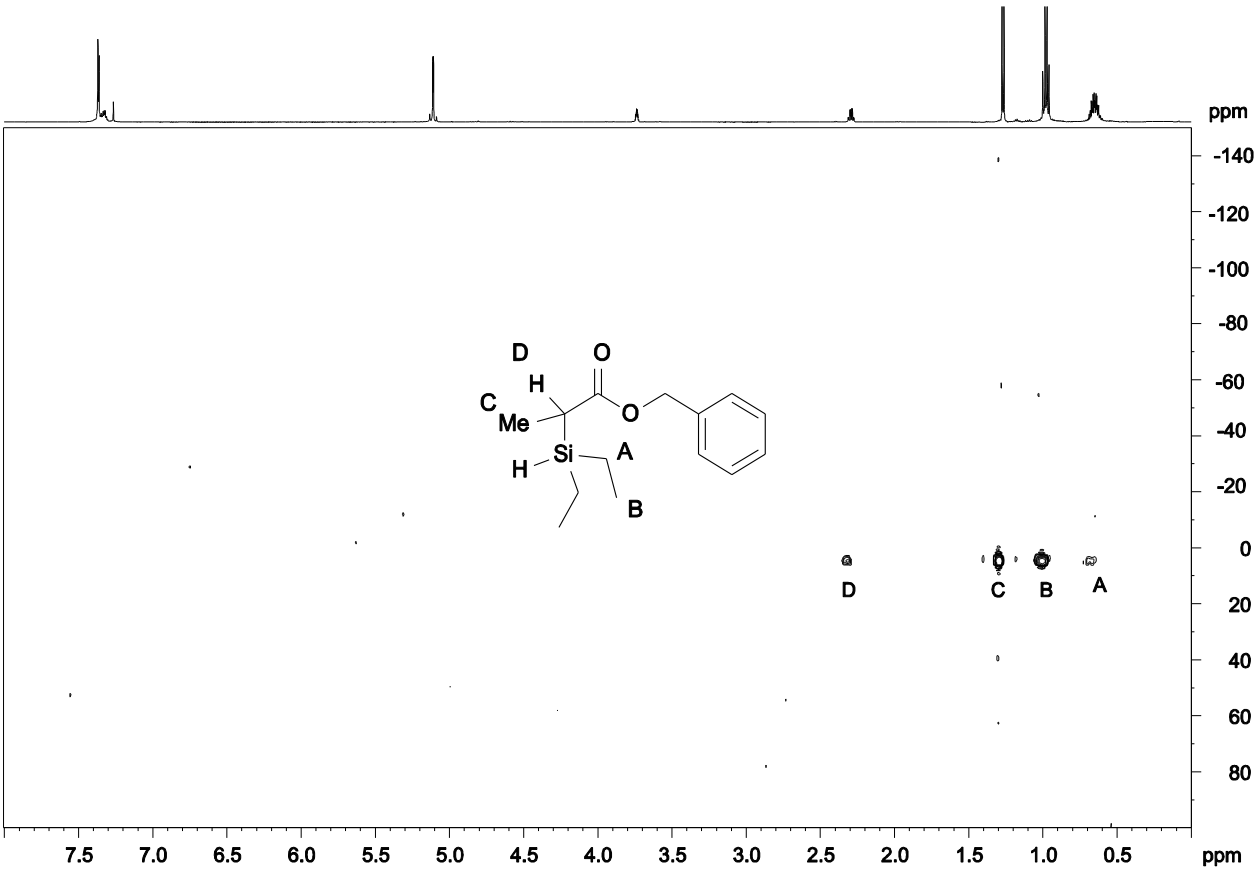

Figure S33. ^{1}H-^{29}Si NMR HMBC experiment (119 MHz, chloroform-*d*) for catalytic reaction of benzyl acrylate and Et_2SiH_2 to yield $Et_2HSi(H)MeCCO_2CH_2Ph$.

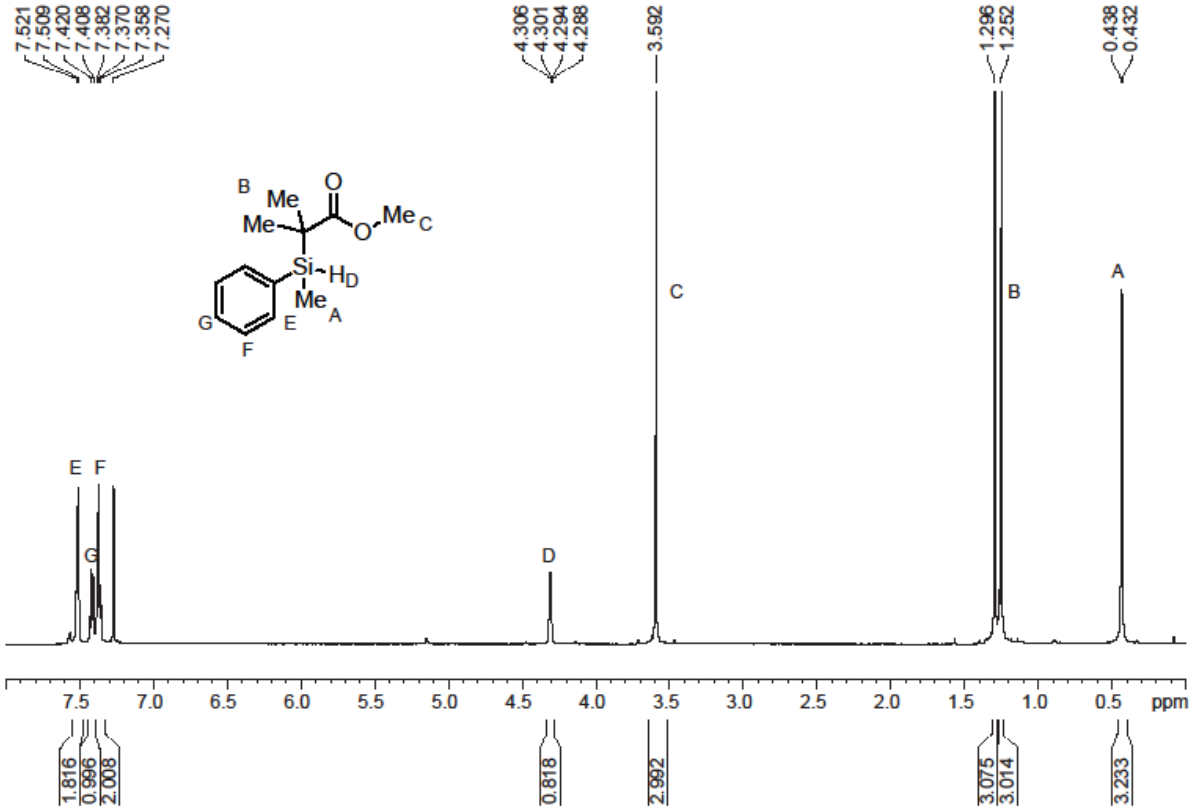

Figure S34. ^{1}H NMR spectrum (600 MHz, chloroform-*d*) for catalytic reaction of methyl methacrylate and $PhMeSiH_2$ to yield $PhMeHSiCMe_2CO_2Me$.

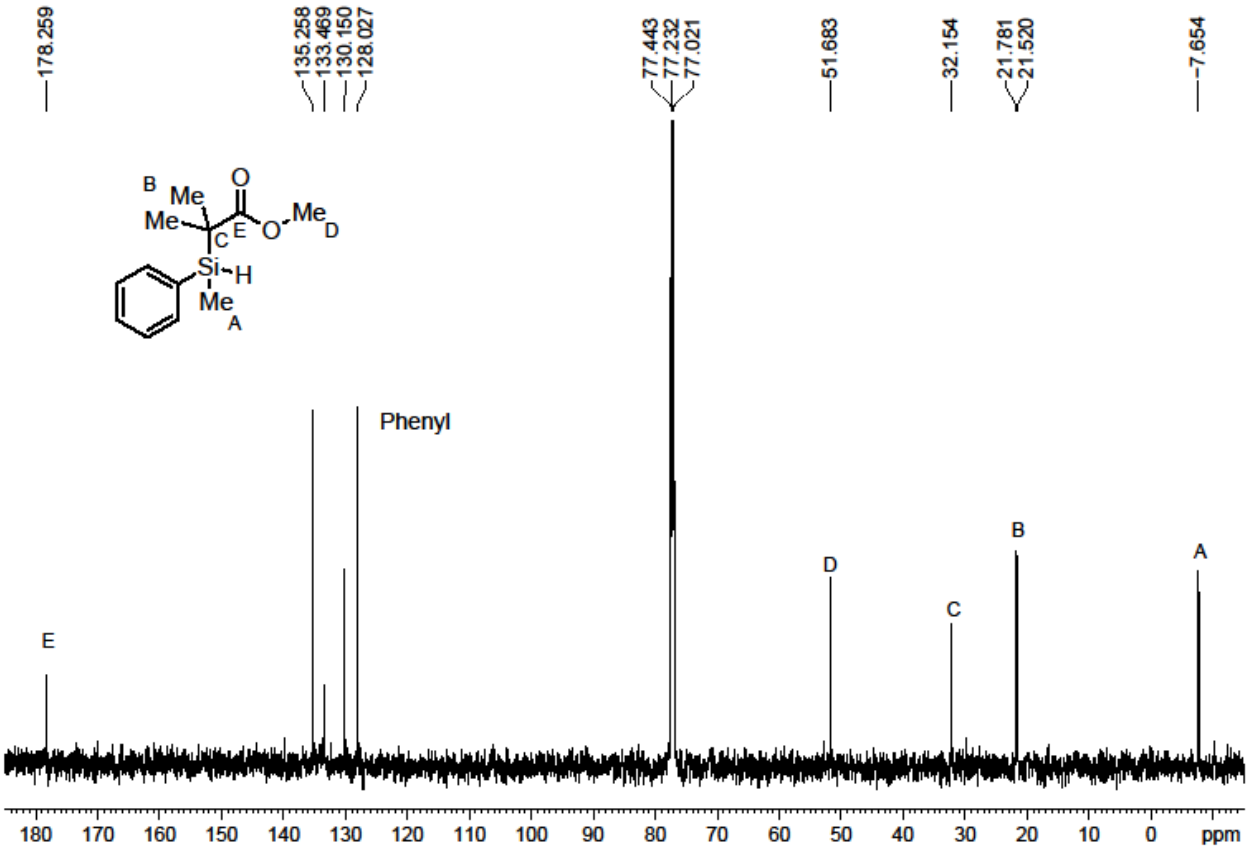

Figure S35. $^{13}C\{^{1}H\}$ NMR spectrum (150 MHz, chloroform-*d*) for catalytic reaction of methyl methacrylate and $PhMeSiH_2$ to yield $PhMeHSiCMe_2CO_2Me$.

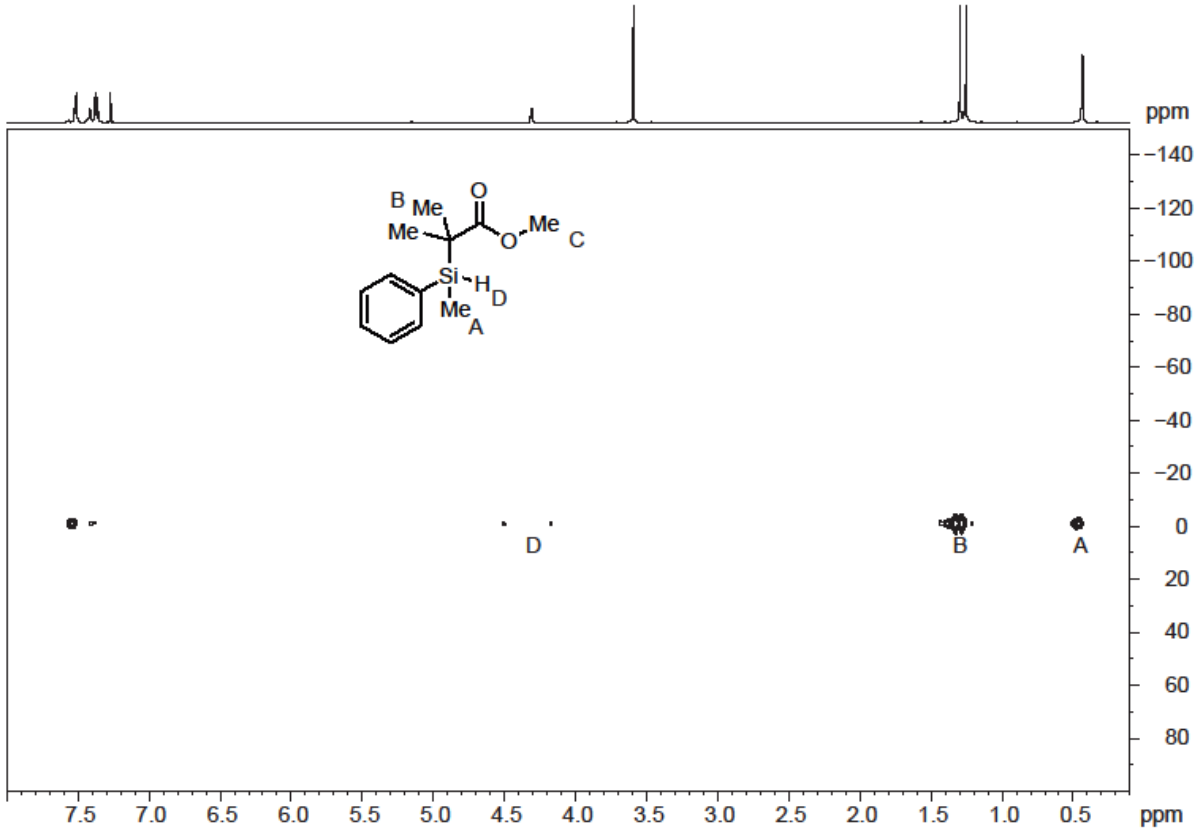

Figure S36. ^{1}H-^{29}Si NMR HMBC experiment (119 MHz, chloroform-*d*) for catalytic reaction of methyl methacrylate and $PhMeSiH_2$ to yield $PhMeHSiCMe_2CO_2Me$.

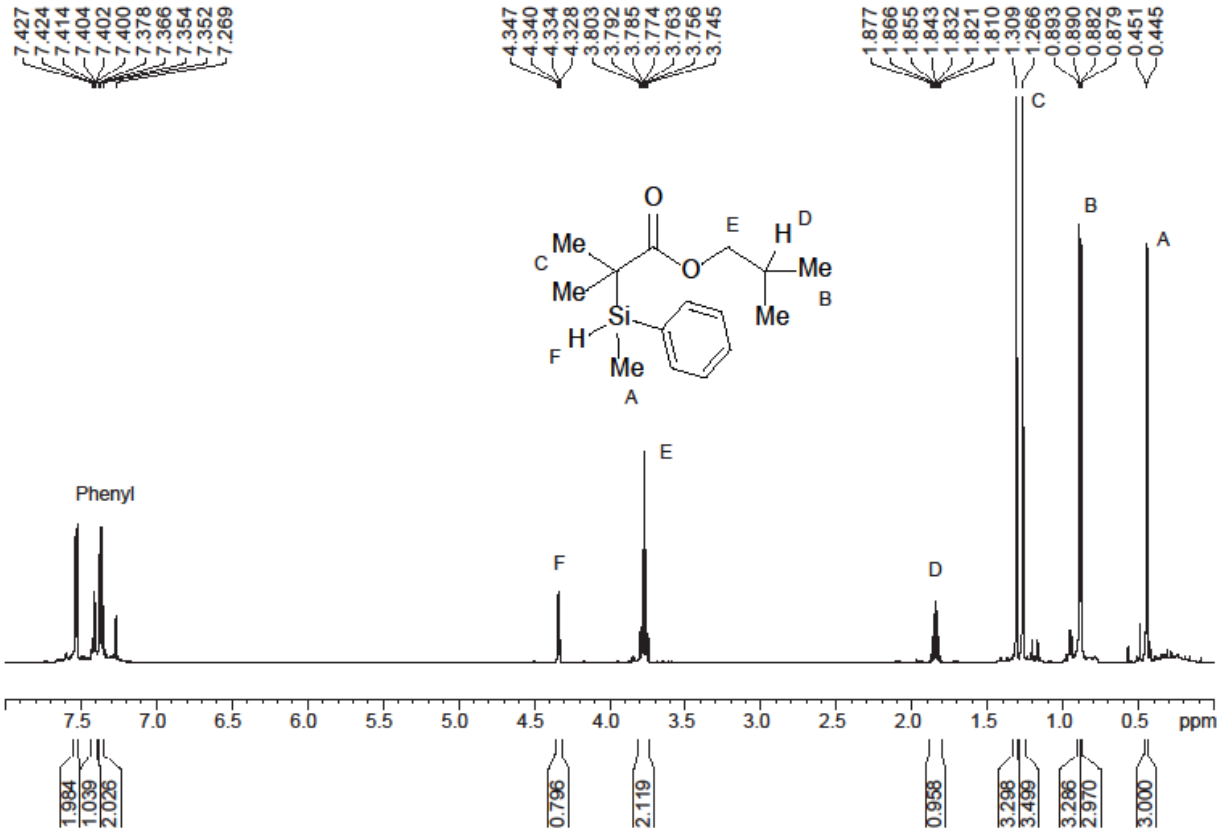

Figure S37. ^{1}H NMR spectrum (600 MHz, chloroform-*d*) for catalytic reaction of isobutyl methacrylate and $PhMeSiH_2$ to yield $PhMeHSiCMe_2CO_2CH_2CHMe_2$.

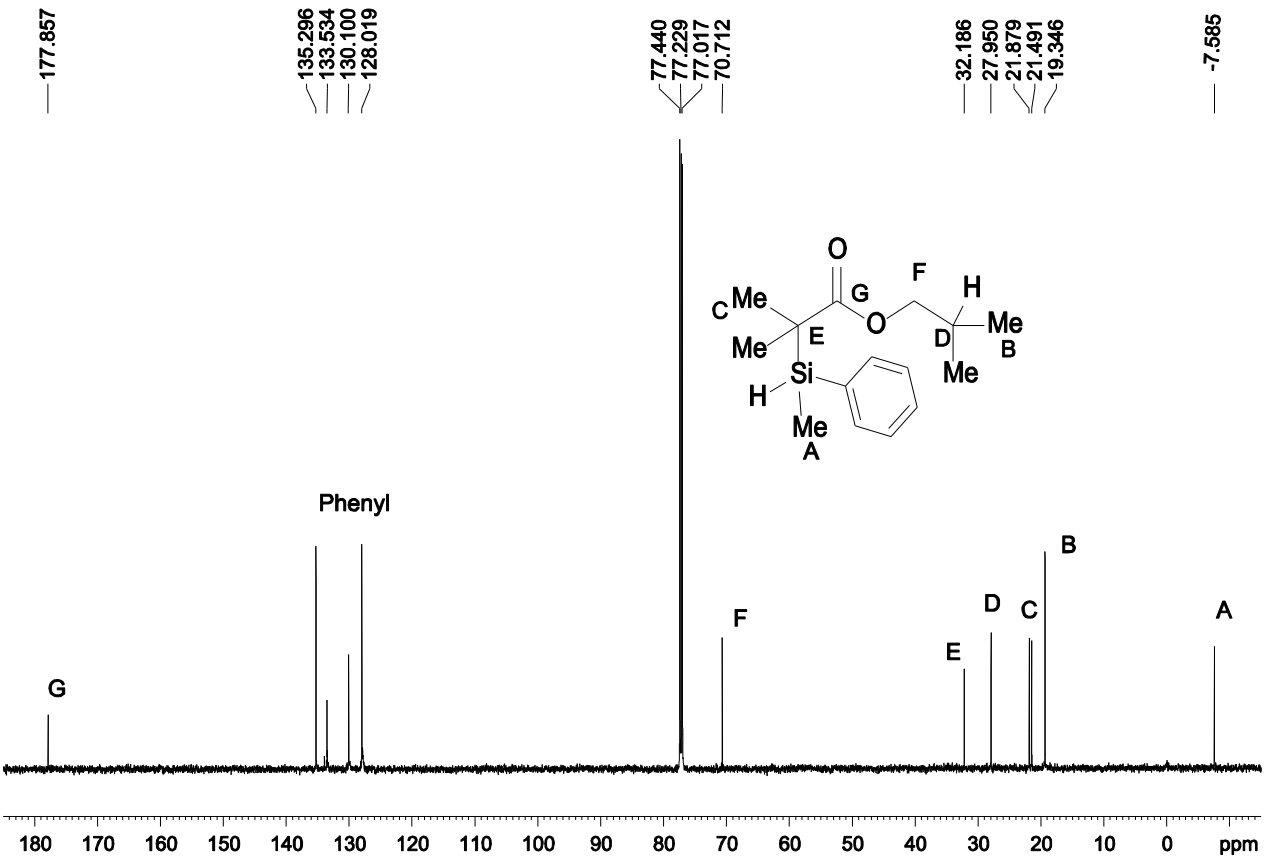

Figure S38. $^{13}C\{^{1}H\}$ NMR spectrum (150 MHz, chloroform-*d*) for catalytic reaction of isobutyl methacrylate and $PhMeSiH_2$ to yield $PhMeHSiCMe_2CO_2CH_2CHMe_2$.

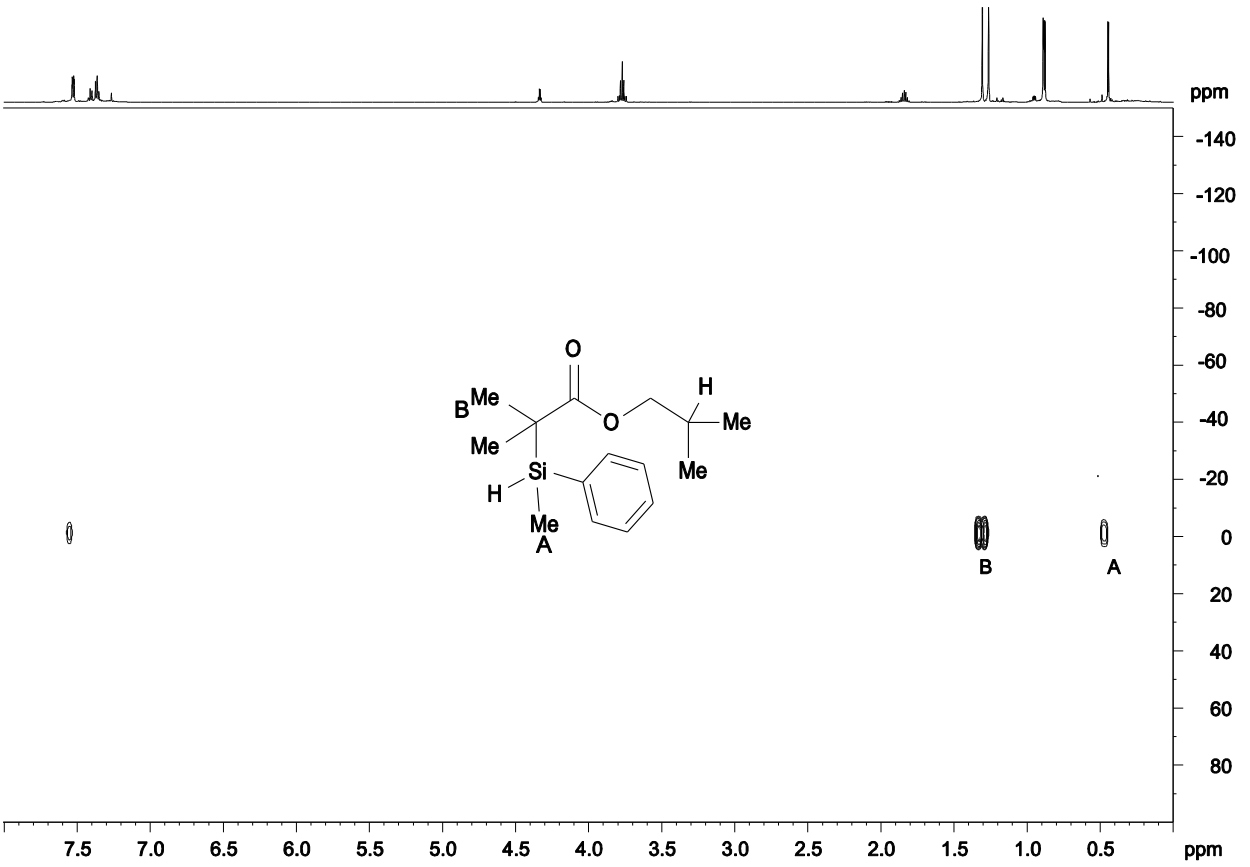

Figure S39. ^{1}H-^{29}Si NMR HMBC experiment (119 MHz, chloroform-*d*) for catalytic reaction of isobutyl methacrylate and $PhMeSiH_2$ to yield $PhMeHSiCMe_2CO_2CH_2CHMe_2$.

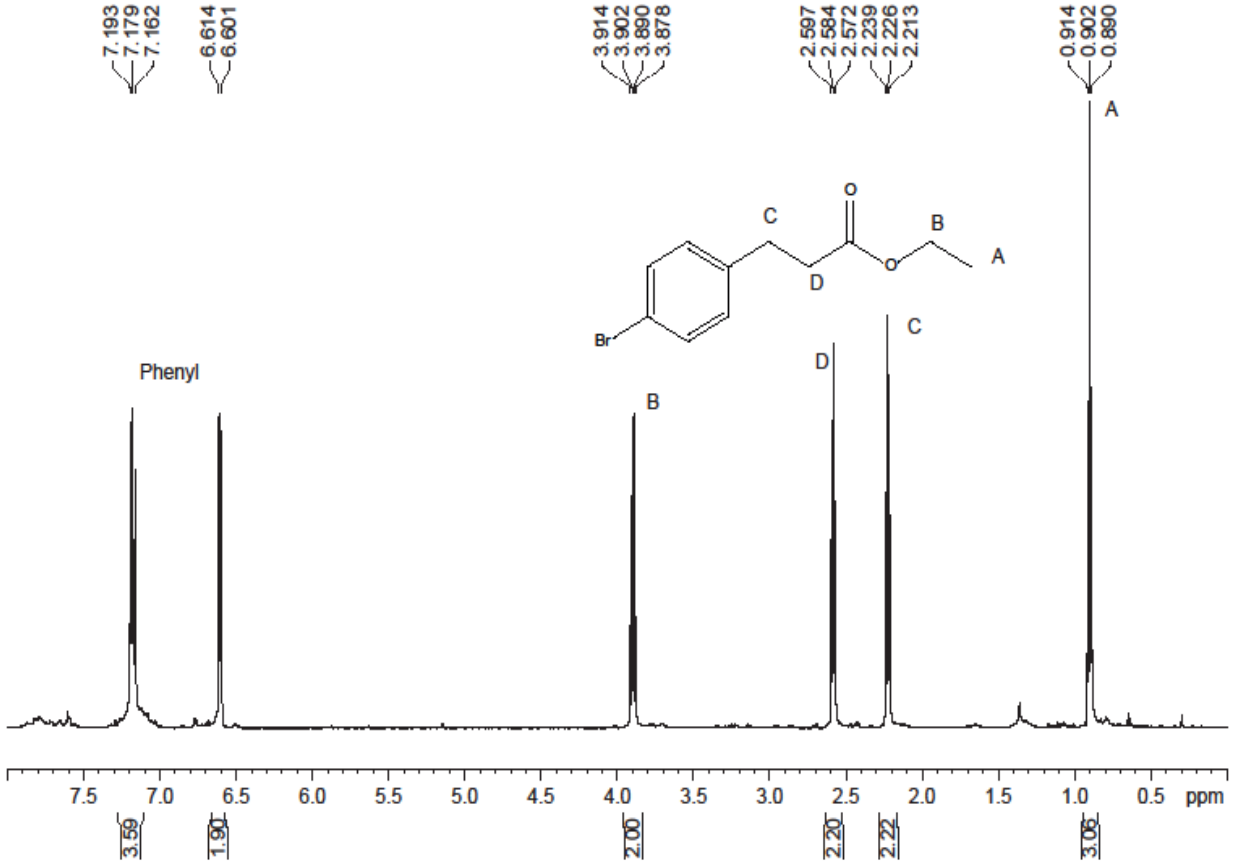

Figure S40. ^{1}H NMR spectrum (600 MHz, benzene-d_6) for catalytic reaction of ethyl trans-4-bromocinnamate and Ph_2SiH_2 to yield ethyl 3-(4-bromophenyl)propanoate as 1,4-addition product followed by hydrolysis.

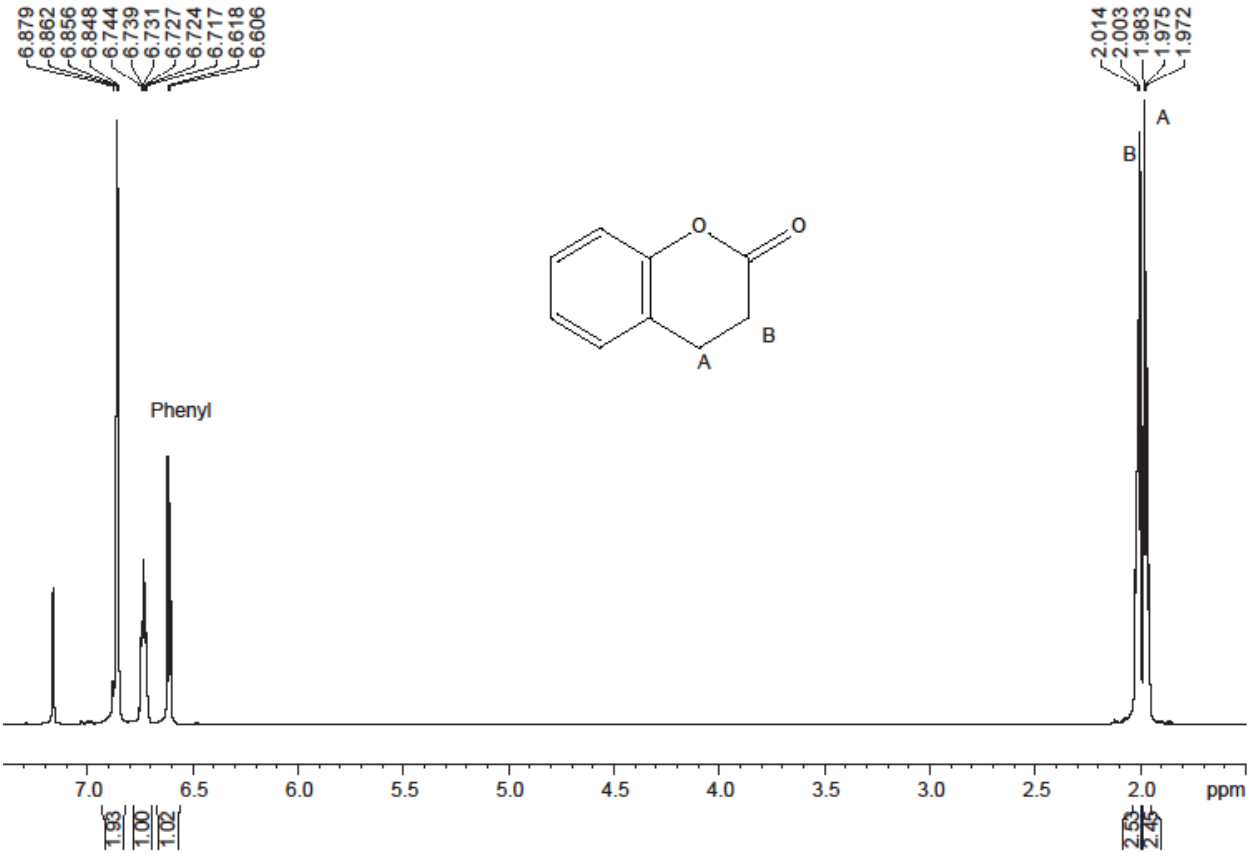

Figure S41. ^{1}H NMR spectrum (600 MHz, benzene-d_6) for catalytic reaction of coumarin and Et_2SiH_2 to yield chroman-2-one as 1,4-addition product followed by hydrolysis.

CHAPTER 4: HOMOLEPTIC DIVALENT DIALKYL LANTHANIDE-CATALYZED CROSS-DEHYDROCOUPLING OF SILANES AND AMINES

Modified from a paper accepted in *ACS Organometallics*

Aradhana Pindwal, Arkady Ellern, Aaron D. Sadow*

Abstract

The rare earth bis(alkyl) compound $Sm\{C(SiHMe_2)_3\}_2THF_2$ (**1b**) is synthesized by reaction of samarium(II) iodide and two equiv. of $KC(SiHMe_2)_3$ in THF. This synthesis is similar to that of previously reported $Yb\{C(SiHMe_2)_3\}_2THF_2$ (**1a**), and compounds **1a** and **1b** are isostructural. Reactions of **1b** and one or two equiv. of $B(C_6F_5)_3$ afford $SmC(SiHMe_2)_3HB(C_6F_5)_3THF_2$ (**2b**) or $Sm\{HB(C_6F_5)_3\}_2THF_2$ (**3b**), respectively, and the 1,3-disilacyclobutane $\{Me_2Si\text{-}C(SiHMe_2)_2\}_2$ byproduct via β-hydrogen abstraction. IR spectra of **2b** and **2b** contain bands from 2300-2400 cm^{-1} assigned to BH stretching modes. The ^{11}B NMR spectra contain highly shifted signals indicating that $HB(C_6F_5)_3$ is closely associated with the paramagnetic samarium center. Compounds **1a** and **1b** react with the bulky N-heterocyclic carbene (NHC) 1,3-di-tert-butylimidazol-2-ylidene (Im*t*Bu) to displace both THF ligands and give the mono-adducts $Ln\{C(SiHMe_2)_3\}_2Im$*t*Bu (Ln = Yb (**4a**), Sm (**4b**)). Complexes **4a** and **4b** catalyze cross-dehydrocoupling of organosilanes with primary and secondary amines at room temperature to give silazanes and H_2, whereas **1a** or **1b** are not effective catalysts. Linear second-

order plots of ln{[Et_2NH]/[Ph_2SiH_2]} vs. time for **4a**-catalyzed dehydrocoupling indicate first-order dependence on silane and amine. However, changes in experimental rate law with increased silane concentration or decreasing amine concentration indicate inhibition by silane. In addition, excess Im*t*Bu or THF inhibit the reaction rate. This data, along with the structures of **4a** and **4b** suggest that the bulky carbene favors low coordination numbers, which is important for the catalytically active species.

Introduction

Lanthanide–carbon bonds in rare earth alkyls react via insertion, σ-bond metathesis, and protonolytic ligand substitution reactions that are important elementary steps in catalytic processes including olefin polymerization,[1] hydrosilylation,[2] and dehydrocoupling.[3] Trivalent rare earth alkyls are typical catalysts for these processes, whereas fewer catalytic processes involve divalent rare earth alkyl compounds.[4] In the few cases involving divalent lanthanides, the metal center is typically a precatalyst that is activated by a one-electron oxidation, for example in the initiation of acrylate polymerizations.[4b, 5] Moreover, while homoleptic tris(alkyl) lanthanide compounds are useful and versatile starting materials for rare earth organometallic chemistry,[6] fewer homoleptic bis(alkyl) ytterbium(II),[7] europium(II),[8] and samarium(II)[4d, 9] compounds are known, with samarium(II) being the most reducing (–1.55 V) followed by ytterbium(II) (–1.15 V) and europium(II) (–0.35 V).[10]

We recently reported the synthesis of homoleptic bis(alkyl) ytterbium(II) compounds, Yb{$C(SiHMe_2)_3$}$_2L_2$ (L_2 = THF_2 or TMEDA), investigated their non-classical M⇠H-Si-containing structures,[11][note that the statement on agostic-like, 3-center-2-electron as equivalent

names, the reverse polarity of SiH vs CH suggests that agostic interactions in the former are distinct from non-classical SiH][12] and demonstrated that the β-SiH groups react with electrophiles and undergo abstraction with $B(C_6F_5)_3$.[11] Because only a few divalent bis(alkyl) lanthanide compounds have been employed in catalytic processes, we decided to investigate $Ln\{C(SiHMe_2)_3\}_2THF_2$ (Ln = Yb, Sm) as catalysts for the dehydrocoupling of organosilanes and amines. In this reaction's initiation, $Ln\{C(SiHMe_2)_3\}_2L_2$ could undergo protonolysis to give a rare earth amide. Amide transfer to an organosilane through a σ-bond metathesis-like group transfer step would provide the silazane product. These steps might be facile with divalent bis(alkyl) rare earth compounds, or their zwitterionic monoalkyl derivatives. Catalytic cross-dehydrocoupling of silanes with amines is an excellent method for silazane preparation because hydrogen gas is the only byproduct, the degree of amine silylation or silane amination can, in principle, be controlled by the catalysts, and stoichiometric salt byproducts are not formed as is the case in halosilane amination. Silazanes are used extensively as bases,[13] ligands,[14] and silylating agents[15] including as protecting groups in synthesis.[16] f-Element,[17] yttrium,[18] and magnesium complexes,[19] early metals,[20] along with Lewis acids[21] and Lewis bases[22] are well known catalysts for SiH/NH cross-coupling. In SiH/NH dehydrocoupling reactions catalyzed by bis(disilazido)ytterbium(II) compounds, Cui and co-workers[4f] observed that an N-heterocyclic carbene (NHC) ligand is required for efficient conversion. The rate of cross-dehydrocoupling of organosilanes and amines catalyzed by bis(disilazido) $Yb\{N(SiMe_3)_2\}_2L$ (L = 1,3-diisopropyl-4,5-dimethyl-imidazole-2-ylidene ($Im\textit{i}C_3H_7$) and 1,3-bis(2,4,6-trimethylphenyl)-imidazole-2-ylidene (ImMes)) is dramatically increased in comparison to THF-coordinated analogues.

Despite this example, the reactivity of carbene-coordinated rare earth complexes,[23] and the role of NHC ligands in transition-metal catalyzed processes,[24] the catalytic chemistry of

carbene-coordinated rare earth alkyl compounds is underdeveloped. In terms of homoleptic rare earth alkyls, the series of trivalent compounds $Ln(CH_2SiMe_3)_3Im\textit{i}C_3H_7$ (Ln = Er, Lu)[25] and $Ln(CH_2SiMe_3)_3$ImDipp (Ln = Y, Lu; ImDipp) = 1,3-bis(2,6-diisopropylphenyl)imidazol-2-ylidene[26] have been prepared by substituting THF with NHC. In addition, only a handful of Yb(II) and Sm(II) alkyl carbene compounds are crystallographically characterized.[27] To the best of our knowledge, N-heterocyclic carbene-coordinated divalent bis(alkyl)lanthanide complexes were previously unknown. This fact, as well as the increase in catalytic activity affected by an NHC ligand for Yb(II)-catalyzed amine-silane dehydrocoupling motivated our preparation of "only carbon ligand coordinated" divalent rare earth bis(alkyl) compounds.

Here, we report the synthesis of a divalent samarium bis(alkyl) compound for comparison of the reactivity of $Yb\{C(SiHMe_2)_3\}_2THF_2$ toward Lewis acids and toward coordination of carbene ligands. In addition, these compounds have been demonstrated to be efficient precatalysts for cross-dehydrocoupling of organosilanes and primary and secondary amines, and kinetic studies have provided a rational for the enhanced activity of NHC-coordinated divalent catalysts.

Results and Discussion

Synthesis of $Sm\{C(SiHMe_2)_3\}_2THF_2$. The homoleptic bis(alkyl)samarium compound $Sm\{C(SiHMe_2)_3\}_2THF_2$ (**1b**) is synthesized by the reaction of SmI_2THF_2[28] and 2 equiv. of $KC(SiHMe_2)_3$, which proceeds in THF over 12 h at room temperature. The solution changes color from blue-green to dark green upon mixing and then to black after 1 h. The diamagnetic isostructural analogues, $Yb\{C(SiHMe_2)_3\}_2THF_2$ (**1a**) and $Ca\{C(SiHMe_2)_3\}_2THF_2$ (**1c**), were

previously synthesized under similar conditions, but the synthesis of those diamagnetic compounds do not show the dramatic color changes observed for samarium.[11] $Sm\{C(SiHMe_2)_3\}_2THF_2$ is isolated by crystallization from pentane at –40 °C as black blocks.

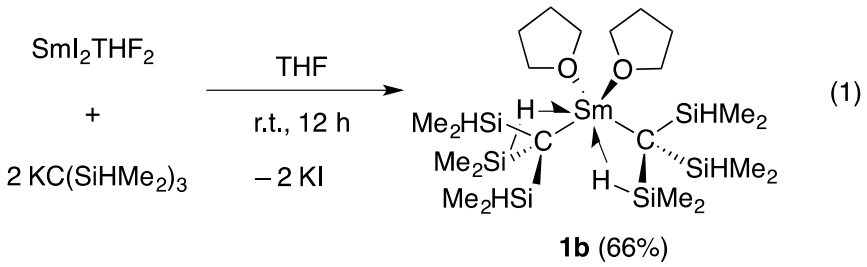

(1)

1b (66%)

The ^1H NMR spectrum of **1b** (all NMR spectra reported were acquired in benzene-d_6 at room temperature unless otherwise specified) contained signals assigned on the basis of their relative integrated ratio, chemical shifts, and linewidths. That latter two properties are influenced by the nuclei's interaction with the paramagnetic center. The highly upfield, broad resonance at –66.5 ppm (6 H, 342 Hz at half height) and the sharp singlet at –1.12 ppm (36 H, 32 Hz at half height) were assigned to the $C(SiHMe_2)_3$ ligand. The remaining signals at 11.9 and 2.78 ppm were assigned to THF. The ^1H NMR spectrum of **1b** was unchanged after its benzene-d_6 solution was heated at 80 °C for 80 h. ^{29}Si or ^{13}C spectra acquired either through direct (^{29}Si or ^{13}C) or indirect (^{29}Si HMBC, ^{29}Si INEPT, ^{13}C HMBC, ^{13}C HMQC or ^{13}C HSQC) experiments did not contain signals, likely the result of the paramagnetic Sm(II) center.

The infrared spectrum of **1b** contained signals at 2107, 2062 and 1867 cm^{-1} (KBr) that were attributed to silicon-hydrogen stretching modes. The first was assigned to a two-center-two electron bonded SiH, while lower energy signals were assigned to groups engaged in three-center-two-electron interactions with the samarium(II) center. These lower frequency bands move closer together in energy (to 2005 and 1990 cm^{-1}) in spectra measured in benzene. Three comparable stretching modes were observed in ytterbium and calcium analogues (**1a**: 2101, 2065

and 1890 cm^{-1}; $Ca\{C(SiHMe_2)_3\}_2THF_2$ (2107, 2066, and 1905 cm^{-1}), suggesting that the paramagnetic samarium compound is isostructural with ytterbium and calcium derivatives.[11]

A single-crystal X-ray diffraction study shows that the samarium center in **1b** adopts a distorted tetrahedral environment similar to the ytterbium complex **1a**. The ∠O1-Sm1-O1# angle of 89.24(7)° is acute, while the ∠C1-Sm1-C1# angle is larger 133.96(7)°. The Sm1-C1 interatomic distance of 2.733(2) Å is ca. 0.14 Å longer than the corresponding distance in **1a**, as expected based on the larger ionic radii of 7-coordinate Sm^{+2} (1.22 Å) than 7-coordinate Yb^{+2} (1.08 Å).[29] The Sm1-C1 interatomic distance is significantly longer than the other characterized Sm(II) alkyl compounds including $Sm\{C(SiMe_3)_3\}_2$[4d] (2.58 Å) and $(C_5Me_5)SmCH(SiMe_3)_2(\mu\text{-}C_5Me_5)K(THF)_2$[4c] (2.64(1) Å) but shorter than $Sm\{C(SiMe_3)_2(SiMe_2OMe)\}_2THF$ (2.787(5) and 2.845(5) Å).[9] These examples are the only three crystallographically characterized dialkyl samarium(II) compounds found in the Cambridge Structural Database. The second notable feature of **1b** is the conformation of $C(SiHMe_2)_3$ ligands as a result of classical and non-classical Sm←H-Si interactions. As in the ytterbium analogue, the two $C(SiHMe_2)_3$ ligands are related by a crystallographic C_2 axis that bisects the C1-Sm1-C1# angle. Within each ligand, one SiH points toward the Sm center, and the resulting Sm1-H1s interatomic distance of 2.64(2) Å is shorter than the Sm1-Si1 distance of 3.303(5) Å. The longer Sm1-Si2 (3.644(6) Å) and Sm1-H2s (3.572(3) Å) distances are similar (as are the Sm1-Si3 (3.599(7) and Sm1-H3s (3.694(2) Å) indicating long, side-on coordination.

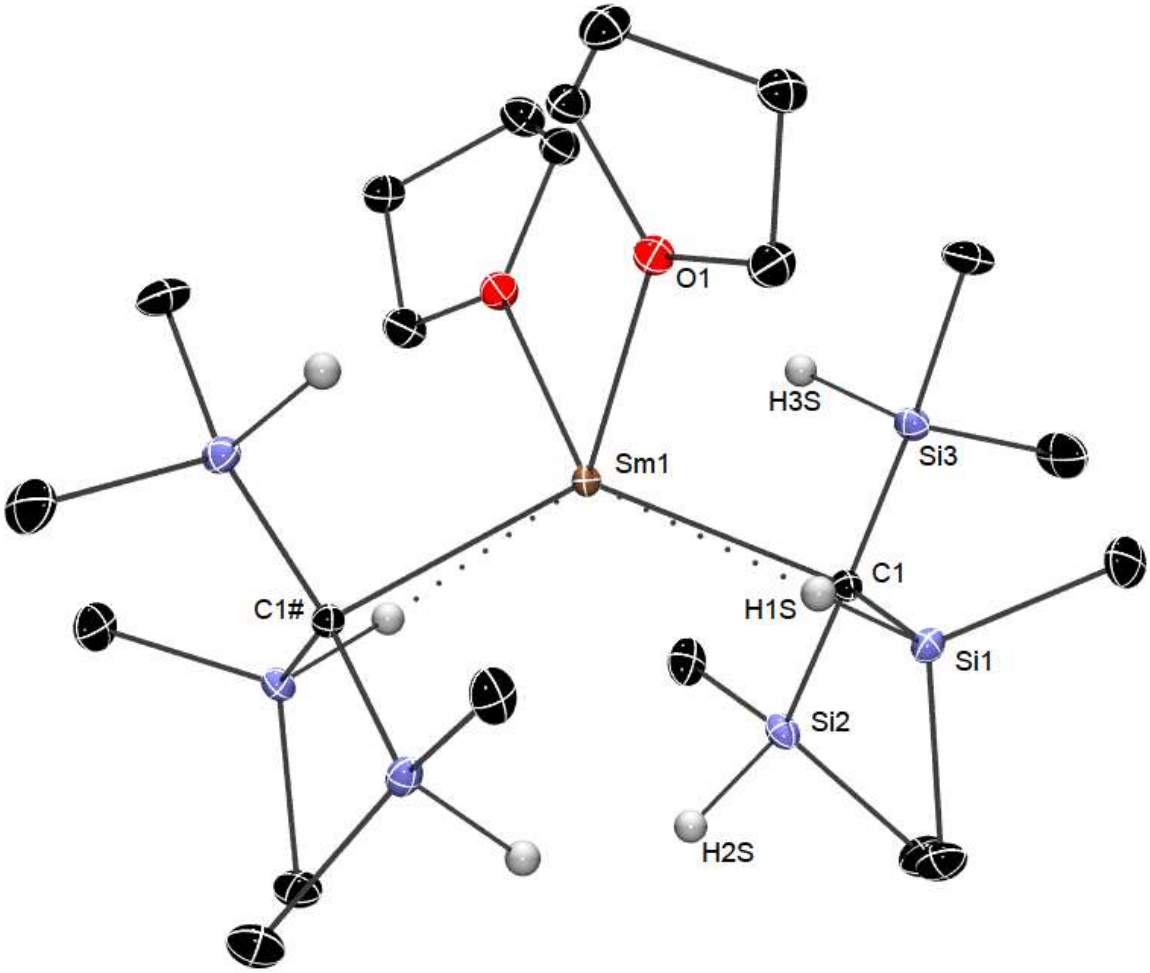

Figure 1. Rendered thermal ellipsoid plot of $Sm\{C(SiHMe_2)_3\}_2THF_2$ (**1b**). Ellipsoids are plotted at 35% probability. Hydrogen atoms bonded to silicon were located objectively in the Fourier difference map and were refined isotropically. All other H atoms are not plotted for clarity. Significant interatomic distances (Å): Sm1-C1, 2.733(2); Sm1-Si1, 3.303(5); Sm1-Si2, 3.644(6); Sm1-Si3, 3.599(7); Sm1-H1s, 2.64(2). Significant interatomic angles (°): C1-Sm1-C1#, 133.96(7); O1-Sm1-C1, 108.57(5); O1-Sm1-O1, 89.24(7); Si1-C1-Sm1, 90.94(7); Si2-C1-Sm1, 104.48(7); Si3-C1-Sm1, 102.49(7).

Reactions with $B(C_6F_5)_3$. The samarium compound **1b** and $B(C_6F_5)_3$ react to transfer hydride from the $C(SiHMe_2)_3$ ligand to the Lewis acid giving zwitterionic hydridoborate compounds. These reactions follow the pathway observed for interactions of the ytterbium complex **1a** and $B(C_6F_5)_3$, despite the more reducing nature of Sm vs. Yb.[11] Thus, **1b** and one or two equiv. of $B(C_6F_5)_3$ give $SmC(SiHMe_2)_3HB(C_6F_5)_3THF_2$ (**2b**) or $Sm\{HB(C_6F_5)_3\}_2THF_2$ (**3b**), respectively (Scheme 1). The byproduct of each hydride transfer is 0.5 equiv of 1,3-disilacyclobutane $\{Me_2Si\text{-}C(SiHMe_2)_2\}_2$, which is the head-to-tail dimer of the silene $Me_2Si{=}C(SiHMe_2)_2$.

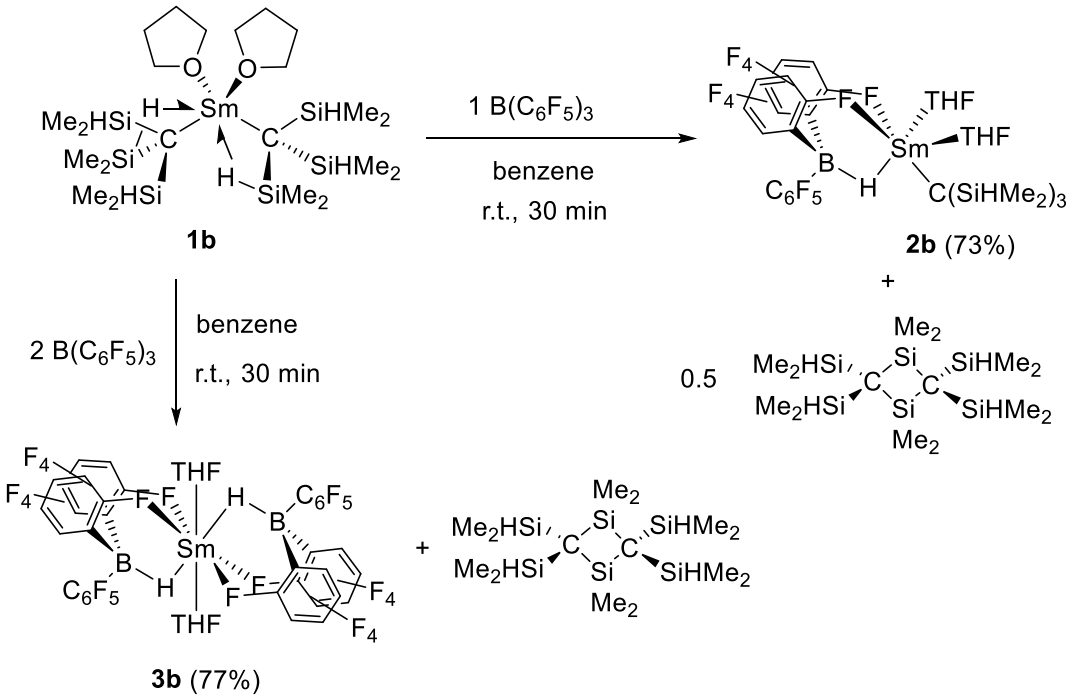

Scheme 1. Reactions of **1b** and one or two equiv. of $B(C_6F_5)_3$.

X-ray quality crystals are not yet available for zwitterionic compounds **2b** and **3b**. The infrared spectra (KBr) of analytically pure **2b**, easily isolated after pentane washes, showed three characteristic bands at 2389 (ν_{BH}), 2306 (ν_{BH}) and 2110 cm^{-1} (ν_{SiH}). In contrast, the IR spectrum of **2a** (KBr) contained bands at 2310 (ν_{BH}), 2074 (ν_{SiH}), 1921 cm^{-1} (ν_{SiH}). The presence of only one SiH band at high energy in **2b** suggests that the $C(SiHMe_2)_3$ group lacks non-classical Sm-

H-Si interactions present in **2a**. In addition, the IR spectrum of **3b** contained bands at 2388 and 2318 cm^{-1} assigned to B-H stretching modes, while no bands were detected in the region associated with Si-H stretching modes (2100-1800 cm^{-1}).

Direct comparisons between samarium and ytterbium structure by NMR are complicated by paramagnetic effects. Nonetheless, signals in the ^{11}B and ^{19}F NMR spectra of **2b** and **3b** indicate that perfluorophenylhydridoborate groups are closely associated with the samarium center. The ^{11}B NMR spectra acquired in bromobenzene-d_5 for **2b** and **3b** contained paramagnetically shifted broad signals at –88.4 and –100.4 ppm, respectively, whereas ^{11}B NMR signals for diamagnetic ytterbium analogues appeared at –20.8 (**2a**) and –26.4 (**3a**). Only two signals were observed in the ^{19}F NMR spectrum in the ratio of 1:2, assigned to the *para*- and *meta*-fluorine on C_6F_5 groups for compounds **2b** and **3b**, compared to the Yb analogues' spectra that revealed three signals for *ortho*-, *meta*-, and *para*-fluorines.[11]

Reaction with 1,3-di-tert-butylimidazol-2-ylidene (Im*t*Bu). Compounds **1a** or **1b** and one equiv. of 1,3-di-tert-butylimidazole-2-ylidene (Im*t*Bu) react almost instantaneously at room temperature in benzene or pentane to displace the THF ligands affording Ln{C(SiHMe$_2$)$_3$}$_2$Im*t*Bu (Ln = Yb (**4a**), Sm (**4b**)) quantitatively in *in situ* reactions (Scheme 2). Recrystallization from pentane at –40 °C affords red crystals of Yb{C(SiHMe$_2$)$_3$}$_2$Im*t*Bu (**4a**) or dark red crystals of Sm{C(SiHMe$_2$)$_3$}$_2$Im*t*Bu (**4b**) in moderate isolated yields.

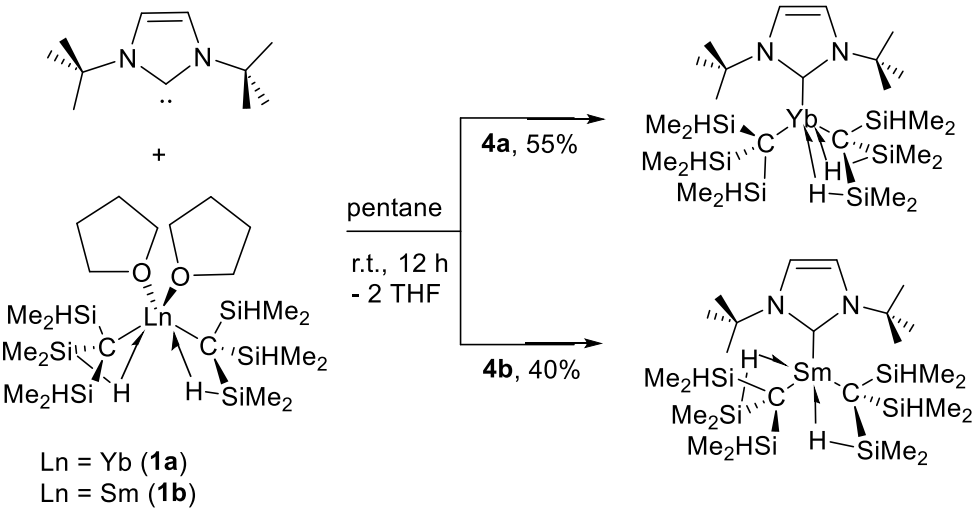

Scheme 2. Reactions of ytterbium and samarium dialkyls with Im*t*Bu.

The ^{1}H NMR spectrum of diamagnetic **4a**, acquired on a recrystallized sample, contained a doublet at 0.45 ppm ($^{3}J_{HH}$ = 3.6 Hz, 36 H) and a septet at 4.86 ppm with silicon satellites ($^{1}J_{SiH}$ = 144 Hz, 6 H) assigned to the $SiHMe_2$ moiety as well as singlets at 1.43 and 6.33 ppm assigned to the coordinated Im*t*Bu ligand. These signals remain sharp even at spectra acquired at low temperature (~200 K) in toluene-d_8. In the $^{13}C\{^{1}H\}$ NMR spectrum, a signal at 196.9 ppm for the carbene carbon appeared with a similar chemical shift as other lanthanide tris(alkyl) carbene adducts.[25-26] Neither ^{15}N NMR signals of Im*t*Bu nor the ^{29}Si NMR of the $SiHMe_2$ moieties are changed significantly in **4a** in comparison with starting materials.

The SiH region of the infrared spectra for **4a** and **4b** were distinct from each other as well as from **1a** and **1b**. In **4a**, a broad signal at 2058 cm^{-1} is poorly resolved from bands at 2083 and 2114 cm^{-1}, with one low energy band at 1871 cm^{-1}. In contrast, the samarium analogue's spectrum contained sharper signals at 2108, 2076, 2064, and 2044 cm^{-1} as well as two lower energy bands at 1910 and 1796 cm^{-1}. Note that the IR spectra of **1a** and **1b** (described above)

only contained 3 ν_{SiH}, suggesting that compounds **1** and **4** have inequivalent conformations. This idea is supported by single crystal X-ray diffraction analysis.

While compounds **4a** and **4b** (see Figures 2 and 3) both contain three-coordinate distorted trigonal planar metal centers (C1-Ln-C8 > 120°), the two species crystallize in inequivalent space groups (**4a:** P-bca, Z = 8; **4b**: P-1, Z = 2) with distinctly inequivalent conformations of their alkyl ligands. In **4a**, one ligand forms two Yb⋯H-Si interactions and the other ligand containing only normal Si-H groups. The di-agostic-like ligand in **4a** contains two short Yb-H distances (Yb1-H2s, 2.42(3); Yb1-H3s, 2.49(3) Å) and two short Yb-Si distances (Yb1-Si2, 3.118(8); Yb1-Si3, 3.169(8) Å). In **4b**, one alkyl contains one Sm⋯H-Si, while the other alkyl contains two secondary interactions. Short distances Sm1-H2s (2.54(2) Å), Sm1-Si2 (3.2686(6) Å), Sm1-H4s (2.65(2) Å), and Sm1-Si4 (3.2916(6) Å), acute angles for Sm1-C1-Si2 (88.13(7)°) and Sm1-C8-Si4 (90.27(7)°), and coplanar Sm-C and Si-H vectors (Sm1-C1-Si2-H2s, –3.4(9)°; Sm1-C8-Si4-H4s, 9.9(9)°) are consistent with Sm⋯H-Si. A second SiH approaches the Sm center (Sm1-H1s, 2.86(2) Å; Sm1-Si1, 3.2973(6) Å; Sm1-C1-Si1, 89.14(7)°), but the Sm1-C1 and Si1-H1s vectors are not coplanar (Sm1-C1-Si1-H1s, –36(1)°). The differences in alkyl ligand conformation may also be reflected in the distinct IR spectra of **4a** and **4b**, suggesting that the Ln⋯H-Si close contacts effect the vibrational properties (i.e., Si-H force constants). It is somewhat unexpected that the conformations of **4a** and **4b** are inequivalent, however, it is also worth noting that the ionic radii for Sm(II) and Yb(II) are different by 0.14 Å.[29]

As noted above, the central carbons of the $C(SiHMe_2)_3$ ligands, the carbene carbon, and the metal center are co-planar in **4a** and **4b**. The angles between the alkyl ligands and the carbene group deviate from 120° (C1-Yb1-C25 = 106.25(8)° and C8-Yb1-C25 = 115.03(8)°; C8-Sm1-C15 = 113.99(5)° and C1-Sm1-C15 = 114.29(5)°) suggesting that alkyl-alkyl interligand

repulsions are more severe than the carbene-alkyl interactions. The Yb1-C1 and Yb1-C8 distances (2.627(3) and 2.611(3) Å, respectively) are slightly longer than in **1a** (2.596(4) Å).[11] However, the Sm-C distances in **1b** (Sm1-C1, 2.733(2) Å) and **4b** (Sm1-C1, 2.779(2) Å; Sm1-C8, 2.739(2) Å) are similar. This observation may relate to the larger ionic radii of Sm(II) compared to Yb(II), which reduces interligand interactions that could affect Ln-C distances in the former complexes. Interestingly, the two alkyl ligands have similar Sm-C distances, even though one ligand has two non-classical Sm←H-Si interactions and the other ligand contains only 2-c-2-e bonded SiH groups. The Yb1-C25 distance in **4a** (2.605(3) Å) is slightly longer than that for other Yb carbenes, such as Yb{N(SiMe$_3$)$_2$}$_2$ImMes (2.600(3) Å),[4f] (C$_5$Me$_4$Et)$_2$Yb(ImMe) (2.552(4) Å[27a].

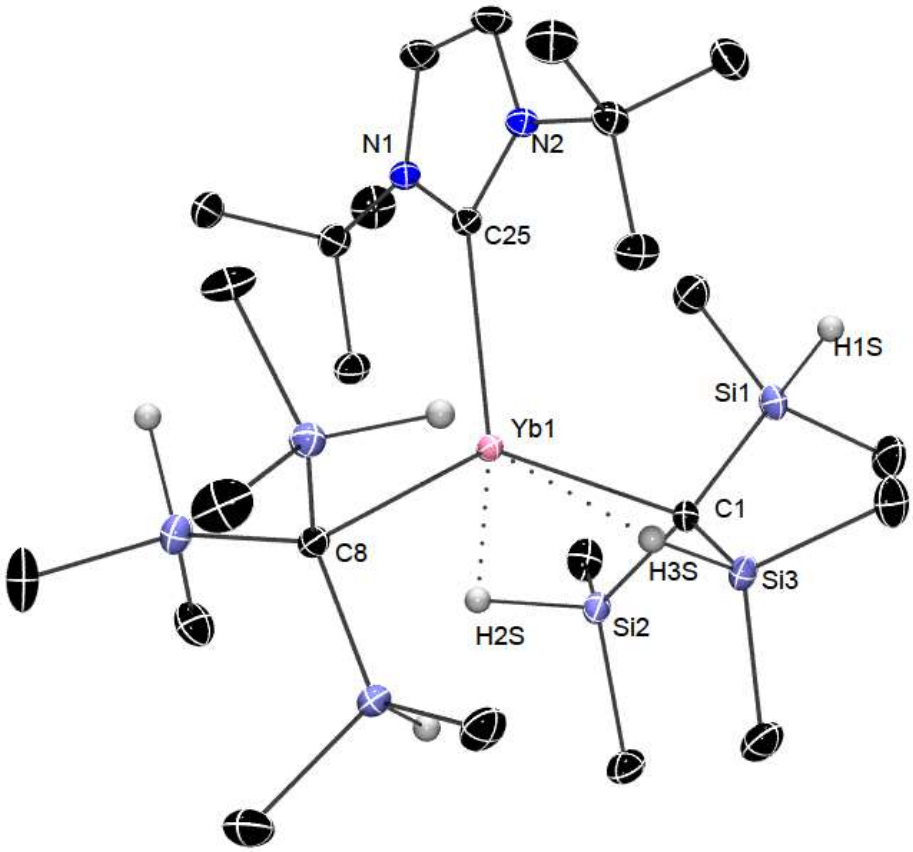

Figure 2. Rendered thermal ellipsoid plot of Yb{C(SiHMe$_2$)$_3$}$_2$Im*t*Bu (**4a**). Ellipsoids were plotted at 35% probability. Hydrogen atoms bonded to silicon were located objectively in the Fourier difference map and were included in the representation. All other H atoms were not plotted for clarity. Significant interatomic distances (Å): Yb1-C1, 2.627(3); Yb1-C8, 2.611(3); Yb1-C25, 2.605(3); Yb1-Si1, 3.825(9); Yb1-Si2, 3.118(8); Yb1-Si3, 3.169(8); Yb1-H1s, 4.16(3); Yb1-H2s, 2.422(3); Yb1-H3s, 2.49(3). Significant interatomic angles (°): C1-Yb1-C8, 138.69(8); C1-Yb1-C25, 106.26(8); C25-Yb1-C8, 115.04(8); Si1-C1-Yb1, 117.0(1); Si2-C1-Yb1, 87.1(1); Si3-C1-Yb1, 89.1(1).

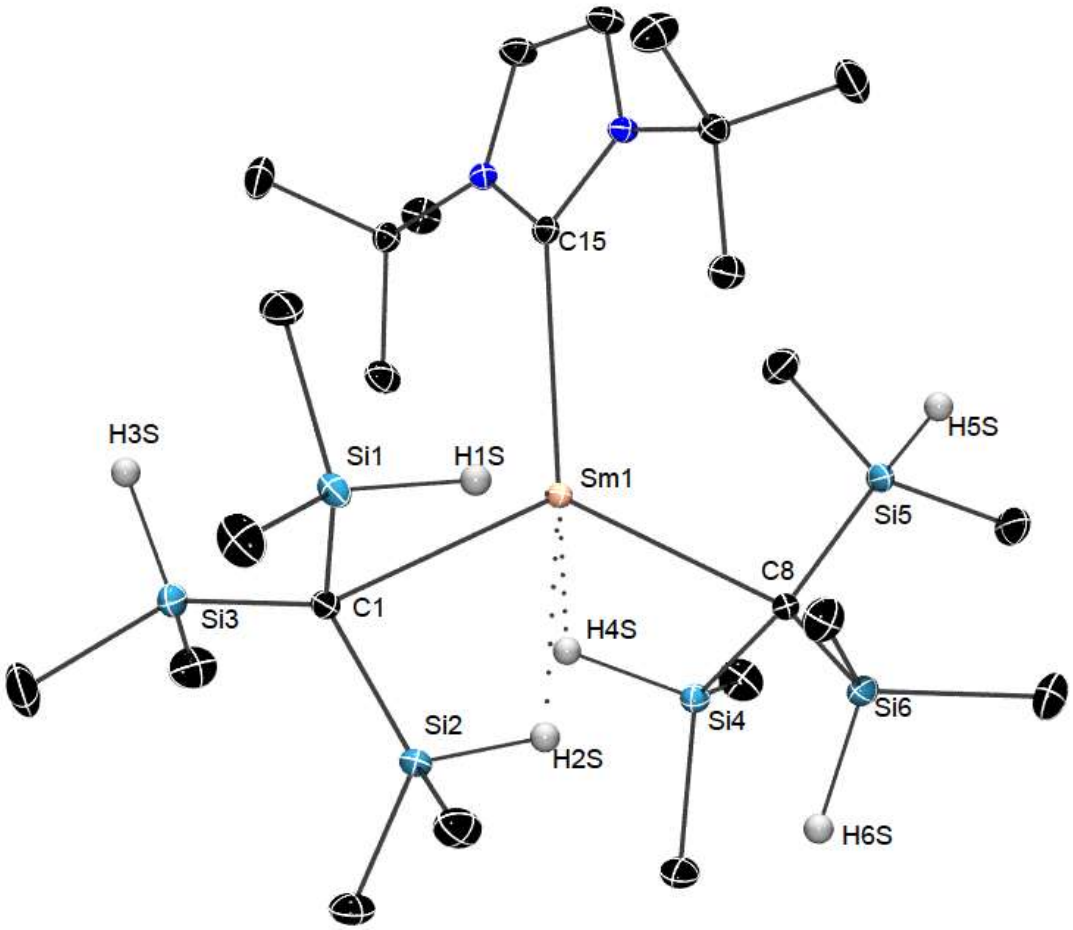

Figure 3. Rendered thermal ellipsoid plot of Sm{C(SiHMe$_2$)$_3$}$_2$Im*t*Bu (**4b**). Significant interatomic distances (Å): Sm1-C1, 2.779(2); Sm1-C8, 2.739(2); Sm1-C15, 2.780(2); Sm1-Si1, 3.297(7); Sm1-Si2, 3.269(8); Sm1-Si3, 4.059(7); Sm1-Si4, 3.292(7); Sm1-Si5,3.702(6); Sm1-Si6, 3.687(7); Sm1-H1s, 2.86(2); Sm1-H2s, 2.54(2); Sm1-H3s, 4.41(2); Sm1-H4s, 2.65(2); Sm1-H5s, 4.03(2); Sm1-H6s, 4.30(3). Significant interatomic angles (°): C1-Sm1-C8, 131.65(8); C1-Sm1-C15, 114.29(6); C15-Sm1-C8, 113.99(6); Si1-C1-Sm1, 89.14(7); Si2-C1-Sm1, 88.13(7); Si3-C1-Sm1, 122.56(9).

Crystals of **4a** and **4b** persist at room temperature for 2 d under an inert atmosphere. Upon heating a solution of **4a** in benzene-d_6 at 80 °C for one day, the alkane HC(SiHMe$_2$)$_3$ is formed at the expense of **4a**. The remaining ^{1}H NMR signals at 1.60 and 4.75 ppm were attributed to a product resulting from transformation of the Im*t*Bu ligand into a new, yet unidentified organic species bonded to ytterbium. The crystals of **4a** and **4b** also decompose under vacuum to HC(SiHMe$_2$)$_3$ and free carbene, and the crystals' color fade from deep red to pale orange during this decomposition process. Hence, these compounds are used only from freshly recrystallized and isolated material by carefully decanting the pentane solution and briefly evaporating residual solvent under vacuum for short amounts of time.

Only starting materials were observed in ^{1}H NMR spectra of mixtures containing the zwitterionic compounds **2a** or **3a** and Im*t*Bu. In contrast, reaction of **4a** and B(C$_6$F$_5$)$_3$ generates YbC(SiHMe$_2$)$_3$(HB(C$_6$F$_5$)$_3$)Im*t*Bu and 0.5 equiv. of 1,3-disilacyclobutane {Me$_2$Si-C(SiHMe$_2$)$_2$}$_2$. The ^{11}B NMR spectrum of the reaction mixture contained a doublet at –21 ppm ($^1J_{BH}$ = 73.6 Hz) and provided good evidence for hydrogen abstraction. The ^{1}H NMR spectrum contained a multiplet at 4.75 ppm (3 H, $^1J_{SiH}$ = 192 Hz) assigned to the SiH and a singlet at 0.74 ppm (18 H,

$SiMe_2$). The large SiH coupling constant indicate classical SiH interactions within the molecule. The integrated ratio of these signals with respect to the carbene resonances at 6.19 and 1.12 ppm indicate formation of a 1:1 adduct. However, repeated attempts of scaling up and isolating the crude from the reaction did not yield isolable product.

UV-Vis spectroscopy. The UV-Vis spectrum of **1b** in THF had two prominent broad bands with λ_{max} values of 387 (ε = 545 $M^{-1}cm^{-1}$) and 407 nm (ε = 529 $M^{-1}cm^{-1}$). The spectrum was similar to that observed in pentane (389 (ε = 556 $M^{-1}cm^{-1}$) and 439 nm (ε = 518 $M^{-1}cm^{-1}$). For compound **4b** in pentane, bands were observed at 405 nm (ε = 551 $M^{-1}cm^{-1}$) and 492 nm (ε = 586 $M^{-1}cm^{-1}$). Peaks between 500 and 600 nm for Sm(II) complexes have been assigned to f→d transitions.[32] The UV-Vis spectrum of **4b** shows an f→d transition at 492 nm while no such transition was observed in compound **1b**. Both compounds' absorption tails through the visible region, accounting for their dark black color. For comparison, the Sm(II) complex $Sm\{N(SiMe_3)_2\}_2THF_2$ (recorded in THF)[33] has two bands at 380 and 558 nm, while the absorption spectrum of SmI_2THF_2 contains four bands at 354, 423, 557 and 623 nm. The shoulder at 370 nm in UV-Vis spectrum of SmI_2THF_2 is assigned to a transition associated with the iodide. Figure 4 shows a comparison of UV-Vis spectra of **1b**, **4b** in pentane. (See Supporting information for UV-Vis spectra of **1b** and the starting material, SmI_2THF_2 in THF). Upon addition of two equiv. of THF to **4b,** the peak at 492 nm diminishes and intensity of the broad peak of **1b** at 439 nm increases. An isosbestic point at 446 nm was apparent in a series of spectra with 2.0, 2.5, 3.0, 3.5 and 4.0 equiv. of THF (Figure 5). Thus, the conversion of **4b** to **1b** upon addition of THF occurs without detectable buildup of intermediates. This process is clearly

reversible, however greater than 8 equiv. are required for the **4b** signals to be overwhelmed by **1b** peaks.

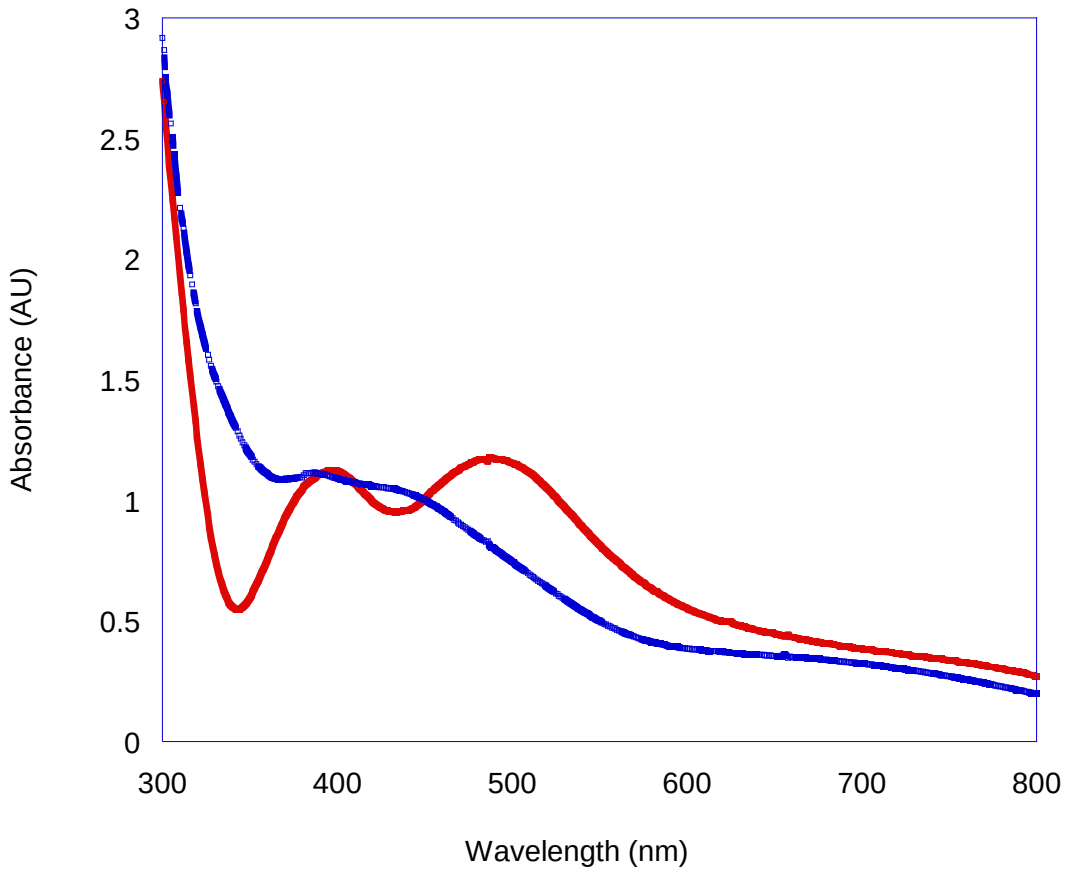

Figure 4. UV-Vis spectra of **1b** and **4b**, 2mM in pentane.

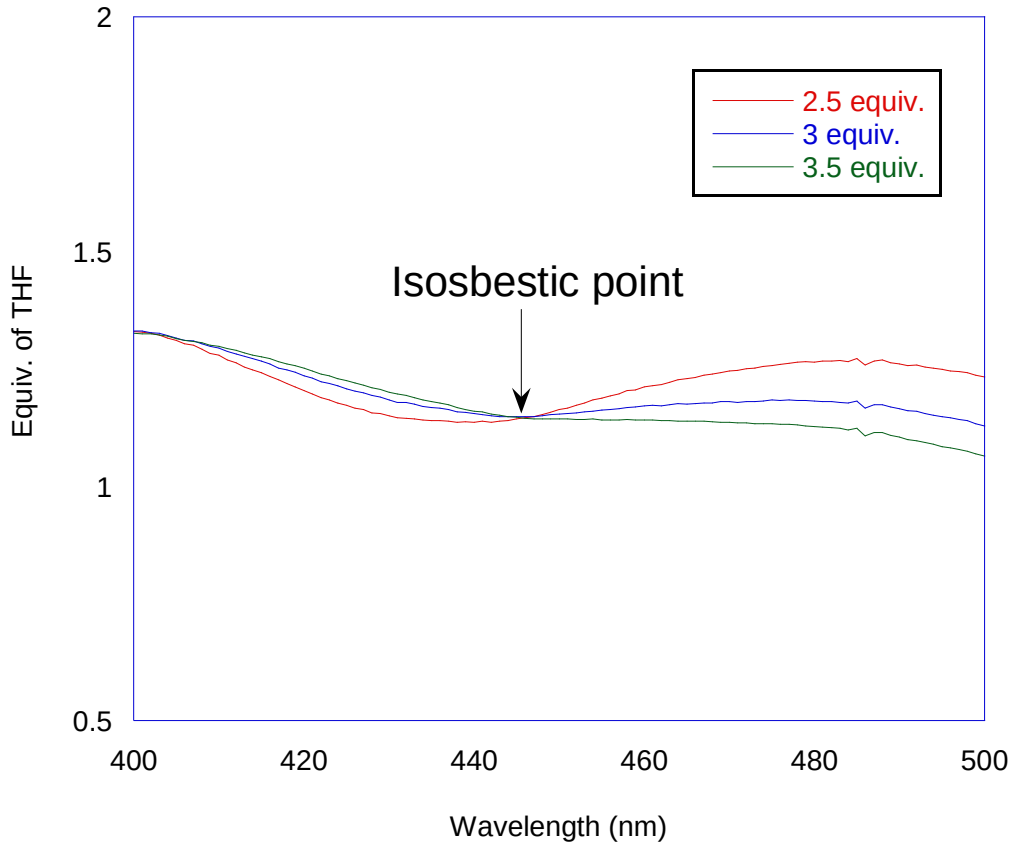

Figure 5. UV-Vis spectra of addition of n equiv. of THF to **4b** to determine the isosbestic point, 2mM in pentane.

The UV-Vis spectra of **2b** and **3b** in bromobenzene showed bands at 364 nm (ε = 948 $M^{-1}cm^{-1}$), 478 nm (ε = 658 $M^{-1}cm^{-1}$) and 533 nm (ε = 587 $M^{-1}cm^{-1}$) for **2b** and 329 nm (ε = 660 $M^{-1}cm^{-1}$), 385 nm (ε = 471 $M^{-1}cm^{-1}$) and 478 nm (ε = 199 $M^{-1}cm^{-1}$) for **3b**. A very weak f→d transition band is observed in both the compounds around 500 nm (see Supporting Information).

Only starting materials were observed in ^{1}H NMR spectra of mixtures containing the zwitterionic compounds **2a** or **3a** and Im*t*Bu. In contrast, reaction of **4a** and $B(C_6F_5)_3$ generates $YbC(SiHMe_2)_3\{HB(C_6F_5)_3\}$Im*t*Bu and 0.5 equiv. of 1,3-disilacyclobutane {Me_2Si-

$C(SiHMe_2)_2\}_2$. The ^{11}B NMR spectrum of the reaction mixture contained a doublet at –21 ppm ($^1J_{BH}$ = 73.6 Hz) and provided good evidence for hydrogen abstraction. The ^1H NMR spectrum contained a multiplet at 4.75 ppm (3 H, $^1J_{SiH}$ = 192 Hz) assigned to the SiH and a singlet at 0.74 ppm (18 H, $SiMe_2$). This large SiH coupling constant suggests that the SiH groups do not interact with the Yb center in this zwitterionic species. The integrated ratio of these signals and the carbene resonances at 6.19 and 1.12 ppm indicate that a 1:1 adduct is formed. Unfortunately, this material has not yet proven isolable.

Cross-dehydrocoupling of organosilanes and amines catalyzed by Ln{C(SiHMe$_2$)$_3$}$_2$Im*t*Bu. The divalent compounds **4a** and **4b** are efficient precatalysts for cross-dehydrocoupling of Si-H and N-H bonds to give Si-N bonds and H_2 (eq. 2).

$$R_3Si\text{-}H + H\text{-}NR'_2 \xrightarrow[\text{r.t., benzene}]{\text{10 mol\% } \mathbf{4a} \text{ or } \mathbf{4b}} R_3Si\text{-}NR'_2 + H_2 \qquad (2)$$

R' = alkyl
Ln = Yb, Sm

Primary and secondary amines effectively couple with primary and secondary silanes to afford the desired silazanes (Table 1), which are readily isolated in good yield by distillation. In the absence of **4a** as a catalyst, only starting materials are observed. Compounds **1a**, **1b**, **2b**, and **3b**, as well as Im*t*Bu were also tested for catalytic activity in the cross-dehydrocoupling of $PhMeSiH_2$ and *t*$BuNH_2$, but only starting materials were observed in ^1H NMR spectra of the reaction mixtures after 1 day at room temperature or 60 °C.

Table 1. Ln{C(SiHMe$_2$)$_3$}$_2$Im*t*Bu-Catalyzed Dehydrocoupling of Silanes and Amines

Entry	**Cat. loading**	**Silane**	**Amine**	**Time (h)**	**Silazane**	**Yield[a] (%)**
1.	5	$PhSiH_3$	4 equiv. 	0.1	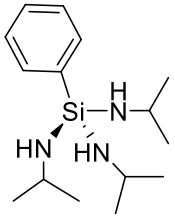	63 (62)
2.	5	2.2 equiv. $PhSiH_3$		0.1	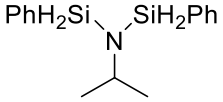	72 (71)
3.	5	$PhSiH_3$	2 equiv. 	15	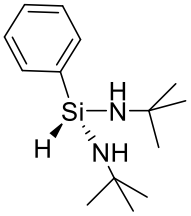	92 (91)
4.	5	2.2 equiv. $PhSiH_3$		15	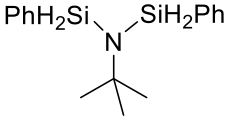	75 (73)
5.	5	$PhSiH_3$	3 equiv. 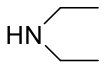	15	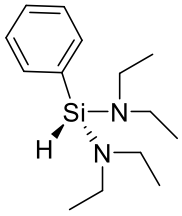	82 (80)
6.	5 [b]	$PhSiH_3$	3 equiv. 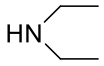	15	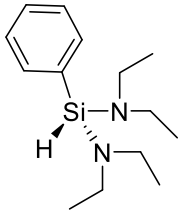	81 (78)

Table 1 continued

7.	10	2 equiv. $PhMeSiH_2$		4	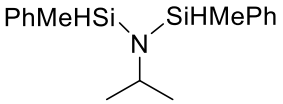	89 (88)
8.	10	$PhMeSiH_2$		4	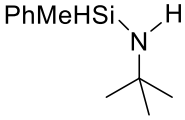	87 (85)
9.	10[b]	$PhMeSiH_2$		4	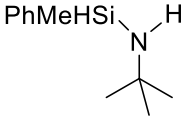	85 (82)
10.	10	$PhMeSiH_2$	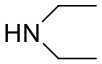	4	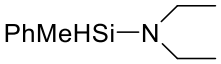	93 (92)
11.	10[b]	$PhMeSiH_2$	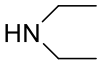	4	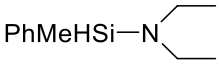	92 (90)
12.	10	Ph_2SiH_2		15	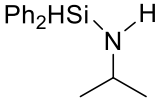	87 (84)
13.	10[b]	Ph_2SiH_2		15	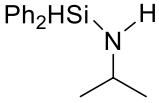	88 (85)
14.	10	Ph_2SiH_2		15	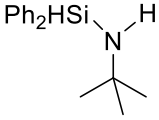	88 (84)
15.	10	Ph_2SiH_2	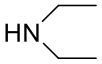	15	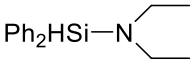	82 (82)

Conditions: Catalyst = **4a**, benzene-d_6 or benzene, room temperature, [a]isolated yields given in parenthesis, [b]catalyzed by **4b**.

In catalytic reactions, the consumption of organosilane and formation of silazane product was evident from the new SiH resonances, which shifted downfield as the SiH were converted into $SiNR'_2$. The $^3J_{HH}$ coupling between SiH and NH provided characteristic splitting patterns for

SiH resonances, which appeared as doublets for silazide RH_2SiNHR' and as triplets in spectra of $RHSi(NHR')_2$. Although reactions of $PhSiH_3$ and $iC_3H_7NH_2$ or $tBuNH_2$ in a 1:1 ratio result in a mixture of these products, reactions with excess silane or excess amine provide control over the product identity. For example, the **4a**-catalyzed reaction of $PhSiH_3$ and 4 equiv. of i-$C_3H_7NH_2$ affords the silyltrisazido $PhSi(NHi\text{-}C_3H_7)_3$. In addition, the amine's steric bulk affects the reaction rate in conversions with $PhSiH_3$. For example, two equiv. of t-$BuNH_2$ and $PhSiH_3$ react to yield the silyldiazido $PhHSi(NHt\text{-}Bu)_2$. The reaction with the secondary amine, Et_2NH (3 equiv.) also requires 15 h to yield the silyldiazido $PhSiH(NEt_2)_2$, but reaction of phenylsilane and $(iC_3H_7)_2NH$ did not result in any silazane formation after 1 day at room temperature or 60 °C.

4a or **4b**-catalyzed reactions of secondary silanes such as $PhMeSiH_2$ and Ph_2SiH_2 and either primary or secondary amines afford monosilazane products, whilst two equiv. of silane react with primary amines gives disilazanes. One such example is illustrated by synthesis of $(PhMeSiH)_2NiC_3H_7$ in 4 h at room temperature. Similar to primary silanes, only starting materials are observed in mixtures of $(iC_3H_7)_2NH$ and secondary silanes. Additionally, only starting materials are observed in mixtures of tertiary silanes such as $BnMe_2SiH$ (Bn = CH_2Ph), Et_3SiH or $(CH_2{=}CH)SiMe_2H$ with primary or secondary amines after 1 day at room temperature or at 60 °C.

The reaction of Ph_2SiH_2 and Et_2NH catalyzed by **4a** yields $Ph_2HSiNEt_2$ as the sole coupling product when a range of silane:amine ratios (1:1 to 1:25) were used. Therefore, this transformation was used as a representative conversion for kinetic studies. Upon addition of catalyst **4a** to mixtures of Ph_2SiH_2 and Et_2NH, free ImtBu and the alkane $HC(SiHMe_2)_3$, resulting from protonolysis, were detected by ^1H NMR spectroscopy. The active catalytic species is part of this mixture, and dehydrocoupling ensues. Four concentration regimes were tested,

namely high and low [Et_2NH] and [Ph_2SiH_2]. Under conditions of low $[Ph_2SiH_2]_{ini}$ (0.081 M) and high $[Et_2NH]_{ini}$ (0.673 M), second-order plots indicate first-order dependence on each reagent. The data analysis is limited by the faster initial consumption of ca. 5 mM of Et2NH during catalyst initiation than during dehydrocoupling. In spite of this limitation, second order rate constants increase in a series of experiments in which [**4a**] is increased.

A plot of observed second-order rate constants vs catalyst concentration (i.e., [**4a**]) reveals a linear dependence on **4a** concentration, giving the ternary rate law $d[Ph_2SiH_2]/dt = k'_{obs}[\mathbf{4a}][Ph_2SiH_2][Et_2NH]$ (k'_{obs} = 1.04 ± 0.07 $\times 10^{-7}$ $mM^{-2}s^{-1}$; Figure 6). The non-zero intercept indicates that a portion of the ytterbium species is not active for catalysis. On the basis of this and the observation of free NHC during the reaction, we hypothesized that additional NHC might increase catalytic activity by disfavoring dissociation. Instead, excess Im*t*Bu, or excess THF, inhibit the rate of catalytic conversion. This inhibition likely results from the ytterbium amide or ytterbium hydride catalytic intermediates coordinating either THF or excess Im*t*Bu, since **4a** and excess Im*t*Bu do not afford detectable quantities of $Yb\{C(SiHMe_2)_3\}_2(Im\textit{t}Bu)_2$. An additional and unexpected, inhibition process was also observed in the second-order rate constant decreases with increasing [Ph_2SiH_2] (Figure 7).

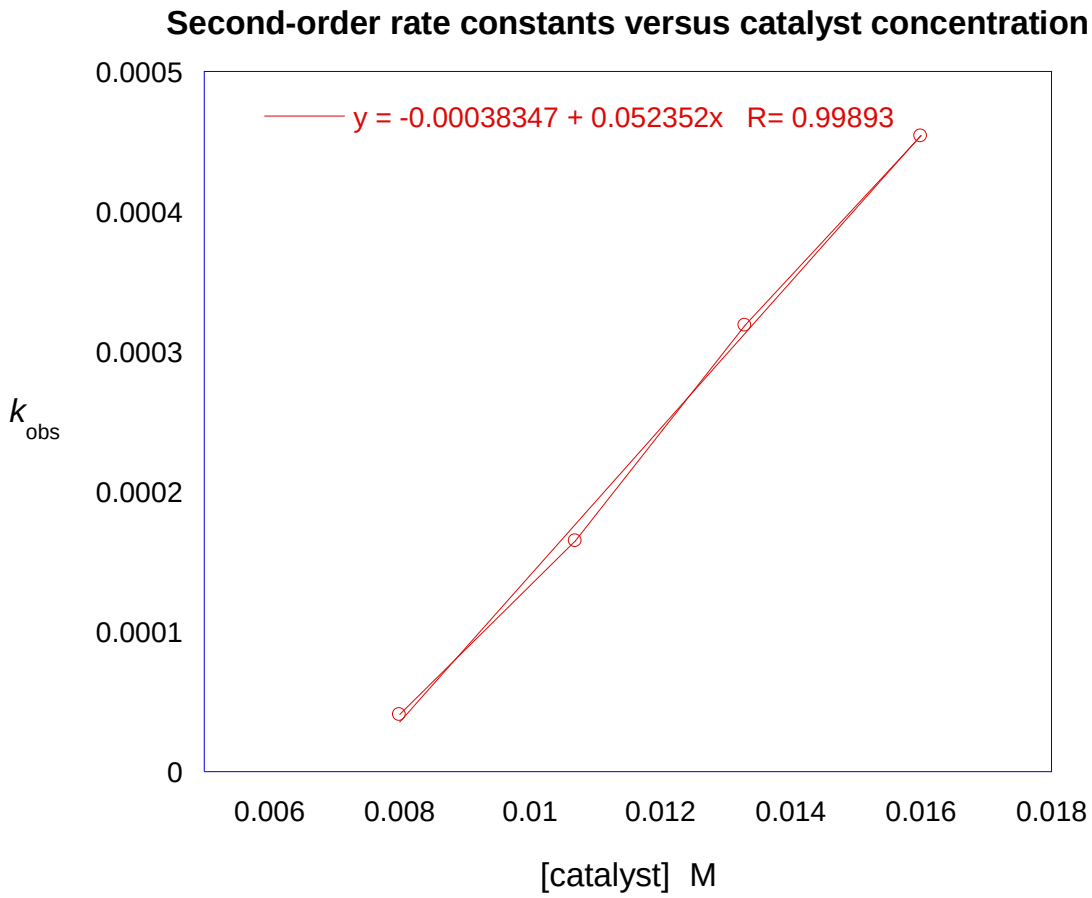

Figure 6. Plot of second-order rate constants versus catalyst concentration [**4a**] for reaction of Et_2NH (0.673 M) and Ph_2SiH_2 (0.081 M) at 298 K.

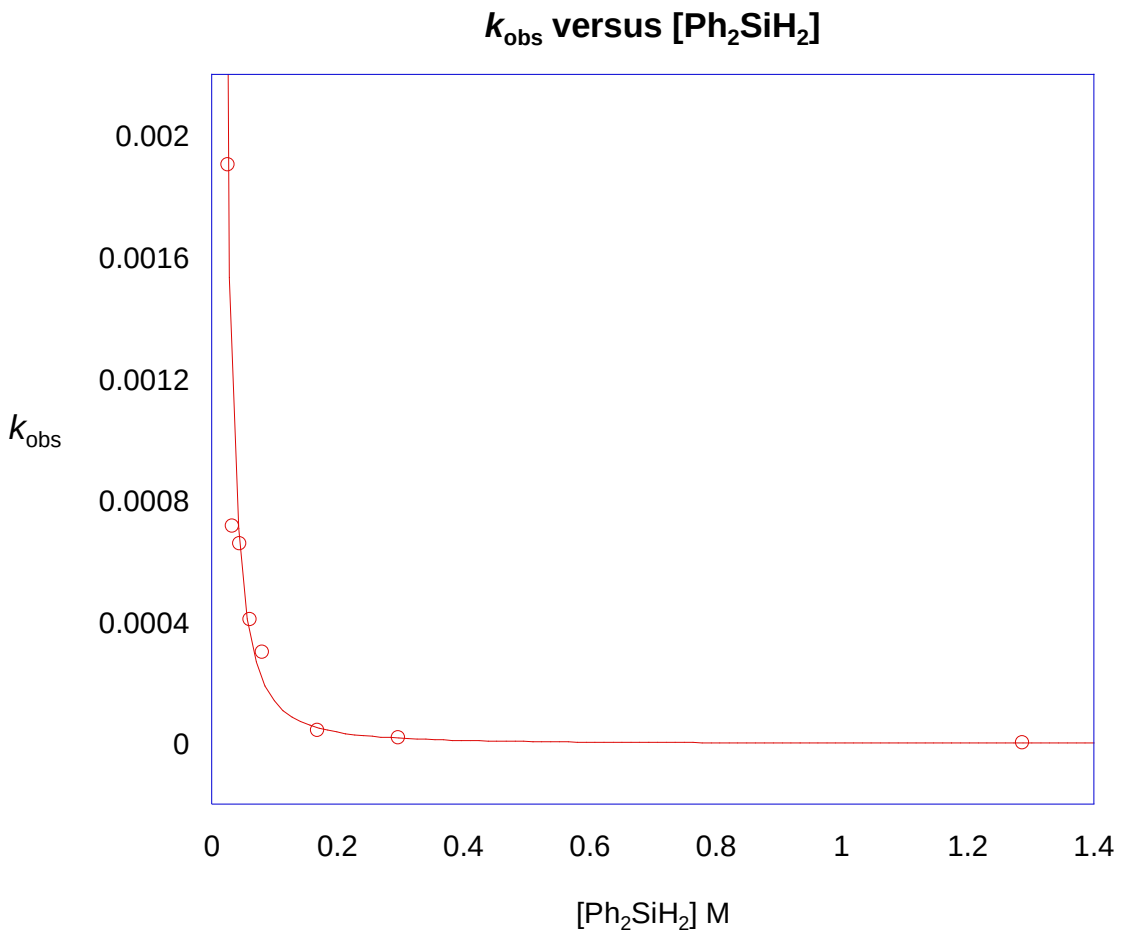

Figure 7. Plot of observed second order rate constant vs varying Ph_2SiH_2 concentration at 298 K in benzene-d_6. The curve is drawn to merely guide the eye and does not represent the results of a least-squares regression analysis.

At low concentrations of amine, the concentration profiles show rapid initial conversion followed by a slower second phase as the reaction approaches completion. Thus, the experimental ternary rate law is likely only valid for given concentration regimes (and not valid at high [Ph_2SiH_2] or low [Et_2NH]). Within the conditions of Figure 6, and taking into account the qualitative observations under the other conditions, a few conclusions are apparent. First, the ternary rate law suggests that interaction of one of the reagents (silane or amine) with catalytic

intermediates is reversible and precedes the turnover limiting step. Because higher concentrations of Ph_2SiH_2 inhibit the catalytic reaction, possibly by formation of an Yb-Ph_2SiH_2 adduct as an off-cycle species, the reversible interaction of catalyst and Ph_2SiH_2 is unlikely to be part of the catalytic cycle. Instead, reversible ytterbium(II)-amine coordination is proposed as a key step for the conversion. This ytterbium amine compound is unlikely to be a hydride, which would rapidly react to give ytterbium amide and H_2. Then, the turnover-limiting step would involve the interaction of a ytterbium amido amine compound (e.g., **A** in Scheme 3) and Ph_2SiH_2. Second, formation of $HC(SiHMe_2)_3$, presumably as part of catalyst initiation, implies that a ytterbium amido species is an intermediate. Note that independent reactions of **4a** and Et_2NH also give $HC(SiHMe_2)_3$, although ytterbium amido products were not isolable. Third, deactivation by excess Im*t*-Bu, THF, or even Ph_2SiH_2 but not Et_2NH suggests that catalysis involves a coordinatively unsaturated species, which must interact with Et_2NH for the reaction to proceed. We propose that deactivation by Ph_2SiH_2 is reversible, because greater than 3 half-lives of conversion were observed under several conditions, and an irreversible catalyst decomposition reaction would likely be noticed with severely non-linear kinetic plots. This coordinatively unsaturated intermediate could be a ytterbium hydride (e.g., **B**), which might form a [Yb]H(H-$SiHEt_2$) related to those proposed for Ru, but could also be a ytterbium amide, such as **C** in Scheme 3. We favor the latter, because if **B**, or its inhibited forms were the catalyst resting state, then second-order dependence on [Et_2NH] would be expected.

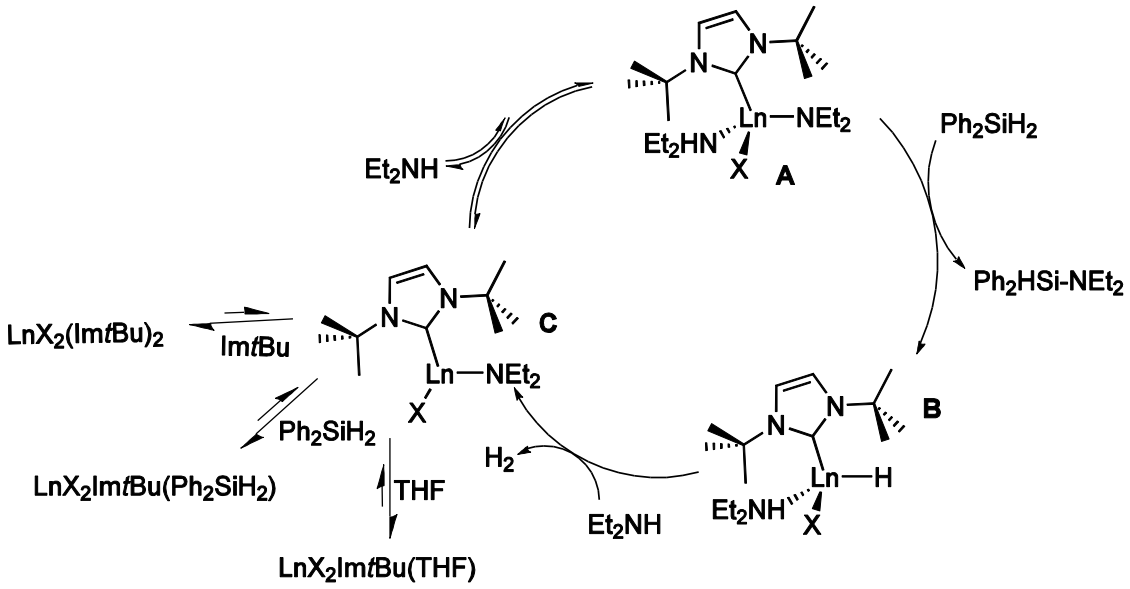

Scheme 3. Proposed catalytic cycle that is consistent with experimental kinetic observation.

Conclusion

The structure and non-redox-based chemistry of ytterbium and samarium compounds $Ln\{C(SiHMe_2)_3\}_2THF_2$, in terms of structure and reactivity toward the Lewis acid $B(C_6F_5)_3$ and substitution of THF ligands by Im*t*Bu, are very similar. In addition, the carbene adducts of both dialkyl rare earth compounds are similarly reactive in dehydrocoupling of amines and organosilanes. However, there are a few notable differences between the samarium and ytterbium compounds, which appear the IR spectra of $LnC(SiHMe_2)_3HB(C_6F_5)_3THF_2$ and the X-ray crystal structures of $Ln\{C(SiHMe_2)_3\}_2$Im*t*Bu. Notably, the ytterbium compound **4a** contains one diagostic-like alkyl ligand and one alkyl ligand lacking secondary interactions, whereas both alkyl ligands in the samarium analogue contain 3c-2e Sm←H-Si structures.

The $LnC(SiHMe_2)_3HB(C_6F_5)_3THF_2$ compounds do not react with Im*t*Bu under the accessible conditions, and apparently the substitution of THF in the zwitterionic compounds is

more difficult that in the neutral **1a** or **1b**. An NHC ligand coordinates to ytterbium in $YbC(SiHMe_2)_3HB(C_6F_5)_3Im\textit{t}Bu$, which is formed from the reaction of **4a** and $B(C_6F_5)_3$. Even so, the Im*t*Bu ligand dissociates from **4a** or **4b** upon addition of small amounts of THF or amines, as suggested by the UV-Vis titration, by the observation of free Im*t*Bu in catalytic reaction mixtures, or even under vacuum. The coordination and substitution chemistry of Yb and Sm in these alkyl compounds affects catalytic dehydrocoupling of amines and silanes. Coordination of substrates and exogenous ligands, including THF and Im*t*Bu, inhibit catalysis, and not all of the ytterbium precatalyst gives active catalytic sites, as shown by kinetic studies. The free Im*t*Bu present during catalysis suggests that irreversible catalyst deactivation involves its dissociation from the rare earth center. Based on these observations, we are currently investigating bidentate hemilabile carbene ligands to access coordinative unsaturation but stabilize lanthanide(II)-ligand interactions in these alkyl compounds.

Experimental Section

All manipulations were performed under a dry argon atmosphere using standard Schlenk techniques or under a nitrogen atmosphere in a glovebox unless otherwise indicated. Water and oxygen were removed from benzene and pentane solvents using an IT PureSolv system. Benzene-d_6 was heated to reflux over Na/K alloy and vacuum-transferred. The compounds YbI_2,[32] SmI_2THF_2,[27] $KC(SiHMe_2)_3$,[33] $B(C_6F_5)_3$,[34] $Yb\{C(SiHMe_2)_3\}_2THF_2$[11] were prepared following literature procedures. 1,3-di-tert-butylimidazol-2-ylidene (Im*t*Bu) was purchased from Sigma Aldrich and used as recieved. The catalytic products $PhSi(NHiPr)_3$, $(PhSiH_2)_2NiPr$, $PhSiH(NHtBu)_2$, $(PhSiH_2)_2NtBu$, $(PhMeSiH)_2NiPr$, $PhMeSiH(NHtBu)$, $PhMeSiH(NEt_2)$,

$Ph_2SiH(NHiPr)$, $Ph_2SiH(NHtBu)$, $Ph_2HSiNEt_2$,[4f] and $PhSiH(NEt_2)_2$,[17] match previously reported NMR spectroscopic data.

^1H, ^{11}B, $^{13}C\{^1H\}$, ^{15}N HMBC and ^{29}Si HMBC NMR spectra were collected on a Bruker DRX-400 spectrometer, a Bruker Avance III-600 spectrometer, or an Agilent MR 400 spectrometer. ^{11}B NMR spectra were referenced to an external sample of $BF_3{\cdot}Et_2O$. ^{15}N chemical shifts were originally referenced to liquid ammonia and recalculated to the CH_3NO_2 chemical shift scale by adding –381.9 ppm. Infrared spectra were measured on a Bruker Vertex 80. Elemental analyses were performed using a Perkin-Elmer 2400 Series II CHN/S. X-ray diffraction data was collected on a Bruker APEX II diffractometer. UV-Vis spectroscopy was measured on Agilent 8453 Diode Array UV-Vis instrument.

$Sm\{C(SiHMe_2)_3\}_2THF_2$ (1b). $KC(SiHMe_2)_3$ (0.159 g, 0.069 mmol) and $SmI_2(THF)_2$ (0.190 g, 0.035 mmol) were stirred in THF (5 mL) at room temperature for 18 h. The resulting black solution was evaporated to dryness under reduced pressure and extracted with pentane (2 × 5 mL) to obtain $Sm\{C(SiHMe_2)_3\}_2THF_2$ (0.154 g, 0.023 mmol, 65.8%). The compound was allowed to crystallize in pentane at –40 °C to yield black crystals of $Sm\{C(SiHMe_2)_3\}_2THF_2$. ^1H NMR (benzene-d_6, 600 MHz, 25 °C): δ 11.93 (s br, 8 H, THF), 2.78 (s br, 8 H, THF), –1.12 (s, 36 H, $SiMe_2$), –66.53 (s br, 6 H, Si*H*Me_2). IR (KBr, cm^{-1}): 2950 s, 2893 m, 2106 s br (ν_{SiH}), 2062 s br (ν_{SiH}), 1867 m br (ν_{SiH}), 1458 w, 1419 w, 1246 s, 1029 s, 945 s br, 885 s br, 832 m br, 764 s, 671 m br, 624 m br. Anal. Calcd for $C_{24}H_{66}O_3Si_8Yb$: C, 39.23; H, 8.68. Found: C, 39.02; H, 8.73. Magnetic susceptibility: $\mu_{eff}^{298\ K} = 3.22\ \mu_B$. Mp, 118-121 °C.

$SmC(SiHMe_2)_3HB(C_6F_5)_3THF_2$ (2b). $B(C_6F_5)_3$ (0.053 g, 0.103 mmol) was added to a benzene (4 mL) solution of $Sm\{C(SiHMe_2)_3\}_2THF_2$ (0.070 g, 0.103 mmol) in small portions. The resulting red mixture was stirred at room temperature for 30 min. The solvent was evaporated under reduced pressure to give a yellow paste. The residue was washed with pentane (3 × 5 mL) and the volatiles were evaporated to dryness in vacuo to give $SmC(SiHMe_2)_3HB(C_6F_5)_3THF_2$ as a red solid (0.081 g, 0.075 mmol, 72.6%). ^{1}H NMR (bromobenzene-d_5, 600 MHz, 25 °C): δ –1.37 (br, 8 H, OCH_2), –3.24 (br, 8 H, CH_2). ^{11}B NMR (bromobenzene-d_5, 192 MHz, 25 °C): δ –88.4 (br). $^{13}C\{^1H\}$ NMR (bromobenzene-d_5, 150 MHz, 25 °C): δ 153.0 (br, C_6F_5), 135.9 (br, C_6F_5), 134.4 (br, C_6F_5). ^{19}F NMR (bromobenzene-d_5, 564 MHz, 25 °C): δ –157.08 (s, 3 F, *para*-F), –161.29 (s, 6 F, *meta*-F). IR (KBr, cm^{-1}): 2964 m, 2899 w, 2389 m (ν_{BH}), 2307 m br (ν_{BH}), 2110 m br (ν_{SiH}), 1645 m, 1603 w, 1515 s, 1466 s br, 1373 m, 1277 br, 1259 br, 1113 s br, 1089 s br, 1023 m br, 965 s br, 899 s br, 839 s br. Anal. Calcd for $BC_{40}F_{15}H_{70}O_2Si_3Sm$: C, 43.15; H, 6.34. Found: C, 43.01; H, 6.04. Mp, 172-174 °C.

$Sm\{HB(C_6F_5)_3\}_2THF_2$ (3b). $B(C_6F_5)_3$ (0.194 g, 0.378 mmol) was added to a benzene (4 mL) solution of $Sm\{C(SiHMe_2)_3\}_2THF_2$ (0.128 g, 0.189 mmol) in small portions. The resulting red mixture was stirred at room temperature for 30 min. The solvent was evaporated under reduced pressure to give a red paste. The residue was washed with pentane (3 × 5 mL) and the volatiles were evaporated to dryness in vacuo to give $Sm\{HB(C_6F_5)_3\}_2THF_2$ as a red solid (0.205 g, 0.145 mmol, 77.0%). ^{11}B NMR (bromobenzene-d_5, 192 MHz, 25 °C): δ –100.8 (br). ^{19}F NMR (bromobenzene-d_5, 564 MHz, 25°C): δ –157.07 (br, 3 F, *para*-F), –161.45 (6 F, *meta*-F). IR (KBr, cm^{-1}): 2968 m, 2899 m, 2389 m (ν_{BH}), 2318 s br (ν_{BH}), 1647 s, 1604 w, 1517 s, 1467 s br,

1374 m, 1274 s br, 1114 s br, 1082 s br, 1018 m, 973 s, 961 s, 927 m, 842 s br, 766 s. Anal. Calcd for $B_2C_{49}F_{30}H_{45}O_2Sm$: C, 40.02; H, 1.37. Found: C, 40.17; H, 1.35. Mp, 177-180 °C.

Yb{C(SiHMe$_2$)$_3$}$_2$Im*t*Bu (4a). 1,3-di-tert-butylimidazol-2-ylidene (Im*t*Bu, 0.028 g, 0.153 mmol) was added to a pentane solution (5 mL) of Yb{C(SiHMe$_2$)$_3$}$_2$THF$_2$ (0.106 g, 0.153 mmol) at room temperature to yield a deep red solution. The solution was allowed to stir at room temperature for 30 min. The reaction mixture was concentrated briefly under reduced pressure to a total volume of 4 mL, and then cooled to –40 °C to yield red needle-like crystals of Yb{C(SiHMe$_2$)$_3$}$_2$Im*t*Bu (0.615 g, 0.84 mmol, 54.8%). ^{1}H NMR (benzene-d_6, 600 MHz, 25 °C): δ 6.33 (s, 2 H, $C_3N_2H_2t$Bu$_2$), 4.86 (sept, $^3J_{HH}$ = 3.6 Hz, $^1J_{SiH}$ = 149 Hz, 6 H, Si*H*Me$_2$), 1.43 (s, 18 H, CMe$_3$), 0.45 (d, $^3J_{HH}$ = 3.3 Hz, 36 H, SiMe$_2$). ^{13}C{^{1}H} NMR (benzene-d_6, 150 MHz, 25°C): δ 196.90 ($C_3N_2H_2t$Bu$_2$), 118.58 ($C_3N_2H_2t$Bu$_2$), 57.75 (*C*Me$_3$), 31.16 (C*Me*$_3$), 11.31 (YbC), 4.00 (SiMe$_2$). ^{1}H-^{15}N HMBC NMR (benzene-d_6, 61 MHz, 25 °C): δ –168.8 ($C_3N_2H_2t$Bu$_2$). ^{1}H-^{29}Si HMBC NMR (benzene-d_6, 119 MHz, 25 °C): δ –19.4 (SiHMe$_2$). IR (KBr, cm^{-1}): 2977 m, 2949 s, 2895 s, 2059 w (ν_{SiH}), 1871 m br (ν_{SiH}), 1463 w, 1243 s, 1023 s, 930 s br, 900 s br, 831 m br, 767 s, 730 s, 673 m br, 634 m br. Anal. Calcd for $C_{24}H_{66}O_3Si_8Yb$: C, 40.95; H, 8.66; N, 3.82. Found: C, 41.09; H, 8.73; N, 3.87. Mp, 181-184 °C.

Sm{C(SiHMe$_2$)$_3$}$_2$Im*t*Bu (4b). (1,3-Di-tert-butylimidazol-2-ylidene) (Im*t*Bu, 0.027 g, 0.15 mmol) was added to a 5 mL pentane solution of Sm{C(SiHMe$_2$)$_3$}$_2$THF$_2$ (0.100 g, 0.15 mmol) at room temperature to yield a dark red solution. The solution was allowed to stir at room temperature for 24 h. After a day, the solution was concentrated and cooled to –40 °C to yield deep red plate-like crystals of Sm{C(SiHMe$_2$)$_3$}$_2$Im*t*Bu (0.042 g, 0.060 mmol, 39.8%). ^{1}H NMR

(benzene-d_6, 600 MHz, 25 °C): δ 13.9 (br, 18 H, $C_3N_2H_2tBu_2$), –0.59 (s, 2 H, $C_3N_2H_2tBu_2$), –2.84 (s, 36 H, $SiMe_2$), –73.9 (s br, 6 H, $SiHMe_2$). IR (KBr, cm^{-1}): 2977 m, 2949 s, 2897 s, 2076 s br (ν_{SiH}), 2064 s br (ν_{SiH}), 2044 s (ν_{SiH}), 1910 s br (ν_{SiH}), 1796 m br (ν_{SiH}), 1463 w, 1397 w, 1372 w br, 1239 s, 1200 m, 1011 w br, 963 s, 930 s br, 896 s br, 832 m br, 764 s, 731 s, 671 m br, 635 m br. Anal. Calcd for $C_{25}H_{63}N_2Si_6Sm$: C, 42.25; H, 8.94; N, 3.94. Found: C, 42.09; H, 8.88; N, 3.85. Mp, 154-157 °C.

General procedure for NMR kinetics measurements. Reaction progress was monitored by single scan acquisition of a series of ^1H NMR spectra at regular intervals on a Bruker DRX400 spectrometer. Hexamethylbenzene was used as a standard of accurately known and constant concentration (0.01 M in benzene-d_6). The temperature in the NMR probe was preset for each experiment at 25 °C, and was kept constant and monitored during each experiment using a thermocouple. A range of silane:amine ratios (1:1 to 1:25) were used to study the catalytic reaction of Ph_2SiH_2 and Et_2NH in benzene-d_6. Kinetic measurements were studied at low concentration of Ph_2SiH_2 (0.081 M) and high concentration of Et_2NH (0.673 M).

Representative example. Catalytic reaction of Ph_2SiH_2 and Et_2NH using 10 mol% Yb{C($SiHMe_2$)$_3$}$_2$Im*t*Bu as catalyst is described. A 5 mL stock solution in benzene-d_6 containing a known concentration of the internal standard hexamethylbenzene (0.0081 g, 0.0499 mmol, 0.01 M) was prepared using a 5 mL volumetric flask. The stock solution (0.50 mL) was added by a 1 mL glass syringe to a known amount of Yb{C($SiHMe_2$)$_3$}$_2$Im*t*Bu (0.0052 g, 0.0071 mmol) in a glass vial. The resulting solution was transferred to a NMR tube, capped with a rubber septum, and a ^1H NMR spectrum was acquired. Neat substrates Ph_2SiH_2 (0.013 g, 0.071 mmol) and

Et_2NH (0.052 g, 0.711 mmol) were added to the NMR tube by injecting through the rubber septum. Then, the NMR tube was quickly placed in the NMR probe. Single scan spectra were acquired automatically at preset time intervals at 25 °C. The concentration of silane and product at any given time was determined by integration of silane and product resonances relative to the integration of the internal standard. Second order rate constants (k_{obs}) were obtained by non-weighted linear least squares fit of the data to the second order rate law, $\ln\{[Et_2NH]/[Ph_2SiH_2]\} = k_{obs}([Et_2NH]_0-[Ph_2SiH_2]_0)t + \ln\{[Et_2NH]_0/[Ph_2SiH_2]_0\}$ providing first order dependence on each substrate at low concentration of silane and high concentration of amine. The experimental third order rate constant, k'_{obs} was obtained by measuring k_{obs} for several catalyst concentrations. A plot of second order rate constants and catalyst concentrations gave a first order dependence on catalyst concentration with an overall rate law, $-d[Ph_2SiH_2]/dt = k'_{obs}[\text{catalyst}][Ph_2SiH_2][Et_2NH]$.

Catalytic synthesis of $PhSi(NHiC_3H_7)_3$ as a representative procedure for the reaction of organosilanes and amines. The pre-catalyst $Yb\{C(SiHMe_2)_3\}_2ImtBu$ (0.030 g, 0.0409 mmol) was dissolved in 4 mL of benzene. The organosilane $PhSiH_3$ (0.088 g, 0.818 mmol) was added to the solution, followed by excess $iC_3H_7NH_2$ (0.193 g, 3.27 mmol, 4 equiv.). The mixture immediately changed color from orange to brown and effervesced, the vial was quickly capped, and the mixture was stirred for 1 h. A brown precipitate formed after 1 h, and this is attributed to catalyst decomposition. The solution was filtered to remove precipitated catalytic material, and volatile materials were removed under vacuum. The product was purified by distillation under vacuum to yield spectroscopically pure, metal, and volatile solvent was removed under vacuum. The product was a colorless oil which was spectroscopically pure $PhSi(NHiC_3H_7)_3$ (0.141 g,

0.504 mmol, 62%). ^{1}H NMR (benzene-d_6, 600 MHz): δ 7.79-7.78 (m, 2 H, *ortho*-C_6H_5), 7.31-7.26 (m, 3 H, *meta*- and *para*-C_6H_5), 3.25 (sept, $^{3}J_{HH}$ = 6.3 Hz, 3 H, CH), 1.07 (d, $^{3}J_{HH}$ = 6.3 Hz, 18 H, CH_3), 0.65 (d, $^{3}J_{HH}$ = 9.8 Hz, NH). ^{13}C{^{1}H} NMR (benzene-d_6, 150 MHz): δ 140.26 (*ipso*-C_6H_5), 135.06 (*ortho*-C_6H_5), 129.49 (*meta*-C_6H_5), 128.18 (*para*-C_6H_5), 42.90 (CH), 28.48 (CH_3). ^{1}H-^{15}N HMBC NMR (benzene-d_6, 61 MHz): δ –331.84. ^{1}H-^{29}Si HMBC NMR (benzene-d_6, 119 MHz): δ –37.56.

$(PhH_2Si)_2Ni C_3H_7$. Following the procedure described above, $PhSiH_3$ (0.195 g, 1.79 mmol, 2.2 equiv.) and *i*$C_3H_7NH_2$ (0.048 g, 0.818 mmol) reacted to give $(PhH_2Si)_2Ni C_3H_7$ (0.158 g, 0.581 mmol, 71%). ^{1}H NMR (benzene-d_6, 600 MHz): δ 7.63-7.62 (m, 4 H, *ortho*-C_6H_5), 7.18-7.17 (m, 6 H, *meta*- and *para*-C_6H_5), 5.25 (s, $^{1}J_{SiH}$ = 207 Hz, 4 H, SiH), 3.29 (sept, $^{3}J_{HH}$ = 6.6 Hz, 1 H, CH), 1.05 (d, $^{3}J_{HH}$ = 6 H, 6.6 Hz, 6 H, CH_3). ^{13}C{^{1}H} NMR (benzene-d_6, 150 MHz): δ 136.04 (*ipso*-C_6H_5), 135.33 (*ortho*-C_6H_5), 130.58 (*meta*-C_6H_5), 128.68 (*para*-C_6H_5), 50.08 (CH), 25.55 (CH_3). ^{1}H-^{15}N HMBC NMR (benzene-d_6, 61 MHz): δ –353.11. ^{1}H-^{29}Si HMBC NMR (benzene-d_6, 119 MHz): δ –29.24.

PhHSi(NH*t*Bu)$_2$. Following the procedure described above, $PhSiH_3$ (0.089 g, 0.818 mmol) and *t*-$BuNH_2$ (0.131 g, 1.79 mmol, 2.2 equiv.) were allowed to stir at room temperature 15 h to yield PhHSi(NH*t*Bu)$_2$ (0.187 g, 0.746 mmol, 91%). ^{1}H NMR (benzene-d_6, 600 MHz): δ 7.79-7.77 (m, 2 H, *ortho*-C_6H_5), 7.29-7.24 (m, 3 H, *meta*- and *para*-C_6H_5), 5.48 (t, $^{3}J_{HH}$ = 3.3 Hz, $^{1}J_{SiH}$ = 214 Hz, 1 H, SiH), 1.19 (s, 18 H, CH_3), 0.82 (br s, 2 H, NH). ^{13}C{^{1}H} NMR (benzene-d_6, 150 MHz): δ 140.76 (*ipso*-C_6H_5), 134.81 (*ortho*-C_6H_5), 129.94 (*meta*-C_6H_5), 128.68 (*para*-C_6H_5), 49.77

(*C*CH_3), 33.94 (CH_3). ^{1}H-^{15}N HMBC NMR (benzene-d_6, 61 MHz): δ –322.58. ^{1}H-^{29}Si HMBC NMR (benzene-d_6, 119 MHz): δ –37.38.

$(PhH_2Si)_2N$*t*Bu. Following the procedure described above, $PhSiH_3$ (0.195 g, 1.79 mmol, 2.2 equiv.) and *t*$BuNH_2$ (0.060 g, 0.818 mmol) were allowed to stir at room temperature 15 h to yield $(PhH_2Si)_2N$*t*Bu (0.174 g, 0.609 mmol, 73%). ^{1}H NMR (benzene-d_6, 600 MHz): δ 7.67-7.66 (m, 4 H, *ortho*-C_6H_5), 7.18-7.16 (m, 6 H, *meta*- and *para*-C_6H_5), 5.38 (s, $^1J_{SiH}$ = 207 Hz, 4 H, SiH), 1.23 (s, 9 H, CH_3). ^{13}C{^{1}H} NMR (benzene-d_6, 150 MHz): δ 137.19 (*ipso*-C_6H_5), 135.03 (*ortho*-C_6H_5), 130.44 (*meta*-C_6H_5), 128.74 (*para*-C_6H_5), 54.11 (*C*CMe_3), 33.06 (CH_3). ^{1}H-^{15}N HMBC NMR (benzene-d_6, 61 MHz): δ –342.66. ^{1}H-^{29}Si HMBC NMR (benzene-d_6, 119 MHz): δ –31.40.

$PhHSi(NEt_2)_2$. Following the procedure described above, $PhSiH_3$ (0.089 g, 0.818 mmol) and Et_2NH (0.179 g, 2.45 mmol, 3 equiv.) were allowed to stir at room temperature 15 h to yield $PhHSi(NEt_2)_2$ (0.164 g, 0.655 mmol, 80%). ^{1}H NMR (benzene-d_6, 600 MHz): δ 7.74-7.73 (m, 2 H, *ortho*-C_6H_5), 7.27-7.23 (m, 3 H, *meta*- and *para*-C_6H_5), 5.18 (s, $^1J_{SiH}$ = 215 Hz, 1 H, SiH), 2.93 (q, $^3J_{HH}$ = 6.3 Hz, 8 H, CH_2), 1.00 (t, $^3J_{HH}$ = 6.4 Hz, 12 H, CH_3). ^{13}C{^{1}H} NMR (benzene-d_6, 150 MHz): δ 138.17 (*ipso*-C_6H_5), 135.25 (*ortho*-C_6H_5), 130.06 (*meta*-C_6H_5), 128.68 (*para*-C_6H_5), 40.26 (CH_2), 15.69 (CH_3). ^{1}H-^{15}N HMBC NMR (benzene-d_6, 61 MHz): δ –346.17. ^{1}H-^{29}Si HMBC NMR (benzene-d_6, 119 MHz): δ –18.76.

$(PhMeHSi)_2N$*i*C_3H_7. Following the procedure described above, $PhMeSiH_2$ (0.102 g, 0.818 mmol, 2 equiv.) and *i*$C_3H_7NH_2$ (0.024 g, 0.409 mmol) were allowed to stir at room temperature 4

h to yield $(PhMeHSi)_2Ni(C_3H_7)$ (0.108 g, 0.361 mmol, 88%). ^{1}H NMR (benzene-d_6, 600 MHz): δ 7.65-7.60 (m, 4 H, *ortho*-C_6H_5), 7.25-7.20 (m, 6 H, *meta*- and *para*-C_6H_5), 5.24 (m, $^1J_{SiH}$ = 199 Hz, 2 H, SiH), 3.27 (m, 1 H, CH), 1.11 (d, $^3J_{HH}$ = 6.2 Hz, 6 H, CH_3), 0.46 (d, $^3J_{HH}$ = 3.3 Hz, 3 H, CH_3), 0.45 (d, $^3J_{HH}$ = 3.3 Hz, 3 H, CH_3). ^{13}C{^{1}H} NMR (benzene-d_6, 150 MHz): δ 138.88 (*ipso*-C_6H_5), 138.82 (*ipso*-C_6H_5), 135.06 (*ortho*-C_6H_5), 135.00 (*ortho*-C_6H_5), 130.01 (*meta*-C_6H_5), 128.67 (*para*-C_6H_5), 48.62 (CH), 48.36 (CH), 26.02 (CH_3), 25.87 (CH_3), –0.94 ($SiCH_3$), –1.31 ($SiCH_3$). ^{1}H-^{15}N HMBC NMR (benzene-d_6, 61 MHz): δ –345.11. ^{1}H-^{29}Si HMBC NMR (benzene-d_6, 119 MHz): δ –18.14.

PhMeHSiNH*t*Bu. Following the procedure described above, $PhMeSiH_2$ (0.051 g, 0.409 mmol) and *t*$BuNH_2$ (0.030 g, 0.409 mmol) were allowed to stir at room temperature 4 h to yield PhMeHSiNH*t*Bu (0.067 g, 0.346 mmol, 85%). ^{1}H NMR (benzene-d_6, 600 MHz): δ 7.67-7.66 (m, 2 H, *ortho*-C_6H_5), 7.24-7.23 (m, 3 H, *meta*- and *para*-C_6H_5), 5.23 (m, $^1J_{SiH}$ = 199 Hz, 1 H, SiH), 1.08 (s, 9 H, CC*H*$_3$), 0.64 (br s, 1 H, NH), 0.30 (d, $^3J_{HH}$ = 2.8 Hz, 3 H, $SiCH_3$). ^{13}C{^{1}H} NMR (benzene-d_6, 150 MHz): δ 140.17 (*ipso*-C_6H_5), 134.65 (*ortho*-C_6H_5), 129.99 (*meta*-C_6H_5), 128.67 (*para*-C_6H_5), 49.79 (*C*CH_3), 33.66 (CH_3), –0.64 ($SiCH_3$). ^{1}H-^{15}N HMBC NMR (benzene-d_6, 61 MHz): δ –329.71. ^{1}H-^{29}Si HMBC NMR (benzene-d_6, 119 MHz): δ –21.35.

PhMeHSiNEt$_2$. Following the procedure described above, $PhMeSiH_2$ (0.051 g, 0.409 mmol) and Et_2NH (0.030 g, 0.409 mmol) were allowed to stir at room temperature 4 h to yield $PhMeSiHNHEt_2$ (0.072 g, 0.372 mmol, 92%). ^{1}H NMR (benzene-d_6, 600 MHz): δ 7.63-7.62 (m, 2 H, *ortho*-C_6H_5), 7.24-7.23 (m, 3 H, *meta*- and *para*-C_6H_5), 5.13 (q, $^3J_{HH}$ = 3.0 Hz, $^1J_{SiH}$ = 199 Hz, 1 H, SiH), 2.81 (q, $^3J_{HH}$ = 6.9 Hz, 4 H, CH_2), 0.94 (t, $^3J_{HH}$ = 6.9 Hz, 6 H, CH_3), 0.36 (d, $^3J_{HH}$

= 3.0 Hz, 3 H, $SiCH_3$). $^{13}C\{^1H\}$ NMR (benzene-d_6, 150 MHz): δ 138.90 (*ipso*-C_6H_5), 134.84 (*ortho*-C_6H_5), 130.04 (*meta*-C_6H_5), 128.68 (*para*-C_6H_5), 41.78 (CH_2), 16.15 (CH_3), –2.50 ($SiCH_3$). ^1H-^{15}N HMBC NMR (benzene-d_6, 61 MHz): δ –353.05. ^1H-^{29}Si HMBC NMR (benzene-d_6, 119 MHz): δ –11.03.

$Ph_2HSiNHiC_3H_7$. Following the procedure described above, Ph_2SiH_2 (0.075 g, 0.409 mmol) and *i*$PrNH_2$ (0.024 g, 0.409 mmol) were allowed to stir at room temperature 15 h to yield $Ph_2HSiNHiC_3H_7$ (0.083 g, 0.343 mmol, 84%). ^1H NMR (benzene-d_6, 600 MHz): δ 7.70-7.69 (m, 4 H, *ortho*-C_6H_5), 7.21-7.16 (m, 6 H, *meta*- and *para*-C_6H_5), 5.64 (d, $^3J_{HH}$ = 1.8 Hz, $^1J_{SiH}$ = 204 Hz, 1 H, SiH), 3.07 (pseudo-sextet, $^3J_{HH}$ = 6.4 Hz, 1 H, CH), 0.97 (d, $^3J_{HH}$ = 6 H, 6.6 Hz, 6 H, CH_3), 0.66 (br s, 1 H, NH). $^{13}C\{^1H\}$ NMR (benzene-d_6, 150 MHz): δ 136.79 (*ipso*-C_6H_5), 135.58 (*ortho*-C_6H_5), 130.44 (*meta*-C_6H_5), 128.55 (*para*-C_6H_5), 44.76 (CH), 27.60 (CH_3). ^1H-^{15}N HMBC NMR (benzene-d_6, 61 MHz): δ –341.95. ^1H-^{29}Si HMBC NMR (benzene-d_6, 119 MHz): δ –20.44.

$Ph_2HSiNHtBu$. Following the procedure described above, Ph_2SiH_2 (0.075 g, 0.409 mmol) and *t*$BuNH_2$ (0.030 g, 0.409 mmol) were allowed to stir at room temperature 15 h to yield $Ph_2HSiNHtBu$ (0.087 g, 0.341 mmol, 84%). ^1H NMR (benzene-d_6, 600 MHz): δ 7.70-7.69 (m, 4 H, *ortho*-C_6H_5), 7.21-7.20 (m, 6 H, *meta*- and *para*-C_6H_5), 5.72 (d, $^3J_{HH}$ = 3.4 Hz, $^1J_{SiH}$ = 204 Hz, 1 H, SiH), 1.11 (s, 9 H, CH_3), 0.94 (br s, 1 H, NH). $^{13}C\{^1H\}$ NMR (benzene-d_6, 150 MHz): δ 137.73 (*ipso*-C_6H_5), 135.52 (*ortho*-C_6H_5), 130.29 (*meta*-C_6H_5), 128.67 (*para*-C_6H_5), 49.97 (CCH_3), 33.63 (CCH_3). ^1H-^{15}N–HMBC NMR (benzene-d_6, 61 MHz): δ –330.65. ^1H-^{29}Si HMBC NMR (benzene-d_6, 119 MHz): δ –24.93.

$Ph_2HSiNEt_2$. Following the procedure described above, Ph_2SiH_2 (0.075 g, 0.409 mmol) and Et_2NH (0.030 g, 0.409 mmol) were allowed to stir at room temperature 15 h to yield $Ph_2HSiNHEt_2$ (0.085 g, 0.333 mmol, 82%). ^{1}H NMR (benzene-d_6, 600 MHz): δ 7.69-7.68 (m, 4 H, *ortho*-C_6H_5), 7.21-7.20 (m, 6 H, *meta*- and *para*-C_6H_5), 5.60 (s, $^1J_{SiH}$ = 204 Hz, 1 H, SiH), 2.90 (q, $^3J_{HH}$ = 7.0 Hz, 4 H, CH_2), 0.95 (t, $^3J_{HH}$ = 7.0 Hz, 6 H, CH_3). $^{13}C\{^1H\}$ NMR (benzene-d_6, 150 MHz): δ 136.47 (*ipso*-C_6H_5), 135.88 (*ortho*-C_6H_5), 130.34 (*meta*-C_6H_5), 128.63 (*para*-C_6H_5), 41.68 (CH_2), 15.83 (CH_3). ^{1}H-^{15}N HMBC NMR (benzene-d_6, 61 MHz): δ –353.82. ^{1}H-^{29}Si HMBC NMR (benzene-d_6, 119 MHz): δ –14.06.

References

[1] a) E. B. Coughlin and J. E. Bercaw, *Journal of the American Chemical Society* **1992**, *114*, 7606-7607; b) P. L. Watson, *Journal of the American Chemical Society* **1982**, *104*, 337-339; c) P. L. Watson and G. W. Parshall, *Accounts of Chemical Research* **1985**, *18*, 51-56.

[2] a) T. Sakakura, H. J. Lautenschlager and M. Tanaka, *Journal of the Chemical Society-Chemical Communications* **1991**, 40-41; b) P. F. Fu, L. Brard, Y. W. Li and T. J. Marks, *Journal of the American Chemical Society* **1995**, *117*, 7157-7168.

[3] a) C. M. Forsyth, S. P. Nolan and T. J. Marks, *Organometallics* **1991**, *10*, 2543-2545; b) E. Lu, Y. Yuan, Y. Chen and W. Xia, *ACS Catalysis* **2013**, *3*, 521-524.

[4] a) W. J. Evans, T. A. Ulibarri and J. W. Ziller, *Journal of the American Chemical Society* **1990**, *112*, 2314-2324; b) E. Ihara, M. Nodono, K. Katsura, Y. Adachi, H. Yasuda, M. Yamagashira, H. Hashimoto, N. Kanehisa and Y. Kai, *Organometallics* **1998**, *17*, 3945-3956; c)

Z. Hou, Y. Zhang, M. Nishiura and Y. Wakatsuki, *Organometallics* **2003**, *22*, 129-135; d) G. Qi, Y. Nitto, A. Saiki, T. Tomohiro, Y. Nakayama and H. Yasuda, *Tetrahedron* **2003**, *59*, 10409-10418; e) Y. Nakayama and H. Yasuda, *Journal of Organometallic Chemistry* **2004**, *689*, 4489-4498; f) W. Xie, H. Hu and C. Cui, *Angew Chem Int Ed Engl* **2012**, *51*, 11141-11144.

[5] H. Yasuda, *Journal of Polymer Science Part A: Polymer Chemistry* **2001**, *39*, 1955-1959.

[6] M. Zimmermann and R. Anwander, *Chemical Reviews* **2010**, *110*, 6194-6259.

[7] a) P. B. Hitchcock, S. A. Holmes, M. F. Lappert and S. Tian, *Journal of the Chemical Society-Chemical Communications* **1994**, 2691-2692; b) C. Eaborn, P. B. Hitchcock, K. Izod and J. D. Smith, *Journal of the American Chemical Society* **1994**, *116*, 12071-12072; c) J. R. van den Hende, P. B. Hitchcock, S. A. Holmes, M. F. Lappert and S. Tian, *Journal of the Chemical Society, Dalton Transactions* **1995**, 3933-3939; d) P. B. Hitchcock, A. V. Khvostov and M. F. Lappert, *Journal of Organometallic Chemistry* **2002**, *663*, 263-268.

[8] C. Eaborn, P. B. Hitchcock, K. Izod, Z.-R. Lu and J. D. Smith, *Organometallics* **1996**, *15*, 4783-4790.

[9] W. Clegg, K. Izod, P. O'Shaughnessy, C. Eaborn and J. D. Smith, *Angewandte Chemie. International edition in English* **1997**, *36*, 2815-2817.

[10] W. J. Evans, *Inorganic Chemistry* **2007**, *46*, 3435-3449.

[11] K. Yan, B. M. Upton, A. Ellern and A. D. Sadow, *Journal of the American Chemical Society* **2009**, *131*, 15110-15111.

[12] M. Brookhart, M. L. H. Green and G. Parkin, *Proceedings of the National Academy of Sciences of the United States of America* **2007**, *104*, 6908-6914.

[13] L. F. Fieser, M. Fieser, J. G. Smith and T.-L. Ho, *Reagents for organic synthesis*, Wiley, New York, NY ; London, **1967**, p.

[14] a) J. S. Ghotra, M. B. Hursthouse and A. J. Welch, *Journal of the Chemical Society, Chemical Communications* **1973**, 669-670; b) D. C. Bradley, J. S. Ghotra and F. A. Hart, *Journal of the Chemical Society-Dalton Transactions* **1973**, 1021-1027; c) B. D. Murray and P. P. Power, *Inorganic Chemistry* **1984**, *23*, 4584-4588; d) J. Eppinger, E. Herdtweck and R. Anwander, *Polyhedron* **1998**, *17*, 1195-1201; e) C. Lehnert, J. Wagler, E. Kroke and G. Roewer, *European Journal of Inorganic Chemistry* **2007**, *2007*, 1086-1090.

[15] Y. Tanabe, T. Misaki, M. Kurihara, A. Iida and Y. Nishii, *Chemical Communications* **2002**, 1628-1629.

[16] M. Grellier, T. Ayed, J.-C. Barthelat, A. Albinati, S. Mason, L. Vendier, Y. Coppel and S. Sabo-Etienne, *Journal of the American Chemical Society* **2009**, *131*, 7633-7640.

[17] J. Wang, A. Dash, J. Berthet, M. Ephritikhine and M. Eisen, *Journal of organometallic chemistry* **2000**, *610*, 49-57.

[18] A. E. Nako, W. Y. Chen, A. J. P. White and M. R. Crimmin, *Organometallics* **2015**, *34*, 4369-4375.

[19] J. F. Dunne, S. R. Neal, J. Engelkemier, A. Ellern and A. D. Sadow, *J Am Chem Soc* **2011**, *133*, 16782-16785.

[20] M. S. Hill, D. J. Liptrot, D. J. MacDougall, M. F. Mahon and T. P. Robinson, *Chemical Science* **2013**, *4*, 4212.

[21] L. Greb, S. Tamke and J. Paradies, *Chem Commun (Camb)* **2014**, *50*, 2318-2320.

[22] R. J. Corriu, R. J. P. Corriu, D. Leclercq, P. H. Mutin, J. M. Planeix and A. Vioux, *Journal of organometallic chemistry* **1991**, *406*, C1-C4.

[23] a) B. Wang, D. Cui and K. Lv, *Macromolecules* **2008**, *41*, 1983-1988; b) Z. R. Turner, R. Bellabarba, R. P. Tooze and P. L. Arnold, *Journal of the American Chemical Society* **2010**, *132*,

4050-4051; c) D. P. Mills, L. Soutar, W. Lewis, A. J. Blake and S. T. Liddle, *Journal of the American Chemical Society* **2010**, *132*, 14379-14381.

[24] a) A. C. Hillier, G. A. Grasa, M. S. Viciu, H. M. Lee, C. Yang and S. P. Nolan, *Journal of Organometallic Chemistry* **2002**, *653*, 69-82; b) S. Würtz and F. Glorius, *Accounts of Chemical Research* **2008**, *41*, 1523-1533; c) G. C. Vougioukalakis and R. H. Grubbs, *Chemical Reviews* **2010**, *110*, 1746-1787.

[25] H. Schumann, D. M. M. Freckmann, S. Schutte, S. Dechert and M. Hummert, *Zeitschrift für anorganische und allgemeine Chemie* **2007**, *633*, 888-892.

[26] W. Fegler, T. P. Spaniol and J. Okuda, *Dalton Transactions* **2010**, *39*, 6774-6779.

[27] a) H. Schumann, M. Glanz, J. Winterfeld, H. Hemling, N. Kuhn and T. Kratz, *Angewandte Chemie International Edition in English* **1994**, *33*, 1733-1734; b) H. Schumann, *Angewandte Chemie* **1994**, *106*, 1829; c) H. Schumann, M. Glanz, J. Winterfeld, H. Hemling, N. Kuhn and T. Kratz, *Chemische Berichte* **1994**, *127*, 2369-2372; d) A. J. Arduengo, M. Tamm, S. J. Mclain, J. C. Calabrese, F. Davidson and W. J. Marshall, *Journal of the American Chemical Society* **1994**, *116*, 7927-7928; e) M. Glanz, S. Dechert, H. Schumann, D. Wolff and J. Springer, *Zeitschrift Fur Anorganische Und Allgemeine Chemie* **2000**, *626*, 2467-2477.

[28] A. P. Ginsberg, *Inorganic Syntheses*, p. 156.

[29] R. D. Shannon, *Acta Crystallographica* **1976**, *A32*, 751-767.

[30] H. F. Yuen and T. J. Marks, *Organometallics* **2008**, *27*, 155-158.

[31] a) Y. Okaue and T. Isobe, *Inorganica Chimica Acta* **1988**, *144*, 143-146; b) R. H. Crabtree, *The organometallic chemistry of the transition metals*, John Wiley & Sons, **2009**, p.

[32] E. Prasad, B. W. Knettle and R. A. Flowers, *Journal of the American Chemical Society* **2002**, *124*, 14663-14667.

[33] A. P. Ginsberg, *Inorganic Syntheses*, p. 147-148.

[34] K. Yan, A. V. Pawlikowski, C. Ebert and A. D. Sadow, *Chem Commun (Camb)* **2009**, 656-658.

[35] A. G. Massey and A. J. Park, *Journal of Organometallic Chemistry* **1964**, *2*, 245-250.

Supporting Information.

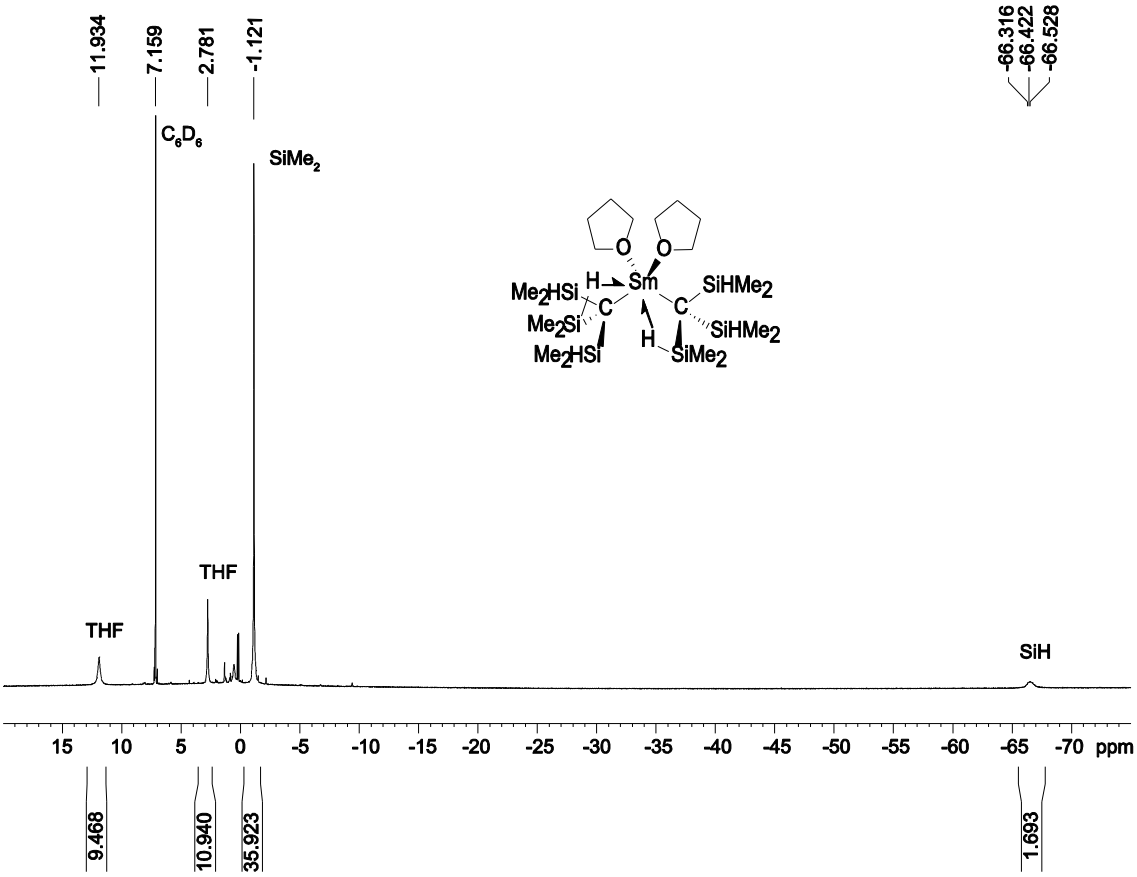

Figure S1. ^{1}H NMR spectrum (600 MHz, benzene-d_6) of Sm{C(SiHMe$_2$)$_3$}$_2$THF$_2$ (**1b**).

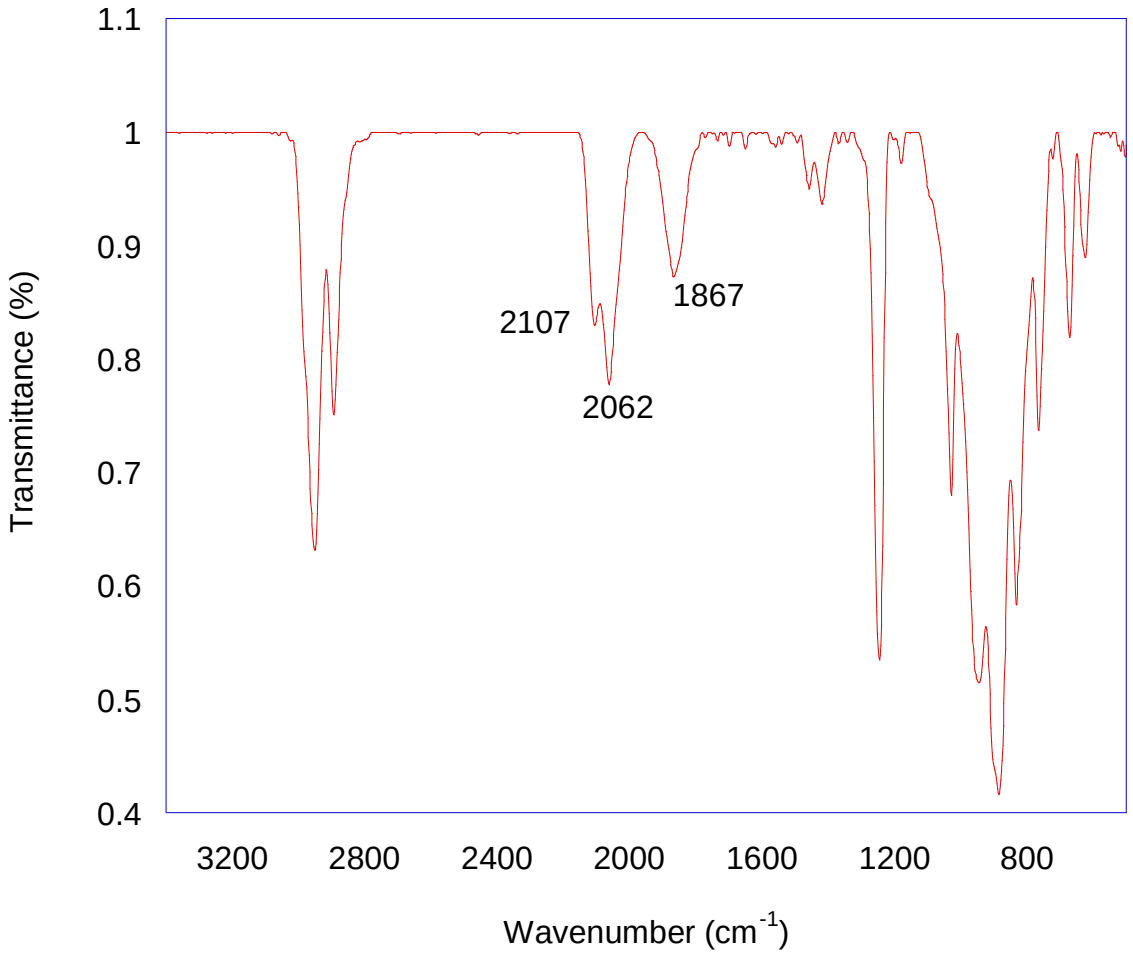

Figure S2. IR (KBr) spectrum of $Sm\{C(SiHMe_2)_3\}_2THF_2$ (***1b***).

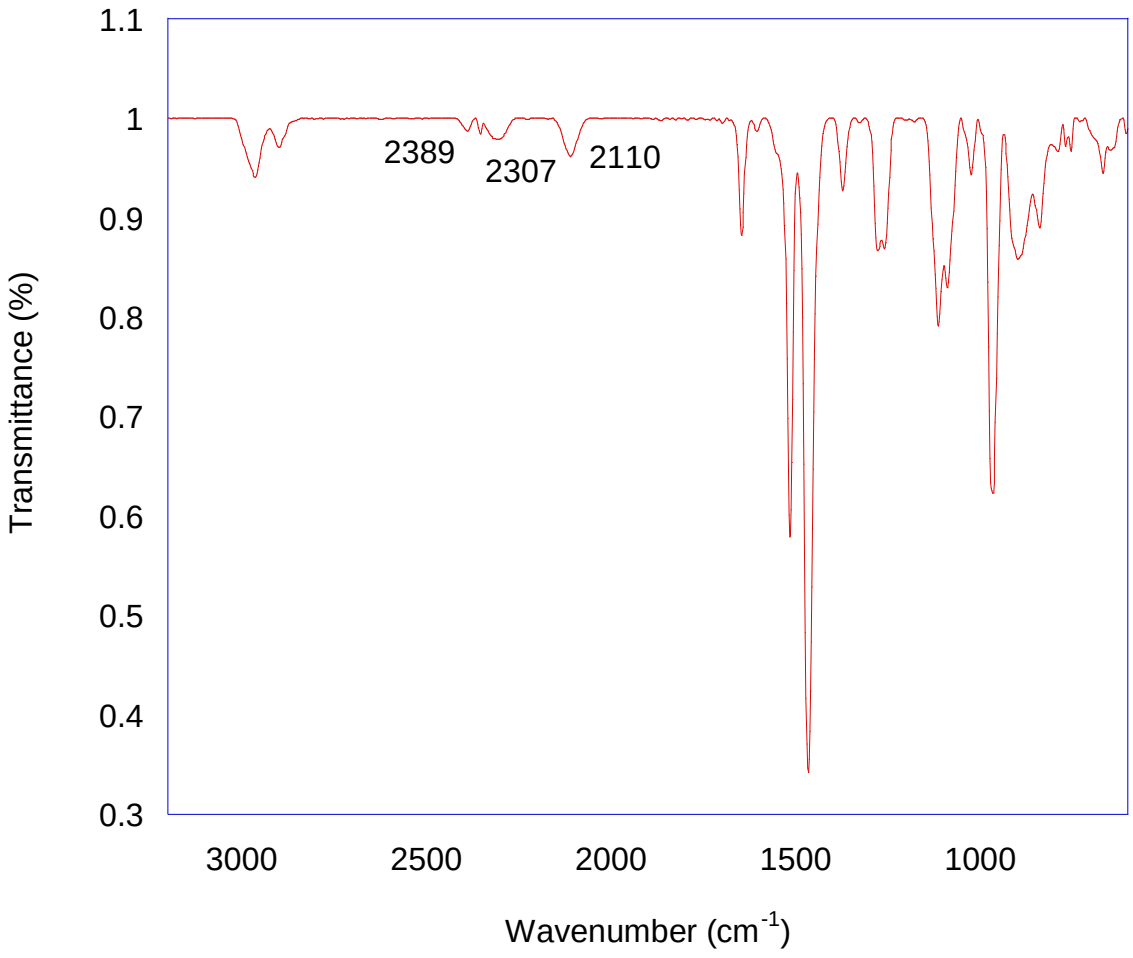

Figure S3. IR (KBr) spectrum of $SmC(SiHMe_2)_3HB(C_6F_5)_3THF_2$ (**2b**).

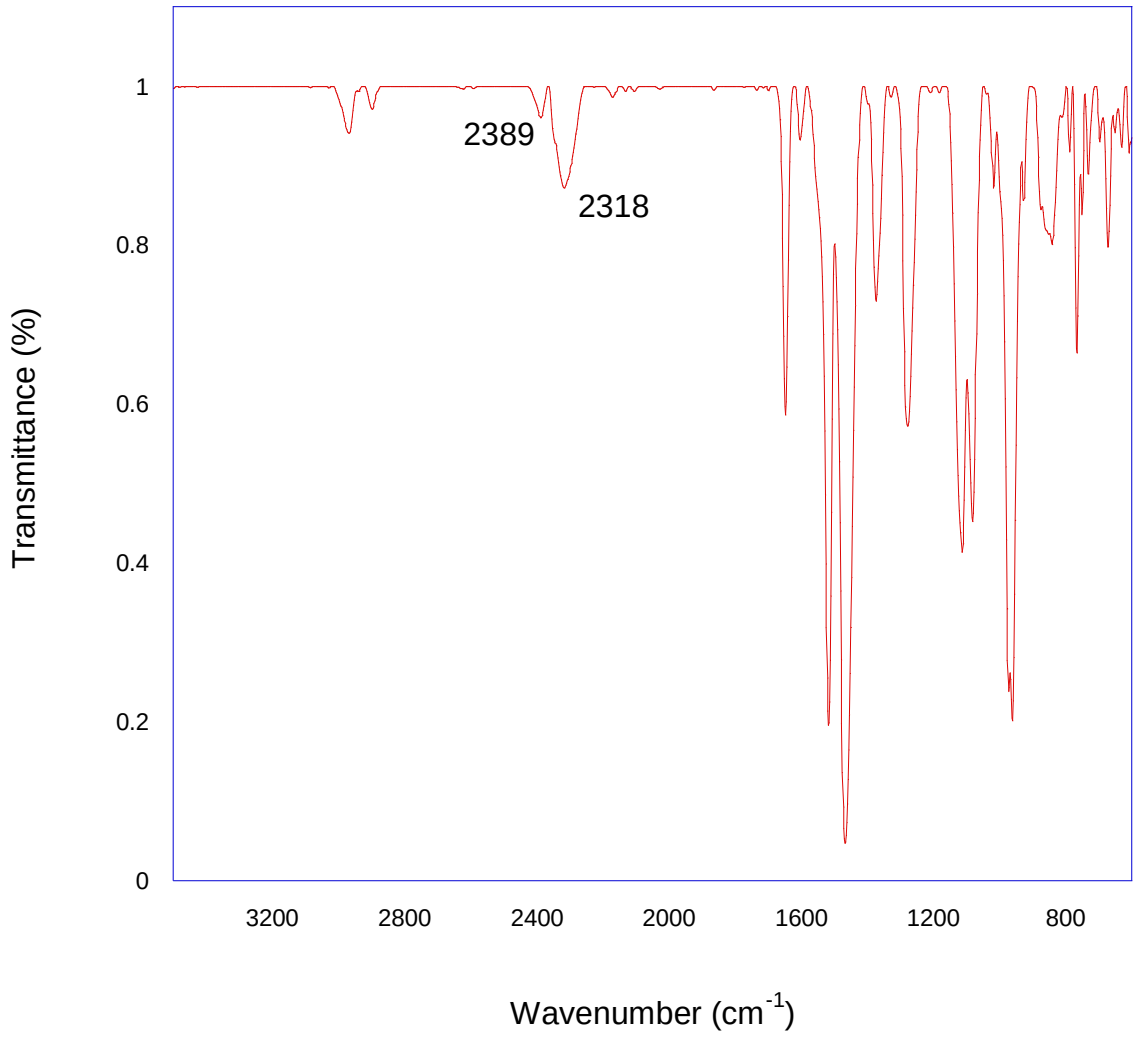

Figure S4. IR (KBr) spectrum of $Sm\{HB(C_6F_5)_3\}_2THF_2$ (**3b**).

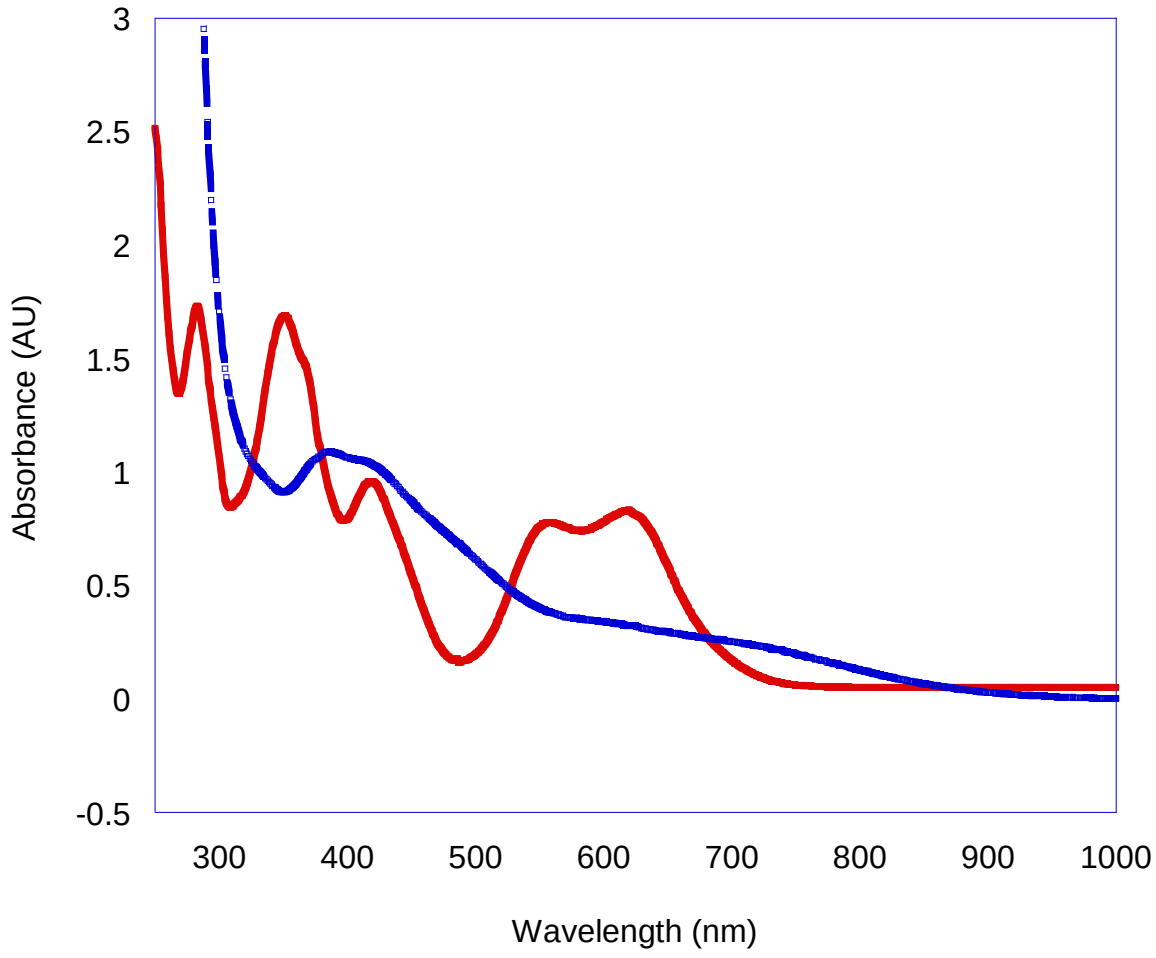

Figure S5. UV-Vis spectra of $Sm\{C(SiHMe_2)_3\}_2THF_2$ (**1b**) and starting material SmI_2THF_2, 2mM in THF.

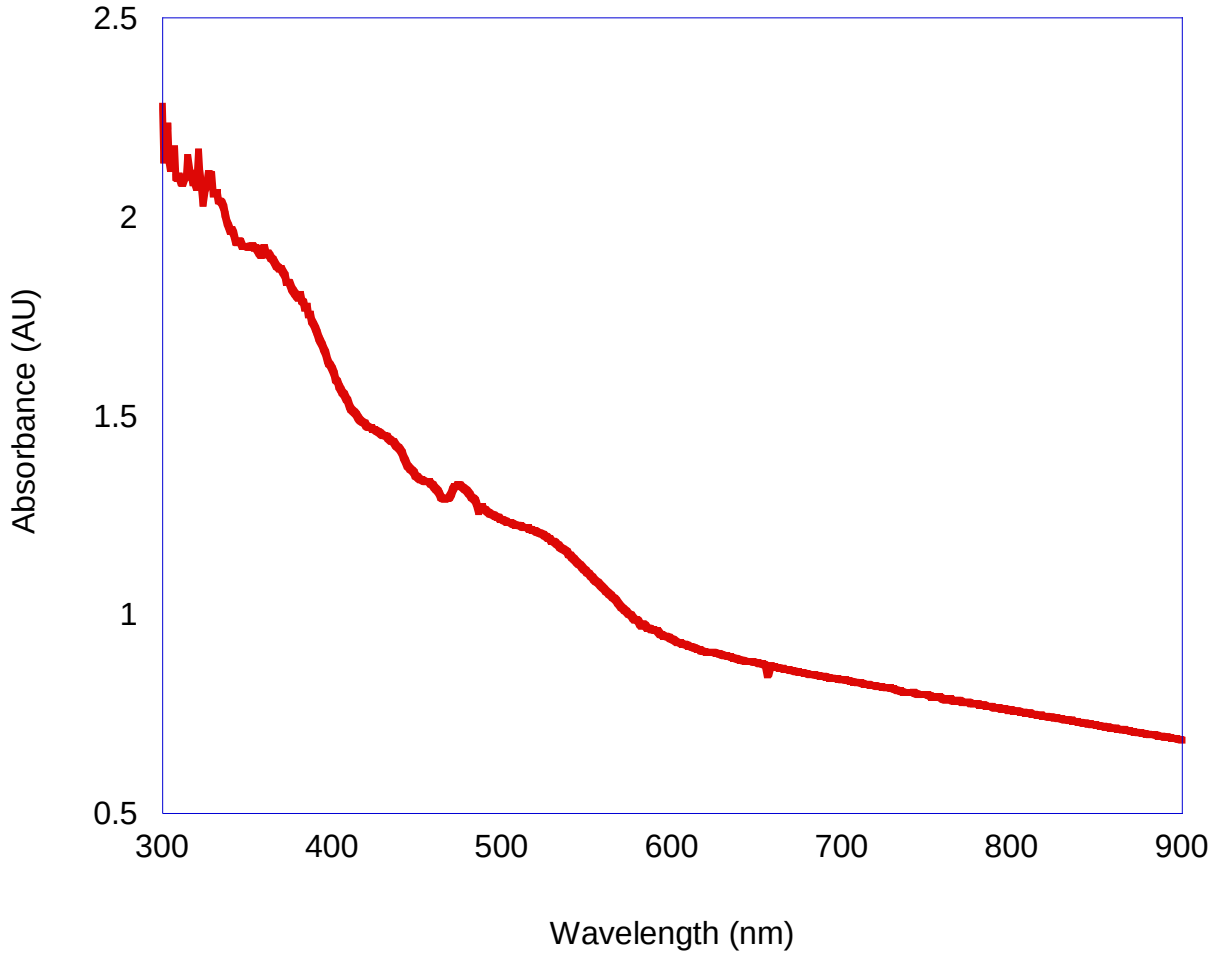

Figure S6. UV-Vis spectrum of $SmC(SiHMe_2)_3HB(C_6F_5)_3THF_2$ (**2b**), 2 mM in bromobenzene.

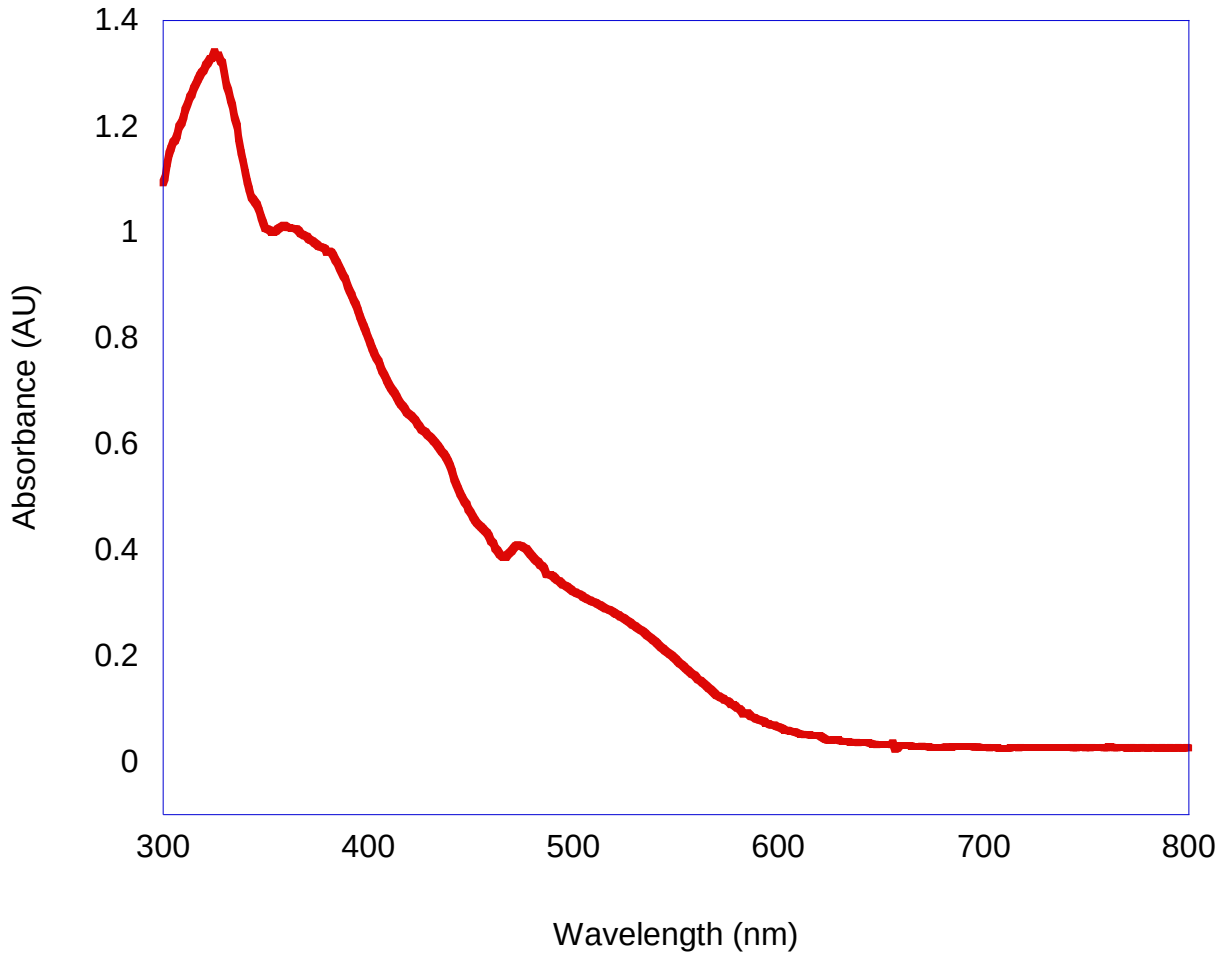

Figure S7. UV-Vis spectrum of $Sm\{HB(C_6F_5)_3\}_2THF_2$ (**3b**), 2 mM in bromobenzene.

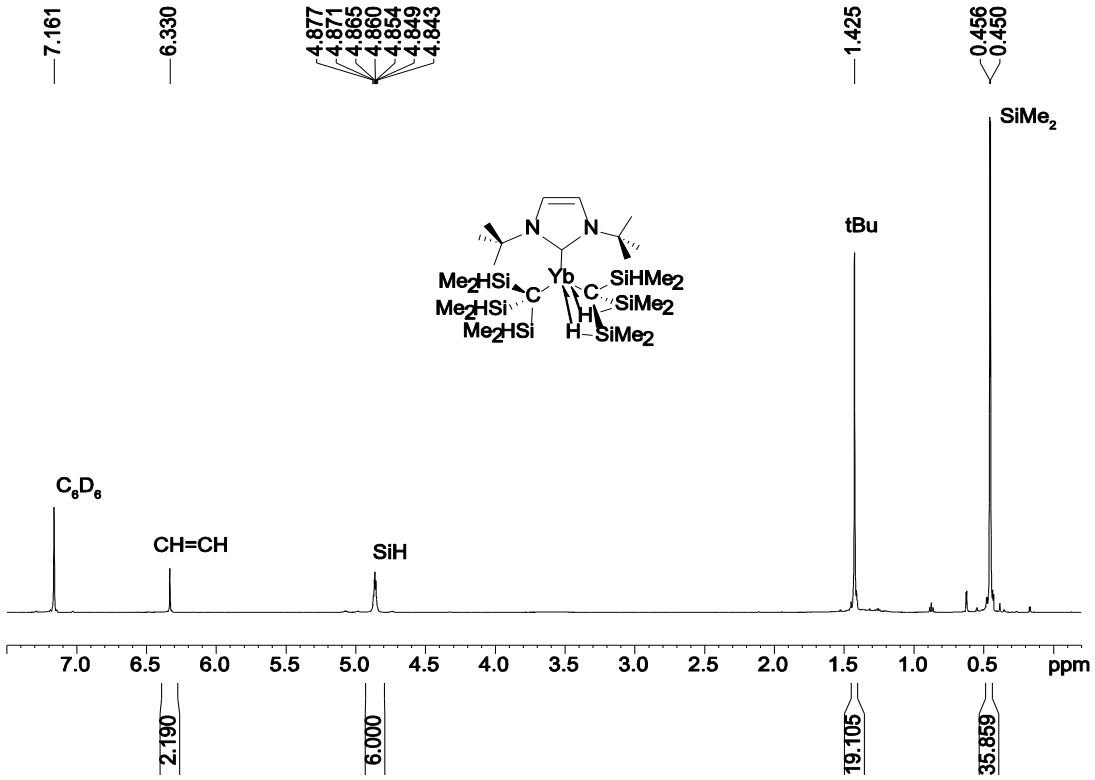

Figure S8. ^{1}H NMR spectrum (600 MHz, benzene-d_6) of Yb{C(SiHMe$_2$)$_3$}$_2$Im*t*Bu (**4a**).

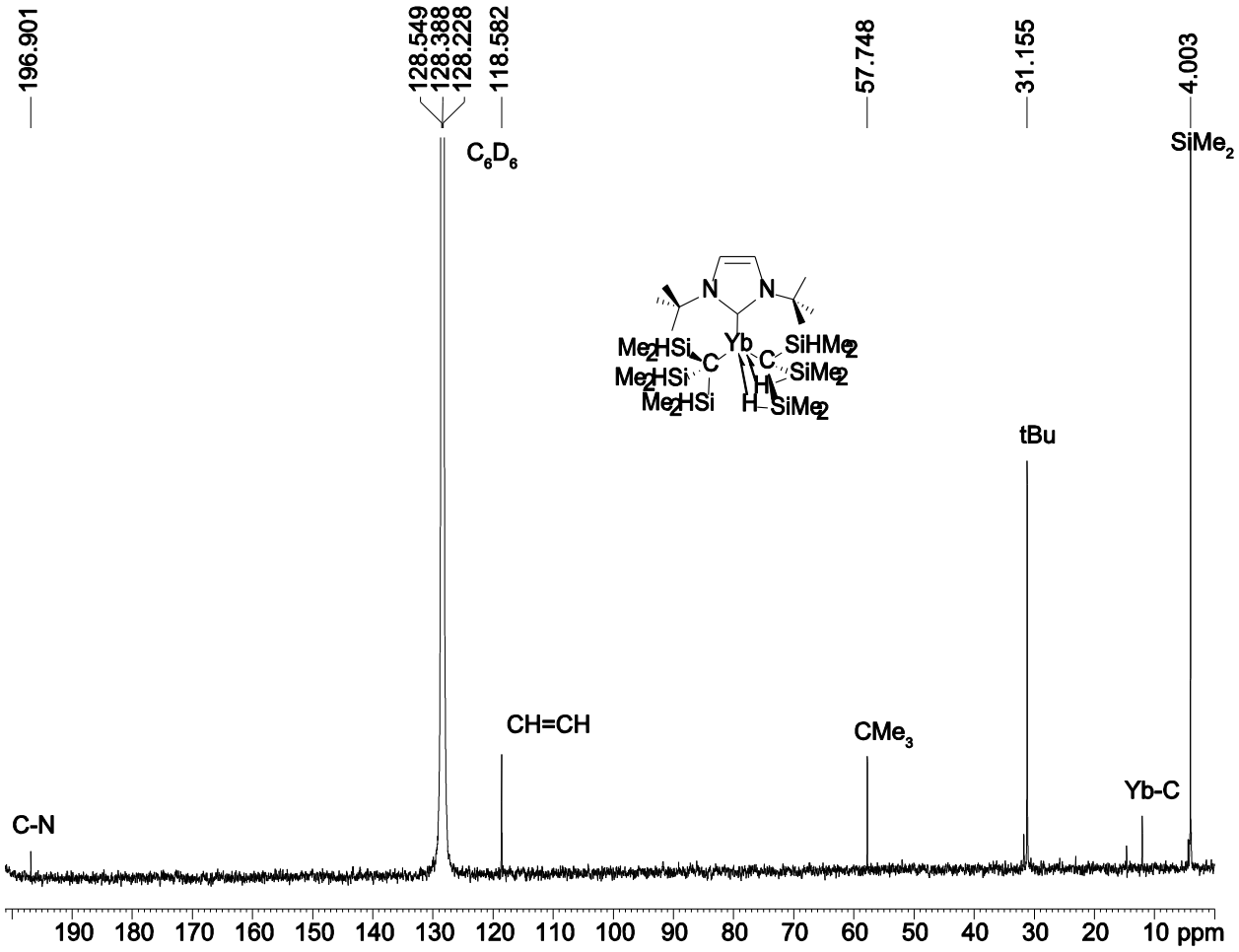

Figure S9. $^{13}C\{^{1}H\}$ NMR spectrum (150 MHz, benzene-d_6) of Yb{C(SiHMe$_2$)$_3$}$_2$Im*t*Bu (**4a**).

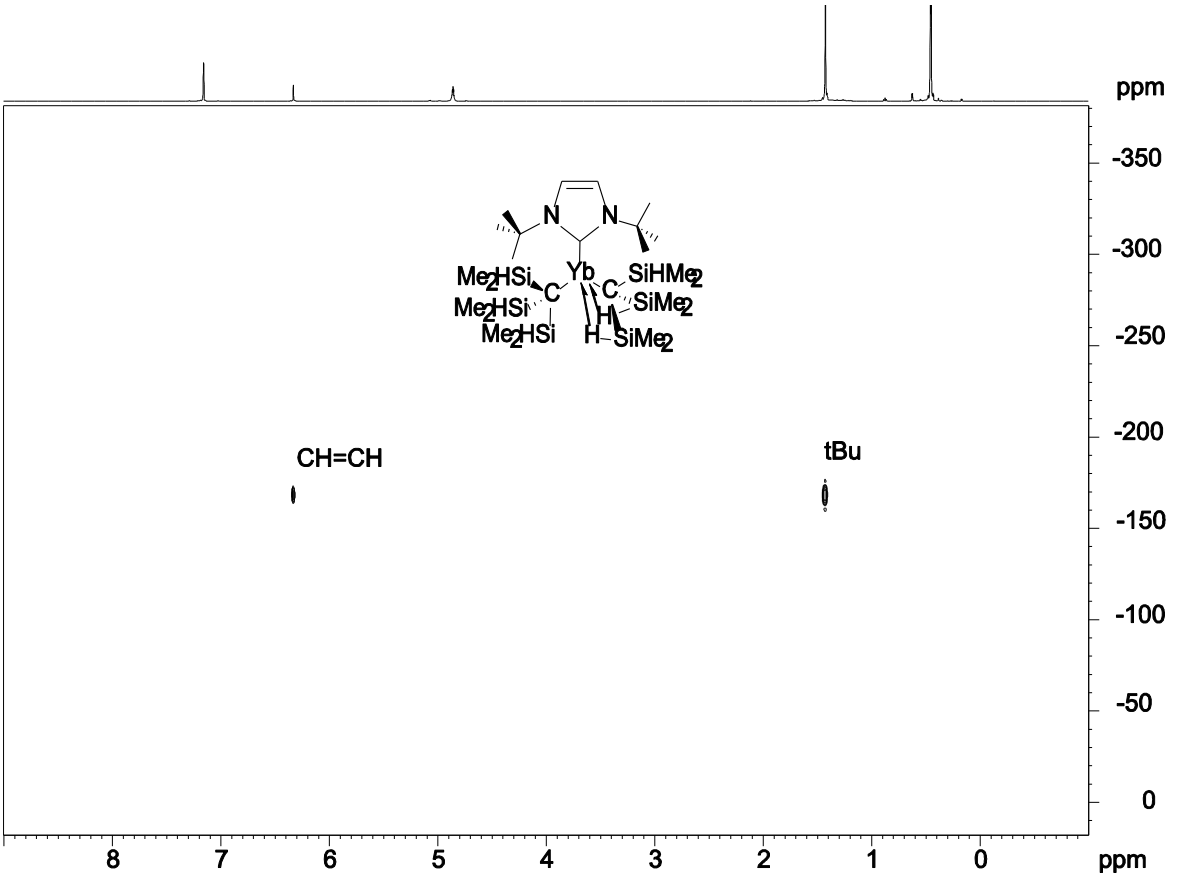

Figure S10. ^{1}H-^{15}N NMR HMBC experiment (61 MHz, benzene-d_6) of Yb{C(SiHMe$_2$)$_3$}$_2$Im*t*Bu (**4a**).

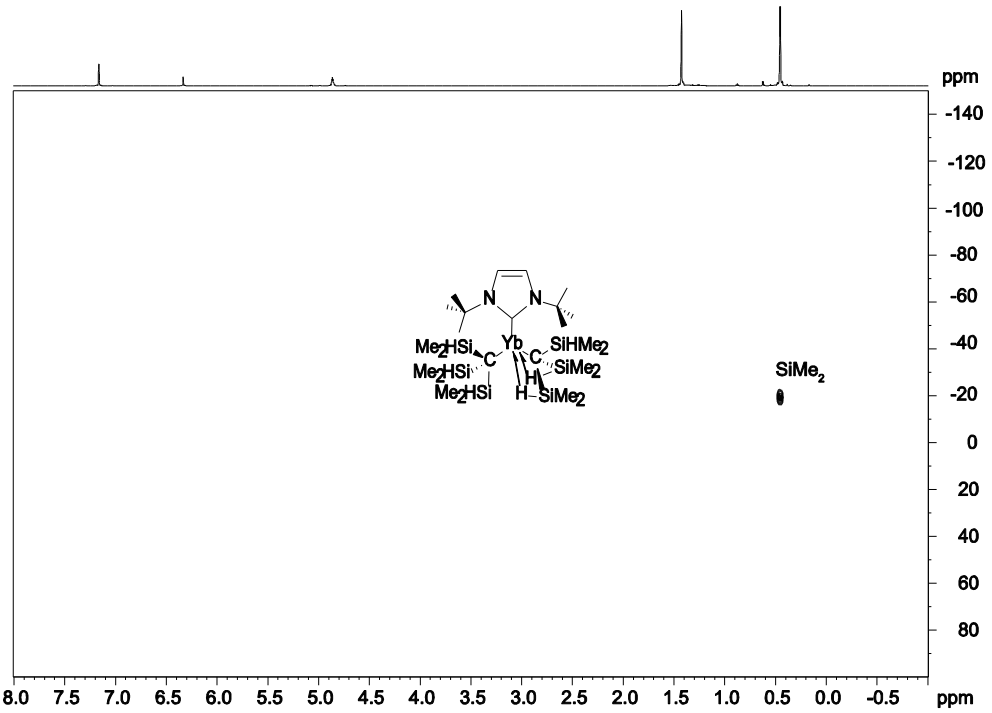

Figure S11. ^{1}H-^{29}Si NMR HMBC experiment (119 MHz, benzene-d_6) of Yb{C(SiHMe$_2$)$_3$}$_2$Im*t*Bu (**4a**).

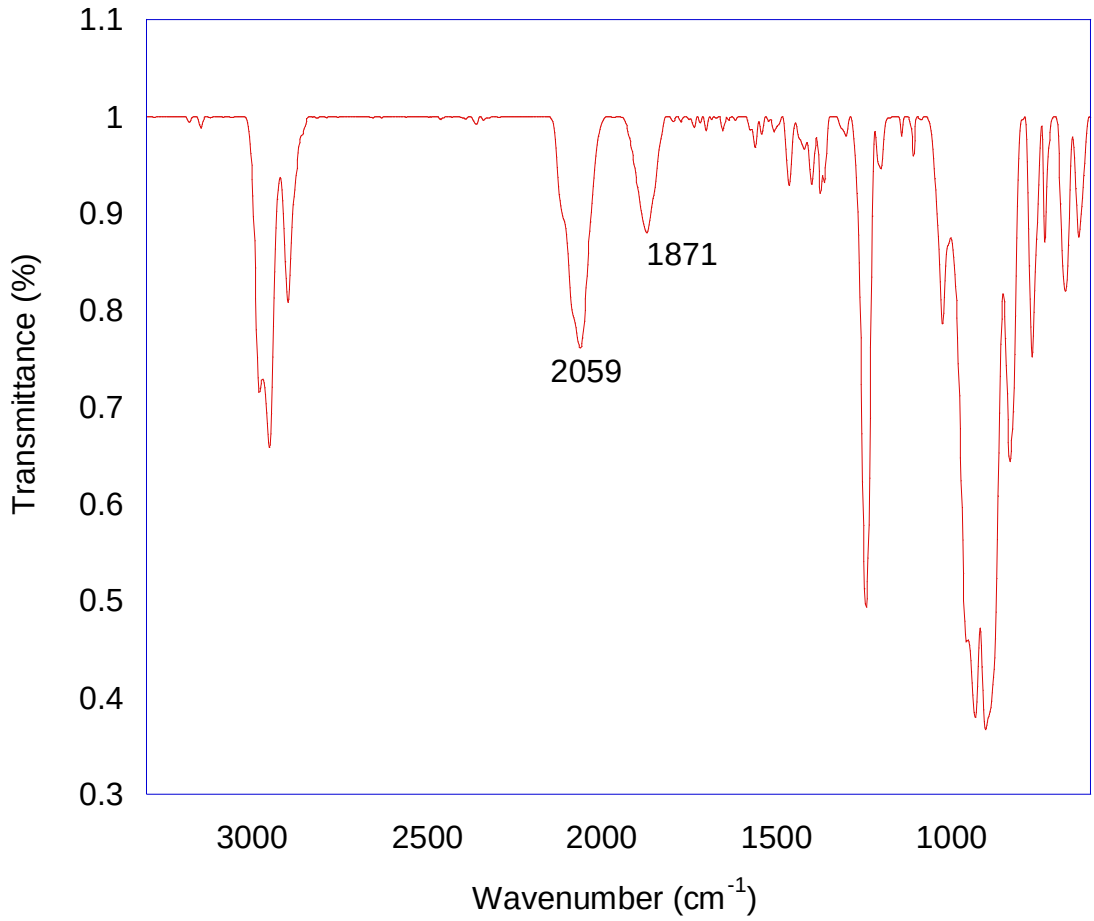

Figure S12. IR (KBr) spectrum of Yb{C(SiHMe$_2$)$_3$}$_2$Im*t*Bu (**4a**).

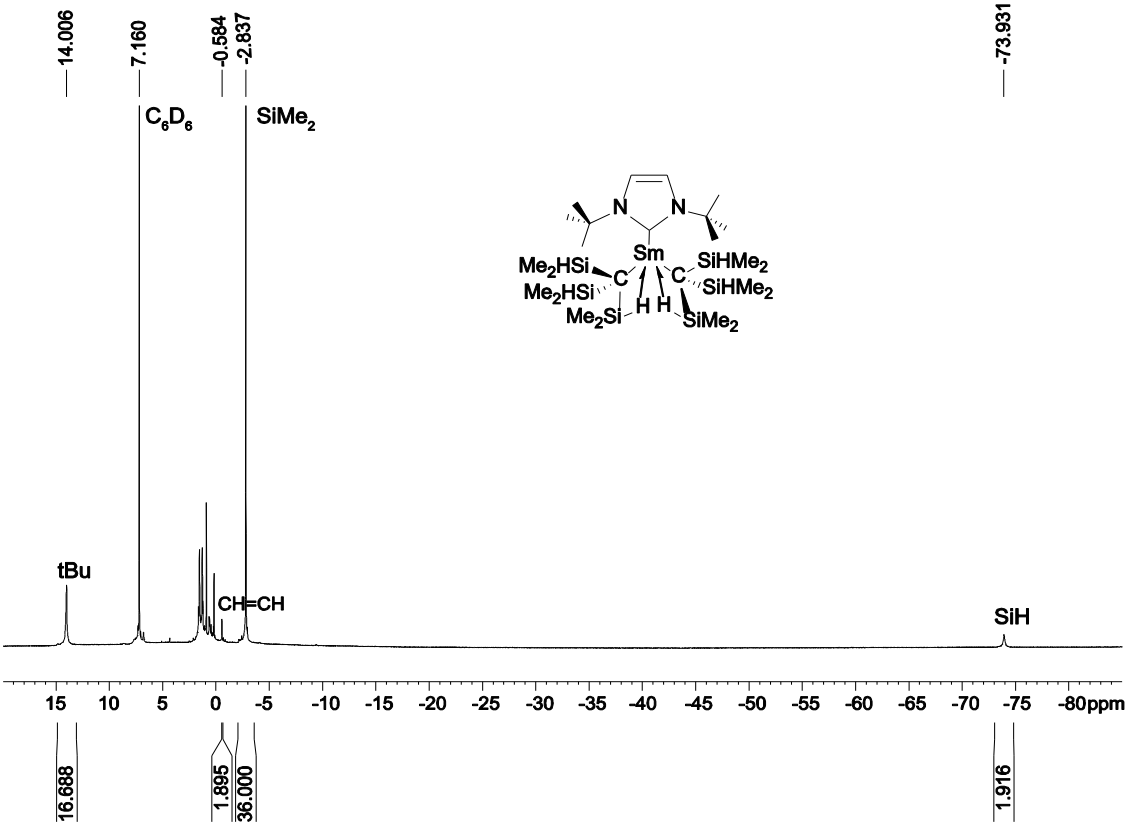

Figure S13. ^{1}H NMR spectrum (600 MHz, benzene-d_6) of Sm{C(SiHMe$_2$)$_3$}$_2$Im*t*Bu (**4b**).

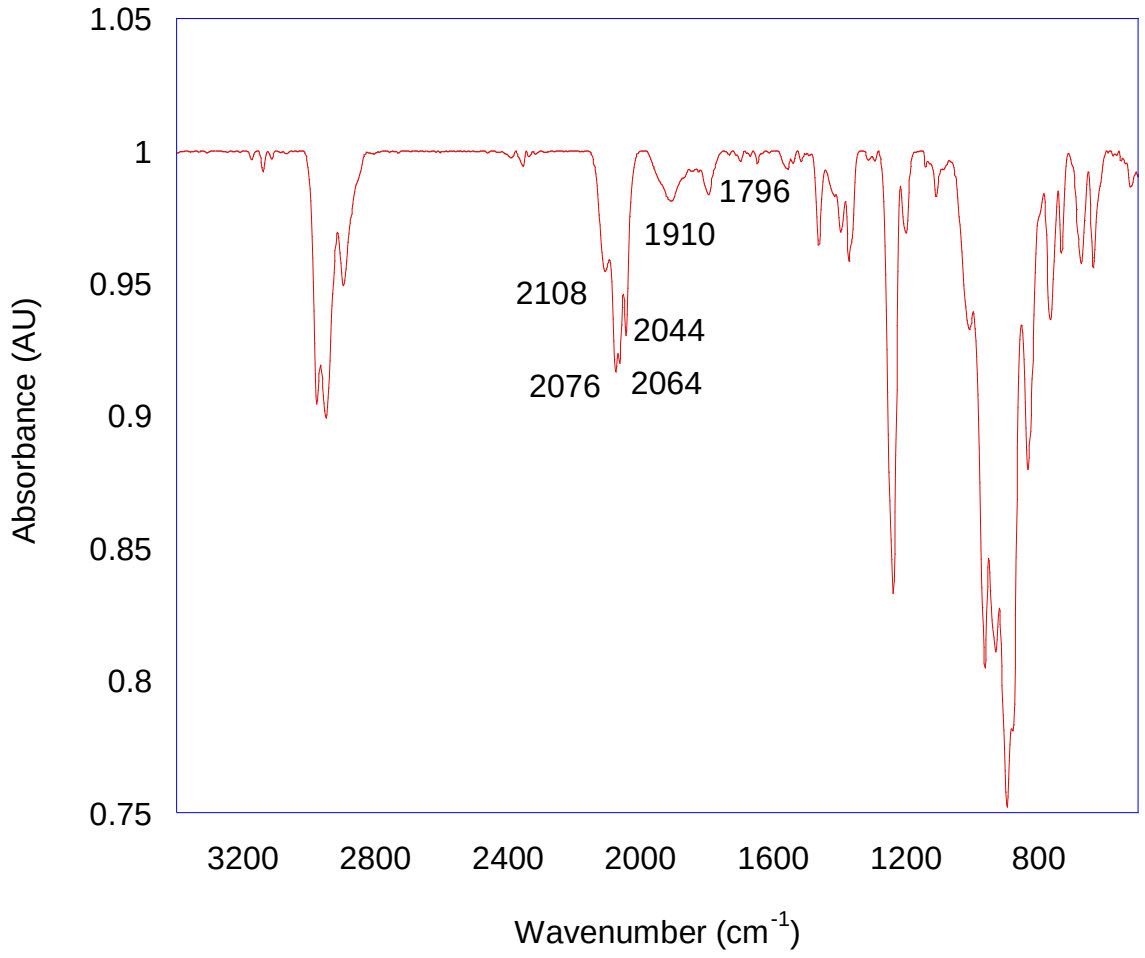

Figure S14. IR (KBr) spectrum of Sm{C(SiHMe$_2$)$_3$}$_2$Im*t*Bu (**4b**).

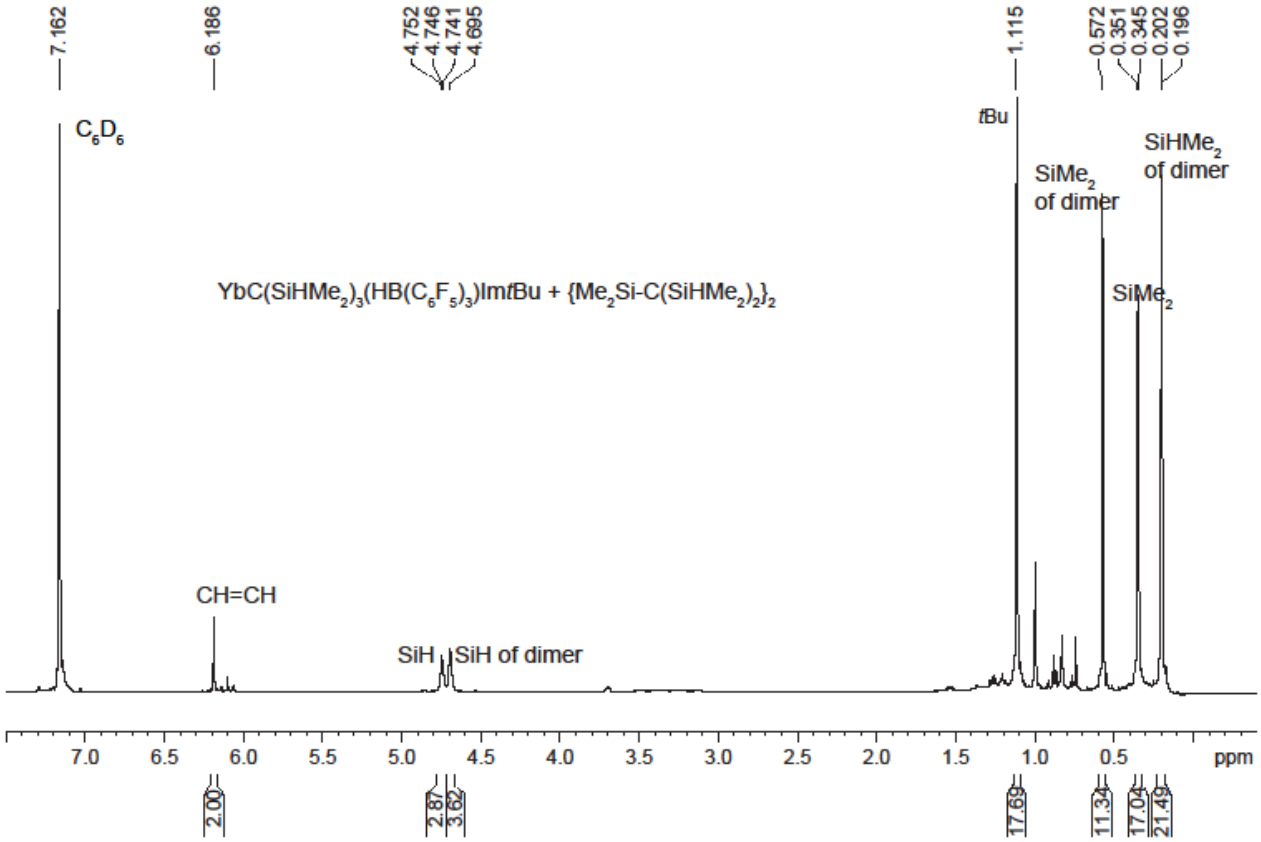

Figure S15. ^{1}H NMR spectrum (600 MHz, benzene-d_6) of YbC(SiHMe$_2$)$_3$(HB(C$_6$F$_5$)$_3$)Im*t*Bu (**5a**).

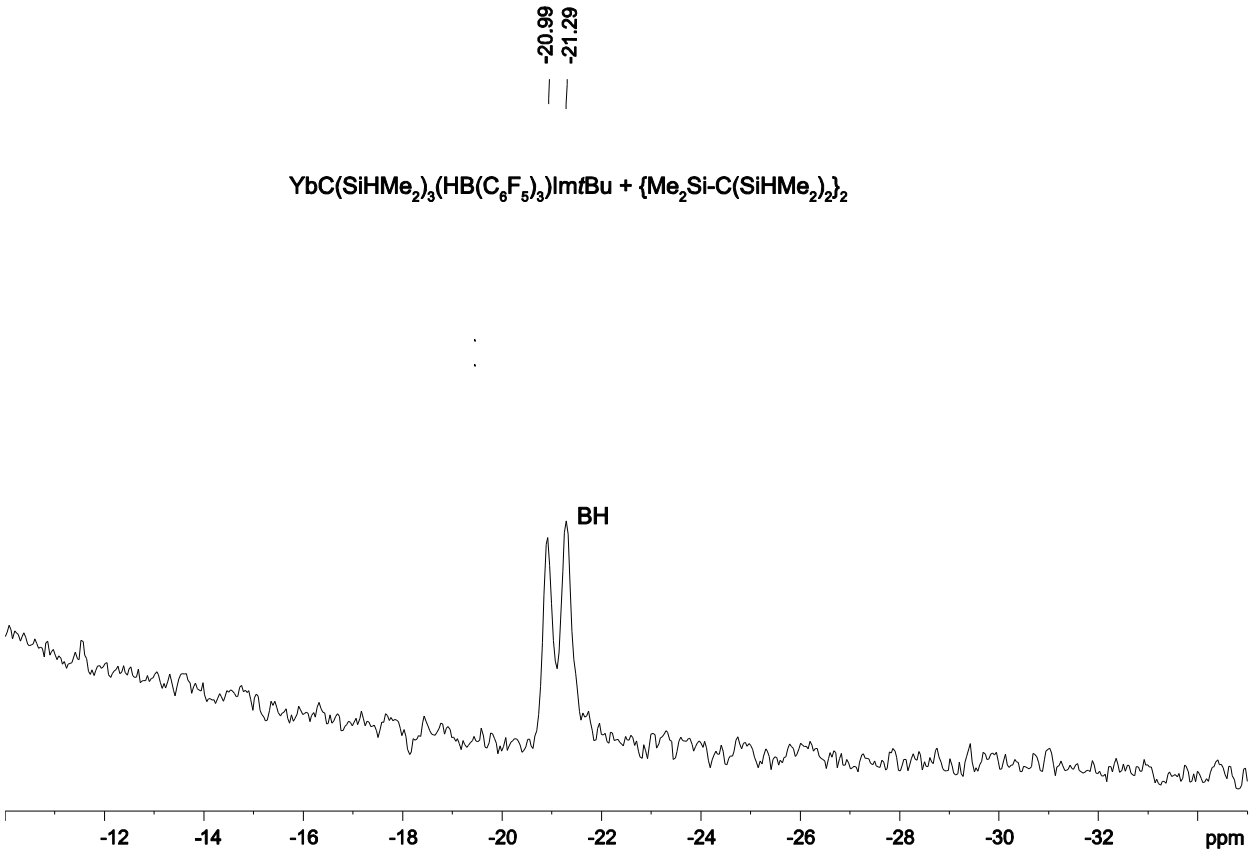

Figure S16. ^{11}B NMR spectrum (192 MHz, benzene-d_6) of YbC(SiHMe$_2$)$_3$(HB(C$_6$F$_5$)$_3$)Im*t*Bu (**5a**).

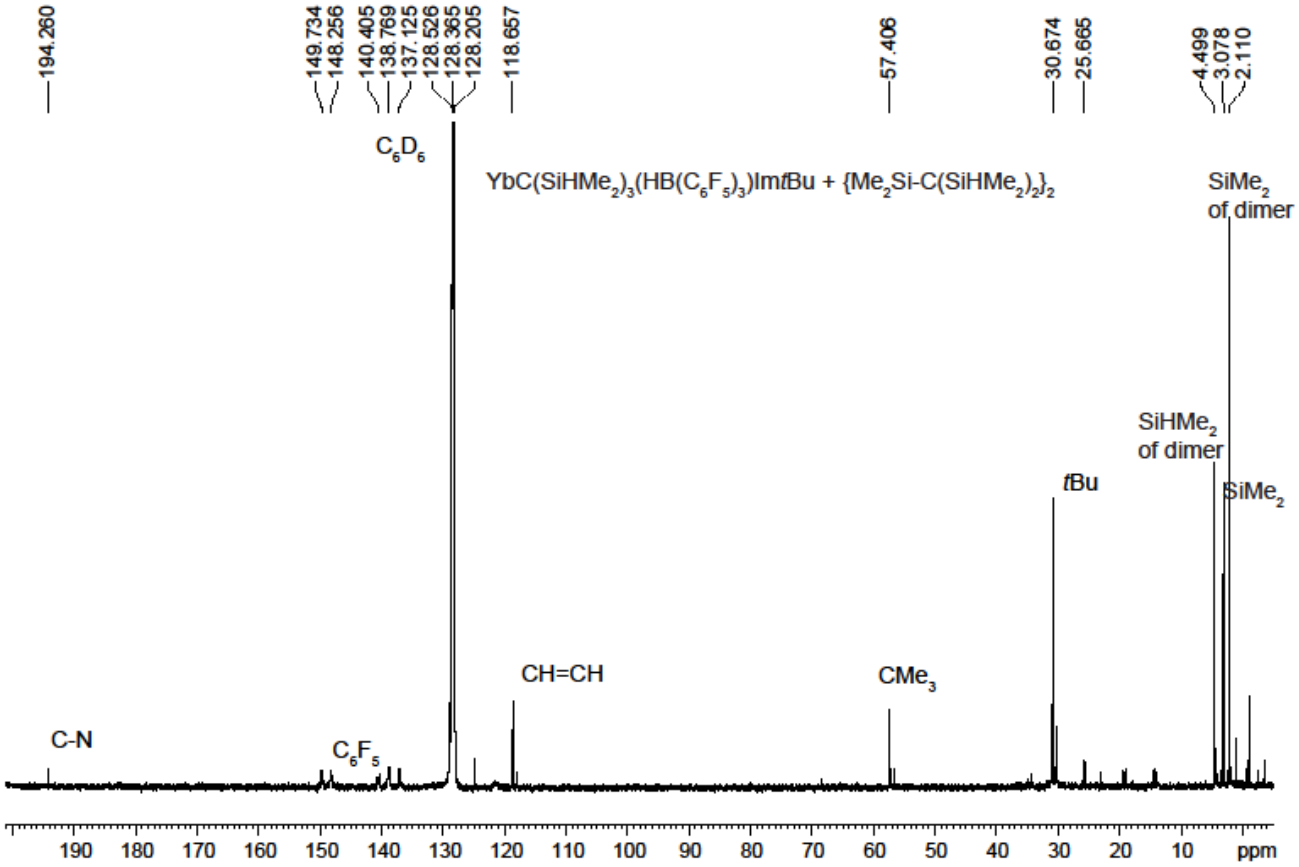

Figure S17. $^{13}C\{^{1}H\}$ NMR spectrum (150 MHz, benzene-d_6) of $YbC(SiHMe_2)_3(HB(C_6F_5)_3)Im\textit{t}Bu$ (**5a**).

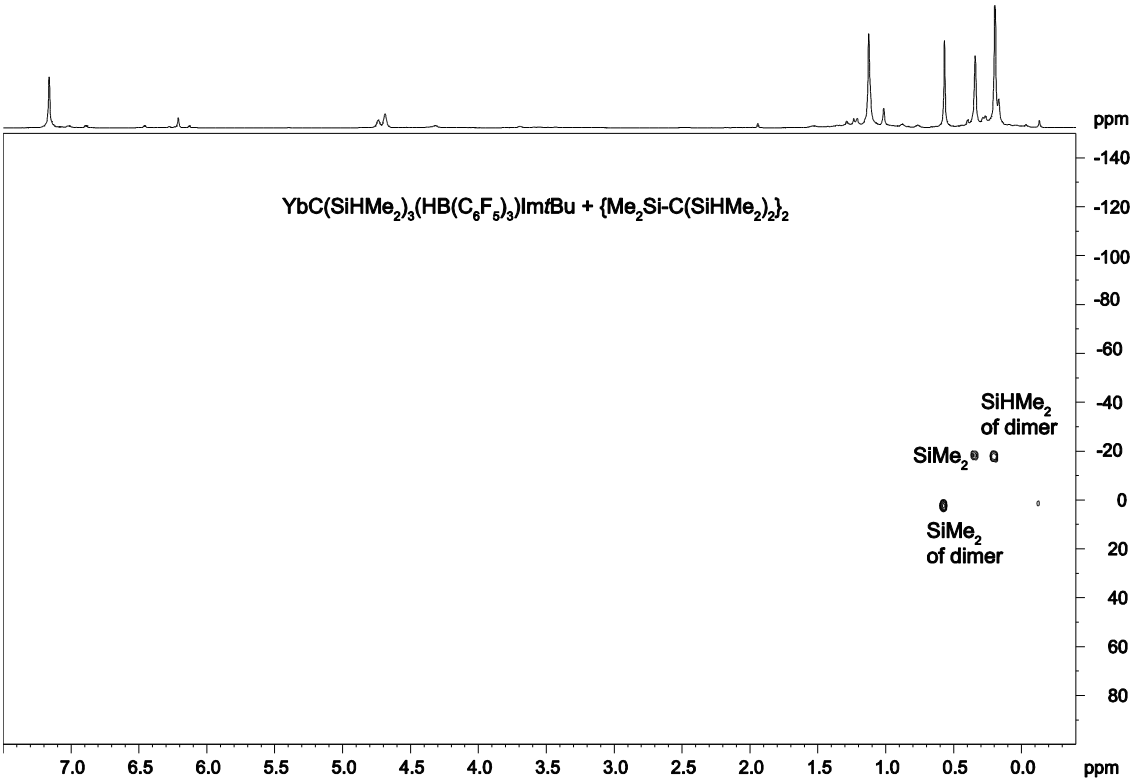

Figure S18. ^{1}H-^{29}Si NMR HMBC experiment (119 MHz, benzene-d_6) of $YbC(SiHMe_2)_3(HB(C_6F_5)_3)Im$*t*Bu (**5a**).

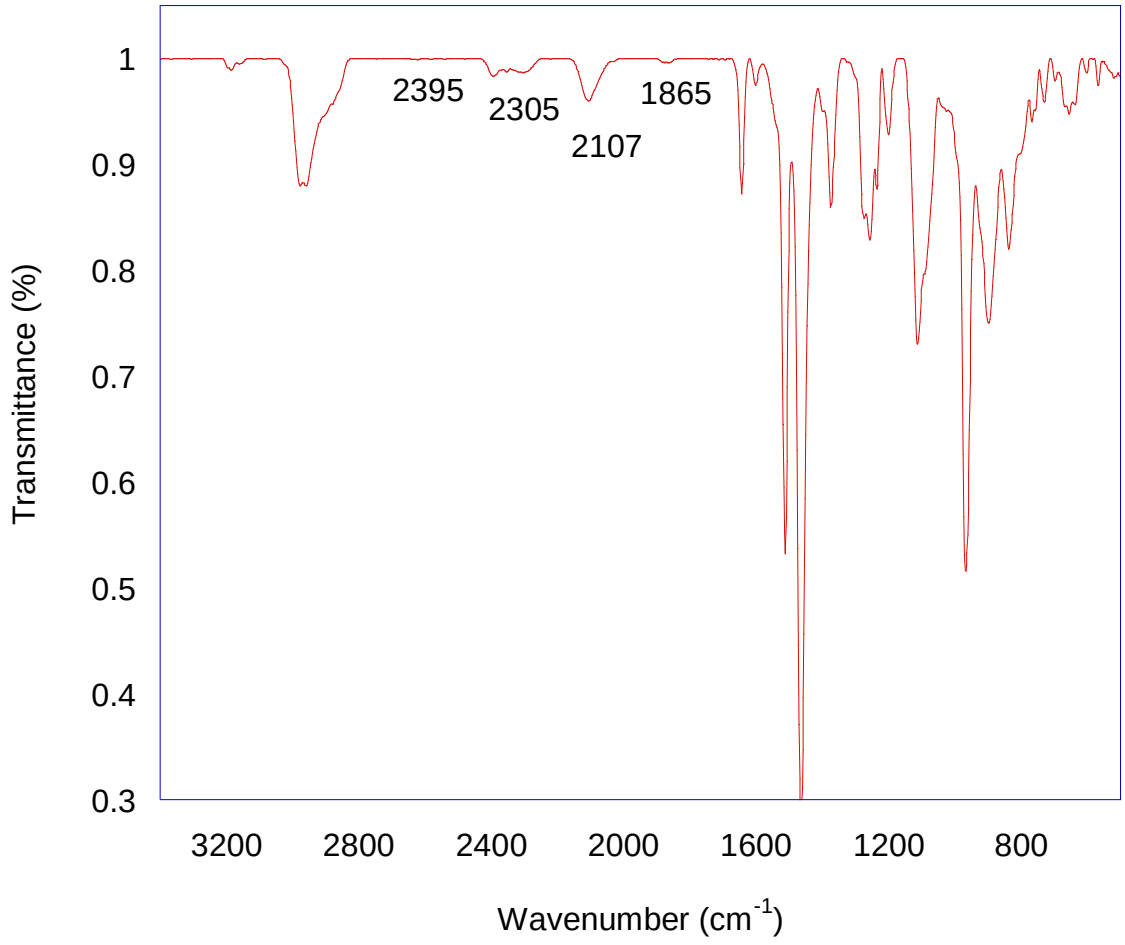

Figure S19. IR (benzene) spectrum of YbC(SiHMe$_2$)$_3$(HB(C$_6$F$_5$)$_3$)Im*t*Bu (**5a**).

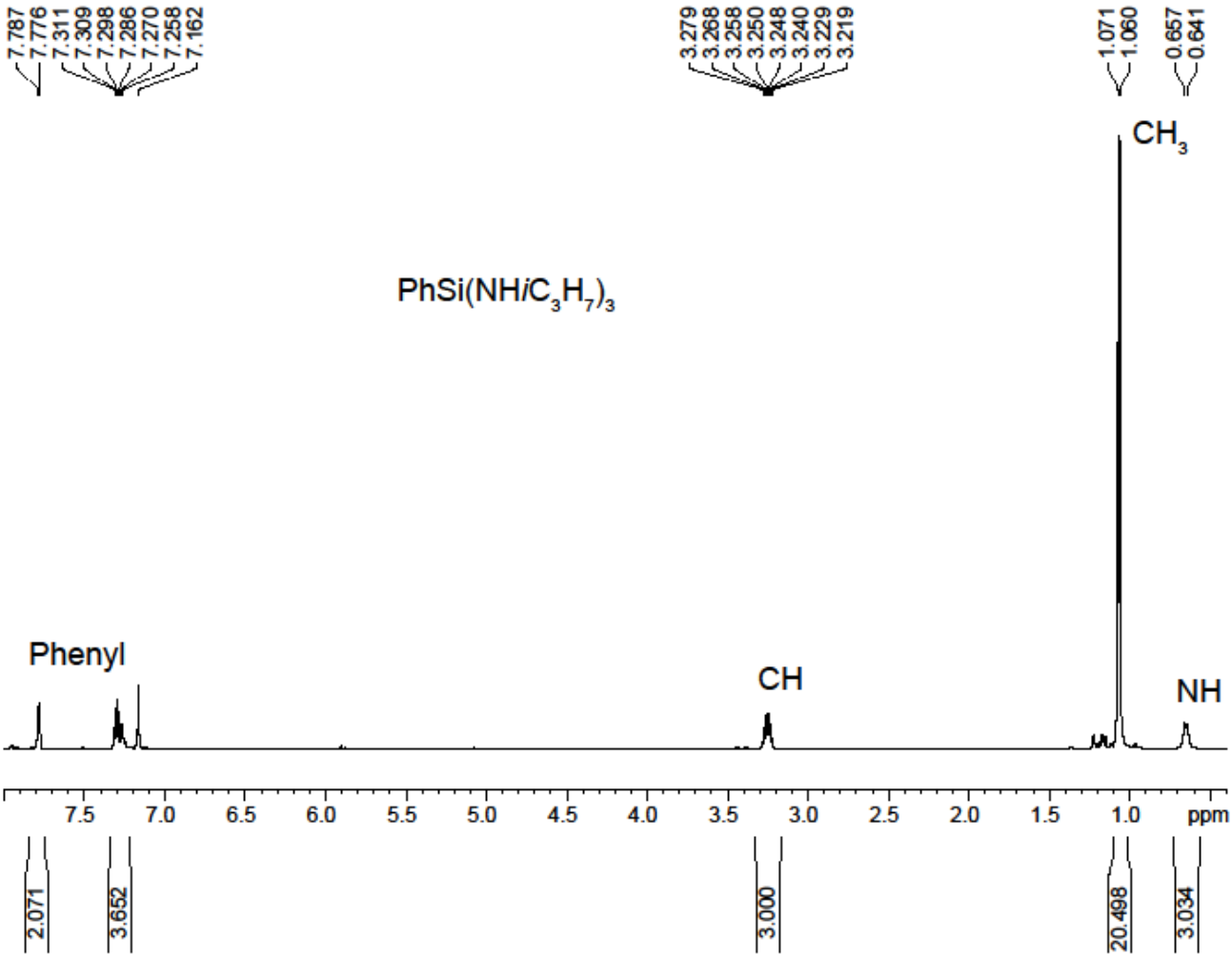

Figure S20. ^{1}H NMR spectrum (600 MHz, benzene-d_6) of PhSi(NH*i*C_3H_7)$_3$ obtained from the reaction of $PhSiH_3$ and 4 equiv. of *i*$C_3H_7NH_2$.

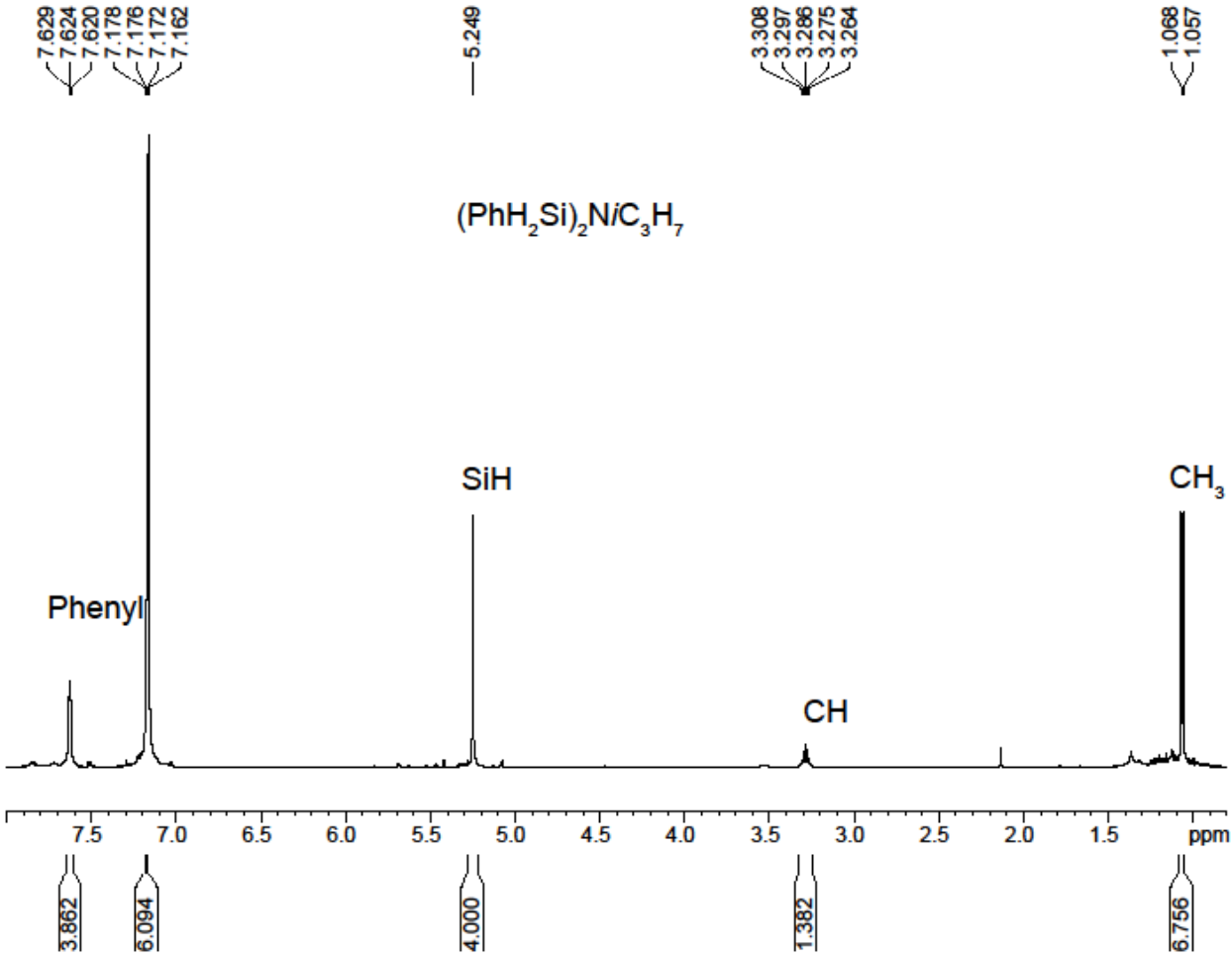

Figure S21. ^{1}H NMR spectrum (600 MHz, benzene-d_6) of $(PhH_2Si)_2NiC_3H_7$ obtained from the reaction of 2.2 equiv. of $PhSiH_3$ and $iC_3H_7NH_2$.

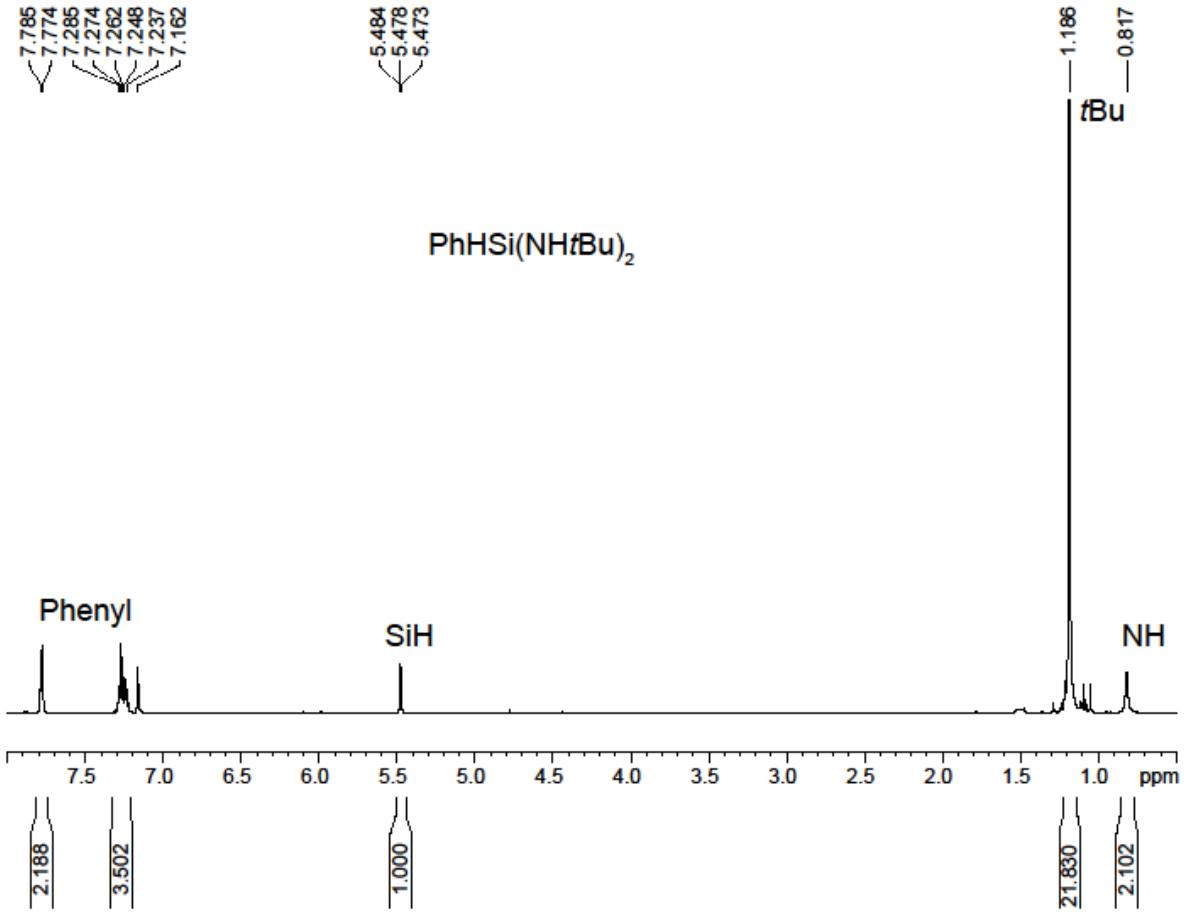

Figure S22. ^{1}H NMR spectrum (600 MHz, benzene-d_6) of PhHSi(NH*t*Bu)$_2$ obtained from the reaction of PhSiH$_3$ and 2 equiv. of *t*BuNH$_2$.

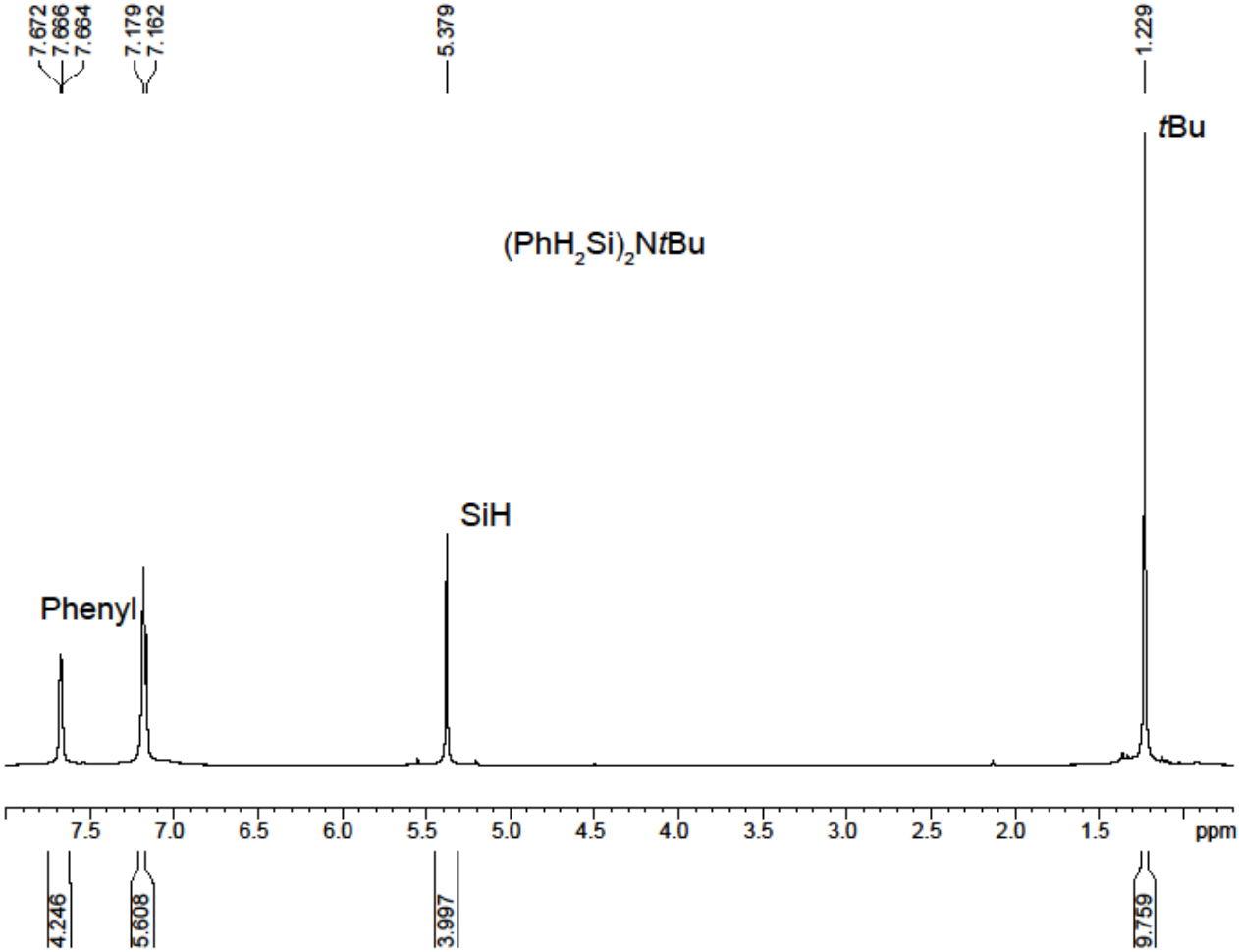

Figure S23. ^{1}H NMR spectrum (600 MHz, benzene-d_6) of $(PhH_2Si)_2NtBu$ obtained from the reaction of 2.2 equiv. of $PhSiH_3$ and $tBuNH_2$.

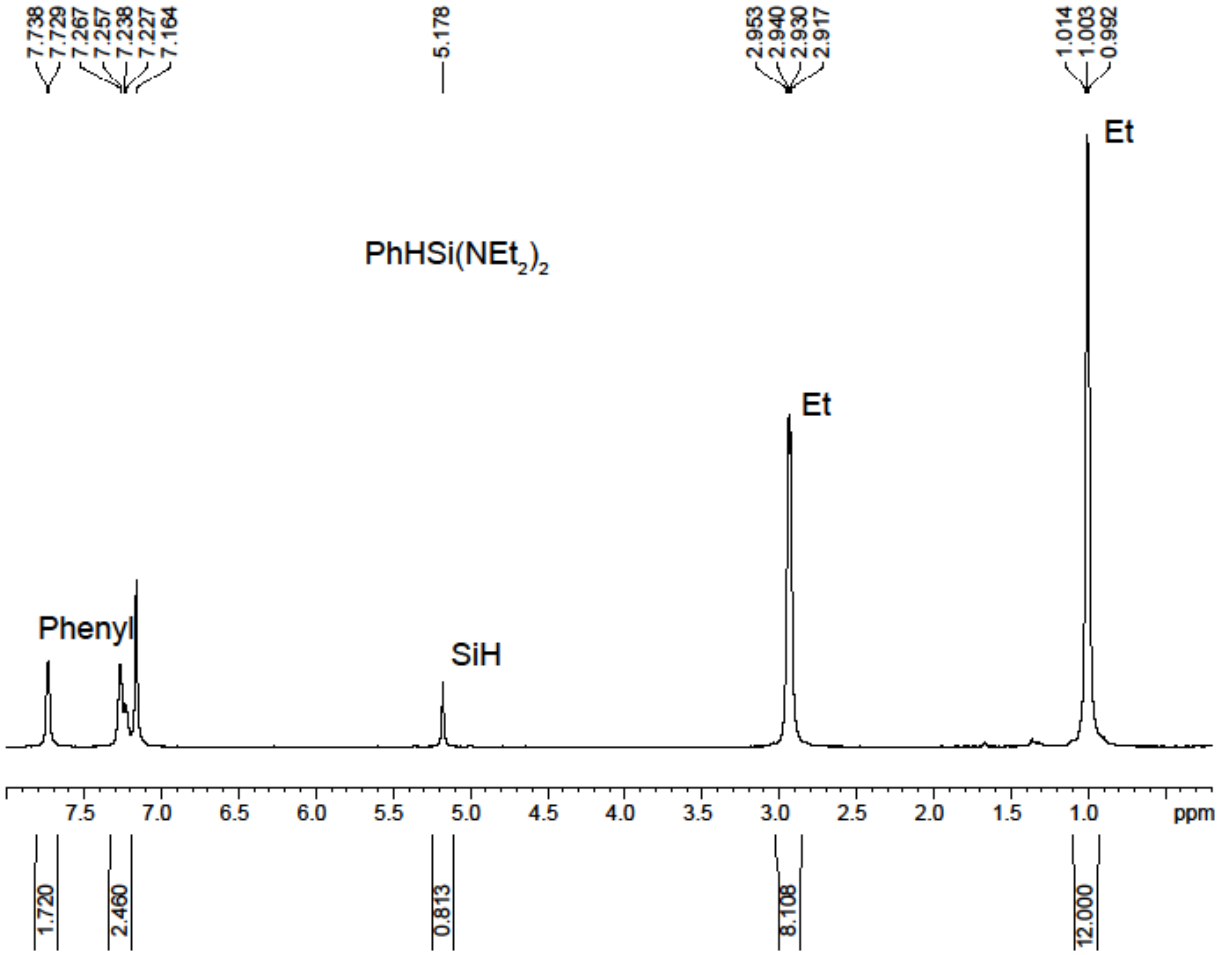

Figure S24. ^{1}H NMR spectrum (600 MHz, benzene-d_6) of $PhHSi(NEt_2)_2$ obtained from the reaction of $PhSiH_3$ and 3 equiv. of Et_2NH.

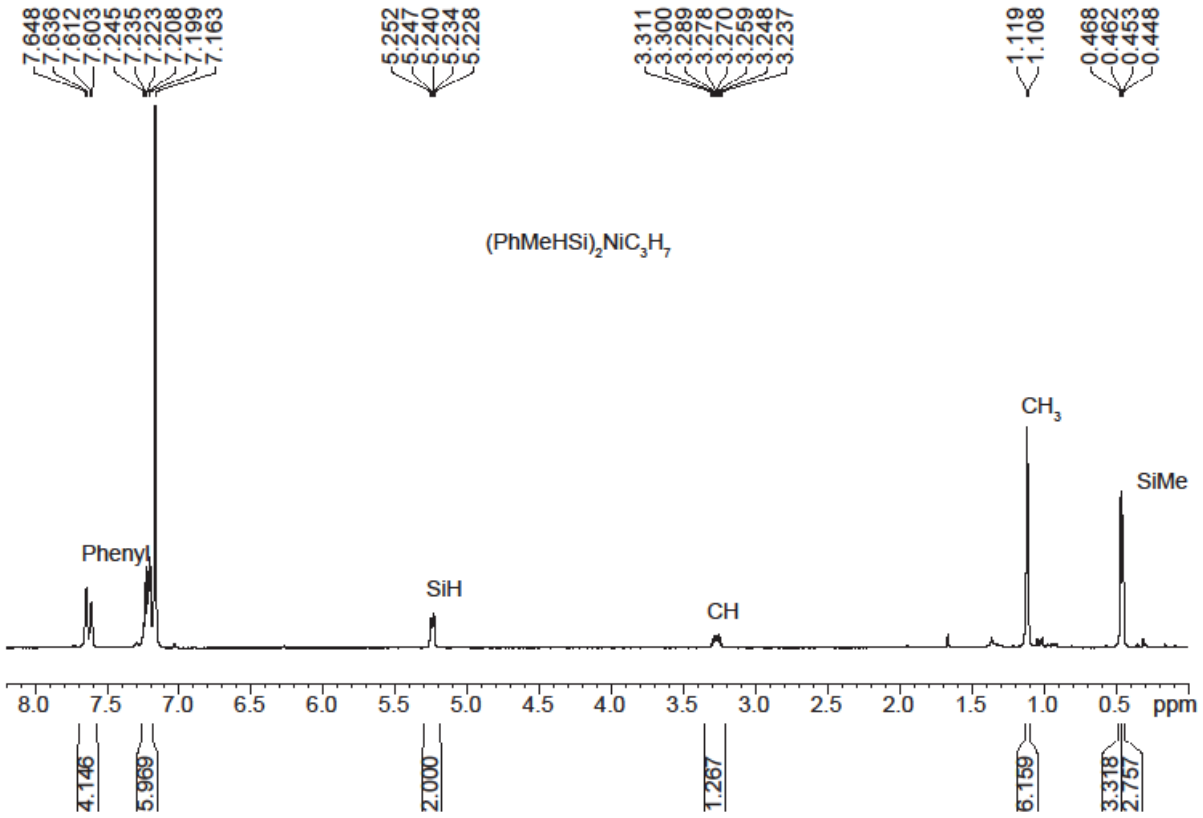

Figure S25. ^{1}H NMR spectrum (600 MHz, benzene-d_6) of (PhMeHSi)$_2$NiC$_3$H$_7$ obtained from the reaction of 2 equiv. of PhMeSiH$_2$ and iC$_3$H$_7$NH$_2$.

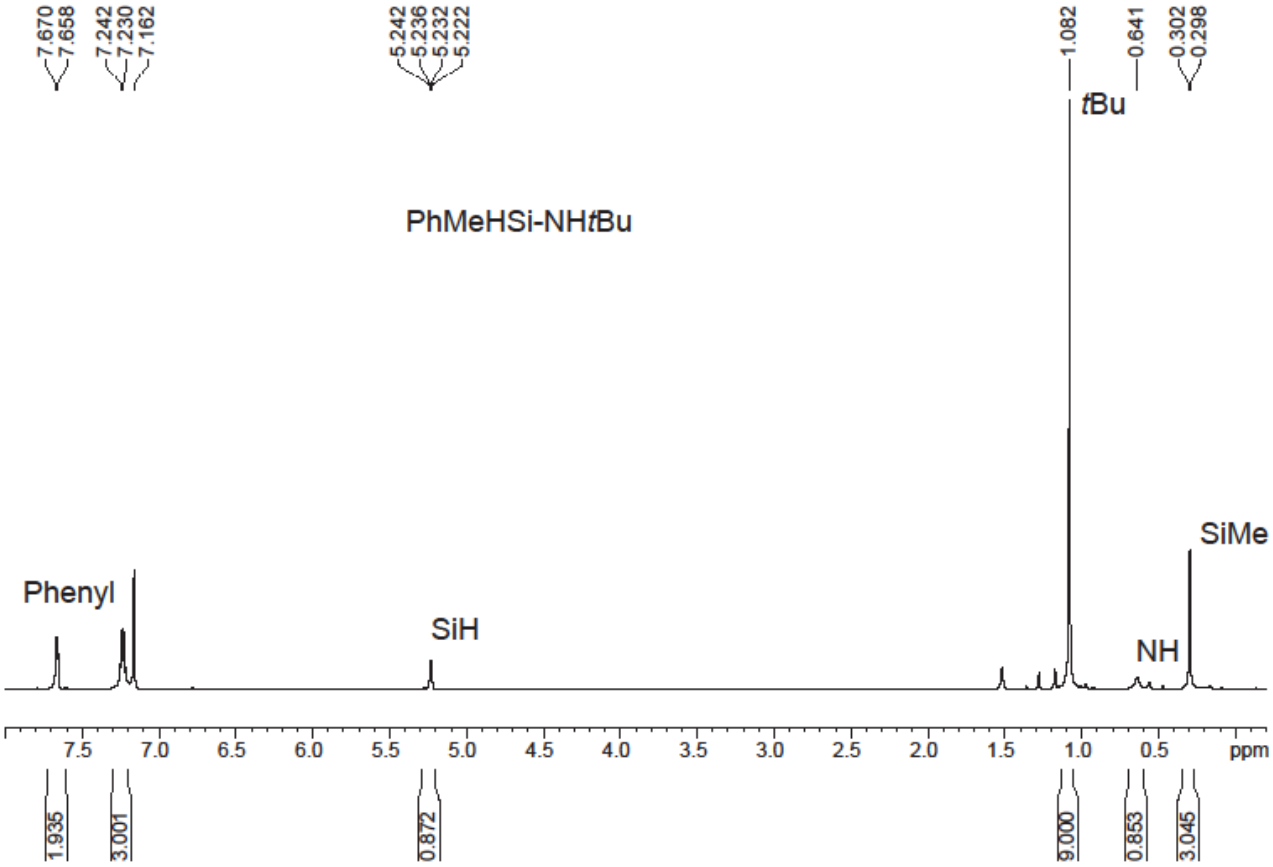

Figure S26. ^{1}H NMR spectrum (600 MHz, benzene-d_6) of PhMeHSi-NH*t*Bu obtained from the reaction of $PhMeSiH_2$ and *t*$BuNH_2$.

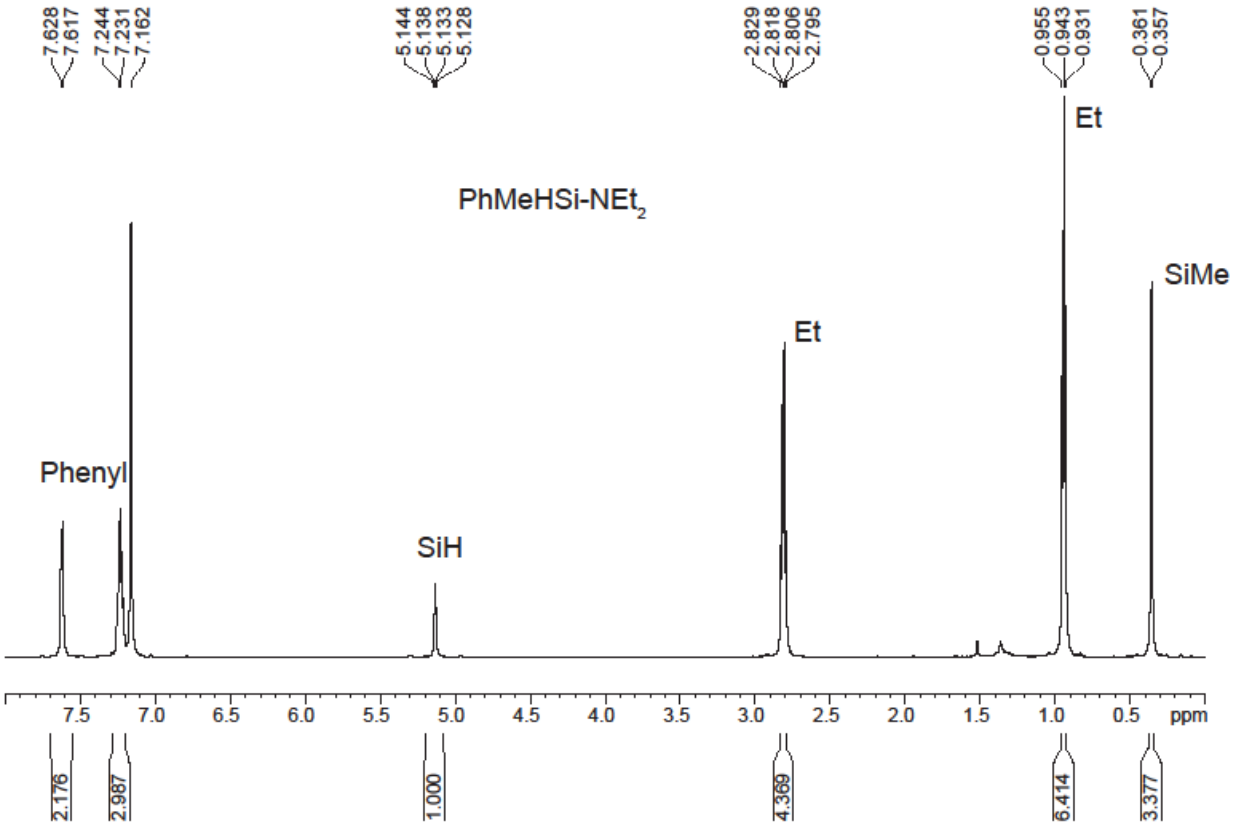

Figure S27. ^{1}H NMR spectrum (600 MHz, benzene-d_6) of PhMeHSi-NEt_2 obtained from the reaction of $PhMeSiH_2$ and Et_2NH.

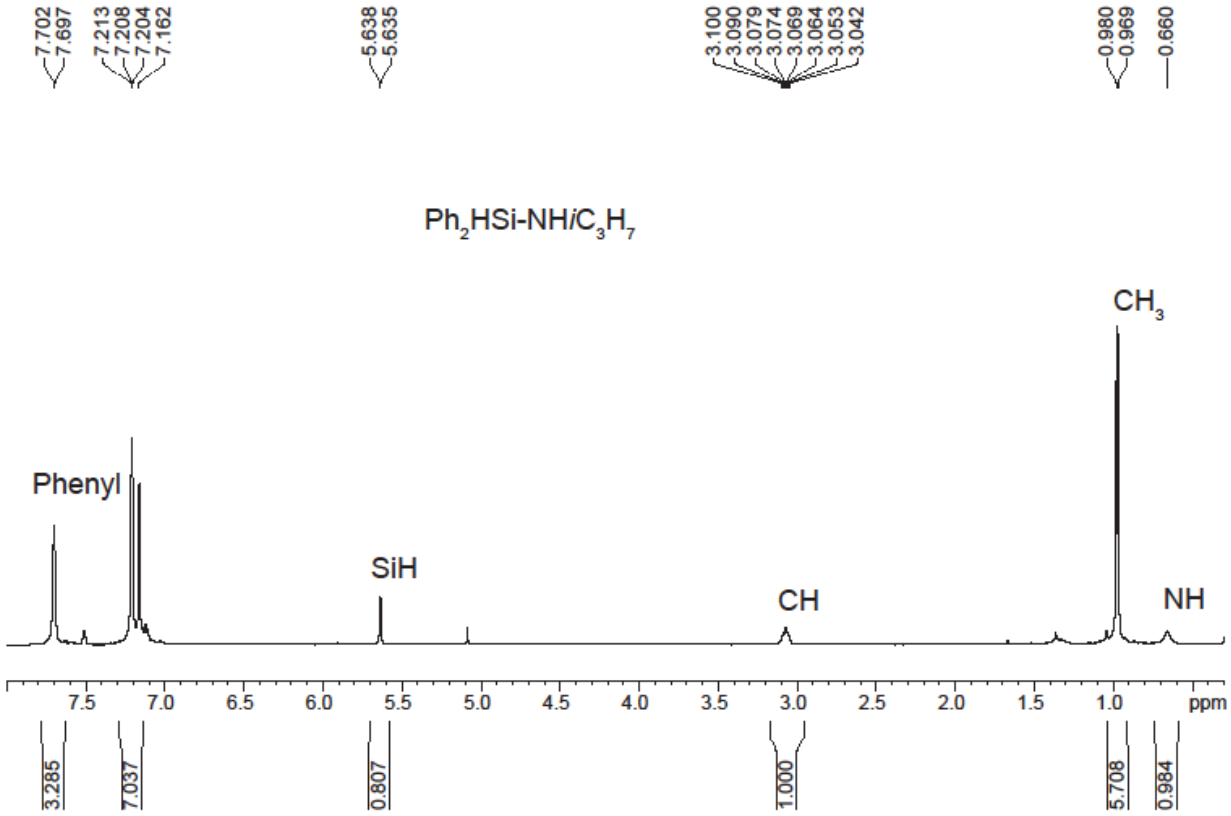

Figure S28. ^{1}H NMR spectrum (600 MHz, benzene-d_6) of $Ph_2HSi\text{-}NHiC_3H_7$ obtained from the reaction of Ph_2SiH_2 and $iC_3H_7NH_2$.

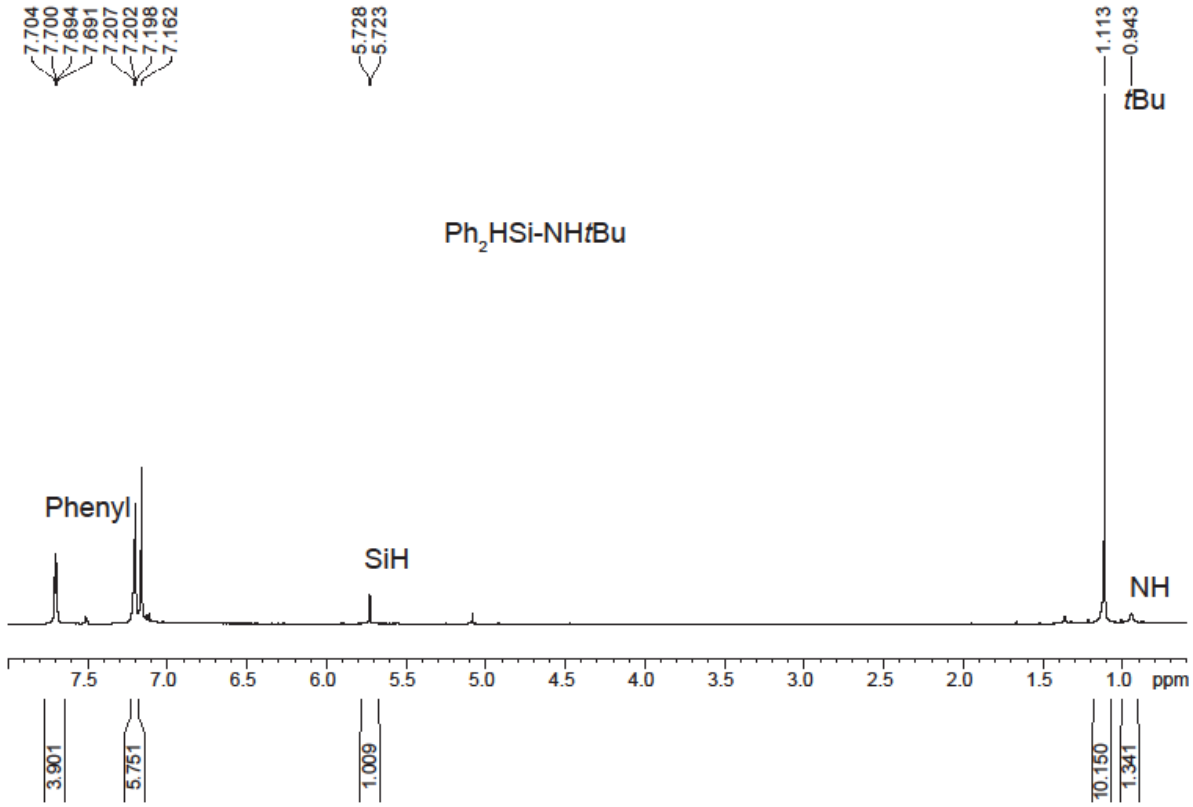

Figure S29. ^{1}H NMR spectrum (600 MHz, benzene-d_6) of Ph_2HSi-NH*t*Bu obtained from the reaction of Ph_2SiH_2 and *t*BuNH_2.

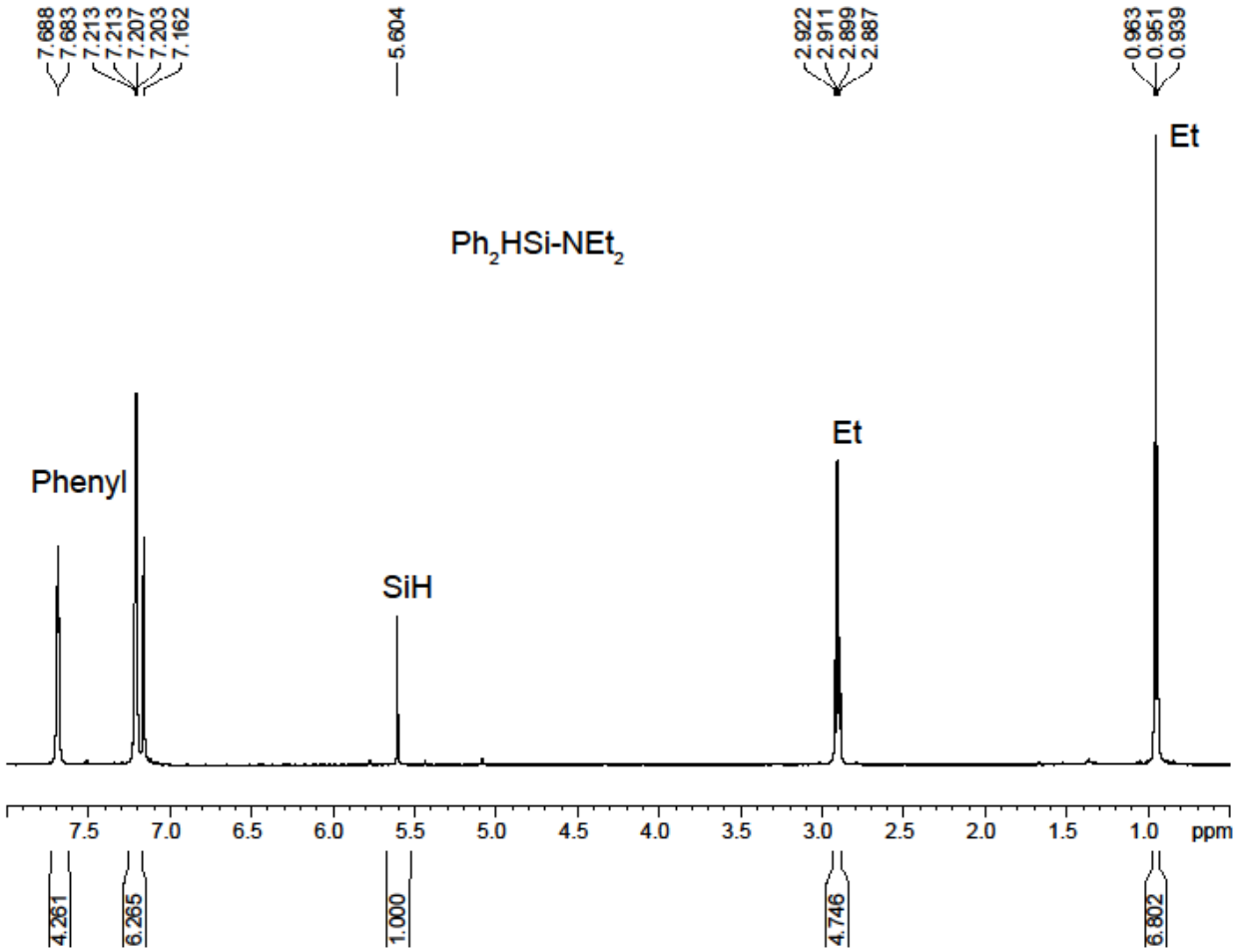

Figure S30. ^{1}H NMR spectrum (600 MHz, benzene-d_6) of $Ph_2HSi\text{-}NEt_2$ obtained from the reaction of Ph_2SiH_2 and Et_2NH.

Kinetic measurements for catalytic reaction between Ph_2SiH_2 and Et_2NH at different concentration of catalyst, 4a in benzene-d_6 at 298 K

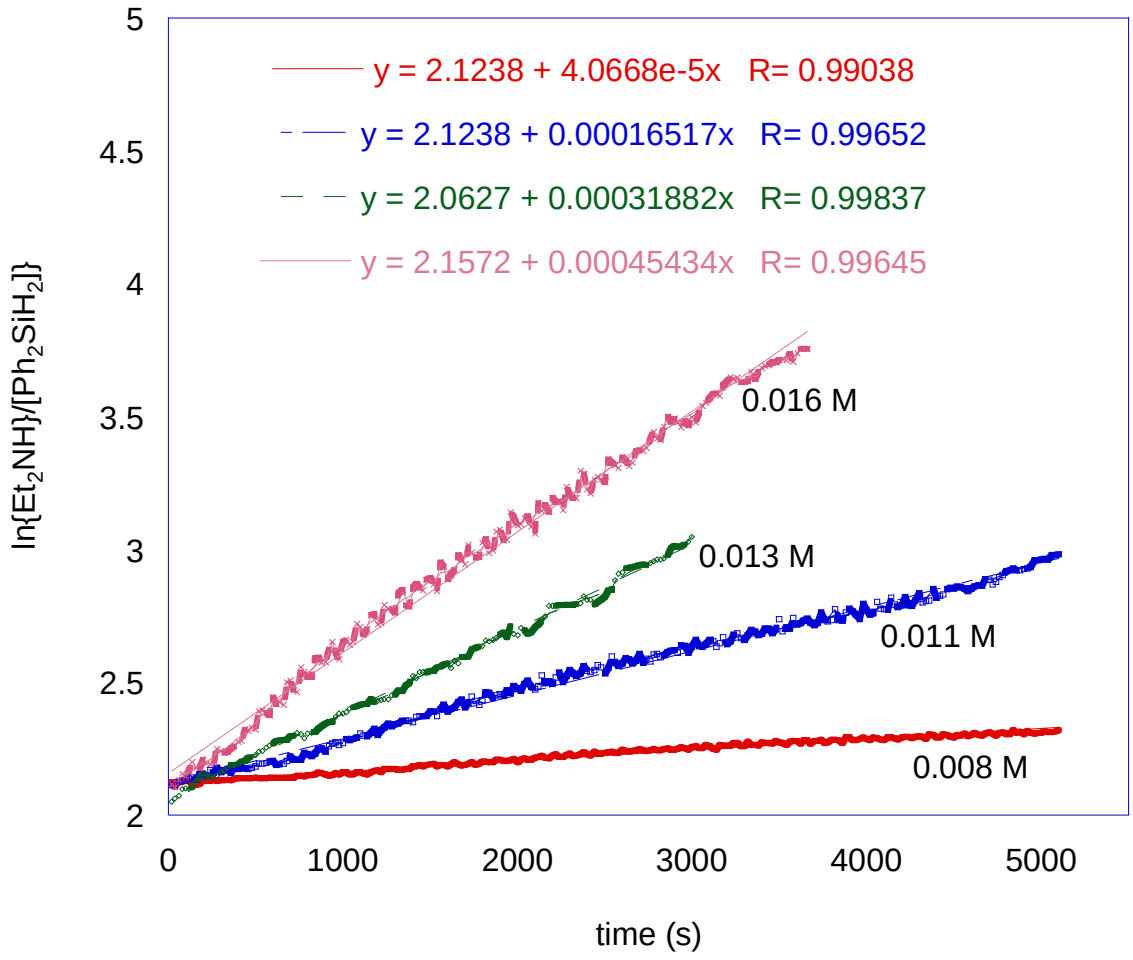

Figure S31. Second-order plot of ln{[Et_2NH]/[Ph_2SiH_2]} versus time for varying concentrations of **4a**.

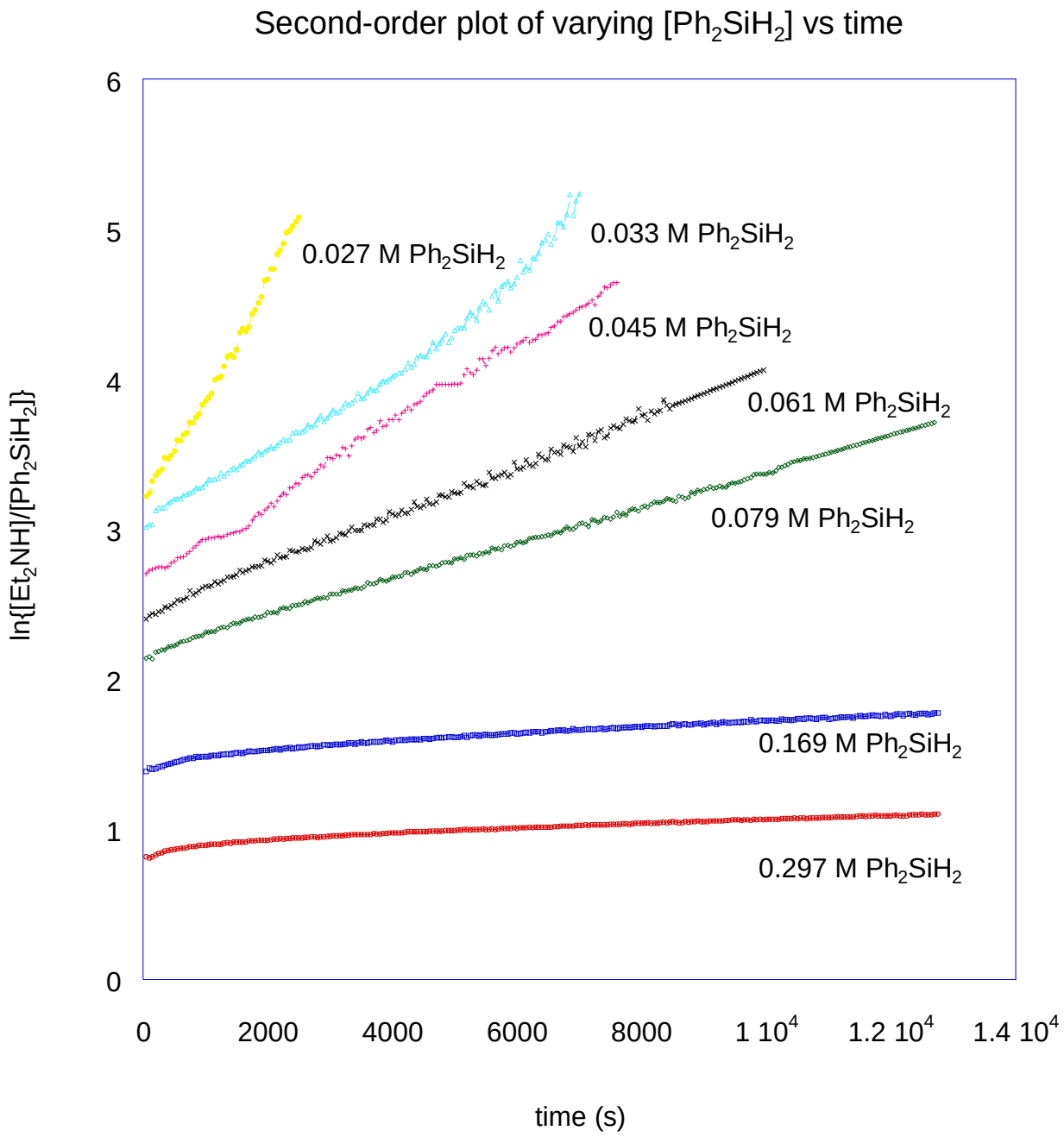

Figure S32. Second-order plot of ln{[Et_2NH]/[Ph_2SiH_2]} versus time for varying concentrations of Ph_2SiH_2.

CHAPTER 5: SYNTHESIS, CHARACTERIZATION AND REACTIVITY OF NEUTRAL YTTERBIUM(II) AND YTTRIUM(III) SILYL COMPLEXES

Modified from a paper to be submitted to a journal

Aradhana Pindwal, Arkady Ellern, Dr. Aaron D. Sadow*

Abstract

The potassium silyl ligand featuring β-SiH groups has been synthesized by reaction of $Si(SiHMe_2)_4$ and KO*t*Bu. Rare earth metal silyl compounds, $Yb\{Si(SiHMe_2)_3\}_2THF_3$ (**1a**) and $Cl_3Y\{Si(SiHMe_2)_3\}_2(Et_2O)].2K(Et_2O)_2$ (**1b**) are synthesized through salt metathesis reactions of the anhydrous lanthanide halide (YbI_2 and YCl_3) and two or three equiv. of $KSi(SiHMe_2)_3$. Compound **1a** is a five coordinate ytterbium center with two silyl ligands, containing β Si-H and three THF molecules while compound **1b** is a potassium salt of yttrium(III) containing two silyl ligands and three chloride group along with ether coordination. These compounds have been isolated and characterized by single crystal X-ray diffraction, NMR and IR spectroscopies and elemental analysis. Such studies reveal absence of non-classical interactions within the molecule, which are observed in the alkyl analogues of **1a**, $Yb\{C(SiHMe_2)_3\}_2THF_2$. Alternatively, the reaction of **1a** and one equiv. of ancillary ligand such as $TlTo^M$ resulted in the formation of $To^M{}_2Yb$, **2a**.

Introduction

The chemistry of transition metal alkyls and silyls compounds has been explored extensively,[1] with much of this work being directed towards better understanding of the reactivity of M-C and M-Si bonds and their comparisons.[2] Such compounds have been employed as catalysts for processes such as, polymerization of olefins,[3] hydrosilylation.[4] Although, chemistry of rare earth metal alkyls ($-CH_2SiMe_3$,[5] $-CH(SiMe_3)_2$,[6] and $-CH_2C_6R_5$)[7] and amides ($-N(SiMe_3)_2$,[8] $-N(SiHMe_2)_2$ and $-N(t\text{Bu}(SiHMe_2))$[9] have been developed extensively, rare earth silyl chemistry has remained under-developed and restricted to $-Si(SiMe_3)_3$ ligand.[10]

Recently, Piers *et. al*.[11] and Baumgartner *et. al*.[12] have demonstrated the synthesis and reactivity of heteroleptic rare earth silyl compounds containing $-Si(SiMe_3)_3$ ligand. Several homoleptic rare earth alkyls[6, 13] and amides[9c, 14] have been synthesized previously but very few homoleptic rare earth silyl compounds are known to date.[15] The chemistry explored thus, far for ligands containing β-SiH groups is limited to the silazide thus, urging us to extend the study to silyl ligands containing β-SiH. Previously, our group has demonstrated synthesis and reactivity of homoleptic rare earth alkyl compounds, $Yb\{C(SiHMe_2)_3\}_2THF_2$[16] and $Y\{C(SiHMe_2)_3\}_3$[17] containing β-SiH. These complexes contain non-classical β Si-H-Ln interactions, but they do not undergo β-H elimination upon thermolysis to 100 °C.

We were, therefore, interested in comparing the synthesis and reactivity of rare earth alkyl compounds with silyl compounds containing β-SiH. Use of these compounds as catalysts or precursors in organometallic chemistry could stem from the fundamental studies aimed at developing the synthesis and exploring the Ln-Si linkages. In this work, we report the synthesis

and characterization of divalent and trivalent rare earth silyl compounds containing β-SiH (Ln = Yb(II) and Y(III)). This presents the first example of such compounds reported thus far. Reaction of bis(silyl) ytterbium(II) compound with ancillary ligand, $TlTo^{M}$ indicates lability of these ligands.

Results and Discussion

Synthesis of $Yb\{Si(SiHMe_2)_3\}_2THF_3$ and $[Cl_3Y\{Si(SiHMe_2)_3\}_2(Et_2O)].2K(Et_2O)_2$. The synthesis and characterization of novel precursor to the synthesis of rare earth silyl compounds, $KSi(SiHMe_2)_3$ has been previously reported. THF ligated homoleptic ytterbium silyl compound, $Yb\{Si(SiHMe_2)_3\}_2THF_3$ (**1a**) is synthesized by a salt metathesis reaction of YbI_2 and two equiv. of $KSi(SiHMe_2)_3$ in THF for one day at room temperature. The crude $Yb\{Si(SiHMe_2)_3\}_2THF_3$ is extracted and recrystallized from pentane at –40 °C to obtain orange needle-like crystals in moderate yield.

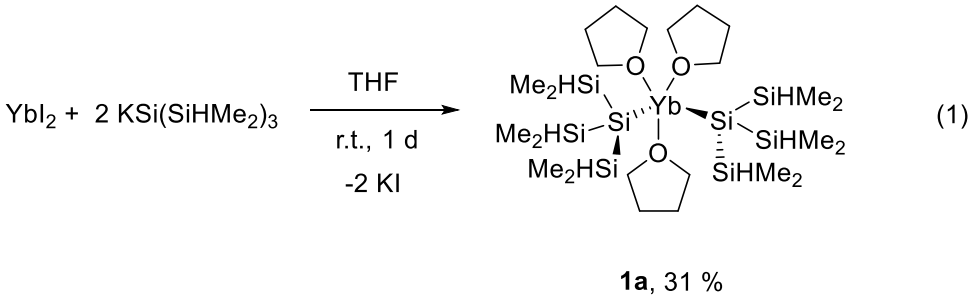

(1)

1a, 31 %

The ^{1}H NMR for **1a** in benzene-d_6 at 25 °C contained a multiplet for six β- SiH at 4.63 ppm ($^{1}J_{SiH}$ = 160 Hz), a doublet at 0.61 ppm for $SiMe_2$ ($^{3}J_{HH}$ = 4.0 Hz) and two THF resonances at 3.73 and 1.42 ppm. For comparison, the SiH resonance in the alkyl analogue of ytterbium(II), $Yb\{C(SiHMe_2)_3\}_2THF_2$[16] was observed at 4.78 ppm ($^{1}J_{SiH}$ = 160 Hz). The $SiHMe_2$ groups, in the silyl ligand as well as in the alkyl ligand, remained equivalent as a result of rapid exchange

on ^{1}H NMR time scale, even at low temperatures (190 K in toluene-d_8). ^{1}H-^{29}Si HMBC experiment showed two cross-peaks at δ –23.6 and –168.1 ppm with $SiMe_2$ resonance at 0.61 ppm for $Si(\mathit{Si}HMe_2)_3$ and $\mathit{Si}(SiHMe_2)_3$, respectively. For comparison, ^{29}Si resonances for $\mathit{Si}(SiHMe_2)_3$ in alkaline earth metal silyl compounds, $Ca\{Si(SiHMe_2)_3\}_2THF_3$ and $Mg\{Si(SiHMe_2)_3\}_2THF_2$, are observed at δ –194 and –184, respectively (unpublished results). These resonances are more upfield than **1a** suggesting Yb is more electronegative than Ca or Mg. On comparing the ^{29}Si resonances with $Yb\{C(SiHMe_2)_3\}_2(THF)_2$, it is upfield at δ –19.5 which is in agreement with C being more electronegative than Si. In Lawless *et al* compound, $Cp^*YbSi(SiMe_3)_3$ ^{29}Si resonance is observed at δ –158 for $\mathit{Si}(SiMe_3)_3$ compared to δ –168.1 for $\mathit{Si}(SiHMe_2)_3$ and $Si(\mathit{Si}Me_3)$ appears at δ –2.9 while $Si(\mathit{Si}HMe_2)_3$ appears at δ –23.6.

Compound **1a** crystallizes in a monoclinic P $2_1/c$ space group with a trigonal bipyramidal geometry around Yb center. The two $Si(SiHMe_2)_3$ groups and one THF molecule occupy the equatorial positions and the other two THF molecules occupy the axial positions. The Yb-Si distances can be categorized as long (~4 Å), intermediate (3.4-3.5 Å), and short (3.14-3.19 Å). The Yb-Si distances in **1a** are 3.020(2) (Yb1-Si1) and 3.012(2) Å (Yb1-Si5) which are consistent with the literature values. For comparison, the Yb-Si distance in $Cp^*YbSi(SiMe_3)_3$ is 3.032(2) Å[10c] while in $Yb\{Si(SiMe_3)_3\}_2THF_3$, it is 3.064(6) Å.[15] The Si1-Yb1-Si5 angle of 129.68(6)° suggests a bent structure around Si1-Yb1-Si5 which is apparent for small sized ytterbium(II) center (6-coordinate Yb^{+2} = 1.02 Å)[18] surrounded by two bulky $Si(SiHMe_2)_3$ groups and three coordinating THF molecules. Unlike $Yb\{C(SiHMe_2)_3\}_2THF_2$ where the SiH groups in the ligand point towards the metal center, thereby exhibiting non-classical interactions, in **1a**, all the SiH groups in $–Si(SiHMe_2)_3$ ligand are oriented such that the hydrogen and methyl groups are directed away from the Yb(II) center. The hydrogen atoms bonded to silicon were located

objectively in the difference Fourier map; the positions of the $SiMe_2$ atoms and the electron density map provide a reasonable estimate of the hydrogen position, subject to the normal limitations associated with X-ray diffraction. The geometry around each Si atom directly bonded to Yb(II) center is distorted tetrahedral with two obtuse angles (120.54(1)°, 111.06(1)°) and two intermediate angles (99.77(2)°, 100.00(2)°). The greater torsion angle for Yb-Si-Si-H at 55.68° suggests absence of non-classical interactions which is also evident from the long Yb-H distances (Yb1-H2s, 5.9(1) Å; Yb1-H3s, 6.01(7) Å; Yb-H4s, 4.55(6) Å) in one ligand.

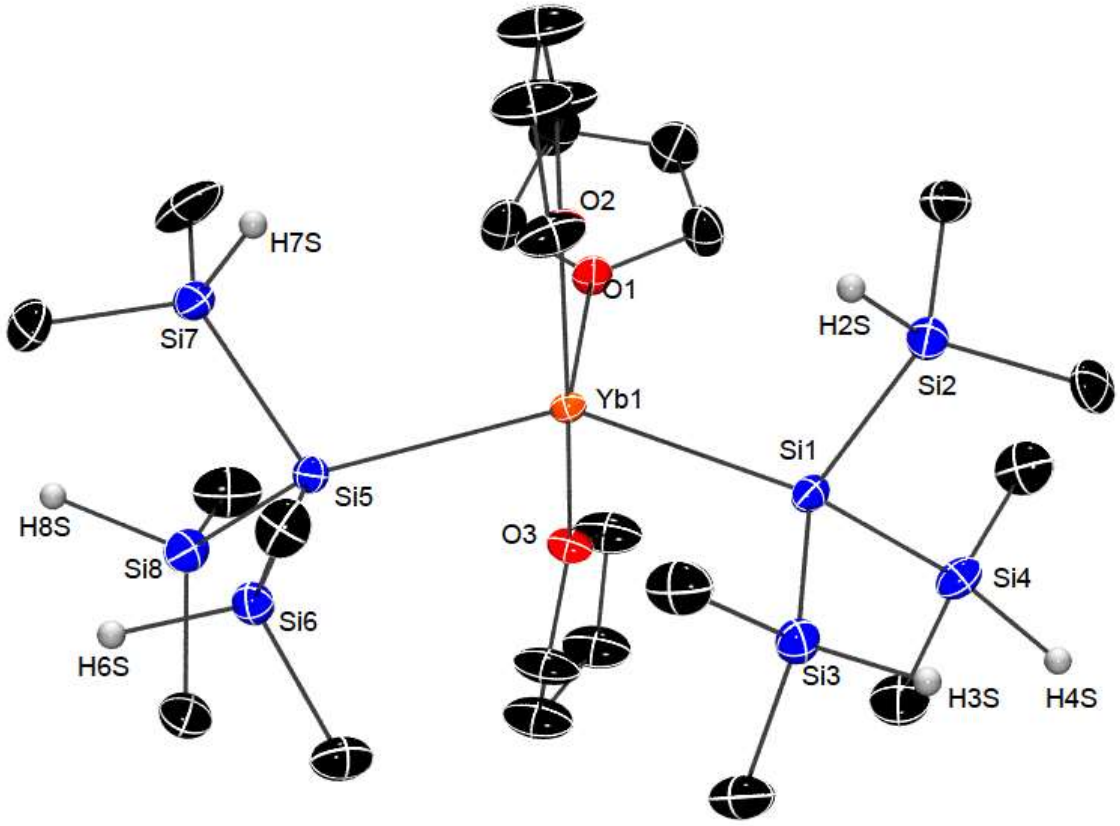

Figure 1. Rendered thermal ellipsoid plot of $Yb\{Si(SiHMe_2)_3\}_2THF_3$ (**1a**). Ellipsoids are plotted at 35% probability. Hydrogen atoms bonded to silicon were located objectively in the Fourier difference map and are included in the representation. All other H atoms are not plotted for

clarity. Significant interatomic distances (Å): Yb1-Si1, 3.020(2); Yb1-Si5, 3.011(2); Yb1-H2s, 5.9(1); Yb1-H3s, 6.01(7); Yb1-H4s, 4.55(6). Significant interatomic angles (°): Si5-Yb1-Si1, 129.69(6); O1-Yb1-Si1, 92.70(1); O2-Yb1-O1, 82.44(2); O2-Yb1-Si5, 112.25(1); O3-Yb1- Si5, 94.31(1).

After synthesis of divalent bis(silyl)ytterbium compound we wanted to extend the study to trivalent rare earth metals and synthesize lanthanide(III) silyl compounds containing β-SiH groups in the ligand. Thus, a series of trivalent lanthanide iodides, such as Y, La, Ce, Pr, Nd and Lu were reacted with 3 equiv. of $KSi(SiHMe_2)_3$ in THF or benzene at room temperature. However, after repeated unsuccessful attempts in synthesizing such compounds at room temperature, it was learnt that these compounds could be synthesized at –78 °C. The reaction of anhydrous YCl_3 and 3 equiv. of $KSi(SiHMe_2)_3$ in ether at –78 °C for 8 h yielded $[Cl_3Y\{Si(SiHMe_2)_3\}_2(Et_2O)].2K(Et_2O)_2$ (**1b**) as a potassium salt, which is the first example of yttrium(III) silyl compound reported in literature. In addition, these compounds are highly temperature sensitive and decomposes in solution at room temperature to several unidentified silyl containing species in the ^{1}H NMR.

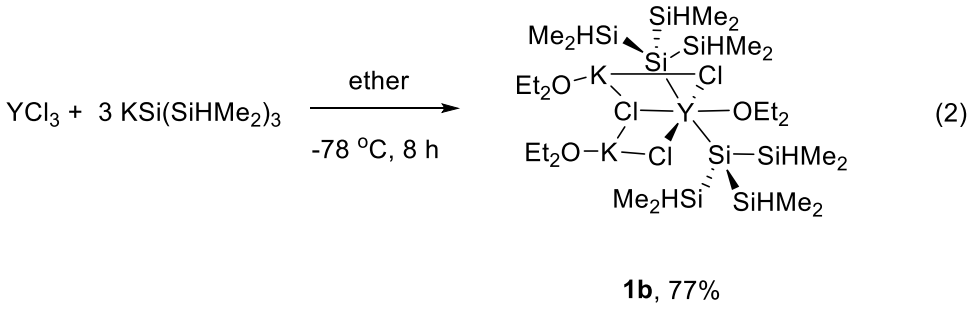

(2)

1b, 77%

Since compound **1b** decomposes at room temperature, the NMR spectroscopy was recorded at 200 K in toluene-d_8. ^{1}H NMR contained a broad resonance at 4.34 ppm assigned to SiH (6 H, $^1J_{SiH}$ = 160 Hz) and another broad resonance at 0.77 ppm assigned to the $SiMe_2$ group

(36 H, $^{3}J_{HH}$ = 4.0 Hz). ^{1}H-^{29}Si HMBC experiment in toluene-d_8 at 200 K contained cross peaks at δ –9.1 and –141.6 ppm for Si(*Si*HMe$_2$)$_3$ and *Si*(SiHMe$_2$)$_3$, respectively which are shifted downfield compared to **1a**. Similar to compound **1a**, IR spectroscopy of **1b** contained only one stretching band at 1999 cm^{-1} thereby indicating absence of non-classical interactions in the molecule. Single crystal X-ray diffraction study of **1b** supports the fact that the molecule lacks non-classical interactions. ORTEP structure of **1b** is shown in Figure 2.

Compound **1b** crystallizes in a monoclinic P 2$_1$/n space group adopting an octahedral geometry around Y center. The two Si(SiHMe$_2$)$_3$ groups occupy the axial positions while one diethyl ether molecule and three Cl atoms occupy the square planar positions. The Si1-Y1-Si5 angle of 171.99^{o} suggests linearity around the atoms. Although the ionic radii of Y(III) is smaller than that of Yb(II) (6-coordinate Yb^{+2} = 1.02 and 6-coordinate Y^{+3} = 0.9 Å)[18] the Ln-Si distances are comparable. The Y-Si distances in **1b** are Y1-Si1, 3.039(1) and Y1-Si5, 3.031(1) Å while in **1a** the Yb-Si distances are Yb1-Si1, 3.020(2) and Yb1-Si5, 3.012(2) Å which are similar. Similar to **1a**, each (SiHMe$_2$)$_3$ groups in the Si(SiHMe$_2$)$_3$ ligand are oriented with hydrogen and methyl groups directed away from the Y center. The hydrogen atoms bonded to silicon were located objectively in the difference Fourier map; the positions of the SiMe$_2$ atoms and the electron density map provide a reasonable estimate of the hydrogen position, subject to the normal limitations associated with X-ray diffraction. The geometry around each Si atom directly bonded to Y is distorted tetrahedral with two obtuse angles (111.21(5)^{o}, 110.69(5)^{o}) and two intermediate angles (101.61(7)^{o}, 96.60(7)^{o}).

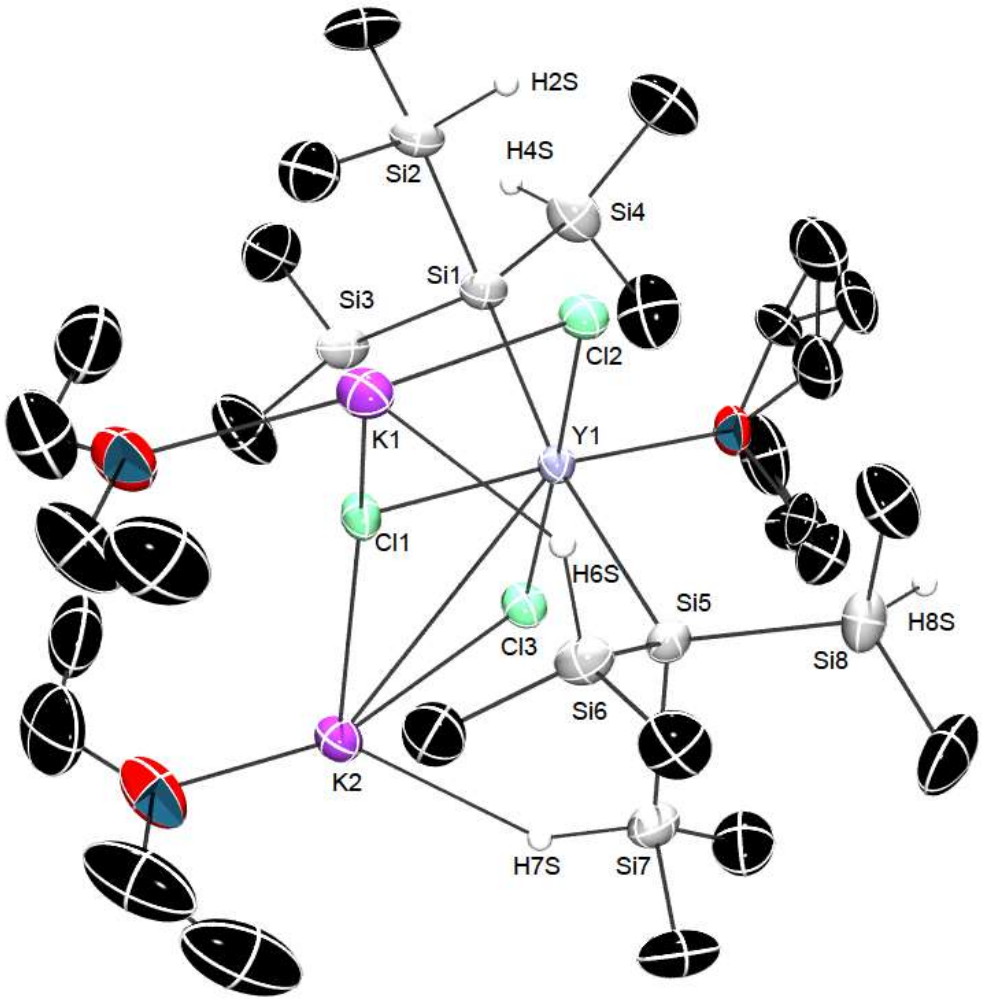

Figure 2. Rendered thermal ellipsoid plot of $[Cl_3Y\{Si(SiHMe_2)_3\}_2(Et_2O)].2K(Et_2O)$ (**1b**). Ellipsoids are plotted at 35% probability. Hydrogen atoms bonded to silicon were located objectively in the Fourier difference map and are included in the representation. All other H atoms are not plotted for clarity. Significant interatomic distances (Å): Y1-Si1, 3.039(1); Y1-Si5, 3.031(1). Significant interatomic angles (°): Si5-Y1-Si1, 171.99(4); Si1-Y1-Cl1, 98.13(4); Cl1-Y1-Si5, 89.74(4).

Reactivity of $Yb\{Si(SiHMe_2)_3\}_2THF_3$. The stoichiometric reaction of **1a** and one equiv. of $TlTo^M$ in benzene at room temperature for 1 day resulted in the formation of THF free, $To^M{}_2Yb$

(**2a**) in good yield (eq. 3). The crude was recrystallized from toluene at –78 °C to obtain red plate-like crystals of **2a**. The formation of **2a** over $To^{M}Yb\{Si(SiHMe_2)_3\}$ suggests that the $Si(SiHMe_2)_3$ groups are very labile and can be cleaved easily.

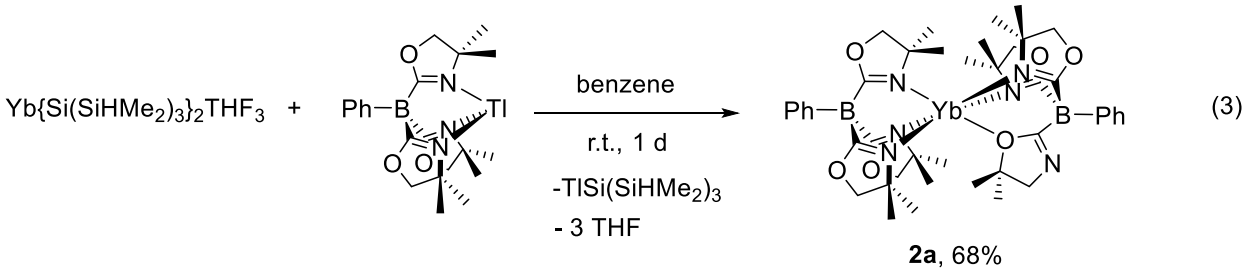

2a, 68% (3)

^{1}H NMR of **2a** acquired in benzene-d_6 at room temperature contained a singlet resonances at 1.14 ppm (36 H) assigned to the oxazolinyl methyl and another singlet at 3.40 ppm assigned to the oxazolinyl methylene group. The singlet resonances for oxazolinyl group suggests the presence of mirror plane of symmetry within the molecule. The ^{11}B NMR contained a resonance at –17.9 ppm which is shifted upfield from the starting material, $TlTo^{M}$.[19] IR spectroscopy studies showed a strong band for C-N stretching frequency at 1572 cm^{-1} suggesting all C-N bonds are equivalent and coordinated to the metal center. The spectroscopic assignments were further confirmed by single crystal X-ray diffraction data.

Compound **2a** crystallizes as monoclinic with P 2_1/c space group having distorted octahedral geometry around Yb center. The structure is κ^3 coordinated through nitrogens on the oxazoline in one To^{M} ligand and two nitrogens and one oxygen of the oxazoline in the other To^{M} ligand making Yb(II) complex 6-coordinated. This observation of coordination of oxazolinyl group through oxygen rather than nitrogen has not been made yet. The Yb-N distances are at an average of 2.513(3) Å while the Yb1-O1 distance is shorter at 2.456(2) Å. The six-coordinate Yb(II) compound adopts a distorted octahedral geometry with an average bond angle around Yb center to be 88.63^{o}.

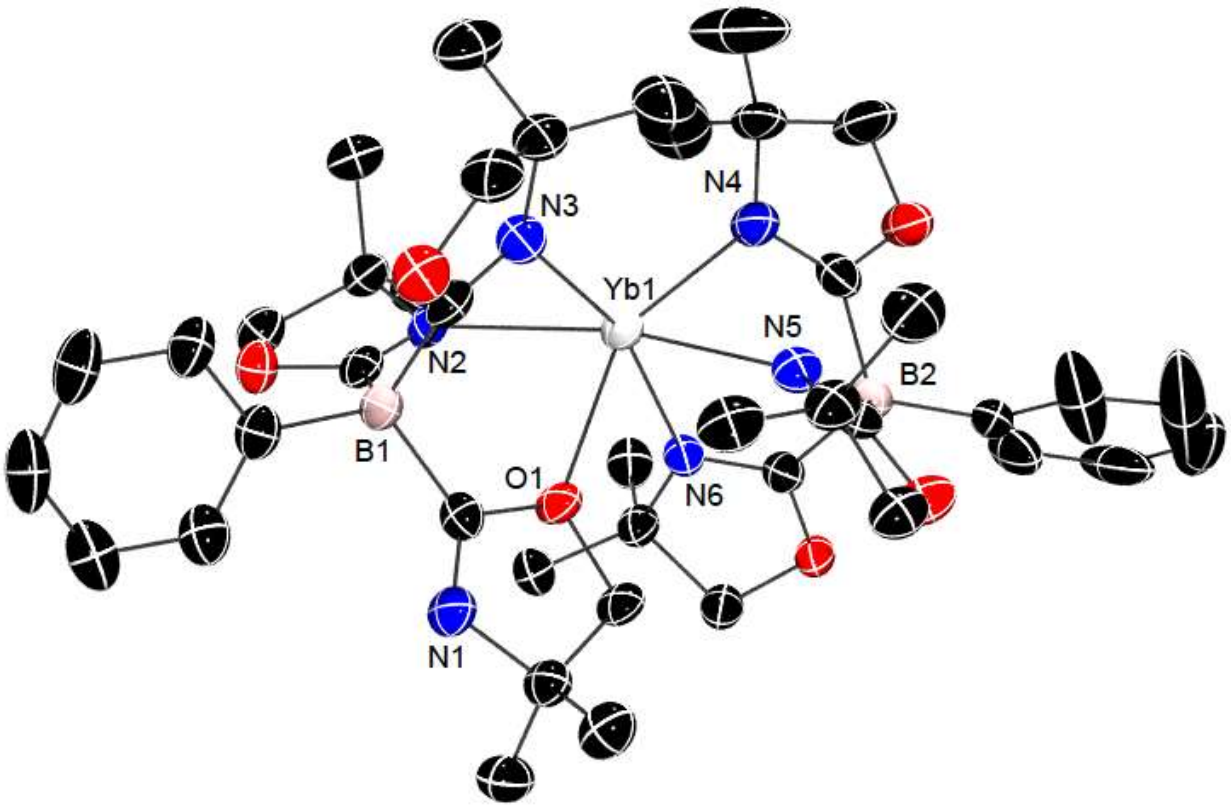

Figure 3. Rendered thermal ellipsoid plot of $To^{M}_{2}Yb$ (**2a**). Ellipsoids are plotted at 35% probability. Hydrogen atoms bonded to silicon were located objectively in the Fourier difference map and are included in the representation. All other H atoms are not plotted for clarity. Significant interatomic distances (Å): Yb1-O1, 2.456(2); Yb1-N2, 2.500(3); Yb1-N3, 2.499(3); Yb1-N4, 2.553(3); Yb1-N6, 2.574(3). Significant interatomic angles (°): O1-Yb1-N2, 85.56(9); N2-Yb1-N6, 94.10(1); N6-Yb1-N5, 78.07(10; N5-Yb1-N4, 78.04(1); N4-Yb1-N3, 97.76(9); O1-Yb1-N3, 98.13(4).

Table 1. Crystallographic Data for compounds 1a, 1b, and 2a.

	1a	**1b**	**2a**
Chemical Formula	$C_{24}H_{66}O_3Si_8Yb$	$C_{26}H_{71}Cl_3K_2O_{3.50}Si_8Y$	$C_{52.50}H_{70}B_2N_6O_6Yb$
Formula Weight	800.53	938.00	1075.81
Crystal System	Monoclinic	monoclinic	Monoclinic
Unit-cell dimensions	a = 13.703(6) Å b = 17.773(7) Å c = 20.932(6) Å α = γ = 90° β = 123.944(19)°	a = 16.020(2) Å b = 21.258(3) Å c = 16.114(2) Å α = γ = 90°; β = 101.253(2)°	a = 19.2786 (16) Å b = 15.5825(13) Å c = 17.9909(15) Å α = γ = 90°; β = 94.2590(10)°
Volume	4229.0(3) Å^3	5382.2(12) Å^3	5389.7(8) Å^3
Space Group	P 1 21/c 1	P 1 21/n 1	P 1 21/c 1
Z	4	4	4
Reflections collected	30722	43291	48058
Independent reflections	7126	9150	11007
R_{int}	0.1044	0.0937	0.0619
R $I>2\sigma(I)$	R_1 = 0.0441 wR_2 = 0.0963	R_1 = 0.0432 wR_2 = 0.1205	R_1 = 0.0353 wR_2 = 0.0808
R_{all}	R_1 = 0.0836 wR_2 = 0.1123	R_1 = 0.0748 wR_2 = 0.1512	R_1 = 0.0509 wR_2 = 0.0858

Conclusion

In conclusion, we have demonstrated the synthesis and characterization of rare earth silyl compounds containing β-SiH which are first of its kinds to be reported in literature. These compounds do not exhibit any non-classical interactions with the metal center as opposed to its alkyl analogue, $Yb\{C(SiHMe_2)_3\}_2THF_2$. This observation could be attributed to longer Yb-Si distances in the molecule. Reaction with $TlTo^M$ indicate the lability of the silyl ligand, thus, limits the scope of synthesis of rare earth silyl compounds.

Experimental Section

All manipulations were performed under a dry argon atmosphere using standard Schlenk techniques or under a nitrogen atmosphere in a glovebox unless otherwise indicated. Water and oxygen were removed from benzene and pentane solvents using an IT PureSolv system. Benzene-d_6 was heated to reflux over Na/K alloy and vacuum-transferred. All reactions were carried out in silylated and flame-dried glassware under an inert atmosphere of dry argon. Starting materials tetrakis(trimethylsilyl)silane,[20] tris(trimethylsilyl)silylpotassium,[21] YbI_2,[22] $TlTo^M$[19] were prepared according to literature procedures. KO^tBu was sublimed prior to use. Trimethylsilyl chloride was distilled before use. ^1H, ^{11}B, $^{13}C\{^1H\}$, and ^{29}Si HMBC NMR spectra were collected on a Bruker DRX-400 spectrometer, a Bruker Avance III-600 spectrometer, or an Agilent MR 400 spectrometer. ^{11}B NMR spectra were referenced to an external sample of $BF_3{\cdot}Et_2O$. ^{15}N chemical shifts were originally referenced to liquid NH_3 and recalculated to the

CH_3NO_2 chemical shift scale by adding –381.9 ppm. Infrared spectra were measured on a Bruker Vertex 80. Elemental analyses were performed using a Perkin-Elmer 2400 Series II CHN/S. X-ray diffraction data was collected on a Bruker APEX II diffractometer.

$KSi(SiHMe_2)_3$. KO^tBu (0.085 g, 0.755 mmol) was added to a benzene (5 mL) solution of $Si(SiHMe_2)_4$ (0.200 g, 0.76 mmol) at room temperature to yield a pale yellow solution. The solution was allowed to stir for 1 h at room temperature. The solvent was evaporated to dryness under reduced pressure and the residue washed with pentane (3 × 5 mL) to give an off-white solid of $KSi(SiHMe_2)_3$ (0.096 g, 0.39 mmol, 51.7%). ^{1}H NMR (benzene-d_6, 600 MHz, 25 °C): δ 4.32 (m, 6 H, $^1J_{SiH}$ = 150 Hz, Si*H*Me_2), 0.60 (d, 36 H, $^3J_{HH}$ = 4.2 Hz, Si*Me*$_2$). ^{13}C{^{1}H} NMR (benzene-d_6, 150 MHz, 25 °C): δ 2.52 ($SiMe_2$). ^{1}H-^{29}Si NMR (benzene-d_6, 119 MHz, 25 °C): δ –23.7 ($SiHMe_2$), –201.2 (*Si*$(SiHMe_2)$. IR (KBr, cm^{-1}): 2943 s, 2887 s, 2015 w (ν_{SiH}), 1416 s, 1242 s, 1002 w, 878 w, 835 w, 755 s, 693 s, 646 s. Anal. Calcd for $C_6H_{21}KSi_4$: C, 29.45; H, 8.65. Found: C, 29.20; H, 8.51. Mp, 132-135 °C.

$Yb\{Si(SiHMe_2)_3\}_2THF_3$ (1a). $KSi(SiHMe_2)_3$ (0.573 g, 2.34 mmol) and YbI_2 (0.500 g, 1.17 mmol) were stirred in 10 mL of THF at room temperature for 24 h The resulting reddish orange suspension was evaporated to dryness under reduced pressure and extracted with pentane (3 × 5 mL). The reddish orange solution was concentrated and recrystallized overnight at –40 °C to obtain reddish orange crystals of $Yb\{Si(SiHMe_2)_3\}_2THF_3$ (0.29 g, 0.36 mmol, 30.9%). ^{1}H NMR (benzene-d_6, 600 MHz, 25 °C): δ 4.63 (m, 6 H, $^1J_{SiH}$ = 160 Hz, Si*H*Me_2), 3.73 (m, 12 H, OCH_2), 1.42 (m, 12 H, CH_2), 0.61 (d, 36 H, $^3J_{HH}$ = 4.0 Hz, $SiMe_2$). ^{13}C{^{1}H} NMR (benzene-d_6, 150

MHz, 25 °C): δ 69.24 (OCH_2CH_2), 25.71 (OCH_2CH_2), 1.88 ($SiMe_2$). $^{29}Si\{^1H\}$ NMR (benzene-d_6, 119 MHz, 25 °C): δ –23.99 ($SiHMe_2$), –168.11 *Si*($SiHMe_2$). IR (KBr, cm^{-1}): 2953 s, 2891 s, 2045 w (ν_{SiH}), 1460 w, 1243 s, 1031 s, 858 w, 680 s, 643 s. Anal. Calcd for $C_{24}H_{66}O_3Si_8Yb$: C, 36.01; H, 8.31. Found: C, 36.83; H, 8.40. Mp, 80 °C, dec.

$[Cl_3Y\{Si(SiHMe_2)_3\}_2(Et_2O)].2K(Et_2O)$ (1b). $KSi(SiHMe_2)_3$ (0.830 g, 3.39 mmol) and YCl_3 (0.22 g, 1.13 mmol) were stirred in 10 mL of ether at –78 °C for 8 h. The resulting pale yellow suspension was filtered and evaporated to dryness under reduced pressure at –78 °C to obtain off-white color, spectroscopically pure **1b**. The compound was crystallized at –40 °C to obtain colorless crystals of $[Cl_3Y\{Si(SiHMe_2)_3\}_2(Et_2O)].2K(Et_2O)$ (0.812 g, 1.06 mmol, 76.6%). ^1H NMR (toluene-d_8, 600 MHz, –80 °C): δ 4.34 (br, 6 H, $^1J_{SiH}$ = 160 Hz, Si*H*Me_2), 3.07 (br, 8 H, OCH_2), 1.10 (br, 24 H, CH_3), 0.77 (br, 36 H, $^3J_{HH}$ = 4.0 Hz, $SiMe_2$). $^{13}C\{^1H\}$ NMR (toluene-d_8, 150 MHz, –80 °C): δ 66.3 (OCH_2CH_3), 16.03 (OCH_2CH_3), 2.89 ($SiMe_2$). $^{29}Si\{^1H\}$ NMR (toluene-d_8, 119 MHz, –80 °C): δ –9.1 ($SiHMe_2$), –141.6 *Si*($SiHMe_2$). IR (KBr, cm^{-1}): 2954 s, 2894 s, 1999 s br (ν_{SiH}), 1462 w, 1419 w, 1365 w, 1244 s, 1201 s, 1023 w br, 862 s, 827 s, 683 s, 645 s.

To^M_2Yb (2a): $Yb\{Si(SiHMe_2)_3\}_2THF_3$ (0.117 g, 0.017 mmol) and $TlTo^M$ (0.197 g, 0.034 mmol) were stirred in 5 mL of benzene at room temperature for 24 h. The resulting reddish solution was filtred and evaporated to dryness under reduced pressure and extracted with benzene (2 × 5 mL). The red solution was crystallized overnight at –40 °C from toluene to obtain red crystals of To^M_2Yb (0.123 g, 0.011 mmol, 68.0%). ^1H NMR (benzene-d_6, 600 MHz, 25 °C): δ 8.35 (d, 4 H,

o-C_6H_5), 7.58 (t, 4 H, *m*-C_6H_5), 7.37 (t, 2 H, *p*-C_6H_5), 3.40 (br, 12 H, $CNCMe_2CH_2O$), 1.14 (br, 36 H, $CNCMe_2CH_2O$). ^{11}B NMR (benzene-d_6, 192 MHz, 25 °C): δ –17.9 (s). $^{13}C\{^1H\}$ NMR (benzene-d_6, 150 MHz, 25 °C): δ 135.24 (*o*-C_6H_5), 127.94 (*m*-C_6H_5), 126.96 (*p*-C_6H_5), 78.14 ($CNCMe_2CH_2O$), 67.74 ($CNCMe_2CH_2O$), 28.48 ($CNCMe_2CH_2O$). IR (KBr, cm^{-1}): 2963 s, 2899 s, 1572 (s ν_{CN}), 1463 s, 1433 s, 1387 w, 1367 s, 1252 s, 1194 s, 1176 m, 1151 m, 1085 w, 995 s, 973 s, 896 s, 837 s, 796 m, 745 m, 702 s, 668 w, 636 m. Anal. Calcd for $C_{42}H_{58}B_2N_6O_6Yb$: C, 53.80; H, 6.24; N, 8.96. Found: C, 53.56; H, 6.18; N, 8.72. Mp, 102 °C, dec.

References

[1] a) H. G. Woo and T. D. Tilley, *Journal of the American Chemical Society* **1989**, *111*, 3757-3758; b) U. Schubert, *Transition Metal Chemistry* **1991**, *16*, 136-144; c) H. G. Woo, R. H. Heyn and T. D. Tilley, *Journal of the American Chemical Society* **1992**, *114*, 5698-5707; d) C. Kayser, D. Frank, J. Baumgartner and C. Marschner, *Journal of Organometallic Chemistry* **2003**, *667*, 149-153; e) M. Zirngast, U. Florke, J. Baumgartner and C. Marschner, *Chem Commun (Camb)* **2009**, 5538-5540.

[2] a) P. Braunstein and M. Knorr, *Journal of Organometallic Chemistry* **1995**, *500*, 21-38; b) V. K. Dioumaev, P. J. Carroll and D. H. Berry, *Angewandte Chemie-International Edition* **2003**, *42*, 3947-3949.

[3] J. Rohrmann and W. A. Herrmann in *Process for the preparation of a chiral stereorigid metallocene, Vol.* Google Patents, **1992**.

[4] a) G. Meurant, *ADVANCES ORGANOMETALLIC CHEMISTRY*, Elsevier Science, **1973**, p; b) T. D. Tilley in *Transition-Metal Silyl Derivatives*, John Wiley & Sons, Ltd, **2004**, pp. 1415-1477.

[5] a) M. F. Lappert and R. Pearce, *Journal of the Chemical Society-Chemical Communications* **1973**, 126-126; b) J. L. Atwood, W. E. Hunter, R. D. Rogers, J. Holton, J. Mcmeeking, R. Pearce and M. F. Lappert, *Journal of the Chemical Society-Chemical Communications* **1978**, 140-142; c) H. Schumann, D. M. M. Freckmann and S. Dechert, *Zeitschrift Fur Anorganische Und Allgemeine Chemie* **2002**, *628*, 2422-2426.

[6] P. B. Hitchcock, M. F. Lappert, R. G. Smith, R. A. Bartlett and P. P. Power, *Journal of the Chemical Society-Chemical Communications* **1988**, 1007-1009.

[7] a) S. Bambirra, A. Meetsma and B. Hessen, *Organometallics* **2006**, *25*, 3454-3462; b) S. Bambirra, D. van Leusen, C. G. J. Tazelaar, A. Meetsma and B. Hessen, *Organometallics* **2007**, *26*, 1014-1023; c) A. J. Wooles, D. P. Mills, W. Lewis, A. J. Blake and S. T. Liddle, *Dalton Transactions* **2010**, *39*, 500-510; d) W. Huang, B. M. Upton, S. I. Khan and P. L. Diaconescu, *Organometallics* **2013**, *32*, 1379-1386.

[8] a) D. C. Bradley, J. S. Ghotra and F. A. Hart, *Journal of the Chemical Society-Dalton Transactions* **1973**, 1021-1027; b) K. H. Denhaan, J. L. Deboer, J. H. Teuben, A. L. Spek, B. Kojicprodic, G. R. Hays and R. Huis, *Organometallics* **1986**, *5*, 1726-1733.

[9] a) W. S. Rees, O. Just, H. Schumann and R. Weimann, *Angewandte Chemie-International Edition in English* **1996**, *35*, 419-422; b) R. Anwander, O. Runte, J. Eppinger, G. Gerstberger, E. Herdtweck and M. Spiegler, *Journal of the Chemical Society-Dalton Transactions* **1998**, 847-858; c) A. R. Crozier, A. M. Bienfait, C. Maichle-Mossmer, K. W. Tornroos and R. Anwander,

Chem Commun (Camb) **2013**, *49*, 87-89; d) A. M. Bienfait, C. Schadle, C. Maichle-Mossmer, K. W. Tornroos and R. Anwander, *Dalton Trans* **2014**, *43*, 17324-17332.

[10] a) H. Schumann, *Journal of organometallic chemistry* **1990**, *390*, 301-308; b) N. S. Radu, T. D. Tilley and A. L. Rheingold, *Journal of the American Chemical Society* **1992**, *114*, 8293-8295; c) M. M. Corradi, A. D. Frankland, P. Hitchcock, M. F. Lappert and G. A. Lawless, *Chemical Communications* **1996**, 2323-2324; d) M. Niemeyer, *Inorganic Chemistry* **2006**, *45*, 9085-9095.

[11] M. J. Sgro and W. E. Piers, *Inorganica Chimica Acta* **2014**, *422*, 243-250.

[12] R. Zitz, H. Arp, J. Hlina, M. Walewska, C. Marschner, T. Szilvási, B. Blom and J. Baumgartner, *Inorganic Chemistry* **2015**, *54*, 3306-3315.

[13] C. Eaborn, P. B. Hitchcock, K. Izod and J. D. Smith, *Journal of the American Chemical Society* **1994**, *116*, 12071-12072.

[14] H. F. Yuen and T. J. Marks, *Organometallics* **2008**, *27*, 155-158.

[15] R. Zitz, J. Hlina, K. Gatterer, C. Marschner, T. Szilvási and J. Baumgartner, *Inorganic Chemistry* **2015**, *54*, 7065-7072.

[16] K. Yan, B. M. Upton, A. Ellern and A. D. Sadow, *Journal of the American Chemical Society* **2009**, *131*, 15110-15111.

[17] K. Yan, A. V. Pawlikowski, C. Ebert and A. D. Sadow, *Chem Commun (Camb)* **2009**, 656-658.

[18] R. D. Shannon, *Acta Crystallographica* **1976**, *A32*, 751-767.

[19] H. A. Ho, J. F. Dunne, A. Ellern and A. D. Sadow, *Organometallics* **2010**, *29*, 4105-4114.

[20] H. Gilman and C. L. Smith, *Journal of the American Chemical Society* **1964**, *86*, 1454-&.

[21] C. Marschner, *European Journal of Inorganic Chemistry* **1998**, 221-226.

[22] A. P. Ginsberg, *Inorganic Syntheses*, p. 147-148.

CHAPTER 6: CONCLUSION

General Conclusions

Rare-earth metals are found in abundance in earth's crust, however, they do not find much use in catalytic chemistry. There is a desperate need to find utilization of these metals in catalysis as they are readily available at low cost. The fundamental study and incorporation of these elements in organometallic reactions and catalysis has lagged behind transition metals and main group metals. The projects described in this thesis have probed new rare-earth metal complexes, incorporating novel ligands, and explored catalytic pathways that are common in transition metal chemistry, but relatively unexplored in lanthanide group metals chemistry.

In this thesis we have described the synthesis of a series of tris(alkyl)lanthanide complexes with multiple β-hydrogens containing $–C(SiHMe_2)_3$ ligand. These compounds show the presence of β-agostic or non-classical interactions with the metal center as observed by single crystal X-ray diffraction and IR spectroscopy. There is no sign of β-hydride elimination even at elevated temperature for these compounds that was often considered as the catalyst degradation pathway in other early metal alkyl complexes bearing β-hydrogen. To explore the reactivity at the nucleophilic β-SiH position reactions with Lewis acids such as, $B(C_6F_5)_3$ were carried out. This reaction allowed us to understand that the most nucleophilic site in the complexes is not the carbanic carbon, but the Si-H bond to form the H-abstracted byproduct, silene dimer $[Me_2SiC(SiHMe_2)_2]_2$ and zwitterionic species $Ln\{C(SiHMe_3)_3\}_2HB(C_6F_5)_3$ (Ln = La, Ce, Pr, Nd).

The synthesis of the new lanthanide alkyl hydridoborate species, $Ln\{C(SiHMe_3)_3\}_2HB(C_6F_5)_3$ allowed us to explore their role as catalysts in hydrosilylation of α,β-unsaturated carbonyl compounds. There has been no precedence in literature of any rare-earth metal to catalyze hydrosilylation reactions of carbonyl compounds. The catalytic site is argued to be the borane Lewis acid as no catalytic activity is observed with tris(alkyl) lanthanide compounds. This suggests the importance of a lanthanide catalyst in the presence of oxygenate substrates working in combination with a borane that lends both nucleophilicity (hydride donor ability) and Lewis acidity (electrophilic boron center).

Another part of my thesis describes the synthesis and characterization of bis(alkyl) lanthanide compounds bearing the multiple β-hydrogens containing $–C(SiHMe_2)_3$ ligand. The difference between Ln(III) and Ln(II) alkyl compounds is the coordination of the donor ligand, THF in the case of Ln(II). The coordination of THF in Ln(II) alkyl compounds allows us to study the reactivity of these compounds at that site. It has been shown that we can displace two THF groups with one bulky N-heterocyclic carbene ligand and this replacement affects the role of the Ln(II) compounds as catalysts for dehydrocoupling of silanes and amine. The compounds, $Ln\{C(SiHMe_2)_3\}_2THF_2$ and $LnC(SiHMe_3)_3HB(C_6F_5)_3$ do not catalyze the cross-dehydrocoupling reaction of organosilanes and amines whereas $Ln\{C(SiHMe_2)_3\}_2Im$*t*Bu (Ln = Yb, Sm) does. This presents the first example of a rare-earth alkyl compound with carbene coordination to catalyze the dehydrocoupling reaction of organosilanes and amines.

Apart from working extensively with rare-earth alkyl compounds, my thesis also describes the synthesis of novel rare-earth silyl compounds. These are the first examples of bis(silyl) lanthanide compounds containing β-hydrogens in the newly developed $–Si(SiHMe_2)_3$ ligand. They are structurally analogous to the Ln(II) alkyl compounds with presence of non-

classical interactions with the metal center. In both the alkyl and silyl chemistry, the presence of β-hydrogen provides a diagnostic IR handle. The SiH group has a characteristic ν_{SiH} band in the range of 2000 – 2100 cm^{-1} region of the IR spectrum and characteristic chemical shifts in the ^{1}H and ^{29}Si NMR spectra. This allows us to explore and extend the scope of study for these classes of compounds. Thus, more in-depth studies and comparisons of the structural and behavioral properties amongst lanthanide compounds, transition metal and main group metal compounds can be performed.

Thus, we have demonstrated the synthesis of highly novel lanthanide compounds and explored their reactivity in catalysis which has remained as an unexplored field in the world of organometallic chemistry. The combination of the tris(alkyl) lanthanide compounds with Lewis acids provides access to utilize rare-earth metal compounds as catalysts. Synthesis of lanthanide alkyl and silyl compounds with chiral ancillary ligands could be developed which could open more avenues for exploring their chemistry and catalytic activity. Catalytic activity of neutral and cationic silyl lanthanide compounds would require additional investigation. The findings presented in this thesis are unique and open up many more areas of study and further exploration towards economical, viable and green chemistry transformations employing rare-earth metals.